

DISSERTATION ZUR ERLANGUNG DES DOKTORGRADES
DER FAKULTÄT FÜR CHEMIE UND PHARMAZIE
DER LUDWIG-MAXIMILIANS UNIVERSITÄT MÜNCHEN



**ANTIBODY DRUGS AT THE LIQUID-AIR INTERFACE:
PHYSICOCHEMICAL CHARACTERISTICS,
AGGREGATION & THE IMPACT OF FORMULATION**

ELLEN DOROTHEE KÖPF

AUS

ULM A. D. DONAU, DEUTSCHLAND

2017

ERKLÄRUNG

Diese Dissertation wurde im Sinne von §7 der Promotionsordnung vom 28. November 2011 von Herrn Prof. Dr. Wolfgang Frieß betreut.

EIDESSTATTLICHE VERSICHERUNG

Diese Dissertation wurde eigenständig und ohne unerlaubte Hilfe erarbeitet.

Basel, den 8. Oktober 2017

.....

ELLEN KÖPF

DISSERTATION EINGEREICHT AM:

9. OKTOBER 2017

GUTACHTER:

PROF. DR. WOLFGANG FRIESS

1. GUTACHTER:

PROF. DR. GERHARD WINTER

MÜNDLICHE PRÜFUNG AM:

24. NOVEMBER 2017

FÜR MEINE ELTERN



ACKNOWLEDGEMENTS

This thesis was prepared at the Department of Pharmacy, Pharmaceutical Technology and Biopharmaceutics at the Ludwig-Maximilians-University Munich (LMU) in cooperation with AbbVie GmbH & Co. KG Ludwigshafen.

Foremost, I want to particularly thank Prof. Dr. Wolfgang Frieß for giving me the opportunity to be part of his group and for his outstanding scientific guidance, encouragement and support. The challenging tasks and questions he raised, the scientific discussions we had and his ongoing interest in the progress of my project contributed fundamentally to the success of this work.

Special thanks also go to Prof. Dr. Gerhard Winter for taking over the co-referee of my dissertation as well as for providing excellent working conditions, and for encouraging scientific discussions on many occasions. Many thanks also go to Prof. Dr. Olivia Merkel, Dr. Julia Engert, Dr. Gerhard Simon, and Sabine Kohler.

AbbVie GmbH & Co. KG is gratefully acknowledged for promoting this project, for funding and material supply, and for giving access to instruments. Especially, I want to thank Dr. Rudolf Schroeder for his supervision, and his scientific and organizational support. My acknowledgements also go to the NBE Formulation Development team for the excellent collaboration, the valuable discussions and their input.

Moreover, I had the great fortune of getting to know Prof. Dr. Gerald Brezesinski from the Max-Planck-Institute of Colloids and Interfaces, Department of Biomolecular Systems in Potsdam-Golm. Thanks to him we got access to and learned very much about several surface-sensitive analytical methods, which have been found to be of great scientific value for this project. Many thanks for welcoming me in Golm, for your interest in the topic and for your encouragement. I also want to thank Irina Berndt, Annelise Heilig and Marina Sturm for supporting and assisting me during my several research stays in Golm.

The Institute of Particle Technology of the Friedrich-Alexander University Erlangen-Nürnberg, Dr. Björn Braunschweig and Manuela Richert are also kindly acknowledged for their support and scientific input.

Many thanks go to the Coriolis Pharma Research GmbH for the opportunity to perform measurements there.

Furthermore, my sincere thanks are owed to my dear colleagues at university for the pleasant working atmosphere, the numerous sports and social activities, and the great times

we are having together. Particularly, I want to thank Corinna, Jacqueline, Christoph (Olaf), Christoph, Kay, Tobias, Teresa, Laura, Randy, Alice, Ben, Ilona and Moritz. Many thanks also go to my lab mates Kerstin, Bifeng and Imke. Thank you, Verena and Stefanie, for all your support and the highly valuable scientific exchange. I especially want to thank Simon for his commitment and enthusiasm for the project during his time as master student – you really did a great job and I always enjoyed working with you! Furthermore, many tanks go to Eva for supporting the project with her very good and dependable work.

Special thanks are also due to my friends for the wonderful time we are having together and for always being there for me. Especially, I want to thank Anna and Benny for offering me the opportunity to combine my several trips to Mannheim/Ludwigshafen with visiting you. Many thanks also go to Kirsten, Steffi, Lara, Martin S., Alex K., Tina, Martin K., Kristina, Simon, Laureen, Alex, Karina, Max, Nick and Flo. Thank you very much Ahmad for being you and for all the rewarding discussions we had. Jasmin Has, I am very grateful for your friendship and your creative input, particularly with the hard cover of my thesis - thank you!

Very special thanks go to Waltraud and Chris for all your encouragement, help and assistance, and of course for proofreading. Above all, I would like to express my deep gratitude to my family. I am very thankful to my parents, Inge and Ernst, for their infinitely great support and for making all of this possible. Thank you Timo, Gaby, Pia and Romy, Frank, Gisi and Mía – it is great to always having you by my side.

My greatest thanks go to Martin: I am exceedingly grateful for your never ending encouragement, for exceptionally motivating and supporting me. I am really happy to always knowing you by my side. Without you I would not be where I am today – thank you so much.

TABLE OF CONTENT

CHAPTER I

GENERAL INTRODUCTION

1. Abstract	1
2. What are Biopharmaceuticals?	2
3. Structure and Organization of Protein Molecules.....	3
4. Instability Reactions of Protein Pharmaceuticals	4
4.1. Chemical Instabilities.....	5
4.2. Physical Instabilities.....	5
5. Immunogenicity of Protein Particles.....	8
6. Methods for the Characterization of Protein Aggregates	8
7. Possibilities for Stabilization.....	9
7.1. Formulation of Liquid Protein Pharmaceuticals.....	10
7.2. Freeze-Drying as Method of Choice for the Improvement of Storage Stability.....	11
7. Innovative Protein Pharmaceuticals	13
8. References	15

CHAPTER II

OBJECTIVES AND OUTLINE OF THE THESIS.....	23
---	----

CHAPTER III

THE FILM TELLS THE STORY: PHYSICOCHEMICAL CHARACTERISTICS OF IGG AT THE LIQUID-AIR INTERFACE

1. Abstract	27
2. Introduction	28
3. Materials and Methods	31
3.1. Materials.....	31
3.2. Surface Pressure Measurements.....	31

3.3.	FT-IR Spectroscopy	32
3.4.	Infrared Reflection-Absorption Spectroscopy (IRRAS)	32
3.5.	Brewster Angle Microscopy (BAM)	34
3.6.	Atomic Force Microscopy (AFM)	34
4.	Results and Discussion.....	35
4.1.	Time & Concentration Dependent Adsorption of IgG	35
4.2.	Repeated Compression-Decompression of Interfacial IgG Films	37
4.3.	Temperature-Induced Unfolding of IgG	39
4.4.	Presence and Secondary Structure of IgG at the Interface	40
4.5.	Structural and Morphological Characterization of the Interfacial Film	44
4.6.	Changes in Film Topography Caused by Compression	44
4.7.	Interfacial Film Thickness in Equilibrium and after Compression	46
5.	Summary & Conclusion.....	49
6.	References	53

CHAPTER IV

NOTORIOUS BUT NOT UNDERSTOOD: HOW LIQUID-AIR INTERFACIAL STRESS TRIGGERS PROTEIN AGGREGATION

1.	Abstract	63
2.	Introduction	65
3.	Materials and Methods	68
3.1.	Materials	68
3.2.	Surface Pressure Measurements	68
3.3.	Agitation Studies	68
3.4.	Mini-Trough Studies	69
3.5.	Compression Speed (c_{speed})	70
3.6.	Compression Factor (c_f)	70
3.7.	Particle Analysis	71

3.7.1.	Visual Inspection and Photo-documentation	71
3.7.2.	Turbidity.....	71
3.7.3.	Light Obscuration.....	71
3.7.4.	Micro-Flow Imaging	71
3.7.5.	Statistical Significance.....	72
3.8.	FT-IR Spectroscopy	72
3.9.	Infrared Reflection-Absorption Spectroscopy (IRRAS)	72
3.10.	Brewster-Angle Microscopy (BAM)	73
4.	Results and Discussion.....	74
4.1.	Adsorption of IgGs to the Liquid-Air Interface	74
4.2.	Physical Resistance of Interfacial Protein Films	75
4.3.	Particle Formation in a Mini-Trough by Liquid-Air Interfacial Stress Only.....	78
4.4.	Structural and Morphological Characterization of the Interfacial Film	80
4.5.	Presence and Secondary Structure of the Protein at the Interface	82
4.6.	Particle Formation by Agitation.....	84
5.	Summary & Conclusion.....	87
6.	References	89

CHAPTER V

MOVE ALONG PLEASE! HOW FORMULATION ADDITIVES AFFECT LIQUID-AIR INTERFACE RELATED PROTEIN INSTABILITY

1.	Abstract.....	99
2.	Introduction	101
3.	Materials and Methods	104
3.1.	Materials.....	104
3.2.	Surface Pressure Measurements.....	104
3.3.	Agitation Studies.....	105

3.4.	Mini-Trough	105
3.5.	Particle Analysis	105
3.5.1.	Visual Inspection and Photodocumentation	105
3.5.2.	Turbidity.....	106
3.5.3.	Light Obscuration.....	106
3.5.4.	Micro-Flow Imaging	106
3.5.5.	Statistical Significance.....	106
3.6.	Infrared Reflectance Absorbance Spectroscopy (IRRAS)	107
3.7.	Brewster Angle Microscopy (BAM)	108
3.8.	Atomic Force Microscopy (AFM)	108
4.	Results and Discussion.....	109
4.1.	Competitive Adsorption	109
4.1.1.	Equilibration Time.....	109
4.1.2.	Equilibrium Surface Pressure	111
4.2.	Repeated Compression and Decompression of Mixed Films.....	113
4.3.	Presence and Secondary Structure of IgG at the Interface.....	116
4.4.	IRRA Spectra of Mixed Protein-Additive Films	117
4.5.	Interfacial Film Structures	120
4.5.1.	Brewster Angle Microscopy	120
4.5.2.	Atomic Force Microscopy	123
4.6.	Impact of the IgG-Additive Mixture Ratio on Particle Formation	125
4.6.1.	By Agitation.....	125
4.6.2.	By Liquid-Air Interfacial Stress (Mini-Trough).....	127
5.	Summary & Conclusion.....	128
6.	Supplemental Information	133
7.	References	135

CHAPTER VI - Part 1

HOW FORMULATION PH AND IONIC STRENGTH AFFECT PHYSICOCHEMICAL PROTEIN BEHAVIOR AT THE LIQUID-AIR INTERFACE

1. Abstract	143
2. Introduction	144
3. Materials and Methods	145
3.1. Materials	145
3.2. Sum Frequency Generation	145
3.3. Surface Pressure Measurements	146
3.4. Electrophoretic Light Scattering	146
3.5. FT-IR Spectroscopy	146
3.6. Infrared Reflection-Absorption Spectroscopy (IRRAS)	147
3.7. Brewster Angle Microscopy (BAM)	148
3.8. Atomic Force Microscopy (AFM)	148
3.9. Mini-Trough	149
3.10. Particle Analysis	150
3.10.1. Light Obscuration	150
3.10.2. Micro-Flow Imaging	150
3.10.3. Statistical Significance	150
4. Results and Discussion	151
4.1. Determination of the interfacial pI of IgG using SFG	151
4.2. Protein Adsorption as Function of pH	152
4.3. Interfacial Film Compressibility	153
4.4. Impact of pH on Secondary Structure: Bulk vs. Interface	154
4.5. Impact of pH on Interfacial Film Structures	157
4.5.1. Brewster Angle Microscopy (BAM)	157
4.5.2. Atomic Force Microscopy (AFM)	160

4.6.	Determination of the Interfacial Film Thickness	162
4.7.	Impact of pH on Particle Formation by Liquid-Air Interfacial Stress (Mini Trough)	167
5.	Summary & Conclusion.....	169
6.	Supplemental Information	172
6.1.	Determination of the isoelectric point (pI) in bulk solution.....	172
6.2.	Interfacial film thickness by IRRAS	173
6.3.	Interfacial film thickness by AFM	176
7.	References	178

CHAPTER VI - Part 2

THE MISSING PIECE IN THE PUZZLE: PREDICTION OF AGGREGATION VIA THE PROTEIN-PROTEIN INTERACTION PARAMETER A_2^*

1.	Abstract.....	187
2.	Introduction	188
3.	Materials and Methods	189
3.1.	Materials.....	189
3.2.	Determination of A_2^* using Dynamic Light Scattering	190
3.3.	Agitation Studies.....	190
3.4.	Particle Analysis	190
3.4.1.	Visual Inspection and Photo-documentation	190
3.4.2.	Turbidity.....	191
3.4.3.	Light Obscuration.....	191
3.4.4.	Micro-Flow Imaging	191
3.4.5.	Statistical Significance.....	191
4.	Results and Discussion.....	192
4.1.	Impact of Protein and pH on A_2^*	192
4.2.	Impact of Protein and pH on Particle Formation by Agitation	193
4.3.	Impact of Ionic Strength on A_2^*	198

4.4. Impact of Ionic Strength on Turbidity and Particle Formation.....	199
5. Summary & Conclusion.....	203
6. References	206

CHAPTER VII

SUMMARY	213
---------------	-----

CHAPTER I

GENERAL INTRODUCTION

1. ABSTRACT

The range of biopharmaceuticals used for therapy or diagnosis include biotechnologically manufactured vaccines, therapeutic enzymes and coagulation factors, numerous hormones, as well as monoclonal antibodies. Because of their insufficient oral bioavailability, protein pharmaceuticals are typically administered parenterally and can therefore come as aqueous solutions or lyophilisates for reconstitution. Proteins show both chemical and physical instabilities such as oxidation and hydrolysis, denaturation and aggregation. The selection of suitable pH and buffer conditions and adding excipients such as surfactants or sugars enables adequate product quality. It is essential to maintain the native conformation for both the efficacy and stability, as well as the compatibility of these large molecules. Moreover, the combination of different analytical methods enables the necessary comprehensive characterization of the protein pharmaceuticals and helps to ensure product stability during development, production and storage.

2. WHAT ARE BIOPHARMACEUTICALS?

The term biopharmaceuticals includes pharmaceutical substances based on protein drugs or nucleic acids, which are used for the therapy or diagnosis of diseases. Moreover, the European Pharmacopeia (Ph. Eur.) defines biopharmaceuticals in a monograph entitled “Products of recombinant DNA technology” as Active Pharmaceutical Ingredients (API), which are “made from genetic modifications [...]” [1]. The first such substance approved for therapeutic use was recombinant human insulin (rHI, trade name Humulin®), which was marketed in 1982. Since then, the biopharmaceuticals market has witnessed significant growth due to increasing prevalence of chronic diseases, rising aging population, but also due to technological advancements and increasing Research and Development (R&D) investments [2]. In addition, the capability of biopharmaceuticals to approach a particular target with high efficacy helps in the treatment of various chronic diseases and disorders. Important therapeutic areas of biopharmaceuticals include diabetes (insulins), multiple sclerosis, rheumatoid arthritis and hepatitis (immunomodulators), cancer (monoclonal antibodies, interferons), metabolic and coagulation disorders (enzymes, coagulation factors) and vaccination (e.g. against cervical cancer or hepatitis B) and are listed in figure 1.

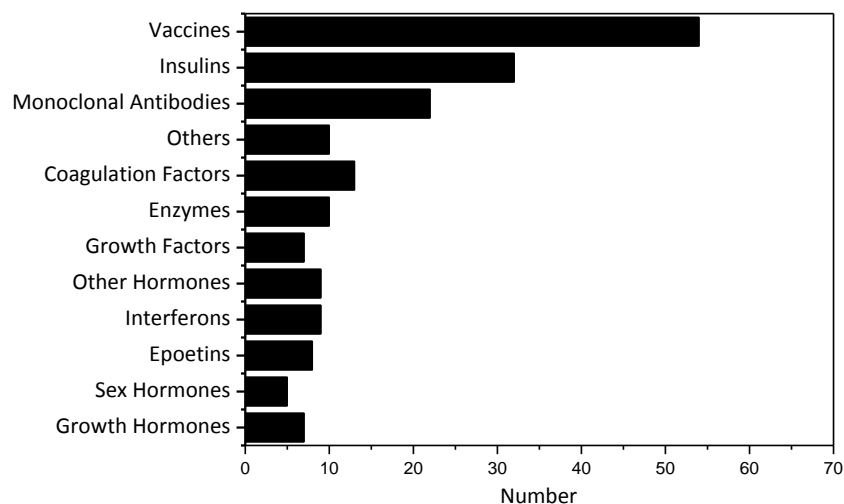


Figure 1: Number of authorized biopharmaceuticals in Germany in 2014 by type (Satista 2015)

Currently, more than 180 protein pharmaceuticals with 138 different recombinantly produced APIs, are approved in Germany; worldwide more than 550 biopharmaceuticals are in clinical trials or in the approval process [3]. In 2014, a total of 47 products containing a new API or new combinations of known APIs have been approved in Germany. Among these new registrations were 14 biopharmaceuticals, including eleven for original products and three biosimilars. Thus, biopharmaceuticals constituted 30 % of all new registrations. Within the current development projects monoclonal antibodies (mABs) have the highest share. Sales of biopharmaceuticals increased in 2014 compared to 2013 by 7% and amounted to around 7.5 billion € [4] (Fig. 2).

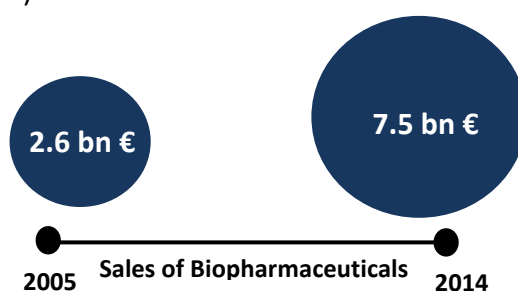


Figure 2: Sales of biopharmaceuticals in Germany from 2005 to 2014 in €

3. STRUCTURE AND ORGANIZATION OF PROTEIN MOLECULES

A protein is primarily defined by its amino acid sequence. Protein pharmaceuticals are much larger compared to small molecule drugs and their therapeutic effect is related to their complex three-dimensional structure. Hence, proteins are macromolecules and have four different structural levels – primary, secondary, tertiary and quaternary. The amino acid sequence makes up the primary structure of the protein, and has a considerable impact on the properties of the protein, such as conformation, charge and solubility [5]. Sequence stretches within a protein molecule have characteristic conformations and the two main types of secondary structure are α -helix and β -sheet. The spatial arrangement of different secondary structural elements to each other results in a unique three-dimensional, the so called tertiary structure. The quaternary structure, such as in case of hemoglobin, describes the structure within macromolecular complexes composed of several protein subunits. The preservation of the native structure and therefore the biological activity of a protein is one of the main tasks of protein formulation.

4. INSTABILITY REACTIONS OF PROTEIN PHARMACEUTICALS

Under physiological conditions, the protein conformation represents an equilibrium between native and denatured (unfolded) state. Exogenous influences during production, storage and transportation might cause a shift in this balance. Additionally, protein molecules may interact and associate forming aggregates of different size ranging from dimers, oligomers and sub-visible particles to visible precipitates [6].

Instability reactions of proteins can be divided into chemical and physical instabilities [7]–[9]. The latter one can further be differentiated in colloidal and conformational instabilities [10]–[12]. A chemical instability is defined as a change within the primary structure induced by a chemical reaction, whereas a physical instability changes the spatial arrangement of the chains towards each other without changes of covalent bonds. The physical stability of a protein is mediated by short, specifically van der Waals, hydrogen bonds and hydrophobic as well as long range, specifically electrostatic interactions. These interactions on the one hand affect the protein secondary and tertiary structure, and on the other hand dictate the interactions between individual molecules in solution [13], [14]. Colloidal instability resulting from attractive protein-protein interactions can result in the formation of protein aggregates. Furthermore, structural changes can trigger aggregation, as hydrophobic patches, previously buried in the interior of the molecule, become exposed at the protein surface leading to increased hydrophobic interactions [15]–[17]. Table 1 lists some important instability reactions of protein molecules.

Table 1: Important instability reactions of proteins in biopharmaceutical formulations

Chemical Instability	Physical Instability
Oxidation	Denaturation
Hydrolysis	Association
Deamidation	Aggregation
Change in disulfid bonds	Precipitation
Racemization, Isomerization	Adsorption on surfaces
β -Elimination	

4.1. Chemical Instabilities

At many points during e.g. manufacturing and shipping of protein pharmaceuticals the problem of instability reactions may be encountered and cause difficulties with respect to product quality. Oxidation processes may cause difficulties as next to oxygen also light and thermal energy are critical factors directly affecting the conformational stability of protein molecules. Amino acids such as cysteine and methionine, as well as aromatic amino acids such as tyrosine or histidine, are particularly sensitive to oxidation reactions. Oxidation of free mercaptan groups (-SH) to sulfoxides is possible. Additionally new intra- or intermolecular disulfide bridges may emerge, whereby the latter results in covalent aggregate formation [18]. Peptide bonds are subject to acidic and alkaline hydrolysis, particularly aspartic acid and proline are prone to undergo such instability reactions [13]. Another typical chemical modification is the deamidation of the chains of asparagine and glutamine to the free carboxylic acid. The rate of deamidation processes thereby very much depends on the structure of the protein and the pH of the solution [19].

4.2. Physical Instabilities

Typical physical degradation reactions are denaturation, aggregation and adsorption onto surfaces. Denaturation renders changes within the spatial structure, whereby in most cases the biological function of the protein gets lost. The unfolded state is colloiddally less stable due to its more hydrophobic state causing the formation of aggregates. Protein aggregates can be soluble and insoluble in nature, can be covalent and non-covalent, and can be reversible or irreversible. Not only partly or fully unfolded protein molecules, but also native molecules can play an important role in the formation of protein aggregates. On the one hand, the emergence of small aggregates can induce the formation of larger aggregates by agglomeration, on the other hand so-called “large native-like particles” often occur spontaneously without continuum from monomer, to dimer to large particles [5].

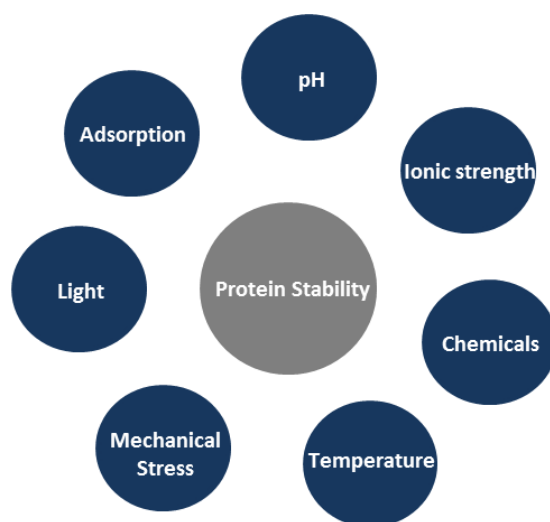


Figure 3: Some important factors influencing protein stability

Temperature or light effects, solvent properties, mechanical stress, denaturing agents or high ionic strength affect protein stability (Fig. 3). Upon heating, non-covalent interactions in the molecule break up leading to a spatial arrangement. The temperature at which 50% of the molecules are in the native state and 50% in the denatured state is referred to as “melting point” (T_m) of a protein. The T_m can be determined by microcalorimetry and provides important information on the conformational stability of a protein in a formulation [12]. Depending on the pH value, side chains are protonated or deprotonated, which has a decisive influence on ionic bonds and conformational stability of the protein [19]. The colloidal stability is typically low at the isoelectric point (pI) where the protein carries no net charge. At pH values away from the pI, electrostatic repulsion between protein molecules increases. However, extreme pH values induce conformational changes due to unfolding induced by intramolecular repulsion and chemical degradation [12], [20]. Hence, determination of pI, e.g. by isoelectric focusing or by capillary electrophoresis, is essential during formulation development. Interactions between the protein molecules, which are primarily determined by pH and ionic strength of the formulation, affect the stability of a protein solution significantly. Hydrophilic and hydrophobic interaction chromatography (HIC) allows to draw conclusions regarding hydrophobicity and isoforms of the protein molecules. The osmotic second virial coefficient provides information on the nature and extent of the interactions and can be determined e.g. by means of static or dynamic light scattering [12] [21], [22].

Another physical instability of proteins is adsorption to material surfaces or to the air-water interface due to hydrophilic and hydrophobic sections in protein molecules. Protein adsorption to containers and stoppers as well as interactions with processing materials or auxiliary materials for application, such as tubings and filters, have to be considered carefully [23]. The adsorption of protein molecules differs in many aspects from the adsorption of e.g. surfactant molecules. Firstly, the adsorption process can accompany the unfolding of protein molecules, although this effect depends on the type of protein and only little is known for IgGs [24], [25]. Secondly, other than in the case of surfactant molecules, no real equilibrium between adsorption and desorption can be reached, as desorption kinetics are hindered due to the emergence of strong intermolecular forces resulting in an interfacial gelation and film formation [26]–[29]. This makes it impossible to use common isotherm models as developed by Henry or Langmuir for the description of protein layers at the liquid-air interface [30]–[32]. In particular, liquid-air interfaces have been identified as critical factor for the occurrence of large protein particles. Although considerable effort has been put into the understanding of protein interfacial behavior, its link to the formation of particles is still poorly understood [33], [34]. Hence, shaking or stirring can cause the formation of aggregates especially in the case of insufficient protection and absence of surface active formulation additives, such as surfactants, in appropriate concentrations [35]–[37]. Most protein pharmaceuticals are packaged in pre-filled syringes or vials made of borosilicate glass (type I). In recent years, delamination, i.e. detachment of inorganic flakes from the inside of vials, and chemical and physical destabilization of the protein by tungsten oxide, which can be formed during the placing of the needle during the production of a pre-filled syringe, were identified as critical factors in the manufacturing process of protein pharmaceuticals [38]. Moreover, the inner wall of a pre-filled syringe is coated with silicone oil to ensure the sliding of the syringe plunger. Already in the 1980s, first studies suggested a clear link between silicone oil and aggregation of insulin [39]. Current studies prove that proteins adsorb to silicone oil-water interfaces in a similar way as to air-water interfaces, and give rise to the hypothesis that due to a rupture of the interfacial film protein aggregates can occur [33], [34], [40].

5. IMMUNOGENICITY OF PROTEIN PARTICLES

Immune reactions to protein pharmaceuticals can be due to the possible formation of so-called “anti-drug antibodies (ADAs), which are antibodies to the therapeutic protein. It is already known that the immunogenic potential depends on the properties of the aggregates, such as size, solubility and conformation. In particular, chemically modified protein particles with non-native conformation were identified as being particularly immunogenic. But also undesired immune reactions due to small, soluble protein aggregates have been reported [41]. Furthermore, non-proteinogenic impurities, such as silicone oil, may intensify an undesired stimulation of the immune system. In case of vaccines this fact is conversely utilized via the addition of adjuvants, e.g. aluminum, to amplify the immune response. Further efforts are needed to fully understand the coherences between protein aggregates and immune response [42].



Figure 4: Protein solution containing aggregates

6. METHODS FOR THE CHARACTERIZATION OF PROTEIN AGGREGATES

The requirement that injections and infusions must be practically free from visible particles as well as the permitted number of non-visible particles, are regulated by the pharmacopoeias. Despite particle testing, a differentiation between protein particles and non-proteinaceous particles does not take place at this point. Moreover, the particle size ranges from a few nanometers in the case of a dimer, up to a few millimeters in the case of large visible aggregates. Therefore, a combination of different analytical methods is required to cover the entire size range, and to differentiate between protein aggregates and other particles. The use of a variety of methods based on different measurement principles, so-

called orthogonal methods, is also proposed by the European Medicines Agency (EMA) for the manufacturing and the quality control of monoclonal antibodies and similar substances. When specifying the particle size, the analytical method used should always be considered. The standard method for the quantification of small oligomers is size exclusion chromatography (SEC). Since SEC results are influenced by interactions of protein molecules with the mobile phase and the stationary phase, the use of analytical ultracentrifugation and field flow fractionation (FFF) as orthogonal methods is recommended. SDS gel electrophoresis is used to identify covalent aggregates and after reduction of the samples it can also be used to differentiate between disulfide bonds and other non-reducible linkages. For the larger nanometer scale, new processes such as nanoparticle tracking or resonance mass measurement have been established [43]. The morphology of a particle may allow the differentiation between foreign particles and protein aggregates. Flow imaging techniques allow this for particles larger than about 5 μm . For example, the spherical silicone oil droplets can easily be distinguished from the irregular and uneven protein aggregates. Below 5 μm silicone oil droplets and protein particles can be distinguished by determining the buoyant mass using resonance mass measurement [44]. Larger particles can also be differentiated by means of infrared and Raman spectroscopy. For the detection of chemical modifications, various chromatographic methods are frequently used, such as reverse phase or ion exchange chromatography, as well as isoelectric focusing, capillary electrophoresis or mass spectrometry. Conformational changes can be investigated using infrared spectroscopy, circular dichroism, or fluorescence measurements [44].

7. POSSIBILITIES FOR STABILIZATION

Aqueous solutions of proteins are usually the most popular because of lower costs and easy administration. Alternatively, protein formulations are lyophilized for stability reasons. All excipients should be safe and satisfy the definition of the GRAS status (generally recognized as safe) by the Food and Drug Administration (FDA). Typical requirements for parenterals, such as sterility, isotonicity and absence of particles of course also apply to protein formulations. As protein unfolding can already set in at a temperature of 40 °C, and chemical instability reactions are accelerated at higher temperatures, storage at 2° to 8 °C and the maintenance of the cold chain during transportation are essential for most liquid formulations. Moreover, freezing of the aqueous solution has to be avoided, since ice

formation and freeze concentration can induce protein aggregation [45]. During storage, light protection has to be assured. Preservatives have to be added to multi-dose aqueous solutions for injections according to the European Pharmacopoeia. Moreover, single-dose aqueous solutions, which are prepared aseptically but which cannot be sterilized in the final container, as is the case with protein solutions, may contain preservatives. Benzyl alcohol, phenol or cresol, are, *inter alia*, commonly used preservatives. Recent studies show, however, that preserving agents may adversely affect the physical stability of protein solutions [46].

7.1. Formulation of Liquid Protein Pharmaceuticals

In the choice of suitable pH value, buffer and ionic strength is crucial for both chemical and physical stability of protein pharmaceuticals. The surface characteristics of a protein molecule are influenced by the pH value due to the protonation or deprotonation of basic and acidic amino acids. Choosing a pH value far away from the isoelectric point (pI) may improve the colloidal stabilization due to stronger repulsion of protein molecules but may put the conformational stability of the protein at risk by a reduction of attractive interactions required for maintenance of the native three-dimensional structure. Typical buffering agents include phosphate, acetate or citrate as well as amino acids, such as histidine. Furthermore, amino acids can complex heavy metals and thus prevent oxidation, but may also introduce impurities [46]. The ionic strength affects the stability of a protein solution significantly. With increased ionic strength, repulsion between the protein molecules can be decreased due to stronger charge shielding thereby fostering aggregation. In contrast, at low ionic strength an increase of the colloidal stability may be observed whereby the nature of the ions themselves has a significant impact on their salting-in effect as described by the Hofmeister series [47]. Already in the late 1980s Timasheff found that the denaturation and aggregation of proteins can be reduced by the addition of excipients [48]. Timasheff developed a thermodynamic model which states that the energy difference between the native and denatured form of a protein must be as large as possible to maintain the intact, native form of the protein. The mechanism of action of common stabilizers is based on their preferred exclusion from the protein sphere (so-called “preferential exclusion”): while the additives are displaced from the surface of the protein, water is preferably attached (so-called “preferential hydration”). For denatured protein molecules,

the contact surface with the solvent is larger compared to the native molecule. Hence, the process of unfolding is, as a result of an increase in free energy, thermodynamically disadvantageous. Therefore, in presence of stabilizing additives, such as sugar alcohols (e.g. mannitol) or sugars (e.g. sucrose or trehalose), the equilibrium is shifted in favor of the native state. Reducing sugars such as glucose or lactose should be avoided to minimize the risk of Maillard reactions. Frequently, surfactants in concentrations slightly above the critical micelle concentration (CMC) are added to the formulations, in particular, polysorbate 20 and 80 or poloxamer 188 [49]. The surfactant molecules compete with the protein molecules for the adsorption to the liquid-air interface preventing interface-related protein aggregation. However, impurities and degradation products of surfactants can cause chemical changes, especially oxidation of protein molecules. Furthermore, fatty acids derived from surfactants may form particles [50]. Hence, not only choosing a high quality of the surfactants added, but also carefully considering an appropriate concentration is important. In order to prevent protein oxidation, antioxidants such as methionine can be added [51].

7.2. Freeze-Drying as Method of Choice for the Improvement of Storage Stability

The process of freeze-drying is divided into the freezing step, followed by primary and secondary drying. Moreover, ice formation leads to the concentration of the API and excipients in solution. During the subsequent primary drying phase, the ice is removed by sublimation. Adsorbed water is removed during secondary drying. Usually, the residual moisture content is less than one percent in order to ensure good protein stability. Different process parameters such as the freezing rate, the temperature control of the shelves, and stabilizing formulation additives can affect product quality significantly. For example, differences in the solubility of buffer salts can cause pH shifts during the freezing process [52]. In addition, the concentration effect may cause a substantial increase in ionic strength affecting protein-protein interactions. Furthermore, the removal of water can be critical for the maintenance of the native state of the protein.



Figure 5: Lyophilized protein formulation

To preserve the stability of the protein during lyophilization, so-called cryo- and lyoprotectors are added to the formulation. Cryoprotectors are substances which contribute to the stabilization of the protein during the freezing process itself, whereas lyoprotectors help to stabilize the protein in the dry state. As with many hydroxyl groups, lyoprotectors can replace the hydration shell of the protein, which is removed during drying (so-called water replacement theory). Therefore, sugars which form amorphous matrices, such as sucrose or trehalose, but also polyalcohols, amino acids, or 2-hydroxypropyl- β -cyclodextrin, can be used as cryo- and lyoprotectors [52], [53]. The low molecular weight components also substantially contribute to the formation of an appealing product cake. The addition of surfactants not only improves the wettability for a fast reconstitution, but can also prevent undesired denaturation at ice interfaces during freezing. The reconstitution and dilution of lyophilized products is a frequent source of error. Strong shaking and foam formation should be avoided to minimize the liquid-air interfacial stress to the protein. Healthcare professionals and patients must be instructed which solvent has to be used for reconstitution or dilution and how dilution has to be performed. In the case of trastuzumab (Herceptin®) dilution with 5% glucose solution instead of the recommended 0.9% sodium chloride solution causes the formation of large aggregates [54].

8. INNOVATIVE PROTEIN PHARMACEUTICALS

Many pharmaceutical companies explore the broad possibilities which protein drugs provide. New protein formats have the potential for improved efficacy and safety compared to conventional structures. Bi- and tri-specific antibodies have multiple binding sites and can therefore recognize different structures and bind to them with high affinity, specificity and potential synergistic effects. In the field of cancer therapy, the first bispecific antibodies have already been approved in the United States, many more based on different technologies such as BiTE[®]-, DART[®]- or DVD[®]-proteins are in development. Antibody-drug conjugates (ADCs) monoclonal antibodies with a covalent coupled to a small molecule. The antibody binds specifically to target cells and brings the highly potent drug molecules selectively to the target. Currently, two ADCs, Adcetris[®] and Kadcyla[®], are approved in oncology. In addition, many candidates are under development or in the approval process. For the formulation of ADCs it is not only important to pay attention to the stability of the antibody, but also to the linker and the small molecule drug [55]. Further investigation will be needed to investigate whether the established formulation strategies are appropriate for standard protein formats as well as for these new types of molecules.

For the high-priced and sensitive protein pharmaceuticals, the choice of primary packaging materials has become more and more important. Schott presented a novel glass syringe (syriQ[™] InJentle) which was especially developed for the filling of biopharmaceuticals and produced without the use of a tungsten pin. Unlike many conventional syringes, the silicone oil is baked-on, whereby free silicone and associated particle formation is reduced. Moreover, the specifically developed design ensures that the protein drug does not come into contact with the needle or the needle adhesive [56]. Interest in developing subcutaneously administrable formulations is particularly high, with the aim of achieving the highest possible user-friendliness. To assure a painless application, the applied volume must be small and therefore the protein concentration must be high. However, highly concentrated protein solutions often have a viscosity which hardly allows subcutaneous injection with conventional injection needles. Therefore, syringe designs with a reduced friction of the plug, auto-injectors, or so-called “thin wall”-needles which have a larger inner diameter at the same outer diameter, provide good options [57].

Furthermore, by adding hyaluronidase, which partly dissolves the extracellular matrix in the injection area, the administered volume can be increased [58]. Herceptin® is the first combination product of a highly-concentrated protein and hyaluronidase.

Thus, many innovations in the field of protein formulation open up new treatment options and significantly contribute to an increased product quality.

9. REFERENCES

- [1] "DNA-rekombinationstechnisch hergestellte Produkte." Europäisches Arzneibuch, Monographie Nr 784.
- [2] I. Krämer, W. Jelkmann, and M. Engelhardt, *Rekombinante Arzneimittel - medizinischer Fortschritt durch Biotechnologie*. Springer Medizin Verlag Heidelberg, 2008.
- [3] "vfa. Verband forschender Pharmaunternehmen," www.vfa.de as available on 30.07.2015, 2015.
- [4] D. Michel and A. Heinemann, "Medizinische Biotechnologie in Deutschland 2009," *Bost. Consult. Gr.*, 2009.
- [5] W. Wang, S. Nema, and D. Teagarden, "Protein aggregation-Pathways and influencing factors," *Int. J. Pharm.*, vol. 390, no. 2, pp. 89–99, 2010.
- [6] J. Brange. Physical stability of proteins. In S. Frokjaer and L. Hovgaards (eds.), *Pharmaceutical Formulation and Development of Peptides and Proteins*, Taylor and Francis, London, 2000, pp. 89–112.
- [7] C. J. Roberts, "Protein aggregation and its impact on product quality," *Curr Opin Biotechnol*, vol. 30, pp. 211–217, 2014.
- [8] R. Tavakoli-Keshe, J. J. Phillips, R. Turner, and D. G. Bracewell, "Understanding the relationship between biotherapeutic protein stability and solid-liquid interfacial shear in constant region mutants of IgG1 and IgG4," *J. Pharm. Sci.*, vol. 103, no. 2, pp. 437–444, 2014.
- [9] J. S. Philo and T. Arakawa, "Mechanisms of protein aggregation.," *Curr. Pharm. Biotechnol.*, vol. 10, no. 4, pp. 348–51, 2009.
- [10] C. Kalonia, V. Tropani, N. Wahome, I. Gabel, C. R. Middaugh, D. Volkin, "Effects of Protein Conformation, Apparent Solubility, and Protein-Protein Interactions on the Rates and Mechanisms of Aggregation for an IgG1 Monoclonal Antibody," *J. Phys. Chem. B*, vol. 120, no. 29, pp. 7062–7075, 2016.
- [11] E. Chi, S. Krishnan, and B. Kendrick, "Roles of conformational stability and colloidal stability in the aggregation of recombinant human granulocyte colony-stimulating factor," *Protein Sci.*, vol. 12, pp. 903–913, 2003.

- [12] T. Menzen and W. Friess, "Temperature-ramped studies on the aggregation, unfolding, and interaction of a therapeutic monoclonal antibody," *J. Pharm. Sci.*, vol. 103, no. 2, pp. 445–455, 2014.
- [13] W. Wang, "Instability, stabilization, and formulation of liquid protein pharmaceuticals," *Int. J. Pharm.*, vol. 185, pp. 129–188, 1999.
- [14] D. Arzenšek, D. Kuzman, and R. Podgornik, "Colloidal interactions between monoclonal antibodies in aqueous solutions," *J. Colloid Interface Sci.*, vol. 384, no. 1, pp. 207–216, 2012.
- [15] S. Simon, H. J. Krause, C. Weber, and W. Peukert, "Physical degradation of proteins in well-defined fluid flows studied within a four-roll apparatus," *Biotechnol. Bioeng.*, vol. 108, no. 12, pp. 2914–2922, 2011.
- [16] J. T. Pelton and L. R. McLean, "Spectroscopic methods for analysis of protein secondary structure.," *Anal. Biochem.*, vol. 277, no. 2, pp. 167–176, 2000.
- [17] L. Wu, J. Zhang, and W. Watanabe, "Physical and chemical stability of drug nanoparticles.," *Adv. Drug Deliv. Rev.*, vol. 63, no. 6, pp. 456–69, May 2011.
- [18] M. Amano, N. Kobayashi, M. Yabuta, S. Uchiyama, and K. Fukui, "Detection of histidine oxidation in a monoclonal immunoglobulin gamma (IgG) 1 antibody," *Anal. Chem.*, vol. 86, no. 15, pp. 7536–7543, 2014.
- [19] J. Y. Zheng and L. J. Janis, "Influence of pH, buffer species, and storage temperature on physicochemical stability of a humanized monoclonal antibody LA298," *Int. J. Pharm.*, vol. 308, pp. 46–51, 2006.
- [20] D. W. Siderius, W. P. Krekelberg, C. J. Roberts, and V. K. Shen, "Osmotic virial coefficients for model protein and colloidal solutions: Importance of ensemble constraints in the analysis of light scattering data," *J. Chem. Phys.*, vol. 136, no. 17, 2012.
- [21] R. M. Fesinmeyer, S. Hogen, A. Saluia, S. R. Brych, E. Kras, L. O. Narhi, D. N. Brems, Y. R. Gokarn., "Effect of Ions on Agitation- and Temperature-induced Aggregation Reactions of Antibodies," *Pharm. Res.*, vol. 26, no. 4, pp. 903–913, 2009.
- [22] G. Yin, Z. Liu, J. Zhan, F. Ding, and N. Yuan, "Impacts of the surface charge property on protein adsorption on hydroxyapatite," *Chem. Eng. J.*, vol. 87, no. 2, pp. 181–186, 2002.

- [23] V. Saller, J. Pott, J. Matilainen, U. Grauschopf, K. Bechtold-peters, and W. Friess, "Particle Shedding from Silicone Tubing used for Peristaltic Pumping in Biopharmaceutical Drug Product Manufacturing," *Pharm. Drug Deliv. Pharm. Technol.*, pp. 2–3, 2015.
- [24] A. Tronin, T. Dubrovsky, S. Dubrovskaya, G. Radicchi, and C. Nicolini, "Role of Protein Unfolding in Monolayer Formation on Air/Water Interface," *Langmuir*, vol. 12, no. 13, pp. 3272–3275, 1996.
- [25] Y. F. Yano, E. Arakawa, W. Voegeli, and T. Matsushita, "Real-time investigation of protein unfolding at an air–water interface at the 1 s time scale," *J. Synchrotron Radiat.*, vol. 20, pp. 980–983, 2013.
- [26] R. Wüstneck, J. Krägel, R. Miller, V. B. Fainerman, P. J. Wilde and D. K. Sarker, "Dynamic surface tension and adsorption properties of b-casein and b-lactoglobulin," *Food Hydrocoll.*, vol. 10, no. 4, pp. 395–405, 1996.
- [27] A. H. Martin, M. B. J. Meinders, M. A. Bos, M. a C. Stuart, and T. Van Vliet, "Conformational Aspects of Proteins at the Air / Water Interface Studied by Infrared Reflection - Absorption Spectroscopy," no. 9, pp. 2922–2928, 2003.
- [28] A. MacKie and P. Wilde, "The role of interactions in defining the structure of mixed protein-surfactant interfaces," *Adv. Colloid Interface Sci.*, vol. 117, no. 1–3, pp. 3–13, 2005.
- [29] J. T. Petkov, T. D. Gurkov, B. E. Campbell, and R. P. Borwankar, "Dilatational and shear elasticity of gel-like protein layers on air/water interface," *Langmuir*, vol. 16, no. 8, pp. 3703–3711, 2000.
- [30] S. Ghazvini, C. Kalonia, D. B. Volkin, and P. Dhar, "Evaluating the Role of the Air-Solution Interface on the Mechanism of Subvisible Particle Formation Caused by Mechanical Agitation for an IgG1 mAb," *J. Pharm. Sci.*, vol. 105, no. 5, pp. 1643–1656, 2016.
- [31] E. A. Vogler, "Protein adsorption in three dimensions," *Biomaterials*, vol. 33, no. 5, pp. 1201–1237, 2012.
- [32] A. V. Makievski, V. B. Fainerman, M. Bree, R. Wüstneck, J. Krägel and R. Miller "Adsorption of Proteins at the Liquid / Air Interface," *Society*, vol. 5647, no. 97, pp. 417–425, 1998.

- [33] S. Rudiuk, L. Cohen-Tannoudji, S. Huille, and C. Tribet, "Importance of the dynamics of adsorption and of a transient interfacial stress on the formation of aggregates of IgG antibodies," *Soft Matter*, vol. 8, p. 2651, 2012.
- [34] J. S. Bee, S. K. Schwartz, S. Trabelsi, E. Freund, J. L. Stevenson, J. F. Carpenter and T. W. Randolph, "Production of particles of therapeutic proteins at the air–water interface during compression/dilation cycles," *Soft Matter*, vol. 8, no. 40, p. 10329, 2012.
- [35] S. Kiese, A. Pappenberger, W. Friess, and H.-C. Mahler, "Equilibrium Studies of Protein Aggregates and Homogeneous Nucleation in Protein Formulation," *J. Pharm. Sci.*, vol. 99, no. 2, pp. 632–644, 2009.
- [36] S. Kiese, A. Pappenberger, W. Friess, and H.-C. Mahler, "Shaken, Not Stirred: Mechanical Stress Testing of An IgG1 Antibody," *J. Pharm. Sci.*, vol. 97, no. 10, pp. 4347–4366, 2008.
- [37] H. C. Mahler, R. Müller, W. Frieß, A. Delille, and S. Matheus, "Induction and analysis of aggregates in a liquid IgG1-antibody formulation," *Eur. J. Pharm. Biopharm.*, vol. 59, no. 3, pp. 407–417, 2005.
- [38] W. Wang, A. A. Ignatius, and S. V. Thakkar, "Impact of Residual Impurities and Contaminants on Protein Stability," *J. Pharm. Sci.*, vol. 103, no. 5, pp. 1315–1330, 2014.
- [39] R. Bernstein, "Clouding and Deactivation of Clear (Regular) Human Insulin: Association With Silicone Oil From Disposable Syringes?," *Diabetes Care*, vol. 10, no. 6, pp. 786–787, 1987.
- [40] L. S. Jones, A. Kaufmann, and C. R. Middaugh, "Silicone oil induced aggregation of proteins," *J. Pharm. Sci.*, vol. 94, no. 4, pp. 918–927, 2005.
- [41] A. J. Freitag, M. Shomali, S. Michalakis, M. Biel, M. Siedler, Z. Kaymakcalan, J. F. Carpenter, T. W. Randolph, G. Winter and J. Engert, "Investigation of the Immunogenicity of Different Types of Aggregates of a Murine Monoclonal Antibody in Mice," *Pharm. Res.*, vol. 32, no. 2, pp. 430–444, 2015.
- [42] W. Wang, S. K. Singh, N. Li, M. R. Toler, K. R. King, and S. Nema, "Immunogenicity of protein aggregates--concerns and realities.," *Int. J. Pharm.*, vol. 431, no. 1–2, pp. 1–11, 2012.

-
- [43] D. Weinbuch, S. Zölls, M. Wiggenghorn, W. Friess, G. winter, W. Jiskoot and A. Hawe, "Micro-flow imaging and resonant mass measurement (archimedes) - complementary methods to quantitatively differentiate protein particles and silicone oil droplets," *J. Pharm. Sci.*, vol. 102, no. 7, pp. 2152–2165, 2013.
- [44] S. Zölls, R. Tantipolphan, M. Wiggenghorn, G. Winter, W. Jiskoot, W. Friess and A. Hawe, "Particles in Therapeutic Protein Formulations, Part 1: Overview of Analytical Methods," *J. Pharm. Sci.*, vol. 101, no. 10, pp. 914–935, 2012.
- [45] N. Rathore and R. S. Rajan, "Current perspectives on stability of protein drug products during formulation, fill and finish operations," *Biotechnol. Prog.*, vol. 24, no. 3, pp. 504–514, 2008.
- [46] P. Heljo, A. Ross, I. E. Zarraga, A. Pappenberger, and H.-C. Mahler, "Interactions Between Peptide and Preservatives: Effects on Peptide Self-Interactions and Antimicrobial Efficiency In Aqueous Multi-Dose Formulations," *Pharm. Res.*, vol. 32, no. 10, pp. 3201–3212, 2015.
- [47] S. Uchiyama, "Liquid formulation for antibody drugs," *Biochim. Biophys. Acta - Proteins Proteomics*, vol. 1844, no. 11, pp. 2041–2052, 2014.
- [48] S. N. Timasheff, "The Control of Protein Stability and Association by Weak Interactions with Water: How Do Solvents Affect These Processes?," *Annu. Rev. Biophys. Biomol. Struct.*, vol. 22, pp. 67–97, 1993.
- [49] T. Serno, E. Härtl, A. Besheer, R. Miller, and G. Winter, "The Role of Polysorbate 80 and HP β CD at the Air-Water Interface of IgG Solutions," *Pharm. Res.*, pp. 1–14, 2012.
- [50] B. A. Kerwin, "Polysorbates 20 and 80 Used in the Formulation of Protein Biotherapeutics: Structure and Degradation Pathways," *J. Pharm. Sci.*, vol. 97, no. 8, pp. 2926–2935, 2008.
- [51] R. J. Elias, D. J. McClements, and E. a Decker, "Antioxidant activity of cysteine, tryptophan, and methionine residues in continuous phase beta-lactoglobulin in oil-in-water emulsions.," *J. Agric. Food Chem.*, vol. 53, no. 26, pp. 10248–53, 2005.
- [52] K. Izutsu, S. Kadoya, C. Yomota, T. Kawanishi, E. Yonemochi, and K. Terada, "Freeze-drying of proteins in glass solids formed by basic amino acids and dicarboxylic acids.," *Chem. Pharm. Bull. (Tokyo).*, vol. 57, no. 1, pp. 43–48, 2009.

- [53] L. Chang, D. Sheperd, J. sun, D. Quelette, K. L. Grant, X. C. Tang, M. J. Pikal, "Mechanism of protein stabilization by sugars during freeze-drying and storage: Native structure preservation, specific interaction, and/or immobilization in a glassy matrix?," *J. Pharm. Sci.*, vol. 94, no. 7, pp. 1427–1444, 2005.
- [54] European Medicines Agency, "Scientific Discussion for the Approval of Herceptin," 2005.
- [55] S. K. Singh, D. L. Luisi, and R. H. Pak, Antibody-Drug Conjugates: Design, Formulation and Physicochemical Stability, vol. 32, no. 11. 2015.
- [56] Schott AG, syriQTM InJentle – Innovative Prefillable Staked Needle Syringe Case Study. 2014, pp. 1–3.
- [57] A. Allmendinger, S. Fischer, J. Huwyler, H. C. Mahler, E. Schwarb, I. E. Zarraga, R. Mueller, "Rheological characterization and injection forces of concentrated protein formulations: An alternative predictive model for non-Newtonian solutions," *Eur. J. Pharm. Biopharm.*, vol. 87, no. 2, pp. 318–328, 2014.
- [58] G. I. Frost, "Recombinant human hyaluronidase (rHuPH20): an enabling platform for subcutaneous drug and fluid administration," *Expert Opin. Drug Deliv.*, vol. 4, no. 4, pp. 427–440, 2007.

PARTS OF THIS CHAPTER WERE PUBLISHED:

Koepf E and Friess W 2016. Proteinformulierung: Vom Molekül zum Medikament, Pharmakon, 2:125-133.

CHAPTER II

OBJECTIVES AND OUTLINE OF THE THESIS

The aim of the thesis is to contribute to a better understanding of the physicochemical behavior of proteins at the liquid-air interface, and related formulation stability issues. Protein pharmaceuticals are exposed to liquid-air interfaces at many points during production, manufacturing and transportation. The objectives of this work focus on a mechanistic comprehension of how protein particles build up in the context of liquid-air interfacial stress exemplarily for antibody molecules. Investigations of the impact of different formulation parameters on the liquid-air interfacial characteristics on the one hand, and on protein-protein interactions in bulk solution on the other, aim to enable a more efficient formulation and process development for protein pharmaceuticals.

As a first objective, novel analytical techniques for the investigation of events and processes at the liquid-air interface were identified, which had not been established for the characterization of proteins so far. In **Chapter III**, different surface sensitive methods were introduced to elucidate the protein adsorption process, protein conformation at the interface, as well as the peculiarities of the interfacial protein film with respect to its resistance, homogeneity and thickness.

Although the link between the presence of a liquid-air interface and the emergence of protein aggregates has been extensively investigated little is known about the underlying mechanisms. As conventional stress by shaking or stirring holds factors such as cavitation, turbulent flow, or interactions with material e.g. stopper or stirrer surfaces, a model was developed to investigate the stimulation of protein aggregation solely by liquid-air interfacial stress (**Chapter IV**).

Formulation additives, especially surfactants, are added to protein formulations, as it is known that this can prevent interface-induced protein aggregation. **Chapter V** focuses on the effect of surface active formulation additives on the interfacial film composition and the physicochemical behavior of the film. The surface sensitive analytical techniques established

before can be used to identify the minimal additive concentration to prevent aggregation. The surfactant concentration should be kept low to reduce negative effect of impurities or oxidative degradation products on protein stability.

In **Chapter VI** the focus was set on the impact of pH and ionic strength on the liquid-air interfacial protein behavior and the protein aggregation process. The charge and charge shielding conditions influence both the colloidal and the conformational stability of a protein formulation. The effect of formulation pH and ionic strength on conformational stability and interfacial film characteristics was addressed in **part 1** of this chapter. The impact of pH and ionic on the colloidal stability in terms of protein aggregation were to be investigated in **part 2**. For this purpose, the protein-protein interaction parameter A_2^* was used as a measure for intermolecular interactions and contextualized to the aggregation rate determined in bulk solution. The combination of these different aspects should enable a clearer mechanistic understanding and formulation strategy.

Overall, this thesis is intended to highlight the complex background of liquid-air interface related protein aggregation. Understanding of the underlying mechanisms will help to improve formulation development, thereby aiming on an increased stability of protein pharmaceuticals which is of great interest for the pharmaceutical industry as well as for each patient.

CHAPTER III

THE FILM TELLS THE STORY: PHYSICOCHEMICAL CHARACTERISTICS OF IGG AT THE LIQUID-AIR INTERFACE

1. ABSTRACT

The presence of liquid-air interfaces in protein pharmaceuticals is known to negatively impact product stability. Nevertheless, the mechanisms behind interface-related protein aggregation are not yet fully understood. Little is known about the physical-chemical behavior of proteins adsorbed to the interface. Therefore, the combinatorial use of appropriate surface-sensitive analytical methods such as Langmuir trough experiments, Infrared Reflection-Absorption Spectroscopy (IRRAS), Brewster Angle Microscopy (BAM), and Atomic Force Microscopy (AFM) is highly expedient to uncover structures and events at the liquid-air interface directly. Concentration-dependent adsorption of a human immunoglobulin G (IgG) and characteristic surface-pressure /area isotherms substantiated the amphiphilic nature of the protein molecules as well as the formation of a compressible protein film at the liquid-air interface. Upon compression, the IgG molecules do not readily desorb but form a highly compressible interfacial film. IRRAS spectra proved not only the presence of the protein at the interface, but also showed that the secondary structure does not change considerably during adsorption or compression. IRRAS experiments at different angles of incidence indicated that the film thickness and/or packing density increases upon compression. Furthermore, BAM images exposed the presence of a coherent but heterogeneous distribution of the protein at the interface. Topographical differences within the protein film after adsorption, compression and decompression were revealed using underwater AFM.

The combinatorial use of physical-chemical, spectroscopic and microscopic methods provided useful insights into the liquid-air interfacial protein behavior and revealed the formation of a continuous but inhomogeneous film of native-like protein molecules whose topographical appearance is affected by compressive forces.

2. INTRODUCTION

Protein pharmaceuticals are among the fastest growing and most important molecules in diagnostics and therapy, and therefore are of significant importance in high-impact areas such as autoimmune diseases and cancer [1]. The large size, the compositional variety and the distinct three-dimensional structure of protein molecules are causal for their sensitivity to undergo degradation processes.

Proteins undergo both chemical and physical degradation such as oxidation and hydrolysis, denaturation and aggregation [2]. Whereas a chemical instability reaction leads to a change in the primary structure of the protein, physical instability reactions result in a change of the spatial arrangement of the protein structure, without modification of covalent bonds. The immunogenic potential of protein pharmaceuticals is directly related to the emergence of aggregates [3]. So, the maintenance of the native conformation is essential for both the efficacy, as well as the safety of a protein drug [4]–[7].

Protein aggregation is highly undesirable due to the profound impact on the stability of the drug product, which can result in a loss of activity and unwanted immunogenic responses. In order to control protein aggregation, it is important to understand the underlying mechanisms. The fundamentals of protein aggregation were first described in the 1960s by the Lumry–Eyring model and are continually developed further [8]–[11].

Under physiological conditions, the three-dimensional structure of a protein represents an equilibrium between native and denatured (unfolded) states [8], [12]–[14]. Exogenous influences during production, storage and transportation can lead to a shift in this balance. In the unfolded state, hydrophobic patches, usually buried in the core, can be exposed to the outside of the molecule, and therefore the denatured proteins are more prone to aggregation. The protein aggregates can be soluble or insoluble in nature, can be composed of covalent and non-covalent bonds, and can be reversible or irreversible [15]. Moreover, not only (partially) unfolded, but also native conformations are involved in the formation of aggregates [16]. In particular, the formation of so-called “large native-like” particles often occurs spontaneously, and no continuous pathway from monomer to dimer and then to large particles can be observed [10]. For instance, a self-association of native protein molecules has been reported for highly concentrated protein solutions as a result of macromolecular crowding-effects [17].

The propensity of protein molecules to accumulate and therefore concentrate at phase boundaries (e.g. solid-liquid, liquid-liquid, and liquid-air) plays an important role in several technological processes, for example during manufacturing and storage of protein pharmaceuticals. The migration of proteins from a bulk phase to an interface is similar to the adsorption process of small amphiphilic solutes, e.g. surfactants. A major distinction, however, is that a small surfactant molecule contains a defined hydrophilic head and hydrophobic tail that can easily partition towards the aqueous and non-aqueous regions of the interface, respectively. Such straightforward partitioning is not possible in the case of proteins. While most of the hydrophilic residues in the tertiary structure of proteins are exposed on the surface, not all hydrophobic residues are buried in the interior and some of them are exposed on the surface what finally imparts amphiphilicity to protein molecules [18]. Therefore, protein molecules adsorb to the liquid-air interface and thereby do not only lower interfacial tension but also form continuous gel-like films of highly concentrated protein via mainly non-covalent interactions [19], [20]. The substantial differences in the surface activity of various proteins must be therefore related to their physical, chemical and conformational properties. Apart from intrinsic molecular factors, surface activity is also dictated by several extrinsic factors, such as pH, ionic strength, temperature or presence of other solution components such as sugars or surfactants. In addition to that, the molecular size of globular proteins affects their adsorption to the liquid-air interface [21], [22].

Interfacial protein gelation and film formation has been identified as important trigger for the aggregation of protein pharmaceuticals [23]–[27]. For instance, adsorption of proteins to silicone oil, such as in prefilled syringes, can enhance protein aggregation [28]. Moreover, particle shedding from silicone tubings in peristaltic dosing pumps has to be considered [29]. Protein aggregation is also known to occur under different mechanical stress conditions, such as shaking [30], [31]. Eliminating the liquid-air interface by removing the headspace in vials prevents agitation-induced aggregation as shown by Kiese *et al.* [32]. Furthermore, several studies suggest a clear connection between the disruption of the highly concentrated protein layer at the liquid-air interface and the occurrence of protein particles in the bulk solution [33], [34]. Choosing appropriate formulation conditions, such as pH, ionic strength and additives (e.g. non-ionic surfactants), can stabilize proteins in pharmaceutical parenteral products against adsorption at surfaces and interface-induced aggregation [35]–[38].

In this study, different surface-sensitive analytical methods were applied for the characterization of important functional properties, such as adsorption, compressibility, as well as structural and topographical features of interfacial protein films. The combinatorial use of different physical-chemical methods enables comprehensive insights into the protein behavior at the interface. These new findings will not only help to understand how protein stability is affected by the events happening at the interface, but also to identify and localize liquid-air interface related mechanisms of aggregation. Examination of particle formation by liquid-air interfacial stress only is not the subject of this study, but was addressed in separate investigations which are to be published soon.

3. MATERIALS AND METHODS

3.1. Materials

Human IgG (Beriglobin™, CSL Behring GmbH, Germany) was used for this study. The market product contains 159 mg/mL human IgG in 22 g/L Glycine and 3 g/L NaCl buffer at pH 6.8. Glycine-NaCl buffer was prepared using highly purified water (ELGA LC134, ELGA LabWater, Germany) and pH was adjusted adding NaOH. All diluted solutions were prepared by the addition of Glycine-NaCl buffer at pH 6.8 to the human IgG stock solution followed by filtration using 0.2 µm sterile PES filters (Sterile Syringe Filter PES, VWR, Germany).

3.2. Surface Pressure Measurements

Surface activity was expressed by surface pressure Π , with $\Pi = \sigma_0 - \sigma$, where σ_0 and σ are the aqueous subphase surface tension and the surface tension of the aqueous protein solution, respectively. Surface pressure measurements were performed in a 5.9 x 39.7 cm² PTFE Langmuir trough equipped with a metal alloy dyne probe (Microtrough XS, Kibron Inc., Finland). For the determination of equilibrium surface pressures, a 3 x 6 Multiwell Plate (V = 0.8 mL) was used. Results are given as mean (n=3) and standard deviation. Equilibrium adsorption pressure is defined as the maximum surface pressure that is reached by adsorption only and stable in a range of +/-0.2mN/m within 0.5 h.

160 mL sample solution was filled into the trough for the repeated compression-decompression measurements. The surface area of the trough can be varied by two mobile PTFE barriers. Temperature was kept at 20 °C (K6-cc circulation thermostat, Peter Huber Kaeltemaschinenbau GmbH, Germany). Compression speed was set to 55 mm/min and compression-decompression cycles were conducted from a maximum surface area of $A_{\max} = 210 \text{ cm}^2$ to $A_{\min} = 52 \text{ cm}^2$. Compression was started after the equilibrium adsorption pressure was reached.

3.3. FT-IR Spectroscopy

For FT-IR measurements spectra were recorded using a Tensor 27 (Bruker Optics GmbH, Germany) connected to a thermostat (DC30-K20, Thermo Haake GmbH, Germany). For each measurement, the protein was formulated at 10 mg/mL in Glycine-NaCl buffer pH 6.8, and for each spectrum 100 absorbance scans were collected at a single beam mode with a resolution of 4 cm⁻¹. Spectra were analyzed by Opus 7.5 (Bruker Optics GmbH) and displayed as vector-normalized second-derivative spectra (calculated with 17 smoothing points according to the Savitzky-Golay algorithms [39]). Infrared spectra of the protein in solution were recorded using an AquaSpec (transmission cell H₂O A741-1) and BioATR (Attenuated Total Reflectance) cell™ II or BioATR (Attenuated Total Reflection) respectively, at 20 °C.

Infrared spectra of the temperature-induced unfolding of the IgG samples were conducted using the BioATR cell, as this sample cell can analyze protein samples either in solution or in suspension. Reference spectra were recorded under identical conditions with only the buffer (Glycine-NaCl buffer pH 6.8) in the cell. Temperature-dependent spectra were acquired every 4 °C from 25 – 93 °C with an equilibration time of 120 s. Recorded infrared spectra were analyzed by Protein Dynamics for Opus 7.5.

3.4. Infrared Reflection-Absorption Spectroscopy (IRRAS)

IRRAS was used to determine the presence and the conformation of the adsorbed protein at the soft liquid/air interface. IRRAS spectra were recorded using a VERTEX FT-IR spectrometer (Bruker Optics GmbH, Germany) equipped with a liquid nitrogen-cooled MCT (mercury cadmium telluride) detector. The spectrometer was coupled to a Langmuir trough (Riegler & Kirstein GmbH, Germany), placed in a sealed container (external air/water reflection unit XA-511) to guarantee constant vapor atmosphere. The IR beam was conducted out of the spectrometer and focused onto the water surface of the Langmuir trough. A computer controlled KRS-5 wire-grid polarizer (thallium bromide and iodide mixed crystal) was used to generate perpendicular (s) and parallel (p) polarized light. The angle of incidence was set to 40° with respect to the surface normal. Measurements were performed using a trough with two compartments and a trough shuttle system [40]–[42]. One compartment contained the protein solution under investigation (sample), and the other (reference) was filled with the pure buffer sub phase. The single-beam reflectance spectrum (R_0) from the reference trough was taken as background for the single-beam reflectance spectrum (R) of the monolayer in

the sample trough to calculate the reflection-absorption spectrum as $-\log(R/R_0)$ in order to eliminate the water vapor signal. IR spectra were collected at 8 cm^{-1} resolution and a scanner speed of 20 kHz. For s-polarized light, spectra were co-added over 200 scans, and spectra with p-polarized light were co-added over 400 scans. To distinguish between the influence of increasing concentration and changed orientation on the signal intensity, the dichroic ratio DR of the amide I band at 1643 cm^{-1} was calculated as $DR = A_p/A_s$, with A_s and A_p being the maximum absorption obtained with s-polarized light and p-polarized light, respectively.

For the determination of the interfacial film thickness in equilibrium and after compression to 30 mN/m, the incidence angle of the IR beam was varied with respect to the surface normal between 30° and 72° in steps of 2° or 3° . IRRAS spectra were simulated using a MATLAB program [43], [44] on the basis of the optical model of Kuzmin and Mikhailov [45], [46]. The intensity and shape of a reflection-absorption band depend on the absorption coefficient k , the full-width of half-height (fwhh), the orientation of the transition dipole moment (TDM) within the molecule α , the molecular tilt angle θ , the polarization and the angle of incidence (AoI) of the incoming light, as well as the layer thickness d and its refractive index n . Simulated spectra were fitted to the experimental data in a global fit, where all spectra recorded at different AoI and different polarizations were fitted in one non-linear least square minimization using the Levenberg-Marquardt algorithm. The polarizer quality was set to $\Gamma = 0.01$. The optical constants of the water sub phase were taken from Bertie et al. [47], [48]. The layer thickness d was determined from a fit of the OH stretching vibrational band ($\nu(\text{OH})$) in the range of $3800\text{--}3000\text{ cm}^{-1}$. Additional experimental details are described elsewhere [49]–[52].

3.5. Brewster Angle Microscopy (BAM)

The morphology of the monolayer was imaged with a Brewster angle microscope, BAM2plus from NanoFilm Technologie GmbH (Goettingen, Germany), equipped with a miniature film balance from NIMA Technology (Coventry, UK). IgG at 1 mg/mL in Glycine-NaCl buffer at pH 6.8 was filled into the trough ($V = 80$ mL). Simultaneous surface pressure measurements during adsorption and compression of the IgG in the Langmuir trough enabled a direct connection of each image with the corresponding surface pressure during adsorption or compression of the protein. The lateral resolution of the BAM was approximately $3\text{ }\mu\text{m}$. The size of the BAM images is $400 \times 720\text{ }\mu\text{m}^2$. Detailed information about the BAM method is given elsewhere [53]–[55].

3.6. Atomic Force Microscopy (AFM)

For AFM, protein films formed during adsorption to equilibrium adsorption pressure or after compression to a desired surface pressure, were transferred by the Langmuir-Schaefer deposition (horizontal transfer of the film) using $1 \times 1\text{ cm}^2$ mica plates (Mica Sheet V5 Quality, Science Services GmbH, Germany) attached to a stamp tool. The mica was lowered onto the surface and pulled off after 2 s of contact time. The mica was removed from the stamp tool and the transferred film was covered with a drop of buffer solution to prevent drying of the sample. The transferred films were analyzed by underwater AFM (Bruker / Veeco / Digital Instruments MultiMode AFM) using a cantilever (Arrow™ NCpt, resonance frequency 285 kHz, spring constant 42 N/m) in tapping mode (Nano World AG, Switzerland). Images were analyzed by NanoScope III 5.12r3 Software (Digital Instruments Inc., US).

For the determination of interfacial film thickness, the film was transferred onto silica by Langmuir-Schaefer technique. A scratch was made using stainless steel tweezers. Film thickness was determined by section analysis from an average of 6 measuring points from the silica substrate to the film (area unaffected by the scratch).

4. RESULTS AND DISCUSSION

4.1. Time & Concentration Dependent Adsorption of IgG

Surface pressure measurements were performed to investigate the adsorption kinetics of the IgG from bulk solution to the liquid-air interface. IgG reveals a pronounced surface activity as shown in Figure 1a. IgG in a concentration 0.01 mg/mL reaches surface pressure values of 6.7 mN/m after 300 min, whereas IgG in a concentration of 0.5 mg/mL reaches an equilibrium surface pressure value of 18.2 mN/m after about 270 min. In case of a 1 mg/mL IgG solution, the equilibrium adsorption pressure is only slightly higher (18.5 mN/m after 240 min). Although the adsorption of globular proteins such as IgG starts immediately, equilibrium adsorption pressures are reached only after several hours and depend on the protein itself and on the formulation conditions [21], [22], [56]. Adsorption of small surfactants, such as polysorbate 20 or 80, is much faster, and equilibrium adsorption pressure values are reached within less than 30 min due to the distinct amphiphilic character and the low molecular weight [18], [36], [57].

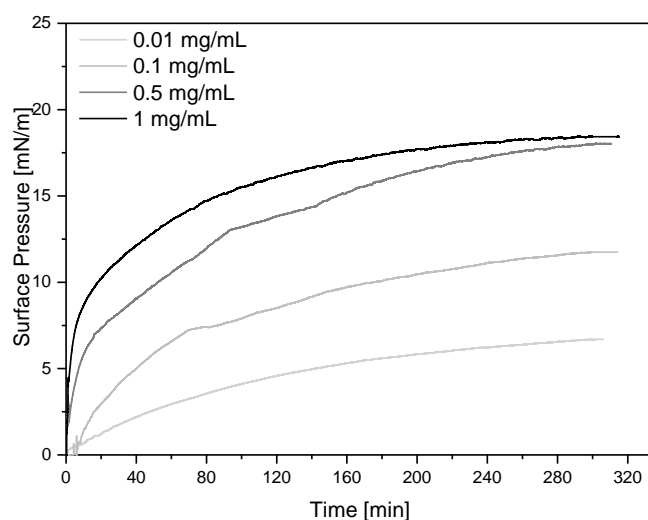


Figure 1a: Time-dependent adsorption of IgG using different bulk concentrations

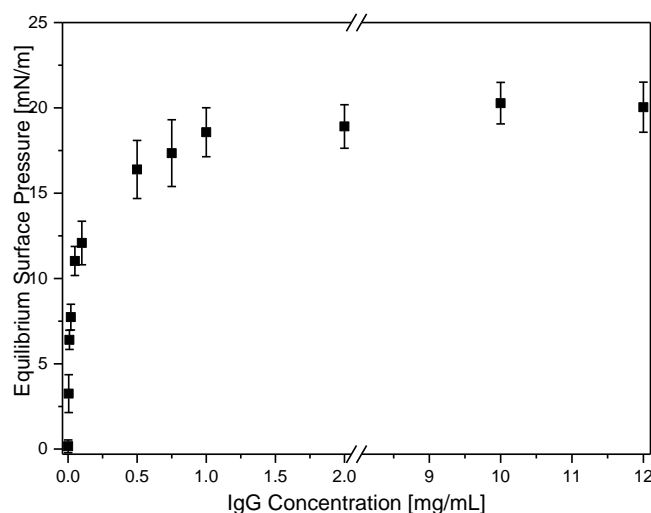


Figure 1b: Concentration-dependent equilibrium adsorption pressure of IgG

Figure 1b shows the concentration-dependent equilibrium adsorption pressure using protein concentrations of 0.001 mg/mL up to 12 mg/mL IgG. At low IgG concentrations in the range from 0.01 mg/mL to 0.1 mg/mL, the concentration-dependent change in surface pressure is pronounced, whereas concentrations ≥ 1 mg/mL do not lead to any further considerable increase in equilibrium adsorption pressure. Therefore, for further experiments a concentration of 1 mg/mL was considered to be adequate. This correlation between protein concentration and equilibrium adsorption pressure can be interpreted in terms of the surface coverage [16], [31]. At protein concentrations ≥ 1 mg/mL IgG, the protein molecules may form multilayers, but these structures do not contribute significantly to the surface pressure [59]. Moreover, a highly viscous protein film is formed, which can be deformed by lifting and lowering the dyne probe (Fig. 2) and is caused by mainly non-covalent interactions of the highly concentrated protein layer at the liquid-air interface [60], [61].

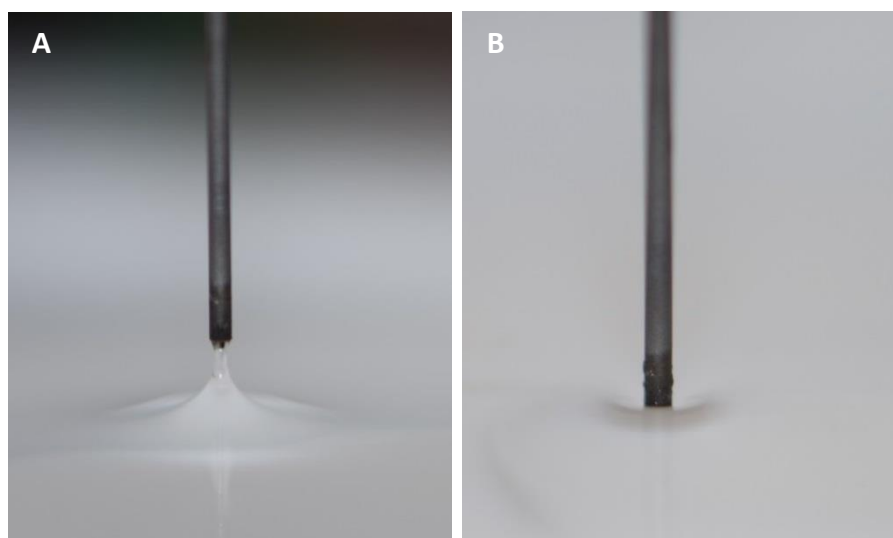


Figure 2: IgG film at equilibrium adsorption pressure deformed by lifting (A) or lowering (B) the dyne probe

4.2. Repeated Compression-Decompression of Interfacial IgG Films

Repeated compression-decompression was performed to investigate the physical resistance of the IgG film at the liquid-air interface. Controlled compression and decompression ensure that mechanical stress is applied to the interfacial IgG film only, while simultaneously the surface pressure is recorded. Movement of the barriers from maximum surface area (A_{\max}) towards the minimum surface area (A_{\min}) results in an increase in surface pressure from the equilibrium adsorption pressure of 18.5 mN/m up to 52 mN/m (Fig. 3). The change in surface pressure upon compression of the film is 33.5 mN/m after the first cycle and does not noticeably change with the following cycles. During the first compression, the slope between 210 cm² (A_{\max}) and 140 cm² is much lower compared to the slope of the isotherm between 120 cm² and $A_{\min} = 52$ cm² (A_{\min}). This indicates a drastic change in compressibility of the protein film. Upon decompression, the surface pressure decreases strongly between 52 cm² and 70 cm², whereas the slope of the isotherm is low between 80 cm² and A_{\max} . Curve progression is nearly identical for each cycle with a slight decrease in the surface pressure at A_{\max} in each cycle. The compression of the film causes a compaction of the proteins connected with a decrease in molecular area modifying the ordering of the protein molecules and the distribution across the interface [62]. This can be connected with an increase in film thickness and/or changes in molecule orientation [63]. Moreover, the surface pressure increase demonstrates that the protein molecules stay at the interface

upon compression. This non-equilibrium between adsorption and desorption can be traced back to the formation of a viscoelastic film where in addition to hydrophobic interactions, hydrogen bonds also contribute substantially to the molecular association [64].

The steep decrease in the initial phase of decompression (between 52 cm² (A_{\min}) and 70 cm²) can be explained by a short-term rupture of the film followed by re-adsorption or re-spreading of protein molecules at the interface, ending in a quasi-equilibrium surface pressure when decompression is completed. Based on the decrease in surface pressure after each cycle compared to the initial value a loss of material from the interface can be assumed [33]. The high compressibility and the appearance of a considerable hysteresis upon compression and decompression substantiate the formation of a viscous protein network at the interface which is in accordance with the film deformation as shown in figure 2. The hysteresis indicates that the protein does not desorb upon compression and that the interfacial film undergoes physical changes during compression and decompression [41], [42], [43].

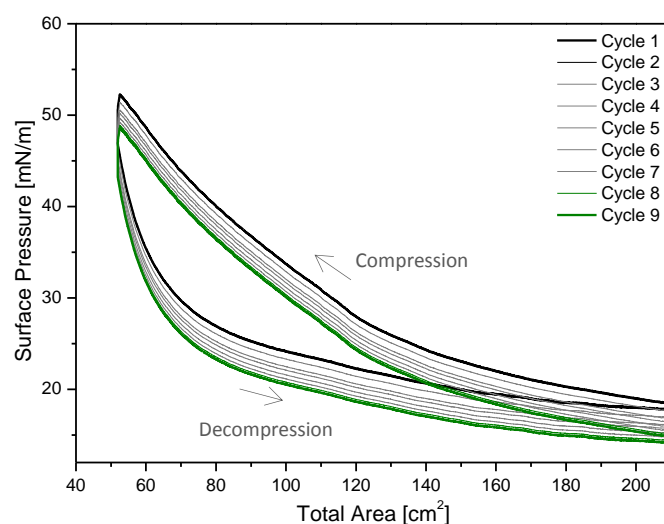


Figure 3: Compression-decompression cycles of IgG in the Langmuir Trough. Compression starts at A_{\max} at equilibrium (18.5 mN/m) adsorption pressure and ends at A_{\min} . Decompression starts at A_{\min} and ends at A_{\max}

4.3. Temperature-Induced Unfolding of IgG

To determine possible changes in the secondary structure, FT-IR spectra were recorded upon heating. The melting temperature (T_m) of IgG was identified to be 72 °C using micro calorimetry [67]. By increasing the temperature above T_m , changes in the secondary structure occurred indicated by changes in the amide I modes (Fig. 4). Starting the temperature ramp, IgG exhibited the amide I band maximum at 1639 cm^{-1} characteristic for intramolecular β -sheet structures (Tab. 1). Additionally, bands with wavenumbers centered around 1620 cm^{-1} and 1690 cm^{-1} assignable to extended strands and to weak intramolecular β -sheet or turns, respectively, can be identified.

Elevation of the temperature resulted in the following spectral changes: the amide I absorbance maximum around 1639 cm^{-1} decreased accompanied by an intensity increase at 1625 cm^{-1} . Additionally, a peak shift from 1690 cm^{-1} to 1695 cm^{-1} occurred representing a shift to intermolecular β -sheet structures. The loss of the native intramolecular β -sheet structure towards a more unordered structure with distinctive bands of intermolecular β -sheet structures (1625 cm^{-1} and 1695 cm^{-1}) is in accordance with the results obtained by Matheus *et al.* [68]. In addition to the formation of intermolecular antiparallel β -sheet structures indicated by peak shifts, the presence of new protein interactions after heating resulted in gel formation of the cooled samples, which is characteristic for extensive intermolecular interactions in protein samples [69].

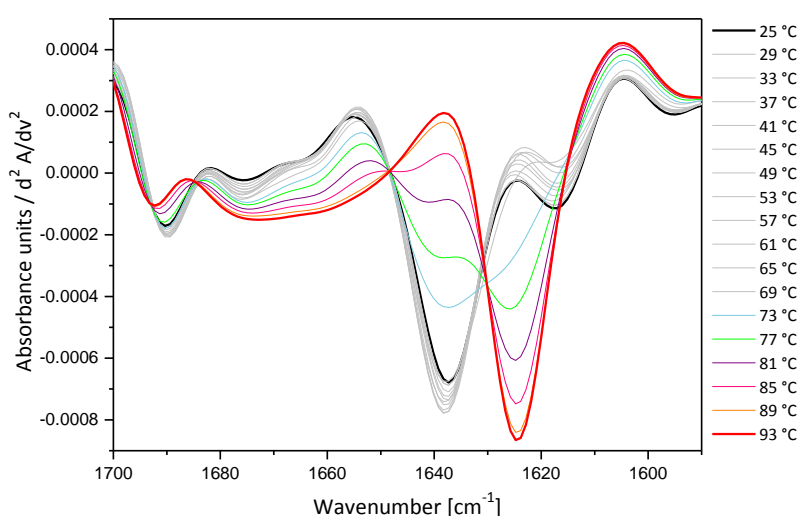


Figure 4: Temperature-induced unfolding of IgG [10 mg/mL in Glycine-NaCl pH 6.8] between 25 °C and 93 °C in steps of 4 °C using FT-IR spectroscopy (BioATR)

4.4. Presence and Secondary Structure of IgG at the Interface

The presence of the IgG at the liquid-air interface can be confirmed by IRRAS measurements. Furthermore, a comparative analysis of secondary structure elements of the IgG in solution and at the interface enables conclusions whether the adsorption to the interface and the compression of the adsorbed protein film cause conformational changes.

The appearance of the water band and the amide A, I and II bands prove the formation of a IgG adsorption layer at the interface. The amide I band is associated mostly with the C=O stretching vibration, and the amide II band results from in-plane NH-bending and CH-stretching vibrations. The amide A band is due to N-H stretching vibration. This vibrational mode does not depend on the backbone conformation but is very sensitive to the strength of hydrogen bonds. Wavenumbers between 3225cm^{-1} and 3280 cm^{-1} have been found for hydrogen bond lengths between 2.69 \AA and 2.85 \AA [70]. The intensity of the bands increases during the adsorption process and also upon compression to surface pressure values above the equilibrium adsorption pressure (Figs. 5 and 6). The intensity of the OH-band around 3600 cm^{-1} is directly connected with the effective adsorption-layer thickness, because the intensity of the water band in the spectrum of the sample trough is reduced in comparison to the one from the reference trough since the protein adsorption layer replaces a water layer of the same thickness [71]. Therefore the increasing intensity of the bands refers to an increasing interfacial protein concentration, film thickness and/or packing density within the film [43], [72]. These results are consistent with the surface pressure measurements, where compression caused a significant increase in surface pressure due to an interfacial compaction of protein material and/or change in molecule orientation.

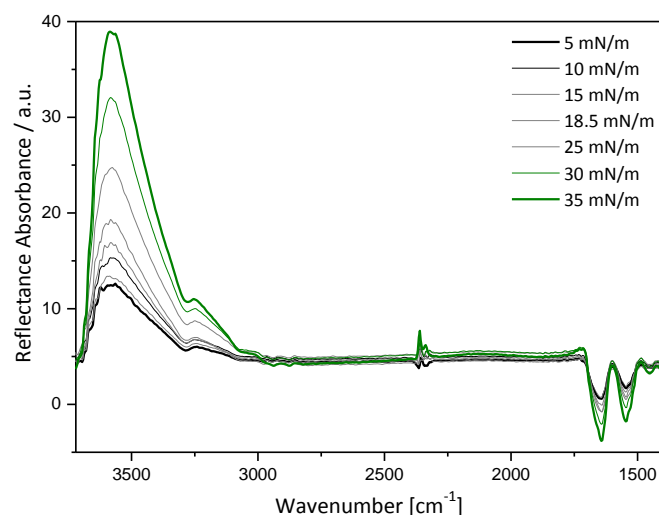


Figure 5: IRRA spectra of IgG with increasing surface pressure (s-polarized light, $A_{ol} = 40^\circ$)

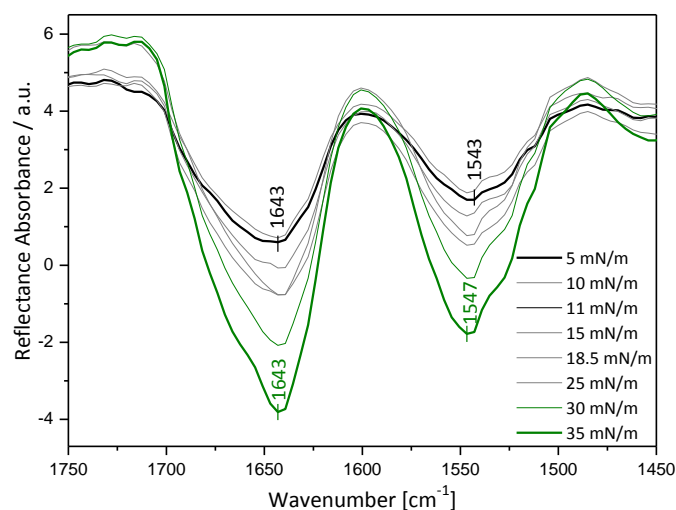


Figure 6: IRRA spectra in the amide I and II regions of IgG with increasing surface pressure (s-polarized light, $A_{ol} = 40^\circ$)

With increasing surface pressure, the intensity of the amide bands increases. The maximum of the amide I band is observed at 1643 cm^{-1} and in the amide II region at $\sim 1543 \text{ cm}^{-1}$ (Fig. 6). The IRRA spectra indicates an intramolecular β -sheet or unordered random coil conformation of the IgG at the interface [73]. The position of the amide I band does not change with increasing surface pressure indicating that the secondary structure of the adsorbed IgG changes neither during adsorption nor during compression.

Figure 7 shows the FT-IR spectrum of the native IgG in solution using the AquaSpec and the BioATR measurement cell, respectively. The band positions of the transmission as well as of the attenuated total reflection (ATR) spectrum can be assigned to a mostly intramolecular β -sheet structure of the IgG in solution. Comparison of the two spectra reveals slight differences in the band positions with 1639cm^{-1} for the AquaSpec, and 1636 cm^{-1} for the BioATR cell. This can be explained by the different measurement techniques as the AquaSpec records transmission spectra of the aqueous protein solution, and the BioATR measures reflectance spectra of a protein film at the silicon crystal. Nevertheless, both measurement principles lead to fairly identical structural elements for the IgG. The position of the bands determined in FT-IR spectra (1639 cm^{-1} or 1636 cm^{-1}) and IRRA spectra (1643 cm^{-1}) differs only marginally. The peaks of the IRRA spectra are broader compared to the FT-IR peaks. This can be explained by the higher resolution of the FT-IR and/or can be due to a peak overlapping within the amide I region of the IRRA spectra, containing not only the band at 1639 cm^{-1} but additional bands beside the band at 1690 cm^{-1} , which is also present in the FT-IR spectrum, reflecting an intramolecular β -sheet structure.

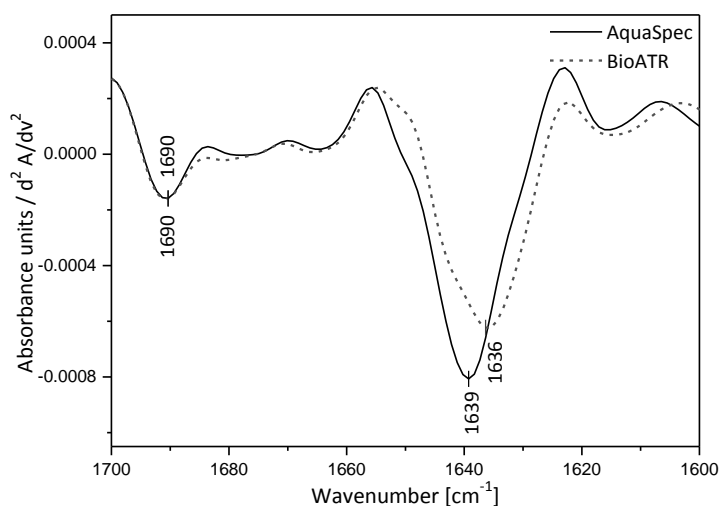


Figure 7: Comparative FT-IR spectra of IgG in solution (AquaSpec vs. BioATR)

Unlike the conformational changes of the IgG induced by heat stress (Fig. 4), where strong peak shifts from the native intramolecular β -sheet structure at 1639 cm^{-1} towards a more unordered structure with a distinctive band of intermolecular β -sheet structure at 1625 cm^{-1} were observed, the adsorption of the IgG to the interface does not induce considerable conformational changes. As no other peaks referring to new structural elements appear, the IgG predominantly retains its native structure during adsorption as well as during compression.

The increase in the intensity of the IRRA bands as well as the increase in surface pressure upon compression can be attributed to an increase in the adsorbed protein amount either due to an increase in film thickness or to changes in the molecule orientation allowing higher packing densities. In order to discriminate between those two effects, the dichroic ratio (DR) was calculated. In figure 8, the DR values at 1643 cm^{-1} are plotted as a function of surface pressure at two different IgG concentrations. No change in DR is observed during adsorption or compression, therefore the molecule orientation does not change with increasing surface pressure. Hence, the increase in surface pressure upon compression and the increase in the intensity of the IRRA bands can be solely explained by an increase in packing density and/or film thickness.

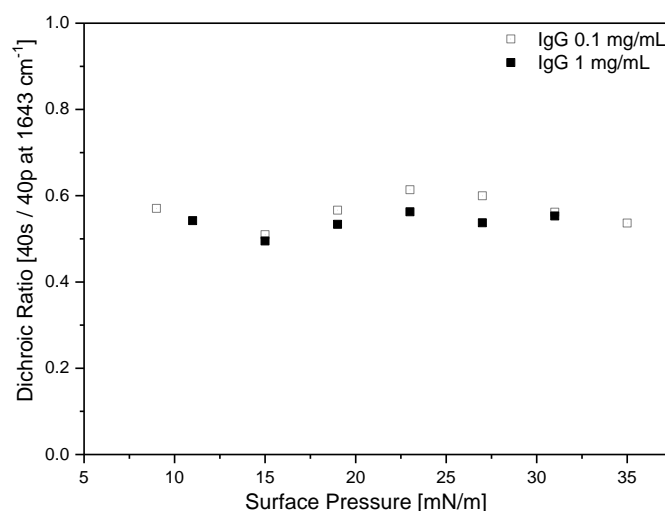


Figure 8: Dichroic Ratio of amide I at 1643 cm^{-1} (p/s-polarized light, $A_{ol} = 40^\circ$) as a function of surface pressure at two different IgG concentrations

4.5. Structural and Morphological Characterization of the Liquid-Air Interfacial Film

BAM was used to visualize the liquid-air interfacial protein film. At the Brewster angle, p-polarized light is not reflected, and the bare buffer surface appears dark. In the case of protein adsorption, the Brewster condition is altered by the presence of the protein film with a different refractive index, indicated by an overall increased brightness as a part of the incident light is reflected (Fig. 9). Areas which appear dark in the BAM images are formed by a thinner but homogeneous film compared to brighter areas. Although the protein covers the entire interface, flickering domains are present immediately as adsorption starts representing differences in packing density. During adsorption, the surface appearance does not change. Moreover, even compression of the film does not affect the BAM images. Areas of increased brightness represent areas of increased packing density and film thickness [60], [74]. The island-like structures demonstrate that the protein is not homogeneously distributed across the interface.

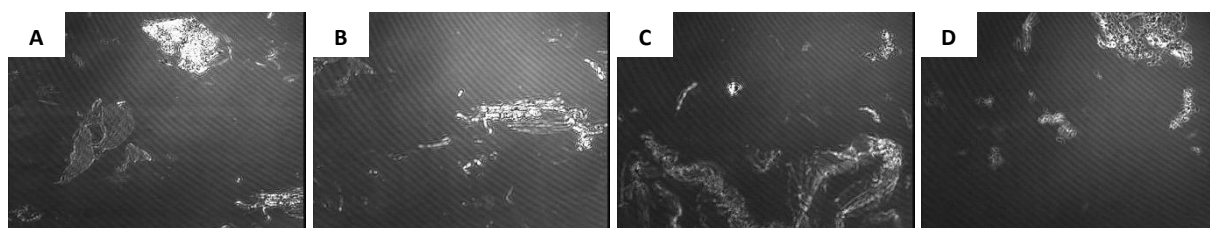


Figure 9: BAM images of IgG during adsorption (A: $\pi = 6.2$ mN/m, B: $\pi = 18.5$ mN/m) and compression (C: $\pi = 25.0$ mN/m, D: $\pi = 35.0$ mN/m)

4.6. Changes in Film Topography Caused by Compression

Underwater Atomic Force Microscopy (AFM) was used to further elucidate the topographical properties of the interfacial protein film on a different scale compared to BAM. The film deposited after adsorption to equilibrium surface pressure confirms the presence of the IgG at the interface (Fig. 10 A). Individual IgG molecules cannot be detected due to the flattening effect during AFM measurements in liquid medium [75]. Nevertheless, as in the BAM images, an inhomogeneous distribution of the protein after adsorption can be confirmed. Bright areas in the deflection image are considered to be protein material that protrudes

above the protein layer with a height of 15 nm. The determined film roughness of 1.0 nm after adsorption is in accordance with literature values for other globular proteins [15], [49]. Upon compression, areas of telescoped material appear (Fig. 10 B) wherein the protein film forms wrinkles that protrude with a height of 18 nm from the remaining part of the compact film. However, a recent study by Ghazvini *et al.* [77] described similar findings for a dried film of an IgG₁ after compression. The presence of those areas of increased film thickness after compression can be explained as follows: compression first increases the packing density in the adsorption layer leading to an increase in surface pressure and the OH- and amide-bands intensities in the IRRA spectra. Some material will be partially excluded from the well-packed film into the subphase during compression.

After decompression, the areas of telescoped material cannot be recognized any more (Fig. 10 C). Thus, decompression results in a decrease of the overall height of the interfacial film, a steep decrease in surface pressure as well as a decrease in surface pressure after each compression-decompression cycle. This can be traced back to a loss of material from the interface [33], [34], [77].

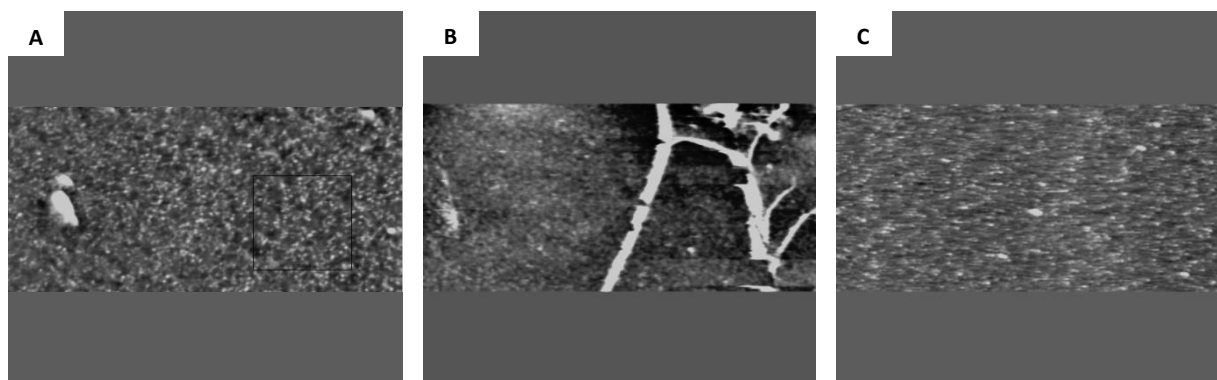


Figure 10: Underwater AFM images in tapping mode (image size: $10 \times 10 \mu\text{m}^2$) of IgG after adsorption to equilibrium surface pressure (A: 18.5 mN/m), compression (B: 30 mN/m) and after decompression of the film

4.7. Interfacial Film Thickness in Equilibrium and after Compression

Interfacial film thickness of the IgG film in equilibrium at 18.5 mN/m and after compression to 30 mN/m was determined by angle-dependent Infrared Reflection Absorption Spectroscopy (IRRAS) measurements and compared to the values obtained by underwater AFM of the films after Langmuir-Schaefer transfer.

The increase in the intensity of the OH-stretching vibration around 3600 cm^{-1} indicates an increase in film thickness upon compression. The two types of polarized light (s and p) have dramatically different reflectivity properties around the Brewster angle ($\sim 53.1^\circ$) with a minimized intensity of the reflected p-polarized light. As shown in figure 11, the reflectance-absorbance (RA) in the region of the OH-stretching vibration changes continuously for s-polarized light as a function of the angle of incidence (Aoi), whereas RA of p-polarized light exhibits a discontinuity around the Brewster angle. The IRRAS spectra taken with p- and s-polarized light have been compared with the corresponding simulated spectra with the OH-stretching vibration $\nu(\text{OH})$ and the amide A band (Fig. 11).

In figure 12, the maxima of the RA intensities of experimental and simulated spectra at different Aoi have been compared. The best fit of the simulated to the experimental data allows the determination of the layer thickness, assuming a refractive index of the protein layer. The presented simulation is based on a refractive index (n) of the protein solution using experimental data. As the refractive index n of the protein solution directly depends on the concentration and packing density, it was set to 1.45 in the adsorption layer at equilibrium with a linearly increasing increment of 0.024 depending on the protein concentration. Therefore, the calculated interfacial film thickness after adsorption to an equilibrium surface pressure amounted to 1.97 nm and increases upon compression to 2.61 nm. Since in the compressed protein layer the concentration is larger, a larger refractive index (1.49) has been used in a second fit.

Moreover, as the secondary structure does not considerably change either during adsorption or during compression, the tertiary structure of the protein could be affected upon adsorption and contribute to a lower interfacial film thickness compared to the dimensions of the molecule in bulk solution. Comparison of the RA intensities in equilibrium to the ones after compression shows a clear increase in the RA intensity of the OH band (see Fig. 12).

Figure 13 shows the AFM images with a scratch of the film in equilibrium and after compression to 30 mN/m. Comparable to fig. 10, the images display a coherent film containing some areas of increased height representing agglomerated protein material (Figs. 13 A + B). Compression caused wrinkling and the formation of a telescoped protein film (Figs. 13 C + D). Section analysis of the AFM height measurements resulted in a mean film thickness of (6.41 ± 2.05) nm in equilibrium and of (5.56 ± 2.94) nm after compression.

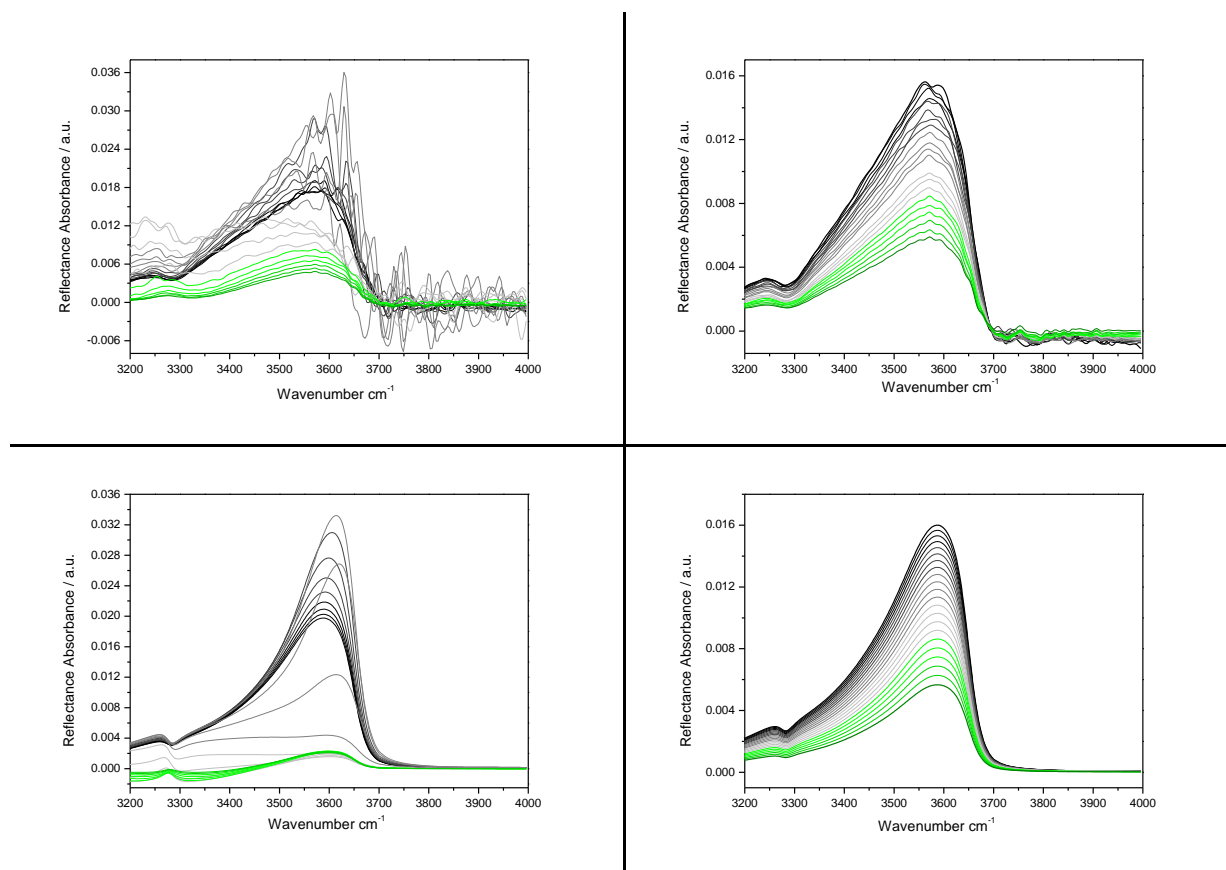


Figure 11: IRRA spectra of the OH-stretching vibration and the amide A band of IgG in equilibrium at 18.5 mN/m at different angles of incidence (AoI) from 30° – 72° (from black via grey to green) in steps of 2°, top: experimental spectra (left: p-polarized light, right: s-polarized light), bottom: the corresponding simulated IRRA spectra

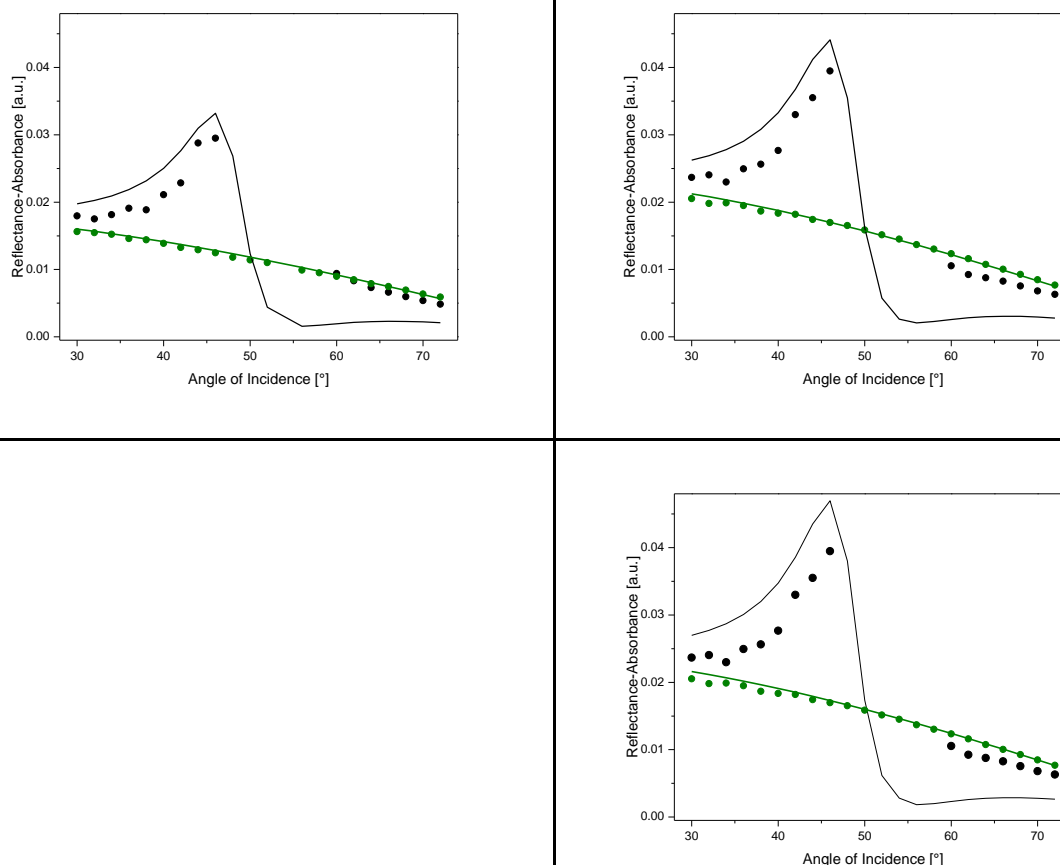


Figure 12: Experimental (dots) and simulated (solid lines) RA intensities using p-polarized (black) and s-polarized (green) light at the maximum position of the OH-stretching vibration. Top left: data obtained at the equilibrium surface pressure, top right: data after compression to 30 mN/m. Top row: a refractive index of 1.45 has been taken for the equilibrium as well as for the compressed layer. Bottom row: An increased refractive index of 1.49 has been taken for the compressed film

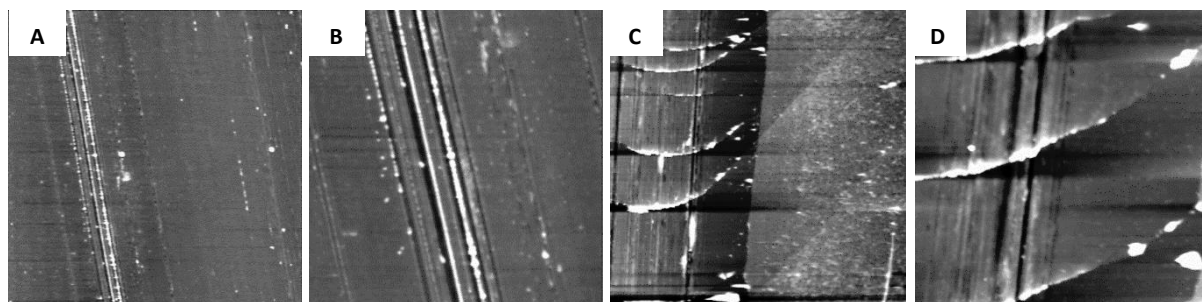


Figure 13: Underwater AFM images incl. scratch for determination of film thickness in tapping mode (image size: A + C: 30 x 30 μm^2 , B + D: 10 x 10 μm^2) of IgG after adsorption to equilibrium surface pressure (A and B: 18.5 mN/m) and after compression (C and D: 30 mN/m)

5. SUMMARY & CONCLUSION

The use of a Langmuir film balance in combination with IRRAS, BAM and AFM is a novel approach for the characterization of films formed by protein biopharmaceuticals at the liquid-air interface. The IgG investigated in this study shows a pronounced amphiphilic behavior. It adsorbs to the liquid-air interface in a time- and concentration-dependent manner, reaching a maximum equilibrium adsorption pressure after about 4 hours at concentrations ≥ 1 mg/mL. An additional concentration dependent measurement series indicated that identical equilibrium surface pressure values were reached at concentrations of 1 mg/mL IgG and above (Fig. 1b).

Adsorption of the IgG results in the formation of a highly viscous protein film wherein the protein covers the entire interface, while showing an inhomogeneous distribution as demonstrated by BAM and AFM. The overall increased brightness in BAM images can be attributed to the presence of the protein film at the interface. The presence of island structures is related to the inhomogeneous IgG adsorption by forming areas of increased thickness or packing density [27], [60]. After adsorption, AFM images reveal a continuous protein film with island structures of condensed protein material similar to BAM but on a smaller scale. The appearance of the OH-vibrational band and amide bands in the IRRAS spectra substantiate the presence of the protein at the interface [41], [78], [79]. Therefore, the accumulation of IgG at the interface was demonstrated by the different methods.

Compression of the film causes a considerable increase in surface pressure above equilibrium values. Not only during adsorption, but all the more upon compression the intensity of the IRRAS bands increases. This signifies an increase in interfacial film thickness [43], [80], [81]. The orientation of the IgG molecules does not change during adsorption or compression as the dichroic ratio does not change with increasing surface pressure. As the dichroic ratio was recorded at different surface pressures during adsorption as well as during compression, possible changes, e.g. in telescoped regions of the compressed film, are considered on average.

During compression, the appearance of the BAM images does not change. In contrast, the AFM images reveal substantial changes of the film topography upon compression. The appearance of telescoped protein material with an increased height compared to the adsorbed film evince that the interfacial film is directly affected by compressive forces [33], [77]. Hence, the protein tends to be trapped at the interface and does not readily desorb

upon compression [82] but forms instead protuberances if the packing density is too high. As secondary structure and molecule orientation were not considerably affected neither by adsorption nor compression, changes in the tertiary structure of the protein could be causative for the compressibility of the interfacial film and the related impeded desorption of protein molecules from the interface.

The IRRAS spectra enable not only conclusions about the presence and film thickness of the IgG at the interface, but also about the protein secondary structure elements. For different types of proteins unfolding upon adsorption to the liquid-air interface has been reported [25], [75], [83], [84]. In contrast to this, our results do not indicate considerable changes in the secondary structure of IgG after adsorption and compression. This can be explained by the fact that IgG molecules belong to the most stable protein types [68], [85]. As no new structural elements show up compared to the native secondary structure in solution the IgG remains in a native-like secondary structure. According to literature, IR methods cover changes of $\geq 2 - 10\%$ in sensitivity [73], [86]. Minor structural perturbations, however, are not detected and cannot be excluded.

The interfacial film thickness was determined from the analysis of the IRRAS intensity of the OH-stretching band as a function of angle of incidence. At equilibrium adsorption pressure (18.5 mN/m), the film thickness amounts to 1.97 nm ($n = 1.45$), and compression to 30mN/m caused an increase in film thickness to 2.61 nm assuming the same refractive index of 1.45 or to 2.4 assuming a higher refractive index of 1.49 for the compressed layer. These values are clearly smaller compared with the ones determined by AFM for the equilibrium film, but in good agreement with the AFM results of the compressed film. The fact, that the calculated film thickness (1.97 nm) is only 30 % of the hydrodynamic radius of the molecule (6.9 nm) can be explained by the loose packing in the equilibrium film. This film contains a substantial amount of water. Algorithms have been devised for estimating the amount of bound water from the amino acid sequence, although these generally do not distinguish between exposed and buried residues. The first ones bind water and the second ones do not. This substantial amount of water in the protein layer leads to the underestimation of the film thickness by IRRAS using the experimentally determined OH-band. Therefore, the thickness of the transferred film determined by AFM is closer to the value of the hydrodynamic radius. On the other hand, it has been stated that IgG molecules preferentially adsorb in flat orientations, which can explain reduced interfacial film

thicknesses compared to the values of hydrodynamic radius measured in solution [87], [88]. *Erickson* [89] determined the minimal radius of a sphere that could contain a protein with 100 kDa to 3.05 nm and for 200 kDa to 3.84 nm. Additionally, they stated the average separation of molecules (center to center) to be 6.9nm [89]. If the film is compressed to 30 mN/m, some water will be squeezed out and the protein film might change to be flatter. Therefore, the thickness of this more densely packed film determined by IRRAS is in good agreement with the value determined by AFM. Although the optical properties could only be estimated from values measured in bulk solution, a qualitative statement on the change in film thickness (packing density) and a differentiation between the film thickness at equilibrium adsorption pressure and after compression can be clearly made.

Compression-decompression cycles reveal compressibility of the protein film [33], [77], [90] indicating a non-equilibrium state of the adsorption layer and therefore drastically reduced desorption kinetics. The considerable hysteresis indicates physical changes within the film as the packing density and film thickness change with compression and decompression. Furthermore, each subsequent cycle ended up in slightly lower surface pressures indicating a loss of material from the interface which is in accordance with the morphology of the protein film exhibiting protrusions after compression. These areas of protein material which are formed by compression and visualized by AFM are no longer present after decompression. Decompression results in a smoother surface compared to adsorption or compression indicated by a decrease in the mean roughness of the film. The decrease in mean roughness also substantiates the assumption for partial loss of material from the interface and compaction of the film by reorganization of the protein molecules, what is in agreement with the results obtained by the surface pressure measurements [33], [34], [77], [91], [92].

Altogether, the combination of physical-chemical, spectroscopic, and microscopic methods for surface characterization provides useful insights into the behavior of proteins at the liquid-air interface. Further investigations will show what impact not only the IgG itself, but also different formulation parameters such as pH and the presence of additives have on the liquid-air interfacial behavior and the tendency of an antibody to aggregate as a measure of protein stability. Moreover, it has already been shown that continuous compression and decompression of an interfacial protein film causes compaction followed by aggregation

[33], [77]. Thus, physical changes within the protein film can be causative for liquid-air interface-related protein aggregation [33], [93].

In conclusion, during adsorption to the soft liquid-air interface IgG forms a continuous but inhomogeneous film of native-like protein molecules whose topographical appearance is affected by compressive forces. As protein pharmaceuticals are exposed to liquid-air interfaces at many points during development, production and storage [94], this comprehensive understanding of the underlying mechanisms is of great importance, as it can help to improve protein stability by choosing appropriate formulation, processing and packing conditions [95], [96].

6. REFERENCES

- [1] J. K. H. Liu, "The history of monoclonal antibody development - Progress, remaining challenges and future innovations," vol. 3, pp. 113–116, 2014.
- [2] N. Rathore and R. S. Rajan, "Current perspectives on stability of protein drug products during formulation, fill and finish operations," *Biotechnol. Prog.*, vol. 24, no. 3, pp. 504–514, 2008.
- [3] A. S. Rosenberg, "Effects of protein aggregates: an immunologic perspective.," *AAPS J.*, vol. 8, no. 3, pp. E501–E507, 2006.
- [4] W. Wang, S. K. Singh, N. Li, M. R. Toler, K. R. King, and S. Nema, "Immunogenicity of protein aggregates-concerns and realities," *Int. J. Pharm.*, vol. 431, no. 1–2, pp. 1–11, 2012.
- [5] E. M. Moussa, J. P. Panchal, B. S. Moorthy, J. S. Blum, M. K. Joubert, L. O. Narhi, and E. M. Topp, "Immunogenicity of Therapeutic Protein Aggregates," *J. Pharm. Sci.*, vol. 105, no. 2, pp. 417–430, 2016.
- [6] W. Jiskoot, T. W. Randolph, D. B. Volkin, C. R. Middaugh, C. Schöneich, G. Winter, W. Friess, D. J. A. Crommelin, and J. F. Carpenter, "Protein Instability and Immunogenicity: Roadblocks to Clinical Application of Injectable Protein Delivery Systems for Sustained Release," *J. Pharm. Sci.*, vol. 101, no. 3, pp. 946–954, 2012.
- [7] C. J. Roberts, "Protein aggregation and its impact on product quality," *Curr. Opin. Biotechnol.*, vol. 30, pp. 211–217, 2014.
- [8] R. Lumry and H. Eyring, "Conformation changes of proteins," *J. Phys. Chem*, vol. 58, no. 2, pp. 110–120, 1954.
- [9] Y. Li and C. J. Roberts, "Lumry-Eyring nucleated-polymerization model of protein aggregation kinetics," *J. Phys. Chem. B*, vol. 113, no. 19, pp. 7020–32, 2009.
- [10] E. Chi, S. Krishnan, B. S. Kendrick, B. S. Chang, J. F. Carpenter, and T. W. Randolph, "Roles of conformational stability and colloidal stability in the aggregation of recombinant human granulocyte colony-stimulating factor," *Protein Sci.*, vol. 12, pp. 903–913, 2003.
- [11] C. J. Roberts, "Kinetics of Irreversible Protein Aggregation: Analysis of Extended Lumry - Eyring Models and Implications for Predicting Protein Shelf Life," pp. 1194–1207, 2003.

- [12] R. J. Green, I. Hopkinson, and R. a L. Jones, "Unfolding and intermolecular association in globular proteins adsorbed at interfaces," *Langmuir*, vol. 15, no. 6, pp. 5102–5110, 1999.
- [13] L. R. De Young, A. L. Fink, and K. A. Dills, "Aggregation of Globular Proteins," *Acc. Chem. Res.*, vol. 26, no. 15, pp. 614–620, 1993.
- [14] R. Wetzel, "Mutations and off-pathway aggregation of proteins," *Trends Biotechnol.*, vol. 12, no. 5, pp. 193–198, 1994.
- [15] J. S. Philo and T. Arakawa, "Mechanisms of protein aggregation.," *Curr. Pharm. Biotechnol.*, vol. 10, pp. 348–351, 2009.
- [16] W. Wang, S. Nema, and D. Teagarden, "Protein aggregation - Pathways and influencing factors," *Int. J. Pharm.*, vol. 390, no. 2, pp. 89–99, 2010.
- [17] S. Zorrilla, G. Rivas, A. U. Acuna, and M. P. Lillo, "Protein self-association in crowded protein solutions: A time-resolved fluorescence polarization study," *Protein Sci.*, vol. 13, no. 11, pp. 2960–2969, 2004.
- [18] S. Damodaran and L. Razumovsky, "Role of surface area-to-volume ratio in protein adsorption at the air-water interface," *Surf. Sci.*, vol. 602, no. 1, pp. 307–315, 2008.
- [19] M. Rodrigueznino, C. Sanchez, V. Ruizhenestrosa, and J. Patino, "Milk and soy protein films at the air-water interface," *Food Hydrocoll.*, vol. 19, no. 3, pp. 417–428, 2005.
- [20] J. M. R. Patino, S. E. M. Ortíz, C. C. Sánchez, R. R. Niño, and C. Anon, "Behavior of Soy Globulin Films at the Air-Water Interface. Structural and Dilatational Properties of Spread Films," vol. 68, pp. 429–437, 2005.
- [21] P. Parhi, A. Golas, N. Barnthip, H. Noh, and E. A. Vogler, "Volumetric interpretation of protein adsorption: Capacity scaling with adsorbate molecular weight and adsorbent surface energy," *Biomaterials*, vol. 30, no. 36, pp. 6814–6824, 2009.
- [22] A. Krishnan, C. A. Siedlecki, and E. A. Vogler, "Traube-Rule Interpretation of Protein Adsorption at the Liquid - Vapor Interface," no. 12, pp. 10342–10352, 2003.
- [23] E. A. Vogler, "Protein adsorption in three dimensions," *Biomaterials*, vol. 33, no. 5, pp. 1201–1237, 2012.
- [24] M. Rabe, D. Verdes, and S. Seeger, "Understanding protein adsorption phenomena at solid surfaces," *Adv. Colloid Interface Sci.*, vol. 162, no. 1–2, pp. 87–106, 2011.
- [25] Y. F. Yano, "Kinetics of protein unfolding at interfaces," *J. physics. Condens. matter*, vol. 24, p. 503101, 2012.

- [26] J. S. Bee, T. W. Randolph, J. F. Carpenter, S. M. Bishop, and M. N. Dimitrova, "Review: Effects of Surfaces and Leachables on the Stability of Biopharmaceuticals," *J. Pharm. Sci.*, vol. 100, no. 10, pp. 4158–4170, 2011.
- [27] P. Wilde, A. Mackie, F. Husband, P. Gunning, and V. Morris, "Proteins and emulsifiers at liquid interfaces," *Adv. Colloid Interface Sci.*, vol. 108–109, pp. 63–71, 2004.
- [28] R. Thirumangalathu, S. Krishnan, M. Ricci, N. Brems, T. W. Randolph, and J. F. Carpenter, "Silicone Oil- and Agitation-Induced Aggregation of a Monoclonal Antibody in Aqueous Solution," *J. Pharm. Sci.*, vol. 98, no. 9, 2009.
- [29] V. Saller, J. Matilainen, U. Grauschopf, K. Bechtold-Peters, H.-C. Mahler, and W. Friess, "Particle Shedding from Peristaltic Pump Tubing in Biopharmaceutical Drug Product Manufacturing," *J. Pharm. Sci.*, vol. 104, no. 4, pp. 1440–1450, 2015.
- [30] A. Eppler, M. Weigandt, A. Hanefeld, and H. Bunjes, "Relevant shaking stress conditions for antibody preformulation development," *Eur. J. Pharm. Biopharm.*, vol. 74, no. 2, pp. 139–147, 2010.
- [31] H. C. Mahler, R. Müller, W. Frieß, A. Delille, and S. Matheus, "Induction and analysis of aggregates in a liquid IgG1-antibody formulation," *Eur. J. Pharm. Biopharm.*, vol. 59, pp. 407–417, 2005.
- [32] S. Kiese, A. Pappenberger, W. Friess, and H.-C. Mahler, "Shaken, Not Stirred: Mechanical Stress Testing of An IgG1 Antibody," *J. Pharm. Sci.*, vol. 97, no. 10, pp. 4337–4366, 2008.
- [33] J. S. Bee, D. K. Schwartz, S. Trabelsi, E. Freund, J. L. Stevenson, J. F. Carpenter, and T. W. Randolph, "Production of particles of therapeutic proteins at the air–water interface during compression/dilation cycles," *Soft Matter*, vol. 8, p. 10329, 2012.
- [34] S. Rudiuk, L. Cohen-Tannoudji, S. Huille, and C. Tribet, "Importance of the dynamics of adsorption and of a transient interfacial stress on the formation of aggregates of IgG antibodies," *Soft Matter*, vol. 8, no. 9, p. 2651, 2012.
- [35] H. J. Lee, A. McAuley, K. F. Schilke, and J. McGuire, "Molecular origins of surfactant-mediated stabilization of protein drugs," *Adv. Drug Deliv. Rev.*, vol. 63, no. 13, pp. 1160–1171, 2011.
- [36] T. Serno, E. Härtl, A. Besheer, R. Miller, and G. Winter, "The Role of Polysorbate 80 and HP β CD at the Air-Water Interface of IgG Solutions," *Pharm. Res.*, pp. 1–14, 2012.

- [37] A. Hawe and W. Friess, "Formulation development for hydrophobic therapeutic proteins," *Pharm. Dev. Technol.*, vol. 12, no. October, pp. 223–237, 2007.
- [38] B. A. Kerwin, "Polysorbates 20 and 80 Used in the Formulation of Protein Biotherapeutics: Structure and Degradation Pathways," *J. Pharm. Sci.*, vol. 97, no. 8, pp. 2926–2935, 2008.
- [39] A. Savitzky and M. J. E. Golay, "Smoothing and Differentiation of Data by Simplified Least Squares Procedures," *Anal. Chem.*, vol. 36, no. 8, pp. 1627–1639, 1964.
- [40] R. Mendelsohn, "External Infrared Reflection Absorption Spectrometry of Monolayer Films at the Air-Water Interface," *Annu. Rev. Phys. Chem.*, vol. 46, pp. 305–334, 1995.
- [41] C. R. Flach, J. W. Brauner, J. W. Taylor, R. C. Baldwin, and R. Mendelsohn, "External reflection FTIR of peptide monolayer films in situ at the air/water interface: experimental design, spectra-structure correlations, and effects of hydrogen-deuterium exchange," *Biophys. J.*, vol. 67, no. 1, pp. 402–410, 1994.
- [42] A. H. Muentert, J. Hentschel, H. G. Borner, and G. Brezesinski, "Characterization of peptide-guided polymer assembly at the air/water interface," *Langmuir*, vol. 24, no. 7, pp. 3306–3316, 2008.
- [43] C. Schwieger, B. Chen, C. Tschierske, J. Kressler, and A. Blume, "Organization of T-shaped facial amphiphiles at the air/water interface studied by infrared reflection absorption spectroscopy," *J. Phys. Chem. B*, vol. 116, no. 40, pp. 12245–56, 2012.
- [44] S. Schrettl, C. Stefaniu, C. Schwieger, G. Pasche, E. Oveisi, Y. Fontana, A. Fontcuberta i Morral, J. Reguera, R. Petraglia, C. Corminboeuf, G. Brezesinski, and H. Frauenrath, "Functional Carbon Nanosheets Prepared from Hexayne Amphiphile Monolayers at Room Temperature," *Nat. Chem.*, vol. 6, no. 6, pp. 468–76, 2014.
- [45] V. L. Kuzmin and A. V. Mikhailov, "Molecular Theory of Light Reflection and Applicability Limits of the Macroscopic Approach," *Opt. Spectrosc.*, vol. 51, no. 4, pp. 383–385, 1981.
- [46] V. L. Kuzmin, V. P. Romanov, and A. V. Mikhailov, "Reflection of Light at the Boundary of Liquid Systems and Structure of the Surface Layer: A Review," *Opt. Spectrosc.*, vol. 73, no. 1, pp. 1–26, 1992.

- [47] J. E. Bertie and Z. Lan, "Infrared Intensities of Liquids XX: The Intensity of the OH Stretching Band of Liquid Water Revisited, and the Best Current Values of the Optical Constants of H₂O(l) at 25°C between 15,000 and 1 cm⁻¹," *Appl. Spectrosc.*, vol. 50, no. 8, pp. 1047–1057, 1996.
- [48] J. E. Bertie, M. K. Ahmed, and H. H. Eysel, "Infrared Intensities of Liquids. 5. Optical and dielectric constants, integrated intensities, and dipole moment derivatives of H₂O and D₂O at 22 °C," *J. Phys. Chem.*, vol. 93, pp. 2210–2218, 1989.
- [49] E. Maltseva, A. Kerth, A. Blume, H. Möhwald, and G. Brezesinski, "Adsorption of amyloid β (1-40) peptide at phospholipid monolayers," *ChemBioChem*, vol. 6, no. 10, pp. 1817–1824, 2005.
- [50] E. Amado, A. Kerth, A. Blume, and J. Kressler, "Infrared reflection absorption spectroscopy coupled with brewster angle microscopy for studying interactions of amphiphilic triblock copolymers with phospholipid monolayers," *Langmuir*, vol. 24, no. 18, pp. 10041–10053, 2008.
- [51] A. Kerth, A. Erbe, M. Dathe, and A. Blume, "Infrared reflection absorption spectroscopy of amphipathic model peptides at the air/water interface," *Biophys. J.*, vol. 86, no. 6, pp. 3750–3758, 2004.
- [52] A. Meister, C. Nicolini, H. Waldmann, J. Kuhlmann, A. Kerth, R. Winter, and A. Blume, "Insertion of lipidated Ras proteins into lipid monolayers studied by infrared reflection absorption spectroscopy (IRRAS)," *Biophys. J.*, vol. 91, no. 4, pp. 1388–401, 2006.
- [53] S. Hénon and J. Meunier, "Microscope at the Brewster angle: Direct observation of first-order phase transitions in monolayers," *Rev. Sci. Instrum.*, vol. 62, no. 4, pp. 936–939, 1991.
- [54] D. Hoenig and D. Moebius, "Direct Visualization of Monolayers at the Air-Water Interface by Brewster Angle Microscopy," *J. Phys. Chem.*, no. 2, pp. 4590–4592, 1991.
- [55] D. Vollhardt, "Brewster angle microscopy: A preferential method for mesoscopic characterization of monolayers at the air/water interface," *Curr. Opin. Colloid Interface Sci.*, vol. 19, no. 3, pp. 183–197, 2014.
- [56] B. C. Tripp, J. J. Magda, and J. D. Andrade, "Adsorption of Globular Proteins at the Air/Water Interface as Measured via Dynamic Surface Tension," *Journal of Colloid and Interface Science*, vol. 173, no. 1, pp. 16–27, 1995.

- [57] H. L. Kim, A. McAuley, B. Livesay, W. D. Gray, and J. McGuire, "Modulation of protein adsorption by poloxamer 188 in relation to polysorbates 80 and 20 at solid surfaces," *J. Pharm. Sci.*, vol. 103, no. 4, pp. 1043–1049, 2014.
- [58] J. Vörös, "The density and refractive index of adsorbing protein layers.," *Biophys. J.*, vol. 87, no. 1, pp. 553–561, 2004.
- [59] D. E. Graham and M. C. Phillips, "Proteins at Liquid Interfaces - III. Molecular Structures of Adsorbed Films," *J. Colloid Interface Sci.*, vol. 70, no. 3, pp. 427–439, 1979.
- [60] R. R. Niño, C. C. Sánchez, V. P. Ruiz-Henestrosa, and J. M. R. Patino, "Milk and soy protein films at the air-water interface," *Food Hydrocoll.*, vol. 19, no. 3, pp. 417–428, 2005.
- [61] J. M. R. Patino, S. E. M. Ortiz, C. C. Sánchez, R. R. Niño, and C. Anon, "Behavior of Soy Globulin Films at the Air-Water Interface. Structural and Dilatational Properties of Spread Films," *Ind. Eng. Chem. Res.*, vol. 42, no. 21, pp. 5011–5017, 2003.
- [62] R. R. Niño, C. C. Sánchez, and J. M. R. Patino, "Interfacial characteristics of β -casein spread films at the air-water interface," *Colloids Surfaces B Biointerfaces*, vol. 12, no. 3–6, pp. 161–173, 1999.
- [63] J. M. R. Patino, C. C. Sánchez, and M. R. Niño, "Structural and morphological characteristics of β -casein monolayers at the air–water interface," *Food Hydrocoll.*, vol. 13, no. 5, pp. 401–408, 1999.
- [64] I. S. Chronakis, A. N. Galatanu, T. Nylander, and B. Lindman, "The behaviour of protein preparations from blue-green algae (*Spirulina platensis* strain Pacifica) at the air/water interface," *Colloids Surfaces A Physicochem. Eng. Asp.*, vol. 173, no. 1–3, pp. 181–192, 2000.
- [65] B. A. Snopok and E. V. Kostyukevich, "Kinetic studies of protein-surface interactions: A two-stage model of surface-induced protein transitions in adsorbed biofilms," *Anal. Biochem.*, vol. 348, no. 2, pp. 222–231, 2006.
- [66] V. M. Kaganer, H. Möhwald, and P. Dutta, "Structure and phase transitions in Langmuir monolayers," *Rev. Mod. Phys.*, vol. 71, no. 3, pp. 779–819, 1999.
- [67] T. Menzen and W. Friess, "Temperature-ramped studies on the aggregation, unfolding, and interaction of a therapeutic monoclonal antibody," *J. Pharm. Sci.*, vol. 103, no. 2, pp. 445–455, 2014.

- [68] S. Matheus, W. Friess, and H. C. Mahler, "FTIR and nDSC as analytical tools for high-concentration protein formulations," *Pharm. Res.*, vol. 23, no. 6, pp. 1350–1363, 2006.
- [69] N. Takeda, M. Kato, and Y. Taniguchi, "Pressure- and thermally-induced reversible changes in the secondary structure of ribonuclease A studied by FT-IR spectroscopy.," *Biochemistry*, vol. 34, no. 17, pp. 5980–7, 1995.
- [70] S. Krimm and J. Bandekar, "Vibrational Spectroscopy and conformation of Peptides, Polypeptides, and Proteins," *Adv. Protein Chem.*, vol. 38, pp. 181–364, 1986.
- [71] A. Meister, A. Kerth, and A. Blume, "Interaction of Sodium Dodecyl Sulfate with Dimyristoyl-sn-glycero-3-phosphocholine Monolayers Studied by Infrared Reflection Absorption Spectroscopy . A New Method for the Determination of Surface Partition Coefficients," *J. Phys. Chem. B*, vol. 108, no. 24, pp. 8371–8378, 2004.
- [72] V. S. Alahverdjieva, K. Khristov, D. Exerowa, and R. Miller, "Correlation between adsorption isotherms, thin liquid films and foam properties of protein/surfactant mixtures: Lysozyme/C10DMPO and lysozyme/SDS," *Colloids Surfaces A Physicochem. Eng. Asp.*, vol. 323, no. 1–3, pp. 132–138, 2008.
- [73] J. Kong and S. Yu, "Fourier transform infrared spectroscopic analysis of protein secondary structures," *Acta Biochim. Biophys. Sin. (Shanghai)*, vol. 39, no. 8, pp. 549–559, 2007.
- [74] F. F. O. Sousa, a. Luzardo-Álvarez, J. Blanco-Méndez, F. J. Otero-Espinar, M. Martín-Pastor, and I. Sández Macho, "Use of ^1H NMR STD, WaterLOGSY, and Langmuir monolayer techniques for characterization of drug-zein protein complexes," *Eur. J. Pharm. Biopharm.*, vol. 85, no. 3, pp. 790–798, 2013.
- [75] T. Furuno, "Atomic force microscopy study on the unfolding of globular proteins in the Langmuir films," *Thin Solid Films*, vol. 552, pp. 170–179, 2014.
- [76] C. Zhou, J.-M. Friedt, A. Angelova, K.-H. Choi, W. Laureyn, F. Frederix, L.A. Francis, A. Campitelli, Y. Engelborghs, and G. Borghs., "Human immunoglobulin adsorption investigated by means of quartz crystal microbalance dissipation, atomic force microscopy, surface acoustic wave, and surface plasmon resonance techniques.," *Langmuir*, vol. 20, no. 11, pp. 5870–5878, 2004.

- [77] S. Ghazvini, C. Kalonia, D. B. Volkin, and P. Dhar, "Evaluating the Role of the Air-Solution Interface on the Mechanism of Subvisible Particle Formation Caused by Mechanical Agitation for an IgG1 mAb," *J. Pharm. Sci.*, vol. 105, no. 5, pp. 1643–1656, 2016.
- [78] S. Y. McLoughlin, M. Kastantin, D. K. Schwartz, and J. L. Kaar, "Single-molecule resolution of protein structure and interfacial dynamics on biomaterial surfaces.," *Proc. Natl. Acad. Sci. U.S.A.*, vol. 110, pp. 19396–401, 2013.
- [79] R. Mendelsohn, G. Mao, and C. R. Flach, "Infrared reflection-absorption spectroscopy: Principles and applications to lipid-protein interaction in Langmuir films," *Biochim. Biophys. Acta - Biomembr.*, vol. 1798, no. 4, pp. 788–800, 2010.
- [80] M. Hoernke, J. A. Falenski, C. Schwieger, B. Koksche, and G. Brezesinski, "Triggers for β -sheet formation at the hydrophobic-hydrophilic interface: High concentration, in-plane orientational order, and metal ion complexation," *Langmuir*, vol. 27, pp. 14218–14231, 2011.
- [81] C. Stefaniu, G. Brezesinski, and H. Möhwald, "Langmuir monolayers as models to study processes at membrane surfaces.," *Adv. Colloid Interface Sci.*, vol. 208, pp. 197–213, 2014.
- [82] L. Wang, D. Atkinson, and D. M. Small, "Interfacial properties of an amphipathic α -helix consensus peptide of exchangeable apolipoproteins at air/water and oil/water interfaces.," *J. Biol. Chem.*, vol. 278, no. 39, pp. 37480–91, 2003.
- [83] Y. F. Yano, E. Arakawa, W. Voegeli, and T. Matsushita, "Real-time investigation of protein unfolding at an air–water interface at the 1 s time scale," *J. Synchrotron Radiat.*, vol. 20, no. 6, pp. 980–983, 2013.
- [84] P. Pal, T. Kamilya, M. Mahato, and G. B. Talapatra, "The formation of pepsin monomolecular layer by the Langmuir-Blodgett film deposition technique," *Colloids Surfaces B Biointerfaces*, vol. 73, pp. 122–131, 2009.
- [85] M. J. Feige, L. M. Hendershot, and J. Buchner, "How antibodies fold," *Trends Biochem. Sci.*, vol. 35, no. 4, pp. 189–198, 2010.
- [86] M. Jackson and H. H. Mantsch, "The Use and Misuse of FTIR Spectroscopy in the Determination of Protein Structure," *Crit. Rev. Biochem. Mol. Biol.*, vol. 30, no. 2, pp. 95–120, 1995.

- [87] R. Saber, S. Sarkar, P. Gill, B. Nazari, and F. Faridani, "High resolution imaging of IgG and IgM molecules by scanning tunneling microscopy in air condition," *Sci. Iran.*, vol. 18, no. 6, pp. 1643–1646, 2011.
- [88] J. G. Vilhena, A. C. Dumitru, E. T. Herruzo, J. I. Mendieta-Moreno, R. Garcia, P. A. Serenaa, and R. Pérez al., "Adsorption orientations and immunological recognition of antibodies on graphene," *Nanoscale*, pp. 13463–13475, 2016.
- [89] H. P. Erickson, "Size and shape of protein molecules at the nanometer level determined by sedimentation, gel filtration, and electron microscopy," *Biol. Proced. Online*, vol. 11, no. 1, pp. 32–51, 2009.
- [90] R. G. Couston, D. A. Lamprou, S. Uddin, and C. F. Van Der Walle, "Interaction and destabilization of a monoclonal antibody and albumin to surfaces of varying functionality and hydrophobicity," *Int. J. Pharm.*, vol. 438, no. 1–2, pp. 71–80, 2012.
- [91] P. A. Wierenga and H. Gruppen, "New views on foams from protein solutions," *Curr. Opin. Colloid Interface Sci.*, vol. 15, no. 5, pp. 365–373, 2010.
- [92] M. Nieto-Suárez, N. Vila-Romeu, and I. Prieto, "Behaviour of insulin Langmuir monolayers at the air-water interface under various conditions," *Thin Solid Films*, vol. 516, no. 24, pp. 8873–8879, 2008.
- [93] I. C. Shieh and A. R. Patel, "Predicting the agitation-induced aggregation of monoclonal antibodies using surface tensiometry," *Mol. Pharm.*, p. 3184–3193, 2015.
- [94] J. S. Bee, J. L. Stevenson, B. Mehta, J. Svitel, J. Pollastrini, R. Platz, E. Freund, J. F. Carpenter, and T. W. Randolph, "Response of a concentrated monoclonal antibody formulation to high shear," *Biotechnol. Bioeng.*, vol. 103, no. 5, pp. 936–943, 2009.
- [95] N. A. Alexandrov, K. G. Marianova, T. D. Gurkov, et al. and A. Lips, "Interfacial layers from the protein HFBII hydrophobin: Dynamic surface tension, dilatational elasticity and relaxation times," *J. Colloid Interface Sci.*, vol. 376, no. 1, pp. 296–306, 2012.
- [96] C. J. Roberts, T. K. Das, and E. Sahin, "Predicting solution aggregation rates for therapeutic proteins: Approaches and challenges," *Int. J. Pharm.*, vol. 418, no. 2, pp. 318–333, 2011.

THIS CHAPTER WAS PUBLISHED:

Koepf E, Schroeder R, Brezesinski G, Friess W 2017. The Film Tells The Story: Physicochemical Characteristics of IgG at the Liquid-Air Interface, *EJPB*, 119:396-407.

CHAPTER IV

NOTORIOUS BUT NOT UNDERSTOOD: HOW LIQUID-AIR INTERFACIAL STRESS TRIGGERS PROTEIN AGGREGATION

1. ABSTRACT

Protein aggregation is a major challenge in the development of biopharmaceuticals as it negatively impacts product quality. The mechanisms and pathways of protein aggregation are manifold. Therefore, good understanding of the factors that influence, control and prevent protein aggregation are essential for a successful formulation development. In particular, the presence of liquid-air interfaces has been identified to trigger the formation of large protein particles. This study focused on the analysis of the physical-chemical behavior of two monoclonal antibodies (IgGs) at the liquid-air interface. In addition, a Mini-trough model was developed what allows a direct comparison of the interfacial film characteristics studied in a Langmuir trough with the impact of interfacial stress only on protein particle formation. Surface pressure measurements exhibited the formation of a highly compressible interfacial film. Moreover, an inhomogeneous protein distribution across the interface with areas of increased packing density and film thickness were discovered by Brewster-Angle microscopy. Repeated compression and decompression of the interfacial film resulted not only in a considerable hysteresis, but also in significantly elevated numbers of particles compared to the controls. Furthermore, the extent and speed of compression directly affected the mechanical properties of the film as well as the number of particles formed. Particularly, compression by a critical factor above 3 was identified to cause a significant increase in particle formation. Above that, with increasing compression speed the number of particles increased, too. Infrared reflection-absorption spectroscopy did not indicate considerable changes in secondary structure compared to FT-IR spectra in solution. Hence, it was proven that the IgG remains in a native-like conformation at the interface.

Consequently, the physical-chemical methods applied in combination with the newly-designed Mini-trough provided substantial indications of the mechanisms of interface-related protein aggregation. The characterization of not only the interfacial film but also the aggregation process itself by a trough method exclusively has not been described before but provides additional understanding and enables testing of different formulations under controlled stress conditions.

2. INTRODUCTION

Protein aggregation is a major challenge in the development of protein pharmaceuticals. Particularly, interfacial stress as encountered during manufacturing, filling and shipping directly affects protein stability and can result in the formation of protein particles.

Protein aggregates can be soluble or insoluble in nature, can be a result of intermolecular covalent or non-covalent bonds and can be reversible or irreversible [1]. On the one hand, the emergence of small aggregates can induce the formation of larger aggregates by further association, thereby exceeding the solubility limit and leading to protein precipitates. On the other hand, so-called “large native-like particles” can occur spontaneously without continuum from monomer to dimer to large particles [2]. Hence, not only (partly) unfolded, but also native molecules can play an important role in the formation of protein aggregates [3], [4]. Due to their partly amphiphilic nature, protein molecules exhibit a certain surface activity and therefore have a high propensity to adsorb to interfaces, e.g. to container surfaces or to the liquid-air interface [5]–[9]. Choosing appropriate formulation conditions, such as pH and ionic strength as well as the addition of surfactants can stabilize proteins against adsorption to surfaces and interface-induced aggregation [10]–[14].

Using the pendant drop technique, Beverung *et al.* described the time dependent adsorption of several proteins, including ovalbumin, β -casein, lysozyme, and bovine serum albumin (BSA) into 3 regimens: after an induction period where the molecules diffuse to the subsurface with a minimal reduction in surface tension only, a steep decrease in interfacial tension is caused by a saturation of the interface with protein molecules. Subsequently, the final regime is characterized by a relaxation of the adsorbed layer and the formation of a multi-layer, viscoelastic interfacial film [15]. Hill *et al.* state that the adsorption of proteins at interfaces is an irreversible process as no desorption is detected upon dilution of the bulk phase [16]. This can be attributed to a prohibitively high energy barrier for desorption from an interface. Furthermore, interfacial electrostatic interactions appear to play a particularly important role regarding structure and properties of interfacial protein layers [17].

Liquid-air interfaces are particularly present in protein pharmaceuticals as air bubbles or headspace in solution vials or syringes [18]. It has been stated, that the adsorption process causes protein unfolding and as a consequence results in aggregation [19]–[21]. In contrast, other studies suggest that protein molecules remain in a native-like conformation at the interface [22]–[24]. So-called soft proteins with low structural stability exhibit a stronger

tendency to unfold and on the contrary, so-called hard proteins show structural rigidity [20], [25]. Makievsky *et al.* state that human serum albumin (HSA) does not undergo any significant denaturation at the liquid-air interface [26]. However, unfolding of lysozyme was observed using IRRAS [27] and x-ray reflectivity [19]. The conformation of adsorbed proteins has been reported to be mainly β -sheet. Thus, protein molecules with mainly α -helix or random structure in the native state, such as lysozyme, may be more prone to unfolding upon adsorption to hydrophobic interfaces than e.g. β -sheet rich β -lactoglobulin [28]–[30].

Different stress conditions, such as shaking or stirring, are known to cause the formation of different types and sizes of protein particles [31]–[33]. Kiese *et al.* demonstrated that eliminating the liquid-air interface by removing the headspace in vials prevents agitation-induced aggregation [13]. During shaking, however, not only interfacial stress, but additional effects such as cavitation, flow dynamics and contact materials can affect the aggregation process [34]–[37]. Proteins have been shown to form a compressible viscoelastic adsorbed layer at the interface [38]. Moreover, the protein layer thickens and crumples with increasing surface pressure, and eventually the protein network fails and is displaced from the interface [5], [38]. Martin *et al.* hypothesized that compression to high surface pressures may cause a collapse of the protein film thereby leading to a gradual displacement of protein molecules from the interface [39]. Similarly, Ghazvini *et al.* claimed that interfacial stress initiates protein aggregation at the liquid-air interface, and the presence of protein particles in bulk is the result of mechanical perturbation of the interface [24]. Therefore, mechanical stress by substantial compression and decompression of a concentrated protein film was assumed to result in rupture and loss of material from the interface, and thus in the formation of protein particles [40]. Whereas many studies hypothesized an involvement of the liquid-air interface in the protein aggregation process [24], [40], [41], Lin *et al.* were able to directly prove that interfacial dilatational deformation accelerates particle formation in monoclonal antibody solutions [42].

So, although considerable efforts have been made to elucidate the mechanisms behind protein interfacial behavior and its direct link to protein aggregation, it is still not thoroughly understood [4], [40], [43]. Especially, a direct connection of the physical-chemical properties of the interfacial film and the emergence of large protein particles in solution is an obvious, but not well-understood issue. Therefore, it is essential to localize and analyze the liquid-air interface-related protein aggregation process. In this study, different surface-sensitive

analytical methods were applied to characterize the liquid-air interfacial protein film of two different monoclonal antibodies (IgGs). Infrared Reflection-Absorption Spectroscopy (IRRAS) was used to identify the protein secondary structure at the interface and compared to spectra in solution using FT-IR. Brewster-Angle Microscopy (BAM) was applied to uncover topographical properties of the liquid-air interfacial film. Above that, a model was developed to study the formation of particles by continuous compression and decompression of the interfacial film only. Additionally, this newly designed test model allows an evaluation of the impact of compression rate and speed on the formation of protein particles.

The localization of the aggregation process, the identification of critical factors, as well as the analysis of the secondary structure of the protein are of high importance for a detailed mechanistic understanding of how large protein aggregates emerge upon interfacial stress. Consequently, the physical-chemical methods applied to characterize the interfacial film in connection with the Mini-trough studies represent a valuable tool to screen different formulation candidates for their propensity to undergo interface-related protein aggregation processes.

3. MATERIALS AND METHODS

3.1. Materials

Two monoclonal antibodies (mAB₁ 126 mg/mL pH 6.0 in 20 mM Histidine buffer, and mAB₂ 94 mg/mL pH 5.3 in 15 mM Histidine buffer) were provided by AbbVie Deutschland GmbH & Co. KG, Ludwigshafen am Rhein, Germany. Solutions were prepared using highly purified water (ELGA LC134, ELGA LabWater, Germany) and pH was adjusted with 1 mM NaOH and 1 mM HCl, respectively. All samples were filtrated using 0.2 µm sterile polyethersulfone (PES) syringe filters (Sterile Syringe Filter PES, VWR, Germany).

3.2. Surface Pressure Measurements

Surface pressure measurements and compression-decompression experiments were performed in a 59 x 397 mm² PTFE Langmuir trough equipped with a metal alloy dyne probe (Kibron Inc., Finland). The trough was filled with a 160 mL sample solution. The surface area can be adjusted by two mobile PTFE barriers with a maximum area of 234 cm². Temperature was set to 20 °C by connecting the trough to a K6-cc circulation thermostat (Peter Huber Kaeltemaschinenbau GmbH, Germany). Compression speed was set to 55 mm/min at a compression factor (c_f) of 8.3. Three cycles of continuous compression and decompression were performed. For the compression-decompression experiments, the mAb concentration was set to 1 mg/mL in 15 mM Histidine buffer at pH 6.0. Equilibrium surface pressure was defined as the maximum surface pressure that is reached by adsorption and changes less than 0.1 mN/m within 0.5 h. Results are given as mean and standard deviation (SD).

3.3. Agitation Studies

Agitation studies were performed on a horizontal orbital shaker [GfL 3017, Gesellschaft für Labortechnik mbH, Germany) at 100 rpm for 48 h. Each vial (vial size: 6 mL - 6R) was filled with 4 mL or without headspace, respectively. mAb concentration was set to 1 mg/mL in 15 mM Histidine buffer at pH 6.0 for all measurements. The stoppers (without and with needle) are in-house products and made of borosilicate glass (glass type I). The glass needle was generated by manual pull out of the glass stoppers after heating the glass until deformable (in-house production).

The vials were sealed using a viton O-ring (DuPont - E. I. du Pont de Nemours and Company, U.S.) and spring steel clips or conical joints KCM (Keck™ by Schott Medica, Germany). Tests were performed in triplicates and analyzed for turbidity and by LO, MFI.



Figure 1: 6R vials with glass stopper sealed by a viton O-ring and spring steel clip, and glass stopper with needle

3.4. Mini-Trough Studies

The so-called “Mini”-trough was designed and built in-house. It consists of a PTFE trough with same proportions and functionality as the Kibron Langmuir trough already described (see Materials and Methods: Surface Pressure Measurements) without a surface pressure measurement unit. Automated and continuous compression-decompression cycles can be performed to stress the liquid-air interface only. In relation to the Langmuir trough, the dimensions of the Mini-trough are reduced by a factor of 8.7 with a maximum area $A_{\max} = 27.0 \text{ cm}^2$. This results in a trough length of 9.0 cm, a width of 3.0 cm and a depth of 0.5 cm. To maximize contact between the sample surface and the barriers, the trough was slightly overfilled and therefore the sample volume was set constant to 14.5 mL for all experiments. Particle contamination was minimized by washing with ethanol (commercial grade, absolute) and repeated washing with highly purified water. A plastic enclosure covers the PTFE trough and the barriers (Fig. 2). mAb concentration was set to 1 mg/mL in 15 mM Histidine buffer at pH 6.0 for all measurements. The samples were stressed by 100 cycles started after an equilibration time of 2.5 h.



Figure 2: Mini-Trough for repeated compression-decompression experiments

3.5. Compression Speed (c_{speed})

The Mini-trough enables the adjustment of compression speed (c_{speed}). One compression-decompression cycle describes a bidirectional barrier movement by 2×39.6 mm. Compression speeds of 25, 55, 95 or 115 mm/min have been used.

3.6. Compression Factor (c_f)

Compression factor (c_f) is defined as the ratio between the maximum and minimum surface area. It can be varied by manual setting of the barriers end positions as illustrated in figure 2.2. To investigate the impact of the compression factor, compression speed was kept constant at 55 mm/min.

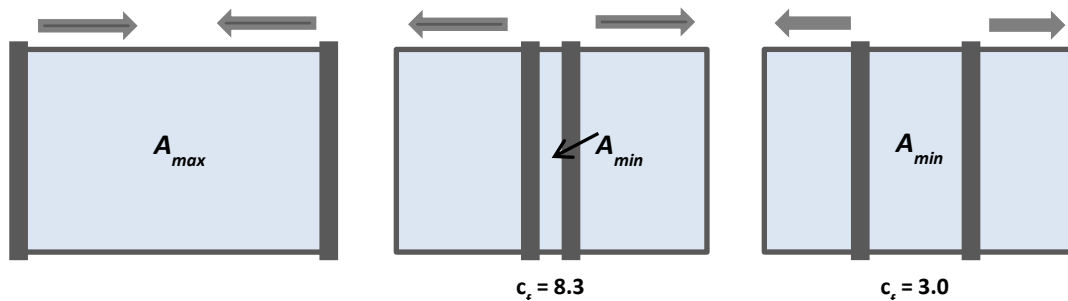


Figure 3: Schematic illustration of barrier movement and related area restriction from maximum surface area (A_{max}) to the minimum surface area (A_{min}) dependent on compression factor (c_f) for $c_f = 8.3$ and $c_f = 3$

Table 1 lists some compression factors chosen and the corresponding barrier movement and cycling times.

Table 1: Compression factors (c_f) and related area, barrier movement and cycling time

c_f	A_{min} [cm ²]	Barrier Movement [cm]	Time for 100 cycles [h]
2	13.5	4.5	1.4
3	9.0	6.0	1.8
5	5.4	7.2	2.2
8.3	3.2	7.7	2.4
11	2.5	8.2	2.5

3.7. Particle Analysis

3.7.1. Visual Inspection and Photo-documentation

Samples were analyzed for particles by visual inspection in a box with a blackboard equipped with a white light lamp for 5 s each and recorded by photo-documentation (Nikon D5300 SLR digital camera, Nikon Corporation, Japan). Each sample was categorized according to table 2.

Table 2: Four Categories for visual inspection (following Ph. Eur. 2.9.19)

0	1	2	3
Free from particles	Practically free from particles	Several particles	Many particles

3.7.2. Turbidity

Samples were analyzed for turbidity according to Ph. Eur. 2.2.1. A sample volume of 1.8 mL was analyzed using a Nephla turbidimeter (Dr. Lange, Duesseldorf, Germany). Data is given as formazine nephelometric units (FNU).

3.7.3. Light Obscuration

Samples were analyzed for particles in the micrometer range by light obscuration (in analogy to USP 788 and Ph. Eur. 2.9.19. requirements) with a SVSS-C instrument (PAMAS, Partikelmess- und Analysesysteme GmbH, Rutesheim, Germany). After a pre-run volume of 0.5 mL, each sample was analyzed in triplicates of 0.3 mL at a filling and emptying rate of 10 mL/min. Before each run, the system was rinsed with at least 5 mL of highly purified water. Data was collected using PAMAS PMA Program V 2.1.2.0. Results are given as mean and SD.

3.7.4. Micro-Flow Imaging

Particle size and number were additionally measured using a micro-flow imaging (MFI) system DPA4100 from Brightwell Technologies Inc. (Ottawa, Canada) equipped with a high-resolution 100 µl flowcell and the MFI™ View Application Software. Pre-run volumes of 0.3 mL and sample volumes of 0.65 mL were drawn through the flow cell by a peristaltic pump at a flow rate of 0.1 mL/min. To optimize illumination and to provide a clean baseline the system was rinsed with highly purified water before and after the measurements. Results are given as mean and SD.

3.7.5. Statistical Significance

A t-test was performed with * for $p \leq 0.05$, ** for $p \leq 0.01$ and *** for $p \leq 0.001$.

3.8. FT-IR Spectroscopy

FT-IR spectra of 10 mg/mL mAB in 15mM Histidine buffer pH 6 were recorded using a Tensor 27 (Bruker Optik GmbH, Ettlingen, Germany) equipped with an AquaSpec (transmission cell H₂O A741-1) or a BioATR (Attenuated Total Reflectance) cell™ II (Harrick) at 20 °C connected to a thermostat (DC30-K20, Thermo Haake). For each spectrum, a 100 scan interferogram was collected at a single beam mode with a 4 cm⁻¹ resolution. Recorded spectra were analyzed by Opus 7.5 (Bruker Optik GmbH) and displayed as vector-normalized second-derivative amide I spectra (calculated with 17 smoothing points according to the Savitzky-Golay algorithms [26]). Infrared spectra of the temperature-induced unfolding of the IgG samples were conducted using the BioATR measurement cell as the sample cell. Temperature-dependent spectra were acquired every 4 °C from 25 – 93 °C with an equilibration time of 120 s. Recorded infrared spectra were analyzed by the software Protein Dynamics for Opus 7.5.

3.9. Infrared Reflection-Absorption Spectroscopy (IRRAS)

Infrared spectroscopy was used to determine the presence and the conformation of adsorbed protein. IRRAS spectra were recorded using a VERTEX FT-IR spectrometer (Bruker, Germany). The spectrometer was coupled to a Langmuir trough (R&K, Germany), placed in a sealed container to guarantee constant vapor atmosphere. The IR beam was conducted out of the spectrometer and focused onto the water surface of the Langmuir trough. A computer- controlled KRS-5 wire-grid polarizer was used to generate perpendicular (s) polarized light. The angle of incidence was set to 40° with respect to the surface normal. Measurements were performed using a trough with two compartments and a trough shuttle system. One compartment contained the protein solution under investigation (sample), while the other (reference) was filled with the pure subphase. The single-beam reflectance spectrum of the reference trough was ratioed as background to the single beam reflectance spectrum of the sample to calculate the reflection absorption spectrum as $-\log(R/R_0)$. IR spectra were collected at 4 cm⁻¹ resolution using 200 scans.

3.10. Brewster-Angle Microscopy (BAM)

A Langmuir trough (KSV NIMA, Finland) was connected to a KSV NIMA Brewster Angle Microscope to enable image measurements at the Brewster-Angle (53.06°, p-polarized light). mAB at 0.1 mg/mL in 15mM histidine buffer was filled into the trough ($V = 80$ mL). Simultaneous surface pressure measurements in the Langmuir trough enabled a direct allocation of each image to a certain adsorption or compression state of the protein film. The BAM images covered an area of $400 \times 720 \mu\text{m}^2$.

4. RESULTS AND DISCUSSION

4.1. Adsorption of IgGs to the Liquid-Air Interface

The surface activity of the two mABs was investigated by surface pressure measurements. The surface pressure does not depend on the geometry of the trough as a continuous protein film is formed, and the surface tension is considered to be uniform across the interface [45].

The adsorption to the liquid-air interface ends up in concentration and time-dependent equilibrium surface pressure values as a result of molecule arrangement within the adsorbed film [46]. mAB₁ reached a maximum equilibrium surface pressure of 13.5 mN/m at concentrations ≥ 1 mg/mL (Fig. 4), and mAB₂ a maximum equilibrium surface pressure of 14.4 mN/m at ≥ 1 mg/mL, respectively. Moreover, at bulk concentrations of ≥ 1 mg/mL no further increase in surface pressure was observed. This can be explained by a saturation of the interface with protein molecules [5], [42]. Other proteins, such as human serum albumin (HSA) and β -lactoglobulin reach similar surface pressure values of 18.8 mN/m [26] and 24.0 mN/m, respectively [47]. Absolute surface pressure values have been reported to be affected by molecular size as well as by the relative affinity to the liquid-air interface [47]. Upon adsorption, protein molecules get enriched at the interface resulting in a thin layer of concentrated solution [17]. Consequently, the antibody molecules adsorb irreversibly are not only kinetically trapped at the interface but rather stabilized by protein-protein interactions what results in the formation of an interfacial, viscoelastic film network [17], [48]–[50].

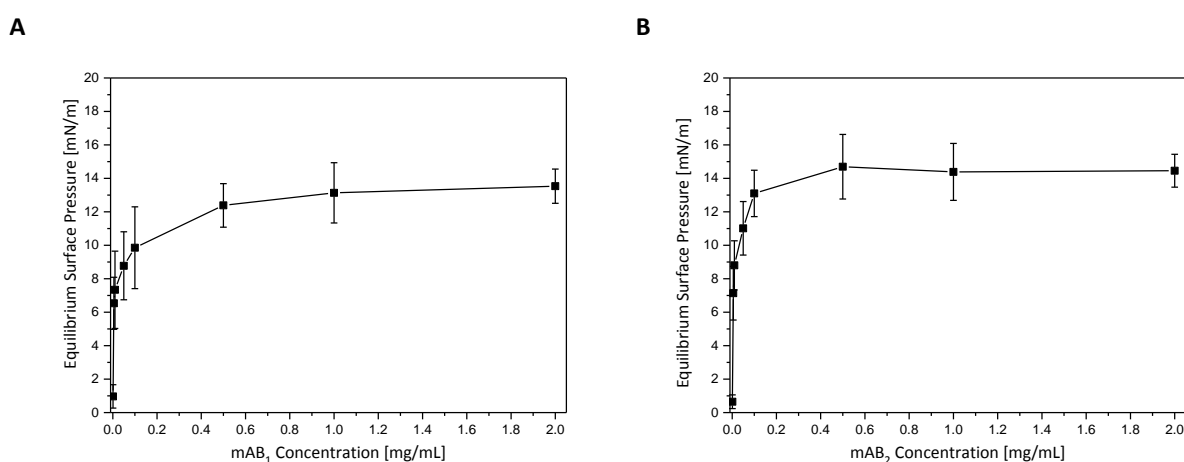


Figure 4: Concentration-dependent equilibrium surface pressure values of A: mAB₁, B: mAB₂

4.2. Physical Resistance of Interfacial Protein Films

Controlled compression and decompression of the liquid-air interfacial film and simultaneous recording of surface pressure was performed to investigate the impact of mechanical stress on the physical resistance of the film. Movement of the barriers from A_{\max} to A_{\min} resulted in an increase of surface pressure (Fig. 5). Measurements were started after equilibrium surface pressure was reached and set to zero. Upon compression, the protein molecules do not desorb upon compression but form a coherent and compressible film indicated by an increase in surface pressure [51]. Furthermore, the distribution and ordering of the molecules changes as the area per molecule decreases and a densely-packed adsorption layer is formed. Hence, surface pressure depends on the occupation rate of molecules within the adsorption layer as well as on the film thickness [52], [53]. The formation of a strong network capable of enduring considerable stresses is probably due to a complex interplay of hydrophobic interactions, hydration, and hydrogen bonds [45].

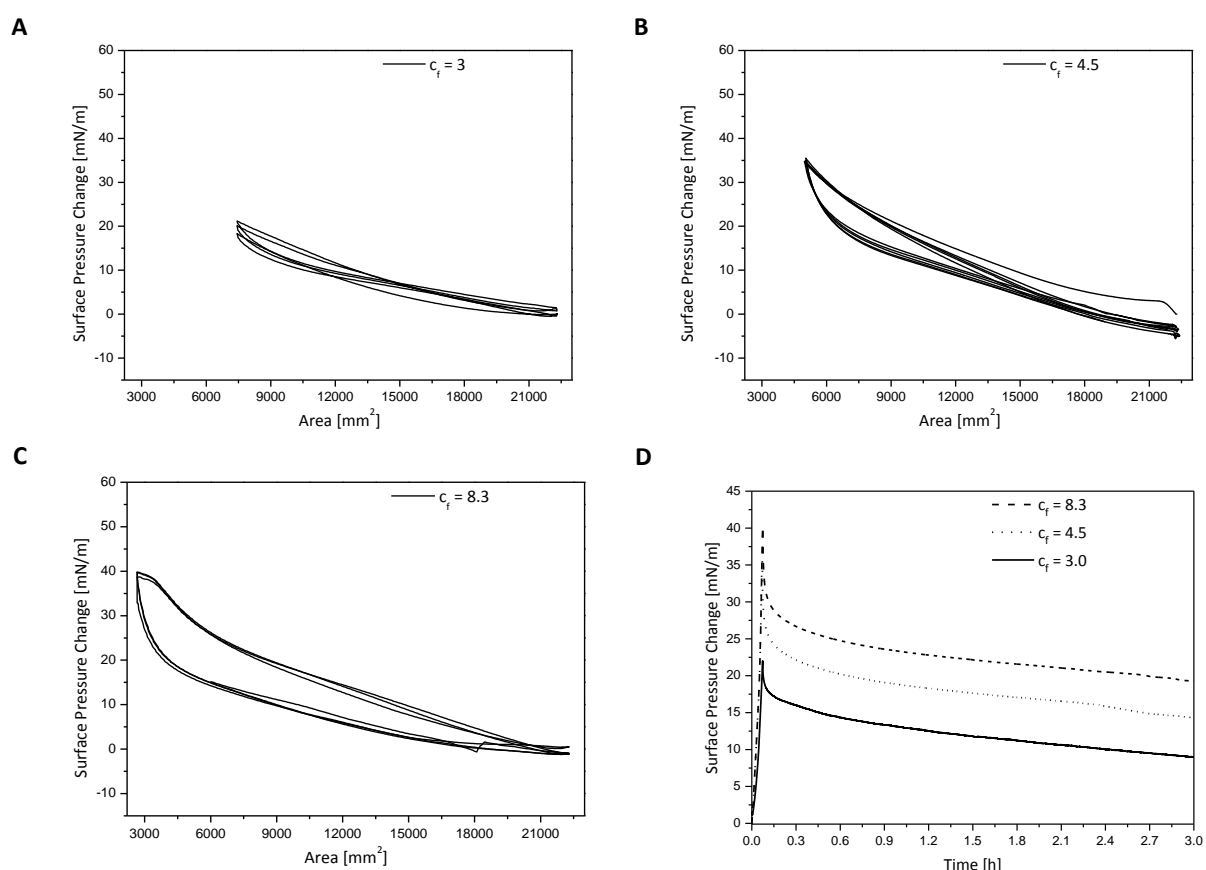


Figure 5: Surface pressure during repeated compression and decompression of mAB₁ at a c_{speed} of 55 mm/min at a c_f of; A: 3, B: 4.5, C: 8.3, D: Impact of c_f on surface pressure over time after compression to A_{\min} without decompression

Compression of the interfacial film leads to stronger protein-protein interactions and this cohesion between the molecules can be partially irreversible and clusters of protein molecules might be formed [54]. Decompression caused an initial steep decrease in surface pressure. The ascending line during compression and the descending line during decompression differ from each other forming a characteristic hysteresis [40]. As a result, upon decompression the surface pressure initially drops drastically presumably due to a rupture of the film. Similarly, Grasso *et al.* showed that changes in the surface electrostatics affected the hysteresis of an insulin monolayer [55]. The way a protein film responds to compression has been described to be determined by the deformability (hardness) of the adsorbed species [30], [39], [56].

The influence of the compression factors from the maximum surface area ($A_{\max} = 26.9 \text{ cm}^2$) towards the minimum surface area ($A_{\min} = 6.0 \text{ cm}^2$) on the change in surface pressure upon compression and decompression was examined at a constant c_{speed} of 55 mm/min (Fig. 5). The maximum change in surface pressure at $c_f = 3$ of 18.3 mN/m was much lower compared to 34.7 mN/m at $c_f = 4.5$, and 39.4 mN/m at $c_f = 8.3$. Moreover, at $c_f = 3$ no considerable hysteresis was detected whereas with increasing compression factor the hysteresis area increased. The protein molecules in the compressed film can relax which requires substantial time and is directly dependent on the compression factor. Hence, compression without decompression resulted in a decrease in surface pressure although surface pressure values remain elevated compared to those of the uncompressed state. Furthermore, compression by a high compression factor of 8.3 resulted in an increased quasi-equilibrium surface pressure compared to less compression by factor 3. Similar findings obtained by Bee *et al.* lead to the assumption of a change in the phase behavior of the interface as indicated by a characteristic kink in the surface pressure versus area isotherm, that were observed around 35 mN/m during compression and around 25 mN/m during decompression [40]. Compression was performed by a reduction in surface area from 260 cm^2 to 30 cm^2 , meaning a compression factor of 8.67, and a compression speed of around 30 mm/min.

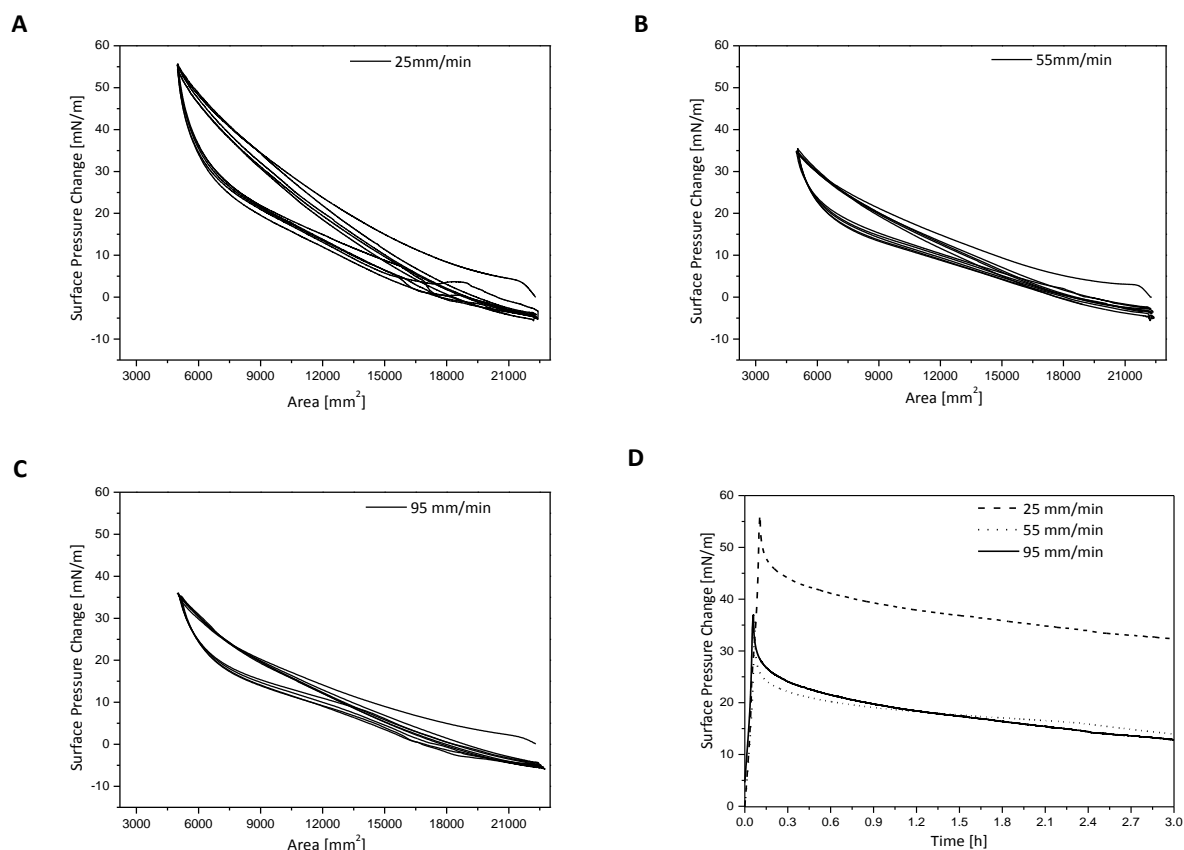


Figure 6: Surface pressure during repeated compression and decompression of mAB₁ [1 mg/mL] at c_f 4.5 at a c_{speed} of A: 25 mm/min, B: 55 mm/min, C: and 95 mm/min, D: Impact of c_{speed} on surface pressure over time of mAB₁ after compression to A_{min} with 55 mm/min without decompression

The impact of different speeds of barrier movement (c_{speed}) at a constant c_f of 4.5 on the interfacial film behavior was analyzed. Upon compression at a c_{speed} of 25 mm/min a maximum change in surface pressure $\Delta\pi_{max}$ of 56.2 mN/m resulted (Fig. 6A). At a higher compression speed of 55 mm/min the maximum change in surface pressure of $\Delta\pi_{max} = 35.7$ mN/m was lower compared to the one resulting at slower compression speed. This could be explained by the fact that faster compression does not allow the molecules to reorder to the same degree, hence packing density is lower, resulting in a lower maximum surface pressure change. Figure 6D shows the progression of surface pressure over time in the compressed state. Independent from c_{speed} the surface pressure decreased by about 20 mN/m within 3 h which can be explained by a decreasing amount of protein material within the film. Furthermore, high compression speeds above 55 mm/min did not further affect the film properties as the curve progression of 55 mm/min and 95 mm/min largely overlap. The persisting elevated surface pressure compared to the equilibrium surface pressure reached

after adsorption indicates the presence of a more concentrated and densely packed film similar as described for the effect of different compression factors.

Overall, the curve progression of each subsequent cycle was almost identical but ended up at marginally lowered quasi-equilibrium surface pressure values after each cycle at A_{\max} . This can be due to a loss of material from the interface due to a rupture of the protein film upon decompression. Furthermore, Petkov *et al.* described a high degree of reproducibility and symmetry between separate compressions and expansions of a β -lactoglobulin film at the liquid-air interface [45]. However, compression was performed at a much lower speed of 0.5 mm/s and the interfacial area was compressed by 2% only [45].

Consequently, compression of the interfacial film caused a pronounced increase in surface pressure, particularly at compression by a factor above 3. In addition, slower compression below 55 mm/min resulted in a much higher surface pressure increase compared to faster compression.

4.3. Presence and Secondary Structure of the IgG at the Interface

A comparison of secondary structural elements of the antibodies investigated by FT-IR in solution and by IRRAS at the interface allows conclusions about possible changes during adsorption and subsequent compression. The amide bands in the IRRAS spectra of mAB₁ and mAB₂ (Fig. 7A-D) gave evidence for the presence of the proteins at the liquid-air interface. The amide bands of mAB₂ appear more distinctive compared to mAB₁. The position of the amide bands does not differ considerably between the two mABs. The strongest amide I contributions are observed at 1639 cm⁻¹ and 1659 cm⁻¹, and in the amide II region around 1551 cm⁻¹ and at 1531 cm⁻¹ for mAB₁ and at 1535 cm⁻¹ for mAB₂. This indicates that the mABs adopt mainly intramolecular β -sheet and unordered random coil conformations at the interface [57]. The intensity, in particular of the OH-stretching vibration around 3580 cm⁻¹, increased upon compression of the interfacial film. This intensity increase as well as that of the amide bands upon compression indicates an increase in interfacial protein concentration and effective film thickness [5], [58]–[60]. The position of the amide I band and thus the mAB secondary structure did not change during compression of the film.

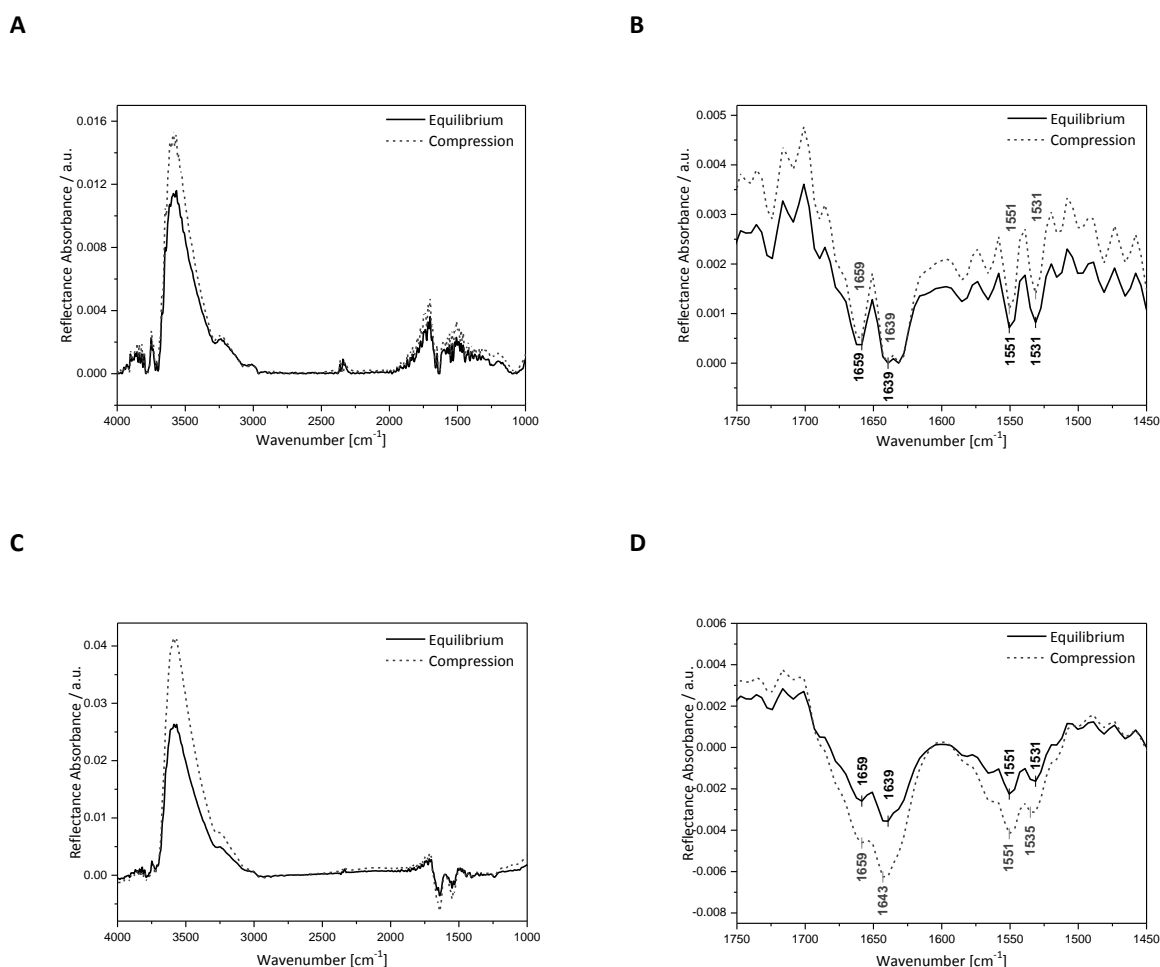


Figure 7: IRRA spectra of mAB₁ after adsorption to equilibrium surface pressure $\Pi=13.5$ mN/m (solid line) and after compression by 15 mN/m (broken line), A: entire mAB₁ IRRA spectra; B: mAB₁ amide I and II region, and I of mAB₂ after adsorption to equilibrium surface pressure $\Pi=14.4$ mN/m (solid line) and after compression by 15 mN/m (broken line), C: entire mAB₂IRRA spectra; D: mAB₂ amide I and II region

FT-IR spectra of mAB₁ and mAB₂ in solution revealed a maximum of the amide I band at 1639 cm^{-1} indicating a high intramolecular β -sheet contribution (Fig. 8). The IRRA spectra after adsorption and compression do not demonstrate new peaks referring to new structural elements. In contrast, conformational changes induced by heat stress are connected with strong peak shifts from the native intramolecular β -sheet structure towards a more unordered structure. Thus, adsorption and compression of the two mABs investigated in this study did not cause measurable changes in secondary structure compared to bulk solution. According to literature, IR methods cover changes of $\geq 2 - 10\%$ in sensitivity [57], [61]. Minor structural perturbations, however, cannot be excluded. Damonodaran *et al.* stated that globular proteins essentially remain in the globular shape at the liquid-air interface [47]. Similarly, Roach *et al.* described the high surface curvature to be causative for the stabile

structure of the globular albumin [62]. In contrast, fibrinogen, being rather rod like, gets distorted by wrapping around surface curvature thereby inducing secondary structure loss. Hence, structural rearrangements have been shown to be protein-specific [28].

Finally, the mABs investigated in this study remain in a native-like conformation with a distinctive band of intermolecular β -sheet structure.

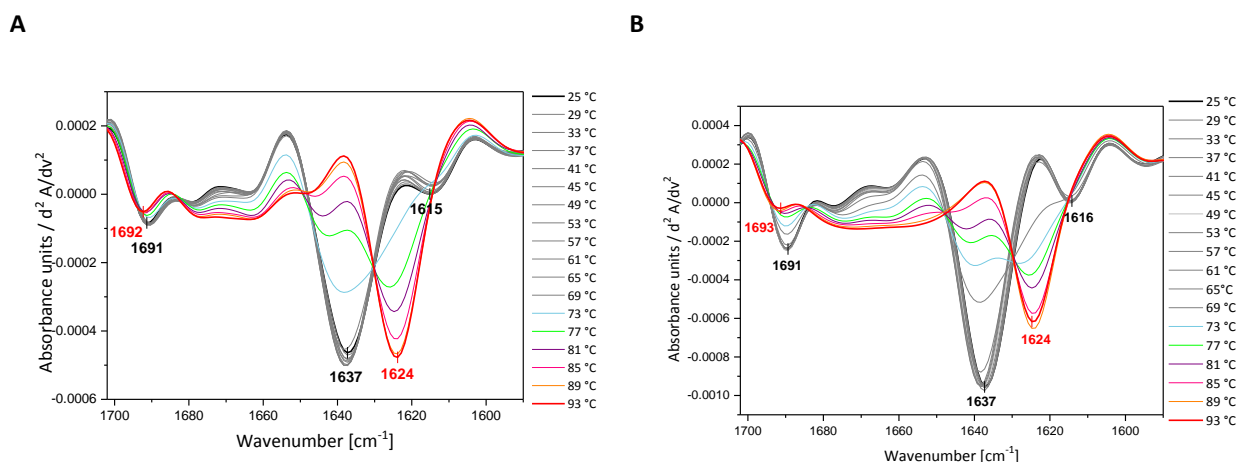


Figure 8: Temperature-induced unfolding of A: mAB₁ and B: mAB₂ from 25 – 93 °C in steps of 4 °C using FT-IR spectroscopy

4.4. Structural and Morphological Characterization of the Liquid-Air Interfacial Protein Film

Brewster-Angle Microscopy in connection to a Langmuir trough was used to additionally visualize and analyze the interfacial protein film morphology. The buffer control yields no signal and the surface appeared dark as no light is reflected at the Brewster angle [66], [67]. Island-like structures appeared during adsorption and indicate an inhomogeneous distribution of protein across the interface. Both mABs did not reveal considerable changes in film morphology with increasing surface pressure during adsorption and compression. For mAB₁, a heterogeneous distribution of the protein across the interface can be assumed, as clods of increased brightness indicating densely packed protein material exist next to darker areas representing regions of a homogeneous and thin protein film (Fig. 9). In contrast, mAB₂ showed an overall increased grey level with less pronounced island-like structures, and line-type structures suggest protein layers of different packing density or film thickness being aligned next to each other (Fig. 10). BAM images did not reveal considerable differences in the interfacial film structure upon compression or decompression. Overall, BAM

demonstrates that protein material accumulates at the interface resulting in inhomogeneously distributed clusters. The observed areas of increased packing density or film thickness might represent an early stage of protein particles when brought into solution by e.g. interfacial stress. This is in accordance with previous studies where heterogeneous structures and regions with different thickness were visualized in a liquid-air interfacial film of soy protein and the existence of large regions of agglomerated protein at the interface was assumed [66]. Particularly, interactions between protein molecules have been ascribed to be responsible for the formation of clusters of different proteins at interfaces [68].

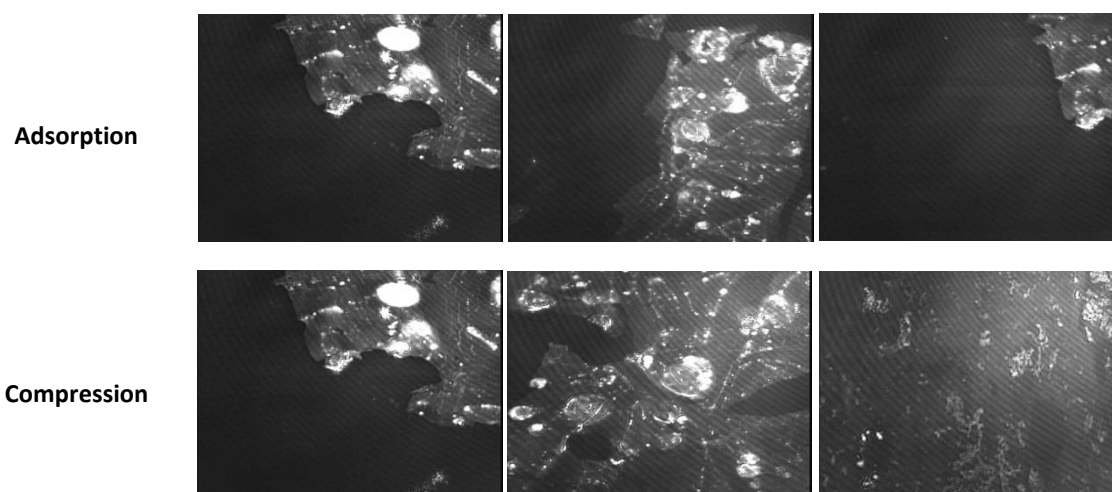


Figure 9: BAM images of mAB₁ during adsorption and compression (with increasing surface pressure from left to right)

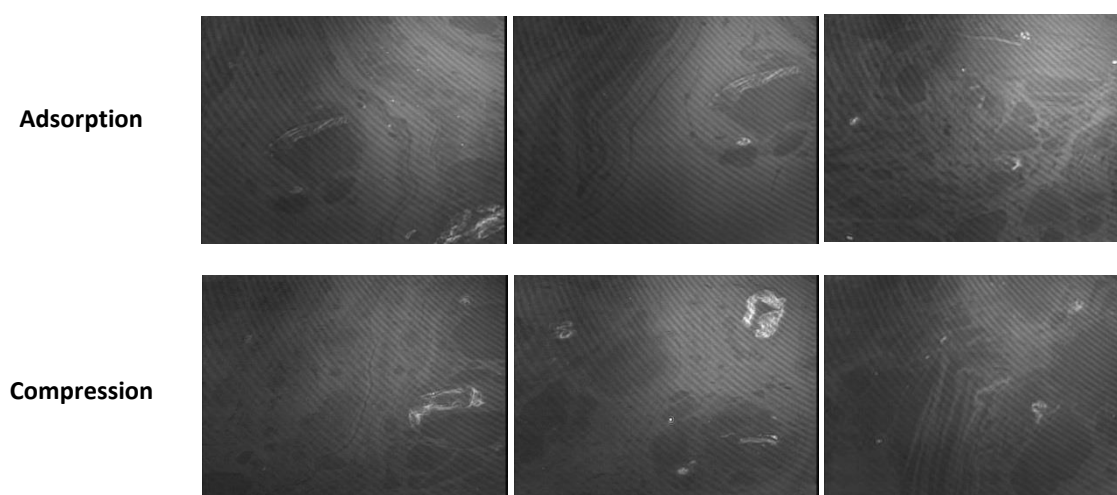


Figure 10: BAM images of mAB₂ during adsorption and compression with increasing surface pressure from left to right)

4.5. Particle Formation by Agitation

Agitation studies were performed to evaluate the impact of mechanical stress by shaking on the emergence of protein particles, as it is typically performed during formulation development. Shaking renders a repeated compression and decompression of the interface, in a way similar to Langmuir measurements. However, a less aging of the interface has to be considered as this directly affects the interfacial film characteristics as well as particle formation [5], [42]. Furthermore, effects such as turbulent flow by overturning of liquid or cavitation may result in additional mechanical stresses that impact protein particle formation [14], [34], [35]. Shaking studies in vials sealed with a glass stopper to minimize the impact of contact materials caused significantly elevated numbers of particles. After 48 hours of shaking, the visual particles with a mean value of 1.3 of categories 0 – 3 and around 50,000 particles $> 1\mu\text{m}$ / mL were formed, accompanied by an increase in turbidity (Figs. 11, 12). Moreover, in vials filled without headspace and therefore in absence of liquid-air interfaces no particle were formed what is in good accordance with studies by Kiese *et al.* [13]. To evaluate this in comparison with protein films formed at the interface, shaking was additionally performed in presence of a glass needle. Upon disturbance of the interface during shaking a high number of visible (category 3) and subvisible particles built up with around 200,000 particles $> 1\mu\text{m}$ / mL accompanied by an increase in turbidity up to 7.6 FTU. In case the vials including the glass needle were filled without any headspace no considerable particle formation occurred. This again can be traced back to the fact that with the absence of headspace also the presence of a liquid-air interface was excluded what ruled out protein accumulation and therefore also any interfacial disturbance [13].

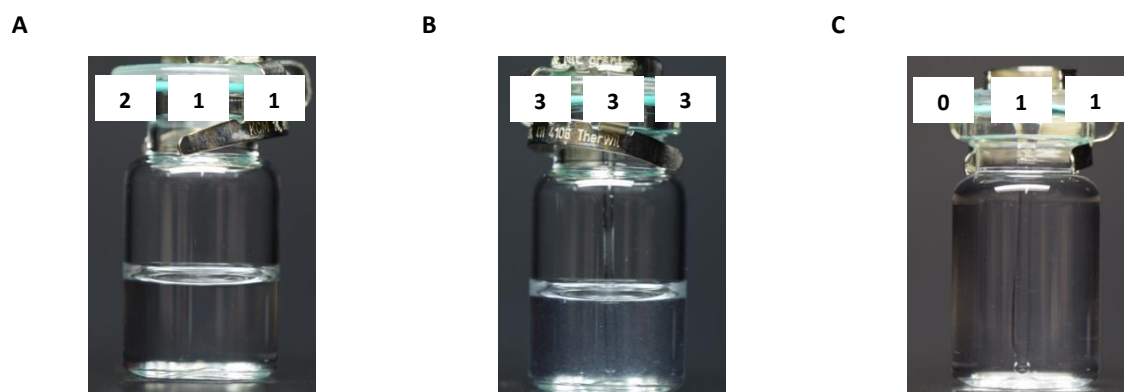


Figure 11: Photo documentation and results of the visual inspection after 48 h shaking of mAB₁ with different stopper types; A: Glass Stopper, B: Glass Stopper + Needle, C: Glass Stopper + Needle without headspace

In a similar way, Rudiuk *et al.* showed that upon transient breakage of the liquid-air interface by a stainless steel needle large protein particles are released from the interface. Furthermore, they stated that so-called primary surface aggregates stay at the interface and do not penetrate into the bulk in the absence of external triggers [22]. Similar findings were reported by Metha *et al.* who showed that rupture of the viscoelastic gel formed at the silicone oil–water interface resulted in particle formation [48], [69]. Gerhardt *et al.* showed that without movement of an air bubble, the protein gel layer formed at the silicone oil–water interface was not disrupted and no particle formation took place [23]. A study by Maa *et al.* pointed out that shear, induced by using a nitrogen bubbling method, in presence of a liquid-air interface caused aggregation of recombinant human growth hormone (rhGH) and aggregation was found to increase with increasing protein concentration and interfacial area [70].

Although the presence of the interface was shown to be involved in the aggregation process in all cases, a direct localization and evaluation of impact factors that contribute to the underlying mechanisms is not given. Ultimately, only the use of a physical-chemical characterization of the IgG at the liquid-air interface in direct combination with controlled interfacial stress at the interface exclusively will allow a mechanistic understanding of interface-induced protein aggregation. Therefore, a model was developed to investigate the effect of liquid-air interfacial stress only on protein particle formation.

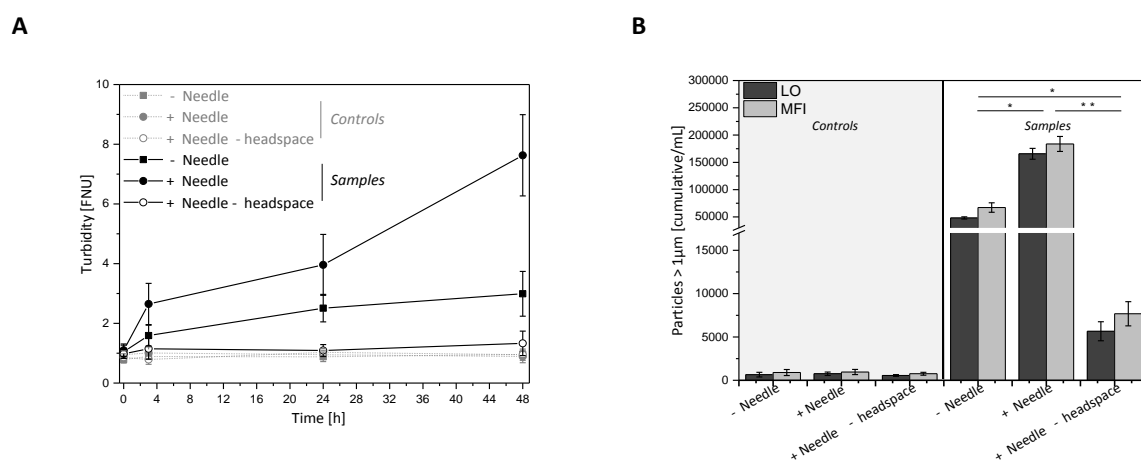


Figure 12: Shaking of mAB₁ (= samples) and buffer (= controls) with different stopper types (glass stopper, glass stopper + needle, glass stopper + needle without headspace), A: turbidity during 48 h shaking, B: number of particles > 1 μm/mL after 48 h shaking

4.6. Particle Formation in the Mini-Trough by Liquid-Air Interfacial Stress Only

A Mini-trough with identical dimensions as the Langmuir trough but on a smaller scale was developed to investigate whether automated, repeated compression and decompression of the interfacial film only can cause the formation of particles. Above that, the Mini-trough enables to analyze the influence of compression speed and factor on the extent of particle formation.

Only very low numbers of particles were detected in unstressed protein solutions by LO and MFI. In contrast, 100 compression-decompression cycles of a 1 mg/mL mAB₁ solution after reaching equilibrium surface pressure caused the formation of significant amounts of particles amounting to around 6000 particles >1 $\mu\text{m}/\text{mL}$ (Fig. 13A). Furthermore, repeated compression and decompression was performed at different c_f and c_{speed} . Figure 13B demonstrates that the number of particles formed was strongly dependent on c_f . Compression by a factor of 2 (at a constant c_{speed} of 55 mm/min) did not cause substantial particle formation. Significant particle formation set in at a c_f of 3 and increased up with increasing compression factor reaching a plateau at c_f values of 8.3 and above. Also, c_{speed} was proven to directly influence the number of particles formed. Already at a c_{speed} of 25 mm/min (at a constant c_f of 8.3) a pronounced number of particles formed upon repeated compression and decompression. However, figure 13C reveals less particle formation at a c_{speed} of 25 mm/min compared to higher c_{speed} . No considerable differences were noticeable at compression speeds higher than 55 mm/min where the number of particles overall ranged between 6000-8000 particles >1 $\mu\text{m}/\text{mL}$. Therefore, both c_f and c_{speed} substantially affected not only the interfacial film behavior as indicated by the surface pressure measurements, but also the formation of particles by interfacial stress only.

Thus, a rupture of the highly concentrated film, especially during decompression, can result in the release of clustered protein material into bulk solution. The island-like distribution of protein observed in the BAM images goes in line with this hypothesis. Furthermore, this assumption is supported by findings of van Aken *et al.* where interfacial compression in a Langmuir trough, equipped with a computer-controlled barrier transport system, caused an increase in surface pressure [71]. Depending on the rate of compression and the type of protein (β -casein, β -lactoglobulin, BSA), sudden drops of the surface pressure were observed during compression that were described to arise from tearing or wrinkling of the adsorbed

protein layer [71]. Using a custom-built bubble tensiometer, Lin *et al.* investigated the effect of continuous contraction of a mAB adsorbed to the liquid-air interface [42]. Deformation of the interface caused a reduction in surface area and forced the adsorbed protein molecules into close proximity of each other. Further contraction provided visual evidence to eventually cause ejection of large, protein aggregates from the interface [42]. Bee *et al.* applied a cyclic compression of an IgG₁ antibody adsorbed to the liquid-air interface where similar findings were observed with regard to hysteresis and compression decompression behavior [40]. Moreover, 6.5 hours of continuous periodic compressions/dilations trough resulted in a very slight increase in visible proteinaceous particles. More comprehensively, however, interface-related aggregation was investigated using rotating vials, meaning an end-over-end rotation where the interface passed through a geometrical maximum and minimum area what resulted in protein particle formation. Therefore, it was hypothesized aggregation takes place at the interface followed by detachment into the bulk solution [40]. The compression ratio was varied via the selection of vial dimensions and ranged between a ratio of 2.9 : 0.78 (= 3.72) to 8.0 : 0.77 (= 10.39). The rotation rate was set to 3–14 rpm, resulting in a period of about 4 to 20 s per rotation. Therefore, at comparable compression factors, compression speed was chosen much higher compared to the experiments in the Mini-trough. Above that, the Mini-trough allows repeated compression-decompression of the interfacial film only without interface turnover.

Certainly, using the Mini-trough method the aggregation process can be localized and ascribed to liquid-air interfacial stress only. Therefore, it represents a valuable tool to screen different proteins and formulations for their propensity to undergo interface related-aggregation as a measure of compression factor and speed.

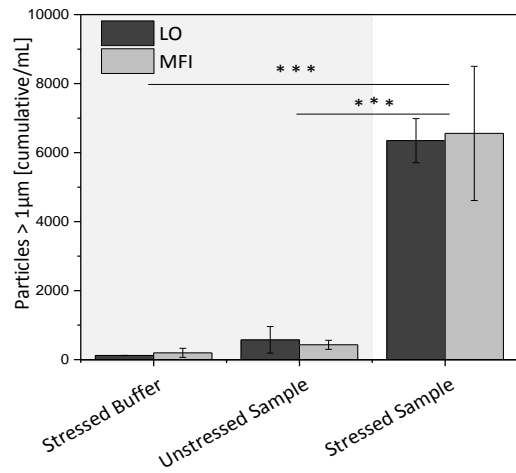
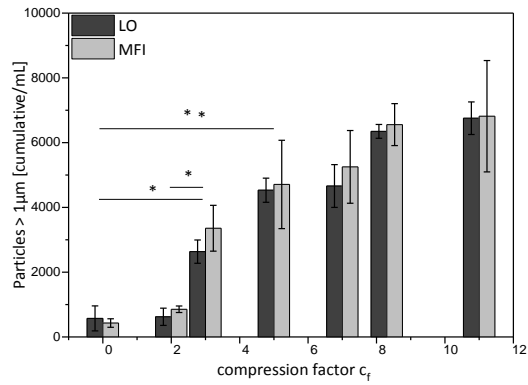
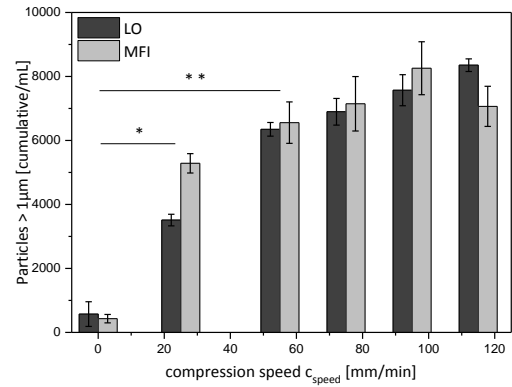
A**B****C**

Figure 12: A: Number of particles $>1 \mu\text{m/mL}$ in the Mini-trough investigated by LO and MFI, $c_f = 8.3$. Stressed buffer: buffer after 100 cycles; Unstressed sample: mAB_1 without barrier movement; Stressed sample: mAB_1 after 100 cycles; and number of particles $\geq 1 \mu\text{m/mL}$ formed for mAB_1 after 100 compression-decompression cycles, B: impact of c_f at a c_{speed} of 55 mm/min, C: impact of c_{speed} at a c_f of 8.3

5. SUMMARY & CONCLUSION

Different methodologies to characterize the liquid-air interfacial film characteristics and related aggregation processes of two IgG molecules were used. The IgGs adsorb to the liquid-air interface in a time- and concentration-dependent manner, thereby forming a coherent but inhomogeneous interfacial protein film. Clusters of protein material were detected by BAM which may represent preliminary stages of protein aggregates emerging at the liquid-at interface already during the adsorption process. Compression caused compaction and concentration within the film as it became obvious by a pronounced hysteresis. The compressibility of the interfacial film was directly affected by the speed and extent of compression. The steep decrease in surface pressure as well as the decreasing surface pressure values with each cycle, indicate a rupture of the film and a potential loss of protein material from the interface. This hypothesis was ascertained not only by a shaking study, but also by controlled compression and decompression of the interfacial film only by a newly designed Mini-trough setup. Thus, a clear connection between interfacial stress and protein particle formation was proven as compression by a factor above 3 and by a speed of 25 mm/min and above resulted in significant particle formation. Consequently, the Mini-trough method is a highly expedient method for the localization and characterization of protein particle formation by liquid-air interfacial stress only. As no major effect on secondary structure was observed by IRRAS, the IgGs are assumed to remain in a native-like conformation. Therefore, we conclude that a major cause of the emergence of large native-like protein particles is a compaction of protein material accompanied by increased protein-protein-interactions, followed by a rupture of the interfacial protein film.

Although considerable effort has been put to gain better understanding of how protein films are characterized and how they behave upon interfacial stress, whether unfolding takes place or not, and how large particles emerge in the bulk, the mechanistic details have not been generally answered to date. Particularly, previous approaches used different and heterogeneous analytical tools to characterize the physicochemical behavior at the interface on the one hand and interface-induced aggregation on the other. The characterization of not only the interfacial film but also the interface-related aggregation process itself by a trough method exclusively has not been described before.

Finally, this approach allows a direct correlation of interfacial stress only and the formation of protein particles. In addition, the Mini-trough method represents a useful tool to screen

different formulations, as it can be directly analyzed whether the condition or additive chosen has a protective effect on interface-related protein aggregation, which is one of the major challenges in the development of protein pharmaceuticals.

6. REFERENCES

- [1] L. O. Narhi, J. Schmit, K. Bechtold-Peters, and D. Sharma, "Classification of protein aggregates.," *J. Pharm. Sci.*, vol. 101, no. 2, pp. 493–8, 2012.
- [2] W. Wang, S. Nema, and D. Teagarden, "Protein aggregation-Pathways and influencing factors," *Int. J. Pharm.*, vol. 390, no. 2, pp. 89–99, 2010.
- [3] E. Chi, S. Krishnan, B. B. S. Kendrick, B. S. Chang, J. F. Carpenter, and T. W. Randolph, "Roles of conformational stability and colloidal stability in the aggregation of recombinant human granulocyte colony-stimulating factor," *Protein Sci.*, vol. 12, pp. 903–913, 2003.
- [4] J. Wiesbauer, R. Prassl, and B. Nidetzky, "Renewal of the air-water interface as a critical system parameter of protein stability: Aggregation of the human growth hormone and its prevention by surface-active compounds," *Langmuir*, vol. 29, no. 49, pp. 15240–15250, 2013.
- [5] E. Koepf, R. Schroeder, G. Brezesinski, and W. Friess, "The film tells the story: Physical-chemical characteristics of IgG at the liquid-air interface," *Eur. J. Pharm. Biopharm.*, vol. 119, pp. 396–407, 2017.
- [6] C. Zhou, J.-M. Friedt, A. Angelova, K.-H. Choi, L. Wim, F. Frederix, L. Francis, A. Campitelli, Y. Engelborghs and G. Borghs, "Human immunoglobulin adsorption investigated by means of quartz crystal microbalance dissipation, atomic force microscopy, surface acoustic wave, and surface plasmon resonance techniques.," *Langmuir*, vol. 20, no. 11, pp. 5870–5878, 2004.
- [7] Z. Liao, J. W. Lampe, P. S. Ayyaswamy, D. M. Eckmann, and I. J. Dmochowski, "Protein assembly at the air-water interface studied by fluorescence microscopy.," *Langmuir*, vol. 27, pp. 12775–81, 2011.
- [8] K. Nakanishi, T. Sakiyama, and K. Imamura, "On the adsorption of proteins on solid surfaces, a common but very complicated phenomenon," *Biosci. Bioeng.*, vol. 91, no. 3, pp. 233–244, 2001.

-
- [9] P. Roach, D. Farrar, and C. C. Perry, "Interpretation of Protein Adsorption : Surface-Induced Conformational Changes Interpretation of Protein Adsorption : Surface-Induced Conformational Changes," *J. Am. Chem. Soc.*, vol. 127, no. 22, pp. 8168–8173, 2005.
- [10] H. J. Lee, A. McAuley, K. F. Schilke, and J. McGuire, "Molecular origins of surfactant-mediated stabilization of protein drugs," *Adv. Drug Deliv. Rev.*, vol. 63, no. 13, pp. 1160–1171, 2011.
- [11] T. Serno, E. Härtl, A. Besheer, R. Miller, and G. Winter, "The Role of Polysorbate 80 and HP β CD at the Air-Water Interface of IgG Solutions," *Pharm. Res.*, pp. 1–14, 2012.
- [12] A. Hawe and W. Friess, "Formulation development for hydrophobic therapeutic proteins.," *Pharm. Dev. Technol.*, vol. 12, no. October, pp. 223–237, 2007.
- [13] S. Kiese, A. Papppenberger, W. Friess, and H. C. Mahler, "Shaken, not stirred: Mechanical stress testing of an IgG1 antibody," *J. Pharm. Sci.*, vol. 97, no. 10, pp. 4347–4366, 2008.
- [14] A. Eppler, M. Weigandt, A. Hanefeld, and H. Bunjes, "Relevant shaking stress conditions for antibody preformulation development," *Eur. J. Pharm. Biopharm.*, vol. 74, no. 2, pp. 139–147, 2010.
- [15] C. J. Beverung, C. J. Radke, and H. W. Blanch, "Protein adsorption at the oil/water interface: Characterization of adsorption kinetics by dynamic interfacial tension measurements," *Biophys. Chem.*, vol. 81, no. 1, pp. 59–80, 1999.
- [16] K. A. Dill, S. Bromberg, K. Yue, K. M. Fiebig, D.P. Yee, P.D. Thomas, and H. Chan, "Principles of protein folding--a perspective from simple exact models," *Protein Sci.*, vol. 10, no. 4, pp. 561–602, 1995.
- [17] E. Dickinson, "Mixed biopolymers at interfaces: Competitive adsorption and multilayer structures," *Food Hydrocoll.*, vol. 25, no. 8, pp. 1966–1983, 2011.
- [18] V. B. Fainerman, S. A. Zholob, M. Leser, M. Michel, and R. Miller, "Competitive adsorption from mixed nonionic surfactant/protein solutions," *J. Colloid Interface Sci.*, vol. 274, pp. 496–501, 2004.

- [19] Y. F. Yano, T. Uruga, H. Tanida, H. Toyokawa, Y. Terada, M. Takagaki, and H. Yamada, "Driving Force Behind Adsorption-Induced Protein Unfolding : A Time-Resolved X-ray Reflectivity Study on Lysozyme Adsorbed at an Air / Water Interface," *Society*, no. 14, pp. 32–35, 2009.
- [20] Y. F. Yano, "Kinetics of protein unfolding at interfaces," *J. physics. Condens. matter*, vol. 24, p. 503101, 2012.
- [21] A. W. P. Vermeer, M. G. E. G. Bremer, and W. Norde, "Structural changes of IgG induced by heat treatment and by adsorption onto a hydrophobic Teflon surface studied by circular dichroism spectroscopy," *Biochim. Biophys. Acta*, vol. 1425, no. 1, pp. 1–12, 1998.
- [22] S. Rudiuk, L. Cohen-Tannoudji, S. Huille, and C. Tribet, "Importance of the dynamics of adsorption and of a transient interfacial stress on the formation of aggregates of IgG antibodies," *Soft Matter*, vol. 8, no. 9, p. 2651, 2012.
- [23] A. Gerhardt, N. R. McGraw, D. K. Schwartz, J. S. Bee, J. F. Carpenter, and T. W. Randolph, "Protein aggregation and particle formation in prefilled glass syringes," *J. Pharm. Sci.*, vol. 103, no. 6, pp. 1601–1612, 2014.
- [24] S. Ghazvini, C. Kalonia, D. B. Volkin, and P. Dhar, "Evaluating the Role of the Air-Solution Interface on the Mechanism of Subvisible Particle Formation Caused by Mechanical Agitation for an IgG1 mAb," *J. Pharm. Sci.*, vol. 105, no. 5, pp. 1643–1656, 2016.
- [25] W. Vegt, H. C. Mei, H. J. Busscher, and W. Norde, "pH dependence of the kinetics of interfacial tension changes during protein adsorption from sessile droplets on FEP-Teflon," *Colloid Polym. Sci.*, vol. 274, no. 1, pp. 27–33, 1996.
- [26] A. V. Makievski, V. B. Fainerman, M. Bree, R. Wu, and J. Kra, "Adsorption of Proteins at the Liquid / Air Interface," *Society*, vol. 5647, no. 97, pp. 417–425, 1998.
- [27] V. S. Alahverdijeva, D. O. Grigoriec, J. K. Ferri, V. B. Fainerman, E. V. Aksenenko, M. E. Leser, M. Michel, and R. Miller, "Adsorption behaviour of hen egg-white lysozyme at the air/water interface," *Colloids Surfaces A Physicochem. Eng. Asp.*, vol. 323, no. 1–3, pp. 167–174, 2008.

- [28] Y. F. Yano, E. Arakawa, W. Voegeli, and T. Matsushita, "Real-time investigation of protein unfolding at an air–water interface at the 1 s time scale," *J. Synchrotron Radiat.*, vol. 20, pp. 980–983, 2013.
- [29] M. B. J. Meinders and H. H. J. De Jongh, "Limited conformational change of β -lactoglobulin when adsorbed at the air-water interface," *Biopolym. - Biospectroscopy Sect.*, vol. 67, no. 4–5, pp. 319–322, 2002.
- [30] A. H. Martin, M. B. J. Meinders, M. A. Bos, M. A. Cohen Stuart, and T. van Vliet, "Conformational Aspects of Proteins at the Air/Water Interface Studied by Infrared Reflection - Absorption Spectroscopy," *Langmuir*, vol. 19, no. 7, pp. 2922–2928, 2003.
- [31] A. J. Freitag, M. Shmali, S. Michalakis, M. Biel, M. Siedler, Z. Kaymakcalan, J. F. Carpenter, T. W. Randolph, G. Winter, and J. Engert, "Investigation of the Immunogenicity of Different Types of Aggregates of a Murine Monoclonal Antibody in Mice," *Pharm. Res.*, vol. 32, no. 2, pp. 430–444, 2015.
- [32] J. Den Engelsman, P. Garidel, R. Smulders, H. Knoll, B. Smith, S. Bassarab, A. Seidl, O. Hainzl, and W. Jiskoot, "Strategies for the Assessment of Protein Aggregates in Pharmaceutical Biotech Product Development," *Pharm. Res.*, vol. 28, no. 4, pp. 920–933, 2011.
- [33] H. C. Mahler, R. Müller, W. Frieß, A. Delille, and S. Matheus, "Induction and analysis of aggregates in a liquid IgG1-antibody formulation," *Eur. J. Pharm. Biopharm.*, vol. 59, pp. 407–417, 2005.
- [34] J. S. Bee, J. L. Stevenson, B. Mehta, J. Svitel, J. Pollastrini, R. Platz, E. Freund, J. F. Carpenter, and T. W. Randolph, "Response of a concentrated monoclonal antibody formulation to high shear," *Biotechnol. Bioeng.*, vol. 103, no. 5, pp. 936–943, 2009.
- [35] W. Lauterborn and C.-D. Ohl, "Cavitation bubble dynamics," *Ultrason. Sonochem.*, vol. 4, pp. 65–75, 1997.
- [36] V. Sharma, A. Jaishankar, Y. Wang, and G. H. McKinley, "Rheology of globular proteins: apparent yield stress, high shear rate viscosity and interfacial viscoelasticity of bovine serum albumin solutions," *Soft Matter*, vol. 7, no. 11, p. 5150, 2011.

- [37] V. Saller, J. Pott, J. Matilainen, U. Grauschopf, K. Bechtold-peters, and W. Friess, "Particle Shedding from Silicone Tubing used for Peristaltic Pumping in Biopharmaceutical Drug Product Manufacturing," *Pharm. Drug Deliv. Pharm. Technol.*, pp. 2–3, 2015.
- [38] P. Wilde, A. Mackie, F. Husband, P. Gunning, and V. Morris, "Proteins and emulsifiers at liquid interfaces," *Adv. Colloid Interface Sci.*, vol. 108–109, pp. 63–71, 2004.
- [39] A. H. Martin, M. A. C. Stuart, M. A. Bos, and T. van Vliet, "Correlation between Mechanical Behavior of Protein Films at the Air / Water Interface and Intrinsic Stability of Protein Molecules," *Langmuir*, vol. 21, no. 9, pp. 4083–4089, 2005.
- [40] J. S. Bee, D. K. Schwartz, S. Trabelsi, E. Freund, J. L. Stevenson, J. F. Carpenter, and T. W. Ranloph, "Production of particles of therapeutic proteins at the air–water interface during compression/dilation cycles," *Soft Matter*, vol. 8, no. 40, p. 10329, 2012.
- [41] S. Amin, G. V. Barnett, J. A. Pathak, C. J. Roberts, and P. S. Sarangapani, "Protein aggregation, particle formation, characterization & rheology," *Curr. Opin. Colloid Interface Sci.*, vol. 19, no. 5, pp. 438–449, 2014.
- [42] G. L. Lin, J. A. Pathak, D. H. Kim, M. Carlson, V. Rigüero, Y. J. Kim, J. S. Buffa, and G. G. Fuller, "Interfacial dilatational deformation accelerates particle formation in monoclonal antibody solutions," *Soft Matter*, vol. 12, no. 14, pp. 3293–3302, 2016.
- [43] I. C. Shieh and A. R. Patel, "Predicting the agitation-induced aggregation of monoclonal antibodies using surface tensiometry," *Mol. Pharm.*, p. 3184–3193, 2015.
- [44] A. Savitzky and M. J. E. Golay, "Smoothing and Differentiation of Data by Simplified Least Squares Procedures," *Anal. Chem.*, vol. 36, no. 8, pp. 1627–1639, 1964.
- [45] J. T. Petkov, T. D. Gurkov, B. E. Campbell, and R. P. Borwankar, "Dilatational and shear elasticity of gel-like protein layers on air/water interface," *Langmuir*, vol. 16, no. 8, pp. 3703–3711, 2000.
- [46] R. Wüstneck, J. Krägel, R. Moller, V. B. Fainerman, P. J. Wilde, D. K. Sarker, D. C. Clark, "Dynamic surface tension and adsorption properties of β -casein and β -lactoglobulin," *Food Hydrocoll.*, vol. 10, no. 4, pp. 395–405, 1996.

- [47] S. Damodaran and L. Razumovsky, "Role of surface area-to-volume ratio in protein adsorption at the air-water interface," *Surf. Sci.*, vol. 602, no. 1, pp. 307–315, 2008.
- [48] S. B. Mehta, R. Lewus, J. S. Bee, T. W. Randolph, and J. F. Carpenter, "Gelation of a monoclonal antibody at the silicone oil-water interface and subsequent rupture of the interfacial gel results in aggregation and particle formation.," *J. Pharm. Sci.*, vol. 104, no. 4, pp. 1282–90, 2015.
- [49] E. Dickinson, "Adsorbed protein layers at fluid interfaces: Interactions, structure and surface rheology," *Colloids Surfaces B Biointerfaces*, vol. 15, no. 2, pp. 161–176, 1999.
- [50] L. A. Pugnali, R. Ettelaie, and E. Dickinson, "Do mixtures of proteins phase separate at interfaces?," *Langmuir*, vol. 19, no. 6, pp. 1923–1926, 2003.
- [51] I. S. Chronakis, A. N. Galatanu, T. Nylander, and B. Lindman, "The behaviour of protein preparations from blue-green algae (*Spirulina platensis* strain Pacifica) at the air/water interface," *Colloids Surfaces Physicochem. Eng. Asp.*, vol. 173, no. 1–3, pp. 181–192, 2000.
- [52] R. R. Niño. C. C. Sánchez, and J. M. R. Patino, "Interfacial characteristics of β -casein spread films at the air-water interface," *Colloids Surfaces B Biointerfaces*, vol. 12, no. 3–6, pp. 161–173, 1999.
- [53] J. M. Rodríguez Patino, C. C. Sánchez, M. R. Rodríguez Niño, "Structural and morphological characteristics of β -casein monolayers at the air–water interface," *Food Hydrocoll.*, vol. 13, no. 5, pp. 401–408, 1999.
- [54] K. Liu, Y. Tian, M. Stieger, E. Van der Linden, and F. Van de Velde, "Evidence for ball-bearing mechanism of microparticulated whey protein as fat replacer in liquid and semi-solid multi-component model foods," *Food Hydrocoll.*, vol. 52, pp. 403–414, 2016.
- [55] E. J. Grasso, R. G. Oliveira, and B. Maggio, "Rheological properties of regular insulin and aspart insulin Langmuir monolayers at the air/water interface: Condensing effect of Zn^{2+} in the subphase," *Colloids Surfaces B Biointerfaces*, vol. 115, pp. 219–228, 2014.

- [56] E. Dickinson, *Food Colloids: Interactions, Microstructure and Processing*. Cambridge: Royal Society of Chemistry (Great Britain), 2004.
- [57] J. Kong and S. Yu, "Fourier transform infrared spectroscopic analysis of protein secondary structures," *Acta Biochim. Biophys. Sin. (Shanghai)*, vol. 39, no. 8, pp. 549–559, 2007.
- [58] A. Meister, A. Kerth, and A. Blume, "Interaction of Sodium Dodecyl Sulfate with Dimyristoyl- sn -glycero-3-phosphocholine Monolayers Studied by Infrared Reflection Absorption Spectroscopy . A New Method for the Determination of Surface Partition Coefficients," pp. 8371–8378, 2004.
- [59] C. Schwieger, B. Chen, C. Tschierske, J. Kressler, and A. Blume, "Organization of T-shaped facial amphiphiles at the air/water interface studied by infrared reflection absorption spectroscopy," *J. Phys. Chem. B*, vol. 116, no. 40, pp. 12245–56, 2012.
- [60] V. S. Alahverdjieva, K. Khristov, D. Exerowa, and R. Miller, "Correlation between adsorption isotherms, thin liquid films and foam properties of protein/surfactant mixtures: Lysozyme/C10DMPO and lysozyme/SDS," *Colloids Surfaces A Physicochem. Eng. Asp.*, vol. 323, no. 1–3, pp. 132–138, 2008.
- [61] M. Jackson and H. H. Mantsch, "The use and misuse of FTIR spectroscopy in the determination of protein structure.," *Crit. Rev. Biochem. Mol. Biol.*, vol. 30, no. 2, pp. 95–120, 1995.
- [62] P. Roach, D. Farrar, and C. C. Perry, "Surface tailoring for controlled protein adsorption: Effect of topography at the nanometer scale and chemistry," *J. Am. Chem. Soc.*, vol. 128, no. 12, pp. 3939–3945, 2006.
- [63] S. de Jong, T. van Vliet, and H. H. J. de Jongh, "The contribution of time-dependent stress relaxation in protein gels to the recoverable energy that is used as a tool to describe food texture," *Mech. Time-Dependent Mater.*, vol. 19, no. 4, pp. 505–518, 2015.
- [64] S. Zölls, M. Wiggenghorn, R. Tantipolphan, G. winter, W. Jiskoot, W. Friess, and A. Hawe, "Particles in Therapeutic Protein Formulations, Part 1: Overview of Analytical Methods," *J. Pharm. Sci.*, vol. 101, no. 10, pp. 914–935, 2012.

- [65] T. Menzen and W. Friess, "Temperature-ramped studies on the aggregation, unfolding, and interaction of a therapeutic monoclonal antibody," *J. Pharm. Sci.*, vol. 103, no. 2, pp. 445–455, 2014.
- [66] R. R. Niño, C. C. Sánchez, V. P. Ruíz-Henestrosa, and J. M. M. Patino, "Milk and soy protein films at the air-water interface," *Food Hydrocoll.*, vol. 19, no. 3, pp. 417–428, 2005.
- [67] F. F. O. Sousa, A. Luzardo-Álvarez, J. Blanco-Méndez, F. J. Otero-Espinar, M. Martín-Pastor, and I. Sández Macho, "Use of ¹H NMR STD, WaterLOGSY, and Langmuir monolayer techniques for characterization of drug-zein protein complexes," *Eur. J. Pharm. Biopharm.*, vol. 85, no. 3, pp. 790–798, 2013.
- [68] M. Kastantin, B. B. Langdon, and D. K. Schwartz, "A Bottom-Up Approach to Understanding Protein Layer Formation at Solid-Liquid Interfaces," *Adv Colloid Interface Sci*, vol. 0, no. 1, p. 240.252, 2014.
- [69] S. B. Mehta, J. F. Carpenter, and T. W. Randolph, "Colloidal Instability Fosters Agglomeration of Subvisible Particles Created by Rupture of Gels of a Monoclonal Antibody Formed at Silicone Oil-Water Interfaces," *J. Pharm. Sci.*, vol. 105, no. 8, pp. 2338–2348, 2016.
- [70] Y. F. Maa and C. C. Hsu, "Protein denaturation by combined effect of shear and air-liquid interface," *Biotechnol. Bioeng.*, vol. 54, no. 6, pp. 503–12, 1997.
- [71] G. A. Van Aken and M. T. E. Merks, "Adsorption of soluble proteins to dilating surfaces," *Colloids Surfaces A Physicochem. Eng. Asp.*, vol. 114, pp. 221–226, 1996.
-

THIS CHAPTER IS INTENDED FOR PUBLICATION:

Koepf E, Eisele S, Schroeder R, Brezesinski G, Friess W. Notorious But Not Understood: How Liquid-Air Interfacial Stress Triggers Protein Aggregation, *International Journal of Pharmaceutics*, submitted on 2017/10/30.

CHAPTER V

MOVE ALONG PLEASE! HOW FORMULATION ADDITIVES AFFECT LIQUID-AIR INTERFACE RELATED PROTEIN INSTABILITY

1. ABSTRACT

The addition of formulation additives is a popular option to protect protein formulations against interface-based stress. However, the addition of surfactants is connected with concerns regarding their variable quality, analytics, and possible negative effects on protein stability. Understanding the behavior of both the protein and the additive at the interface is mandatory for the decision whether and which one to add. In this study, polysorbate 80 (PS 80), poloxamer 188 (P 188), as well as hydroxypropyl- β -cyclodextrin (HP- β -CD) were investigated. Surface pressure measurements combined with studying the interfacial film compressibility allowed conclusions about its composition. Whilst IgG films were highly compressible, compression of an additive solution did not result in a considerable increase in surface pressure. The mixtures exhibit either IgG- or additive-like characteristics depending on the mixing ratio. The appearance of amide bands in Infrared-Reflection-Absorption (IRRA) spectra proved the presence of IgG at the interface in case of mixtures with PS 80 present at concentrations of 0.001 mg/mL and below, and therefore below the critical micellar concentration (CMC). In formulations with 0.01 mg/mL PS 80, 0.01 mg/mL P 188, or 0.349 mg/mL HP- β -CD and above, no amide bands were detected indicating that the interface is fully occupied by the additive molecules. Additive solutions did not supply any signal in Brewster Angle Microscopy (BAM). Therefore, island-like bright domains can be traced back to the presence of IgG clusters at the interface. BAM images demonstrated the presence of IgG molecules at high PS 80 concentrations above CMC (0.01 mg/mL and higher). Similarly, residual IgG clusters were detected in mixtures of IgG with 1 mg/mL P 188 or 34.9 mg/mL HP- β -CD. Clusters of telescoped protein material were detected after

compression of IgG films in Atomic Force Microscopy (AFM) images. In contrast, PS 80 solutions formed smooth and flat films which were not affected by compressive forces. Moreover, at a very low PS 80 concentration of 0.00005 mg/mL bright domains of increased height representing agglomerated protein emerged upon compression. Furthermore, a drastically increased particle formation both upon agitation as well as in repeated compression-decompression experiments was observed. The presence of PS 80 0.01 mg/mL and above, or P 188 0.1 mg/mL and above prevented agitation induced aggregation effectively. Also, HP- β -CD successfully inhibited aggregation at concentrations of 3.49 mg/mL and above, although to a lesser extent. Thus, the combination of the different surface sensitive methods with interfacial stress studies provided new insights into the complex behavior of IgG molecules and formulation additives at the liquid-air interface and a better understanding of interface related protein aggregation.

2. INTRODUCTION

Both chemical and physical stability of protein drugs have to be assured to demonstrate the quality of a drug product [1]. Different to typical small molecule drugs, protein pharmaceuticals are susceptible to physical changes, such as adsorption to hydrophobic interfaces, denaturation and aggregation [2]. Therefore, the successful development of a protein pharmaceutical requires careful assessment of the various possible degradation pathways and a thorough understanding of the mechanisms behind protein aggregation. To overcome these challenges, pH and ionic strength adjustment as well as the addition of excipients are typical strategies for protein stabilization [3]–[6]. In general, formulation additives are frequently utilized as they are known to successfully inhibit surface-induced protein aggregation. Nevertheless, little is known so far about the underlying mechanisms of stabilization [7]. Surfactants, specifically polysorbate 20 (PS 20) and 80 (PS 80) or poloxamer 188 (P 188), belong to the most commonly used additives to stabilize against interface-related mechanical stress [8]. As surfactant molecules exhibit a pronounced surface activity and are much smaller in size, adsorption at interfaces is much faster compared to the proteins. Proteins form a strong viscoelastic network at interfaces. In these films the protein molecules are rather immobilized, tend to stay at the interface and do not readily desorb upon compression [9]. In contrast, surfactants have a high degree of mobility at interfaces [10]. Surfactants can therefore stabilize protein formulations by preferential adsorption to the liquid-air interface, thereby excluding the protein molecules from the interface. By this, PS 80 can suppress aggregation e.g. upon agitation [11]–[13]. Whereas protein molecules tend to strongly interact with one another, surfactants rather move in the direction of the surface tension gradient, as described by the Gibbs–Marangoni effect [14]. Polysorbates were found to prevent protein adsorption by sterically inhibiting proteins from associating with the interface, although no significant surfactant–protein association is assumed to occur in solution [7]. Poloxamers with their collapsed polypropylene oxide (PPO) block form unimeric micelles and higher ordered aggregates and show complex association behavior in solutions [15]. The CMC was found to vary over a wide concentration range depending on temperature and molecular weight [16], [17]. As mechanism of action, poloxamers are thought to form surfactant–protein complexes in solution, independent of their affinity for the interface thereby inhibiting protein adsorption to the interface [15]. Moreover, association into protein-surfactant complexes has been reported for P 188 preventing

proteins from adsorption to surfaces and aggregation. Poloxamers are not expected to form micelles in water except at very high concentrations [7], [18].

Although the inclusion of surfactants in protein formulation brings benefits, they might also come along with some destabilizing effects. For instance, surfactants can stimulate the oxidation of protein molecules, and fatty acids derived from surfactants may induce protein aggregation [19]. Therefore, cyclodextrins, specifically hydroxypropyl- β -cyclodextrin (HP- β -CD), may present an alternative to surfactants [20], [21]. Their ability to suppress aggregation is explained by their ability to bind to exposed hydrophobic amino acid residues on proteins, thereby not only reducing the surface hydrophobicity of the protein but also blocking potential protein-protein interactions [21]. Also a surfactant-like mechanism of stabilization against aggregation has been reported [8], [22]. For example, a stabilizing effect comparable to PS 80 was shown for HP- β -CD upon shaking of a protein solution [23]. In addition, sugar-like effects, particularly based on water replacement, have to be considered [20], [22], [24]. Typically, the critical micellar concentration (CMC) serves as a first reliable hint for the surfactant concentration required to achieve a sufficient stabilization. However, the CMC does not completely describe the surfactant effect on surface-active protein drugs. If the surfactant stabilizes protein molecules by direct binding, the effective surfactant concentration would be related to the molar ratio of surfactant to protein, rather than the CMC [25].

This study aims on the characterization of mixed protein-additive films at the liquid-air interface for different additives and at different mixing ratios. Specifically the question will be addressed whether and if so at which concentration the additive entirely replaces the protein from the interface. This is of importance, particularly for the identification of sufficiently high additive concentrations as well as to better understand and address protein instability at the liquid-air interface. Characterization of the interfacial film composition and its properties is an important prerequisite. A combination of physicochemical investigations and interfacial stress studies was performed using PS 80, P 188 and HP- β -CD in mixtures with a human immunoglobulin (IgG). Surface pressure and compression-decompression experiments allow conclusions about the qualitative composition of the liquid-air interfacial film and thus its mechanical behavior. In combination with Infrared Reflectance-Absorbance spectroscopy (IRRAS), these results provide useful information about whether protein molecules are present at the interface. The topographical features of the liquid-air interfacial

film were analyzed by Brewster Angle microscopy (BAM) as well as by Atomic Force Microscopy (AFM). The effect of the additives at different concentration on protein particle formation was investigated in shaking stress studies as well as by continuous compression-decompression of the interface in a Mini-Trough. Consequently, this study should enable not only to draw conclusions about the impact of formulation additives on the interfacial protein behavior, but may also provide useful insights into interface-related protein aggregation.

3. MATERIALS AND METHODS

3.1. Materials

Human IgG (Beriglobin™, CSL Behring GmbH, Germany) was used for this study. The market product contains 159 mg/mL human IgG in 22 g/L Glycine and 3 g/L NaCl buffer at pH 6.8. Glycine-NaCl buffer was prepared using highly purified water (ELGA LC134, ELGA LabWater, Germany) and pH was adjusted adding NaOH. All diluted solutions were prepared by the addition of Glycine-NaCl buffer at pH 6.8. Polysorbate 80 (PS 80) was obtained from Sigma-Aldrich Chemie GmbH, Germany. The CMC of PS 80 and P 188 was determined to be 0.0026 mg/mL and 0.21 mg/mL in Glycine-NaCl buffer at 20 °C, respectively. Solutions were prepared by dilution in Glycine-NaCl buffer pH 6.8. Solutions of Poloxamer 188 from BASF, Switzerland as well as hydroxypropyl- β -cyclodextrin (HP- β -CD) from Wacker Fine Chemicals, Germany were prepared accordingly. All samples were filtered using 0.2 μ m sterile PES filters (Sterile Syringe Filter PES, VWR, Germany).

3.2. Surface Pressure Measurements

Surface activity was expressed by surface pressure Π , with $\Pi = \sigma_0 - \sigma$, where σ_0 and σ are the aqueous subphase surface tension and the surface tension of the aqueous protein solution, respectively. Surface pressure measurements were performed in a 5.9 x 39.7 cm² PTFE Langmuir trough equipped with a metal alloy dyne probe (Microtrough XS, Kibron Inc., Finland). For the determination of equilibrium surface pressures a 3 x 6 Multiwell Plate (V = 0.8 mL) was used. Results are given as mean (n=3) and standard deviation. Equilibrium adsorption pressure is defined as the maximum surface pressure that is reached by adsorption only and stable in a range of ± 0.2 mN/m within 0.5 h.

160 mL sample solution was filled into the trough for the repeated compression-decompression measurements. The surface area of the trough can be varied by two mobile PTFE barriers. Temperature was kept at 20 °C (K6-cc circulation thermostat, Peter Huber Kaeltemaschinenbau GmbH, Germany). Compression speed was set to 55 mm/min and compression-decompression cycles were conducted from a maximum surface area of $A_{\max} = 210$ cm² to $A_{\min} = 52$ cm². Compression was started after the equilibrium adsorption pressure was reached.

3.3. Agitation Studies

Agitation studies of IgG at 1 mg/mL were performed on a horizontal orbital shaker (GFL 3017, GFL, Germany) at 100 rpm for 48 h. Each vial (6R) was filled with 4 mL or filled without headspace. Borosilicate stoppers (without and with needle) are of in-house production. The needle was made by glassblowing work and therefore pulled from the center the hot glass plate in a way that it forms 3.5 cm (± 0.3 cm) glass fibers of 0.2 cm (± 0.05 cm) diameter (all in one piece). The vials were sealed using a Viton o-ring and spring steel clips KCM (Keck™ by Schott Medica, Germany).

3.4. Mini-Trough

The “Mini-Trough” was designed and manufactured in-house. It consists of a PTFE trough with same proportions and functionality as the Kibron Langmuir trough for bidirectional barrier movement described above, but was reduced in size by a factor of 4.5 (and without surface pressure measurement unit). Automated and continuous compression-decompression cycles can be performed to stress the liquid-air interface only. A sample volume of 14.5 mL was used. A plastic enclosure covers the PTFE trough and the barriers (see Fig.1) to avoid dust and entry. 100 cycles were started after an equilibration time of 2.5 h each. Compression speed (c_{speed}) and compression factor (c_f) were kept constant to 55 mm/min and 4.5, accordingly.

3.5. Particle Analysis

3.5.1. Visual Inspection and Photo-documentation

Samples after shaking and after continuous compression-decompression in the Mini-Trough were investigated for particles by visual inspection with photo-documentation (Nikon D5300 SLR digital camera, Nikon Corporation, Japan). The Ph. Eur. monograph for parenteral preparations in conjunction with the visual particles monograph (Ph. Eur. 2.9.19) requires parenteral preparations (which are not administered using a final filter) to be practically free from (visible) particles. Ph. Eur. monograph ‘Monoclonal antibodies for human use’ requires the formulations to be practically free from particulates that could be detected visually. All samples were categorized according to table 1.

Table 1: Four Categories for visual inspection (following Ph. Eur. 2.9.19)

0	1	2	3
Free from particles	Practically free from particles	Several particles	Many particles

3.5.2. Turbidity

Samples were analyzed for turbidity according to Ph. Eur. 2.2.1 based on the scatter of 860 nm light by the sample at an angle of 90°. A sample volume of 1.8 mL was analyzed using a Nephla turbidimeter (Dr. Lange, Duesseldorf, Germany). Data is given as formazine nephelometric units (FNUs).

3.5.3. Light Obscuration

Samples were analyzed for particles in the micrometer range by light obscuration (in analogy to USP 788 and Ph Eur 2.9.19) with a SVSS-C instrument (PAMAS, Partikelmess-und Analysesysteme GmbH, Rutesheim, Germany). After a pre-run volume of 0.5 mL, each sample was analyzed in triplicates of 0.3 mL at a filling and emptying rate of 10 mL/min. Before each run, the system was rinsed with at least 5 mL of highly purified water. Data was collected using PAMAS PMA Program V 2.1.2.0.

3.5.4. Micro-Flow Imaging

Particle size and number was additionally measured using a micro-flow imaging (MFI) system (DPA4100, Brightwell Technologies Inc., Ottawa, Canada) equipped with a high-resolution 100 µl flow-cell and the MFI™ View Application Software. Pre-run volumes of 0.3 mL and sample volumes of 0.65 mL were drawn through the flow cell by a peristaltic pump at a flow rate of 0.1 mL/min. To optimize illumination and to provide a clean baseline the system was rinsed with highly purified water before and after the measurements.

3.5.5. Statistical Significance

For LO and MFI data a t-test was performed with * for $p \leq 0.05$, ** for $p \leq 0.01$ and *** for $p \leq 0.001$.

3.6. Infrared Reflectance Absorbance Spectroscopy (IRRAS)

Infrared spectroscopy was used to determine the presence of the protein and the additives adsorbed at the liquid-air interface. Moreover, secondary structure of the IgG was analyzed. IRRAS spectra were recorded using a VERTEX FT-IR spectrometer (Bruker Optics GmbH, Germany) equipped with a liquid nitrogen-cooled MCT (mercury cadmium telluride) detector. The spectrometer was coupled to a Langmuir trough (Riegler & Kirstein GmbH, Germany), placed in a sealed container (external air/water reflection unit XA-511) to guarantee constant vapor atmosphere. The IR beam was conducted out of the spectrometer and focused onto the water surface of the Langmuir trough. A computer controlled KRS-5 wire-grid polarizer (thallium bromide and iodide mixed crystal) was used to generate perpendicular (s) and parallel (p) polarized light. The angle of incidence was set to 40° with respect to the surface normal. Measurements were performed using a trough with two compartments and a trough shuttle system [26]–[28]. One compartment contained the protein solution under investigation (sample), and the other (reference) was filled with the pure buffer subphase. The single-beam reflectance spectrum (R_0) from the reference trough was taken as background for the single-beam reflectance spectrum (R) of the monolayer in the sample trough to calculate the reflection-absorption spectrum as $-\log(R/R_0)$ in order to eliminate the water vapor signal. IR spectra were collected at 8 cm^{-1} resolution and a scanner speed of 20 kHz. For s-polarized light, spectra were co-added over 200 scans, and spectra with p-polarized light were co-added over 400 scans.

3.7. Brewster Angle Microscopy (BAM)

The morphology of the monolayer was imaged with a Brewster angle microscope, BAM2plus from NanoFilm Technologie GmbH (Goettingen, Germany), equipped with a miniature film balance from NIMA Technology (Coventry, UK). IgG at 1 mg/mL in Glycine-NaCl buffer at pH 6.8 was filled into the trough ($V = 80$ mL). Simultaneous surface pressure measurements during adsorption and compression of the IgG in the Langmuir trough enabled a direct connection of each image with the corresponding surface pressure during adsorption or compression of the protein. The lateral resolution of the BAM was approximately $3\text{ }\mu\text{m}$. The size of the BAM images is $400 \times 720\text{ }\mu\text{m}^2$. Detailed information about the BAM method is given elsewhere [29]–[31].

3.8. Atomic Force Microscopy (AFM)

For AFM, protein films formed during adsorption to equilibrium adsorption pressure or after compression to a desired surface pressure, were transferred by the Langmuir-Schaefer deposition (horizontal transfer of the film) using $1 \times 1\text{ cm}^2$ mica plates (Mica Sheet V5 Quality, Science Services GmbH, Germany) attached to a stamp tool. The mica was lowered onto the surface and pulled off after 2 s of contact time. The mica was removed from the stamp tool and the transferred film was covered with a drop of buffer solution to prevent drying of the sample. The transferred films were analyzed by underwater AFM (Bruker / Veeco / Digital Instruments MultiMode AFM) using a cantilever (Arrow™ NCpt, resonance frequency 285 kHz, spring constant 42 N/m) in tapping mode (Nano World AG, Switzerland). Images were analyzed by NanoScope III 5.12r3 Software (Digital Instruments Inc., US).

4. RESULTS AND DISCUSSION

4.1. Competitive Adsorption

4.1.1. Equilibration Time

IgG molecules exhibit a certain surface activity because of their partly amphiphilic character. Due to their larger size and less amphiphilic character they adsorb much slower at interfaces compared to the surfactant type formulation additives. An assessment of the time until a stable equilibrium surface pressure is reached therefore provides a first hint on the interfacial film properties. For this purpose, the equilibration time (t_{eq}) was defined as time until a maximum surface pressure is reached by adsorption which changes less than ± 0.2 mN/m within 0.5 h.

In case of the IgG, an equilibrium surface pressure was only reached after 3.9 h. Moreover, t_{eq} decreased with increasing protein concentration (Tab. 1). For all mixtures, t_{eq} was reached much faster (0.1-0.2 h). Additionally, concentration did not have a considerable impact on t_{eq} . For the mixtures, t_{eq} increased with higher amounts of IgG (Tab. 2). In case of PS 80 at a mixture ratio of 2000:1 [C_{IgG} : $C_{PS\ 80}$], in which the surfactant is present well below CMC, t_{eq} was reached after 1.3 h (Fig. 1A, Tab. 2). In contrast, t_{eq} was reached after 0.2 h at high PS 80 concentrations as in case of a ratio of 1:1 [C_{IgG} : $C_{PS\ 80}$]. The IgG molecules compete with the much smaller amphiphiles for the adsorption to the interface as t_{eq} drastically decreases with increasing additive concentration. At PS 80 concentrations well below CMC, but also at higher surfactant concentrations, t_{eq} was elevated for all mixtures compared to pure PS 80 solution (Tab. 2, 3). In mixtures with IgG, the behavior of surfactants can be altered and the apparent CMC values have been described to be increased compared to the CMC values of the surfactants alone [15].

Mixtures of IgG and P 188 revealed highest t_{eq} with up to 1.9 h (e.g. 100:1 ratio of C_{IgG} : C_{P188}). Thus, adsorption kinetics depended on the protein concentration as well as the IgG-additive mixing ratio. P 188 and mixtures of IgG with P 188 revealed the slowest adsorption kinetics which can be traced back to the higher molecular weight of P 188 compared to the other additives investigated. Moreover, the complex behavior of P 188 needs to be considered, as it is known to show a divers aggregation behavior and micelle formation, although the detailed mechanism remains unclear to date [17], [18], [32].

Different to polysorbates, the CMC of poloxamers varies over a broad concentration range depending on temperature and molecular weight ratios of the polymer blocks. We determined a CMC of 0.21 mg/mL which compares well to literature values of 0.334 mg/mL and 0.743 mg/mL [33], [34].

Table 2: Mixing ratios of IgG with P 80, P 188 and HP- β -CD

IgG + Polysorbate 80	
c [mg/mL]	Mixing Ratio [c_{IgG} : $c_{\text{PS 80}}$]
0.1 + 0.00005	2000:1
0.1 + 0.001	100:1
0.1 + 0.01	10:1
0.1 + 0.1	1:1
IgG + Poloxamer 188	
c [mg/mL]	Mixing Ratio [c_{IgG} : c_{P188}]
0.1 + 0.001	100:1
0.1 + 0.01	10:1
0.1 + 0.1	1:1
0.1 + 1	1:10
IgG + Hydroxypropyl- β -cyclodextrin	
c [mg/mL]	Mixing Ratio [c_{IgG} : $c_{\text{HP-}\beta\text{-CD}}$]
0.1 + 0.349	0.29:1
0.1 + 3.49	0.029:1
0.1 + 34.9	0.0029:1
0.1 + 69.8	0.000143:1

Similar to PS 80 and P 188, also the equilibration time of the IgG in mixtures with HP- β -CD in a concentration range of 0.349 mg/mL up to 34.9 mg/mL was analyzed. At HP- β -CD concentrations of 3.49 mg/mL and above, t_{eq} was reached only 0.5 h. In case of the lowest concentration of 0.349 mg/mL, equilibrium surface pressure was reached after 1.1 h, suggesting a contribution of the IgG to the adsorption process.

Cyclodextrins have been reported to bind to exposed hydrophobic residues on proteins causing a shielding of exposed hydrophobic spots thereby inhibiting protein adsorption [21]. Hence, these physicochemical investigations are highly valuable as they give a first hint on the interfacial film characteristics.

Table 3: Equilibration times (t_{eq}) of pure solutions of IgG, PS 80, P 188 and HP- β -CD

IgG		Polysorbate 80		Poloxamer 188		HP- β -CD	
c [mg/mL]	t_{eq} [h]	c [mg/mL]	t_{eq} [h]	c [mg/mL]	t_{eq} [h]	c [mg/mL]	t_{eq} [h]
0.0005	3.1	0.0005	0.2	0.001	0.2	0.349	0.2
0.001	3.6	0.001	0.1	0.01	0.2	3.49	0.2
0.01	3.8	0.01	0.1	0.1	0.1	34.9	0.1
0.1	3.9	0.1	0.1	1	0.1	69.8	0.1

Table 4: Equilibration times (t_{eq}) of mixtures of IgG + PS 80, IgG + P 188 and IgG + HP- β -CD

IgG + Polysorbate 80		IgG + Poloxamer 188		IgG + HP- β -CD	
c [mg/mL]	t_{eq} [h]	c [mg/mL]	t_{eq} [h]	c [mg/mL]	t_{eq} [h]
0.1 + 0.00005	1.3	0.1 + 0.001	1.9	0.1 + 0.349	1.1
0.1 + 0.001	0.7	0.1 + 0.01	1.2	0.1 + 3.49	0.4
0.1 + 0.01	0.5	0.1 + 0.1	0.4	0.1 + 34.9	0.2
0.1 + 0.1	0.2	0.1 + 1	0.1	0.1 + 69.8	0.1

4.1.2. Equilibrium Surface Pressure

Nonionic surfactants evolve their protein stabilizing features by either interfacial competition and / or by direct protein - surfactant interaction [15]. Hence, surface pressure experiments provide evidence about not only the adsorption process but also the interfacial film assembly. The concentration dependent equilibrium surface pressure values (π_{eq}) of IgG mixtures with the additives are shown in figure 1A-C. For IgG, π_{eq} increased with increasing concentration reaching a maximum surface pressure (π_{max}) of 18.5 mN/m at 1 mg/mL. A π_{max} of 31 mN/m was obtained for PS 80 above CMC (determined as 0.0026 mg/mL). The mixtures of IgG and PS 80 behaved similar to pure PS 80 at higher concentrations. At PS 80 concentrations below 0.01 mg/mL, the additional presence of the IgG caused an increase in surface pressure and therefore both surfactant and protein molecules are present at the interface. The π_{eq} of P 188 was determined to 23 mN/m at concentrations of 1 mg/mL and above (Fig. 1B). Different to the results obtained for PS 80, the presence of IgG resulted in higher π_{eq} at all P 188 concentrations, also above the CMC of 0.21 mg/mL. Surface pressure values of IgG - P 188 mixtures with the P 188 present at concentrations above the CMC were overall higher compared to pure P 188. This indicates an additional presence of IgG molecules at the interface. HP- β -CD also exhibited a pronounced surface activity reaching a surface pressure value of 20 mN/m (Fig. 1C). Different to the non-ionic surfactants described

before, no steady state as defined in this study (see materials and methods) was reached. An increase in HP- β -CD concentration caused an increase in surface pressure consistently up to concentrations of 69.8 mg/mL. IgG and HP- β -CD reached comparable surface pressure values and thus, no considerable differences were detectable for the mixtures.

Due to their strong amphiphilic character and smaller molecular weight, surfactants adsorb much faster compared to IgG [35]. Therefore, the IgG can either occupy interspaces which are not accessible by other PS 80 or P 188 molecules, or the IgG competes with the surfactant for the adsorption to the interface. Moreover, it has been stated that poloxamers can inhibit protein adsorption via the formation of protein–surfactant complexes of low adsorption affinity and not by its preferential location at the interface [7]. For the HP- β -CD, no conclusion about the presence of IgG at the interface is possible at this point.

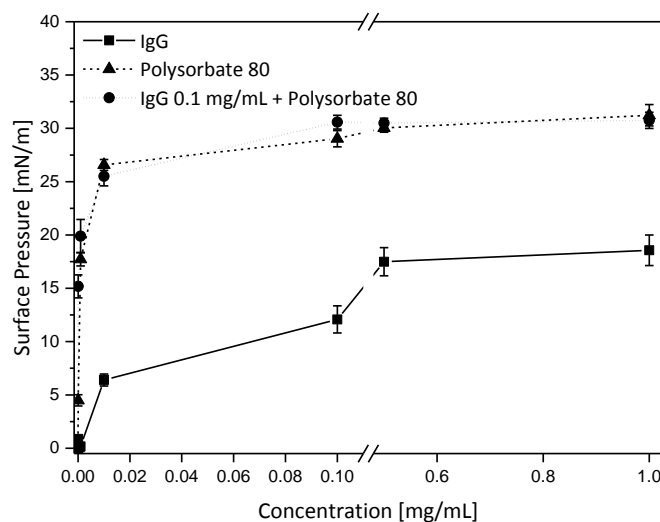


Figure 1A: π_{eq} [mN/m] of IgG and PS 80 and of mixtures of both at different concentrations

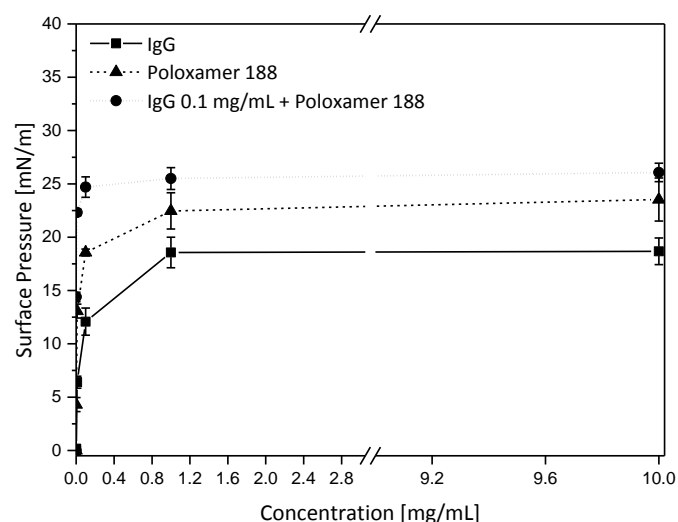


Figure 1B: π_{eq} [mN/m] of IgG and P 188 and of mixtures of both at different concentrations

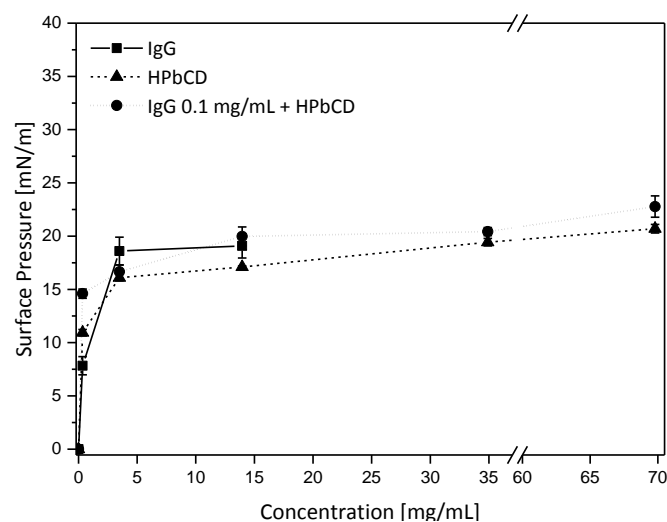


Figure 1C: π_{eq} [mN/m] of IgG and HP- β -CD and of mixtures of both at different concentrations

4.2. Repeated Compression and Decompression of Mixed Protein – Additive Films

Proteins adsorbed to the liquid-air interface behave different than surfactant molecules. While proteins form highly compressible films, surfactant molecules get easily displaced from the surface. Hence the compressibility behavior of the adsorbed film allows conclusions about the composition of the film.

Continuous compression-decompression cycles of the liquid-air interfacial film were performed and surface pressure was recorded simultaneously. Compression of the IgG film caused a substantial increase in surface pressure at a compression factor of 8.3 (Fig. 2A) and the change in surface pressure amounted to 44.9 mN/m. Decompression led to a marked decrease in surface pressure. A substantial hysteresis resulted upon repeated compression and decompression. The equilibrium surface pressure slightly decreased with each cycle. Compression of the liquid-air interface of a PS 80 solution did result in a much less pronounced increase in surface pressure (Fig. 2D). At A_{\min} , a maximum change in surface pressure (π_{\max}) of 14.1 mN/m was reached. Compression and decompression of mixed IgG and PS 80 films revealed a mixture depended compressibility behavior. In case PS 80 was present at a concentration well below CMC, compressibility was protein-like reaching a π_{\max} of 38.5 mN/m (Fig. 2B). In case the PS 80 was present in concentrations above CMC π_{\max} reached 23.3 mN/m (Fig. 2C).

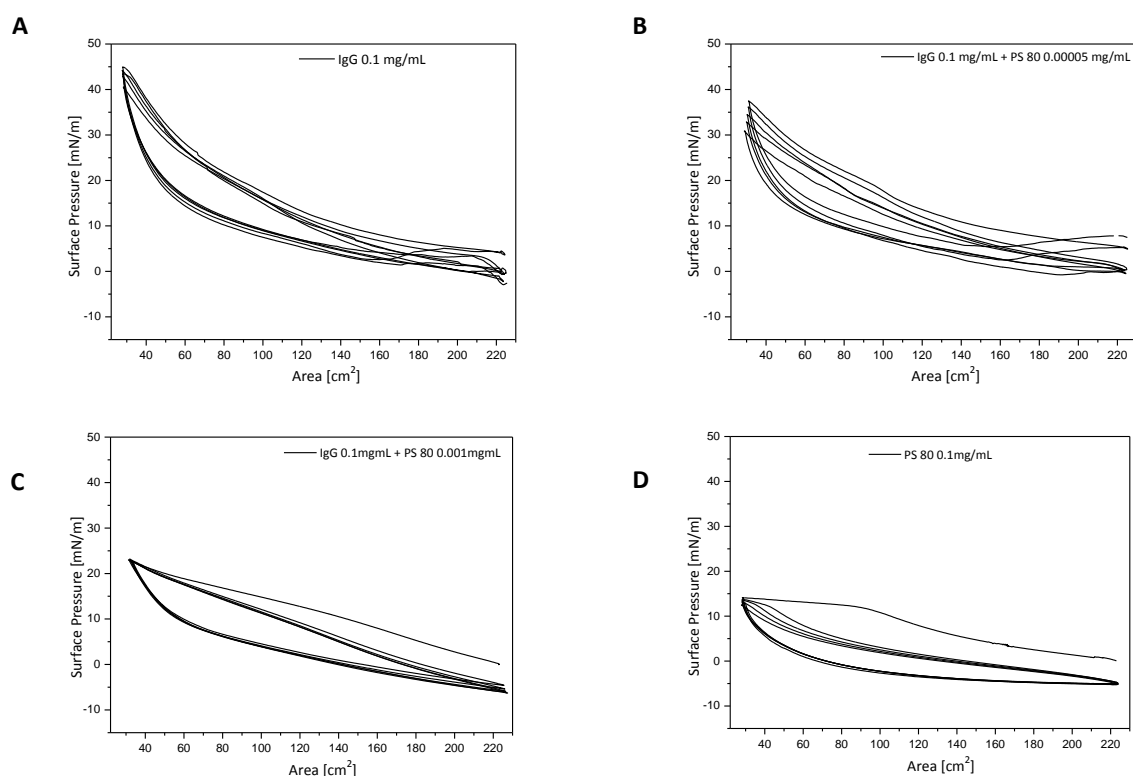


Figure 2: Change in surface pressure [mN/m] vs. total area [cm²] of three continuous compression-decompression cycles of IgG and/or PS 80 at different concentrations. A: IgG 0.1mg/mL, B: IgG 0.1mg/mL + PS 80 0.00005 mg/mL, C: IgG 0.1 mg/mL + PS 80 0.001 mg/mL, D: PS 80 0.1 mg/mL

The compressibility of P 188 films was lower compared to PS 80 (π_{\max} of 3.2 mN/m) (Fig. 3). Moreover, mixtures containing P 188 below CMC (Fig. 3B) and above CMC (Fig. 3C) did not differ much in compressibility with a π_{\max} of 4.5 mN/m and 3.8 mN/m respectively. Compared to pure IgG, compressibility was very low indicating that the film predominantly consists of P 188 molecules with only some IgG molecules present at the interface. Nevertheless, although added in concentrations below CMC compression-decompression showed a surfactant-like behavior of the interfacial film. At comparable mixing ratio the difference in π_{\max} between the mixed and pure surfactant films was more substantial for PS 80 (9.2 mN/m) compared to P 188 (1.3 mN/m). This could be attributed to the complex association behavior of poloxamers forming not only micelles of various geometries but also oligomers and large clusters which occupy a larger surface area compared to polysorbates [16]. Compression did not cause a considerable increase in surface pressure in case of a HP- β -CD solution ($\pi_{\max} = 2.4$ mN/m) as shown in Fig 4. Additional presence of the IgG in mixtures resulted in similar outcomes with $\pi_{\max} = 1.7$ mN/m and $\pi_{\max} = 3.2$ mN/m, respectively. Therefore, no significant differences in the interfacial behavior were recognizable between the mixtures and pure HP- β -CD solutions.

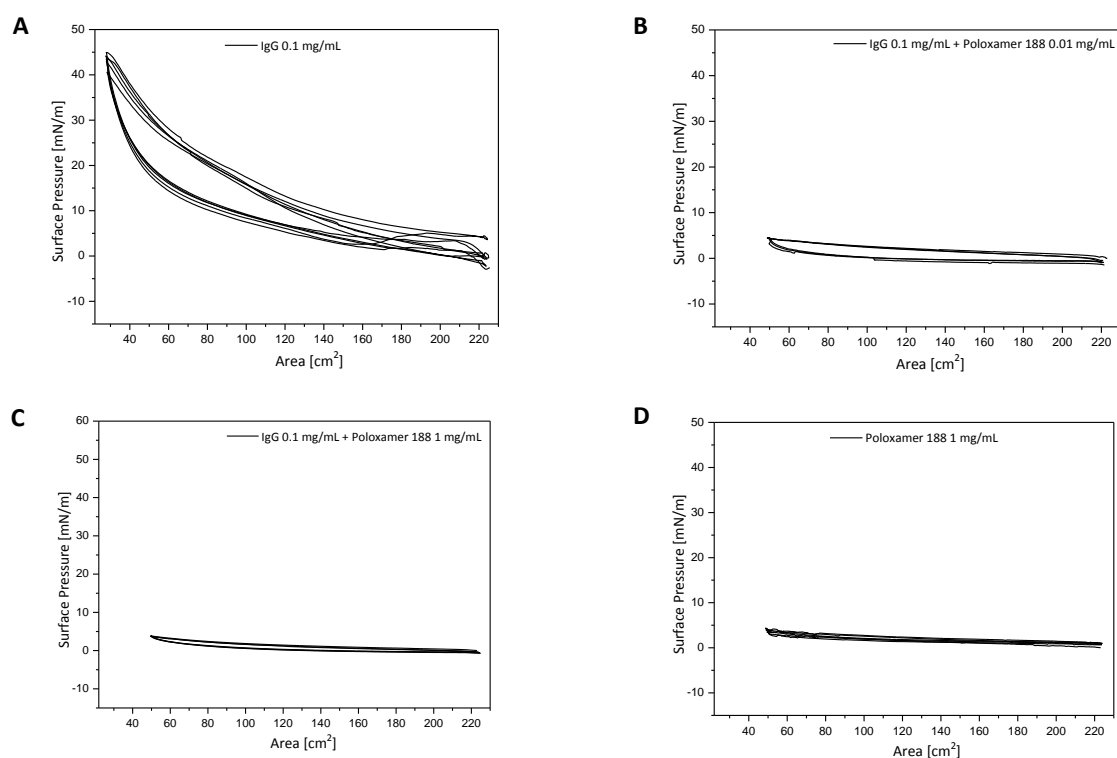


Figure 3: Change in surface pressure [mN/m] vs. total area [cm²] of three continuous compression-decompression cycles of IgG and/or P 188 at different concentrations. A: IgG 0.1mg/mL, B: IgG 0.1mg/mL + P 188 0.01 mg/mL, C: IgG 0.1 mg/mL + P 188 1mg/mL, D: P 188 1 mg/mL

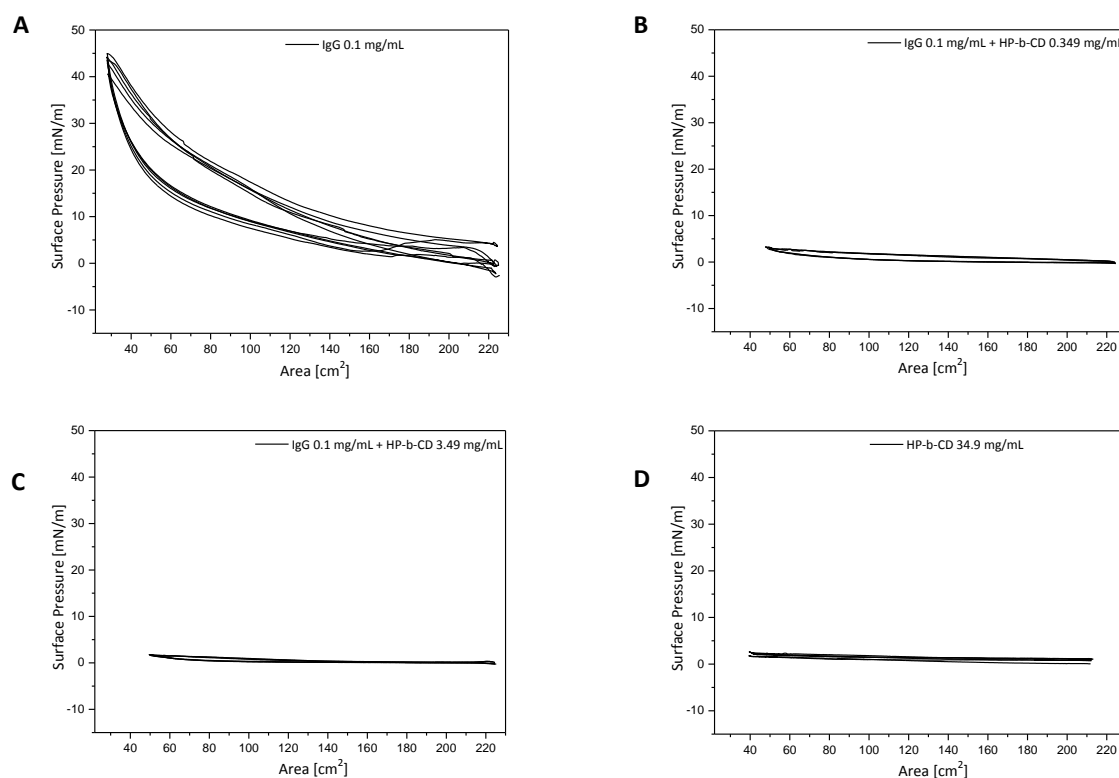


Figure 4: Change in surface pressure [mN/m] vs. total area [cm²] of three continuous compression-decompression cycles of IgG and/or HP-β-CD at different concentrations. A: IgG 0.1mg/mL, B: IgG 0.1mg/mL + HP-β-CD 0.349 mg/mL, C: IgG 0.1 mg/mL + HP-β-CD 3.49 mg/mL, D: HP-β-CD 34.9 mg/mL

4.3. Presence and Secondary Structure of IgG at the Interface

Infrared-Reflectance Absorbance Spectroscopy (IRRAS) was used to determine the presence and secondary structure of the IgG at the liquid-air interface. Figure 5 shows IRRAS spectra of IgG during adsorption to equilibrium surface pressure and during compression up to 35 mN/m. During adsorption as well as during compression the intensity of the OH-stretch vibration around 3600 cm⁻¹ was increasing, as well as the amide I and II bands around 1650 cm⁻¹ and 1550 cm⁻¹. This increase can be assigned to an increasing effective film thickness. Moreover, the position of the amide I band at 1643 cm⁻¹ in the IRRAS spectrum can be assigned to an intramolecular β-sheet structure of the IgG. Compression did not cause considerable changes in the band position and the slight shift of the amide II band from 1543 cm⁻¹ to 1547 cm⁻¹ is within measurement accuracy.

The FT-IR spectrum of the IgG in solution (Fig. 6) reveals a peak maximum at 1639 cm^{-1} and comparison with the IRR spectra proves that the IgG remains in a native-like conformation at the interface as no other peaks referring to new structural elements appear.

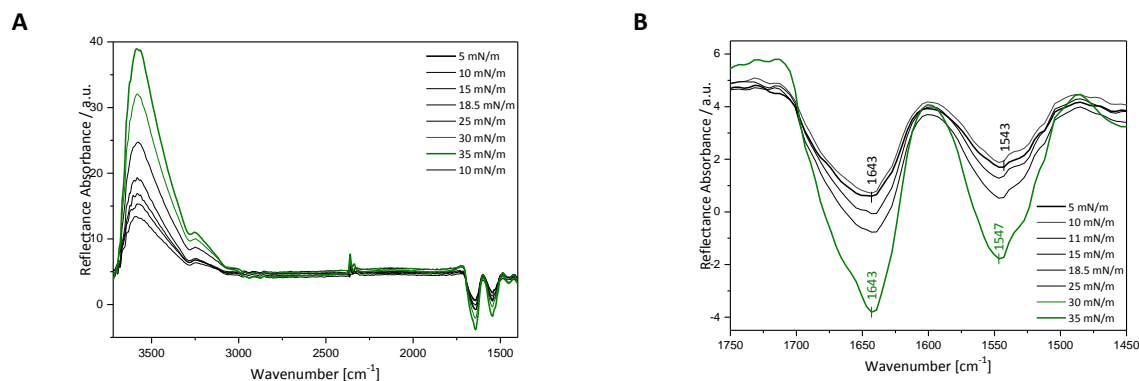


Figure 5: IRR spectra of IgG [1 mg/mL] with increasing surface pressure during adsorption to $\pi_{\text{eq}} = 18.5\text{ mN/m}$ and compression up to $\pi = 35\text{ mN/m}$, A: full spectra, B: Amide I and II band region

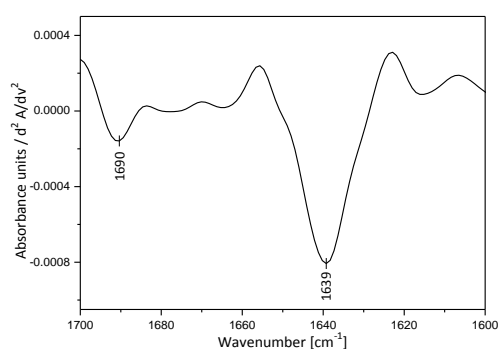


Figure 6: FT-IR spectrum of the amide I region of IgG [10 mg/mL] in solution (AquaSpec)

4.4. IRR Spectra of Mixed Protein-Additive Films

IRRAS provide evidence about the interfacial film composition via an identification of characteristics bands that can be assigned to functional groups of the molecules investigated. Figure 7 shows IRR spectra of IgG, PS 80 and mixtures of both after adsorption and after compression. PS 80 did not reveal characteristic bands but only weak bands around $2964\text{--}2878\text{ cm}^{-1}$ which can be assigned to the CH_2 -groups of the lipid chains.

The mixture of IgG 0.1 mg/mL and PS 80 0.001 mg/mL showed distinct amide bands indicating that some protein molecules must be present at the interface. Compression to 30 mN/m caused a considerable increase, not only of the OH-band but also the amide bands.

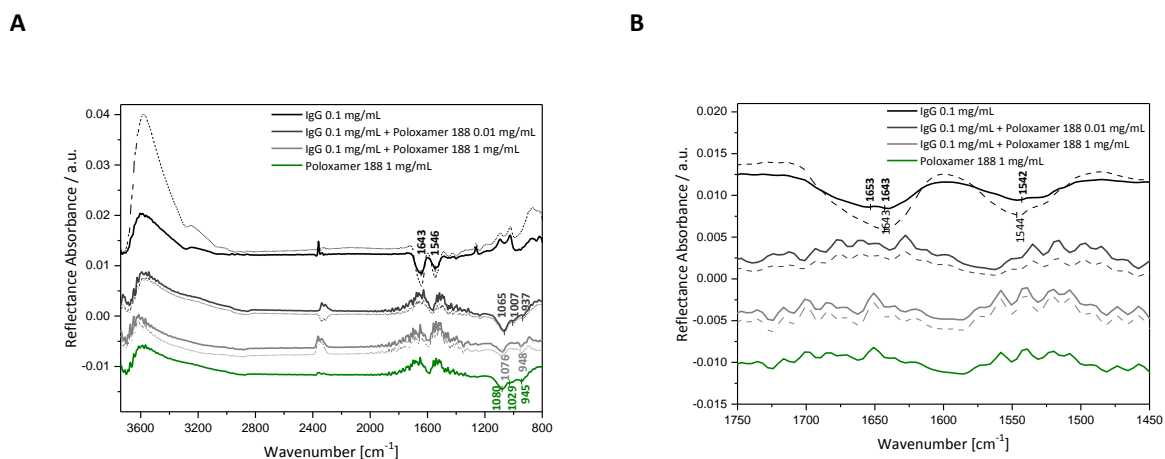


Figure 8: IRRA spectra of IgG and P 188 and mixtures of both in two different concentrations after adsorption to π_{eq} (solid line) and after compression to $\pi = 30 \text{ mN/m}$ (dashed line), A: full spectra, B: amide I and II band region and peak assignment

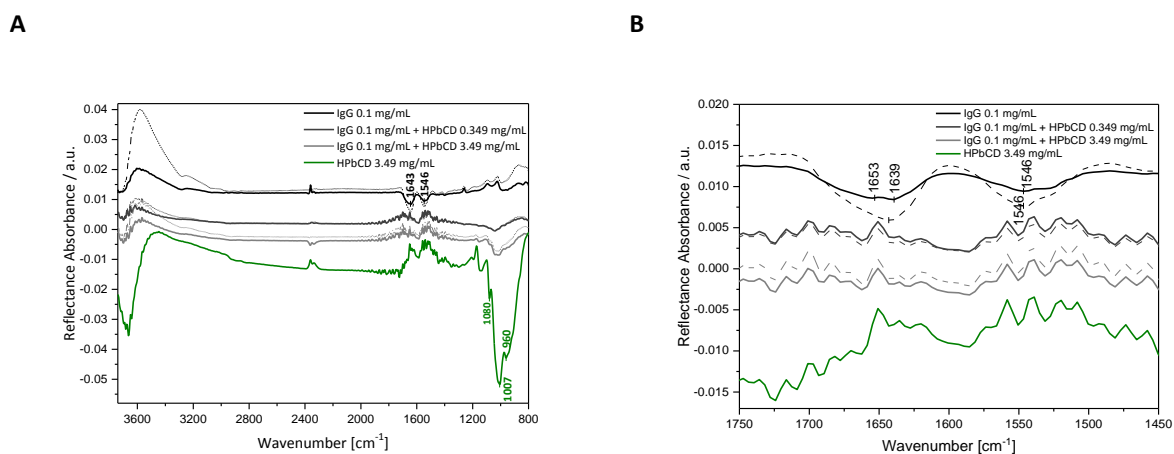


Figure 9: IRRA spectra HP- β -CD of IgG and mixtures of both in two different concentrations after adsorption to π_{eq} (solid line) and after compression to $\pi = 30 \text{ mN/m}$ (dashed line), A: full spectra, B: amide I and II band region and peak assignment

4.5. Interfacial Film Structures

4.5.1. Brewster Angle Microscopy

Brewster Angle Microscopy (BAM) was used to visualize the interfacial film of PS 80, P 188 and HP- β -CD solutions. The Brewster condition was satisfied as the excipient molecules are small and adsorb homogeneously and therefore the interface appeared homogeneously dark (Figs. 11A, 12A, 13A). In contrast, IgG adsorbed inhomogeneously and formed clusters of condensed protein material indicated by bright areas within a continuous film (Fig. 10). In case of IgG-PS 80 mixtures, BAM images appear protein-like in case the surfactant was added in concentrations around or well below CMC (Fig. 11C, D). In case the PS 80 was present at a concentration above the CMC (0.01-0.1 mg/mL), the overall grey level was decreased and the film appearance surfactant-like (Fig. 11B). In mixtures of IgG, even at the lowest tested concentration of P 188 at 0.01 mg/mL and HP- β -CD at 0.349 mg/mL, BAM images on the one hand revealed dark areas referring to regions where no IgG molecules are present. On the other hand, even at the highest additive concentrations some protein clusters are present at the interface (Figs. 11B, 12B, 13B). Similarly, not only IgG but also different proteins such as β -conglycinin and β -casein form flickering domains with increased brightness [9], [36]. The fact, that even at high surfactant concentrations above the CMC some protein clusters are present at the interface indicates that protein adsorption cannot be entirely inhibited. Thus, not necessarily the addition of surfactant at a concentration slightly above CMC is enough to reach maximum stabilization of protein formulations against mechanical stress.

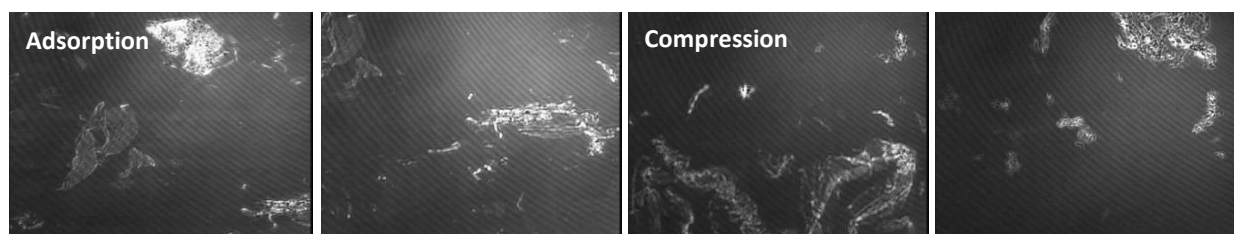


Figure 10: BAM images of IgG 0.1 mg/mL during adsorption and compression

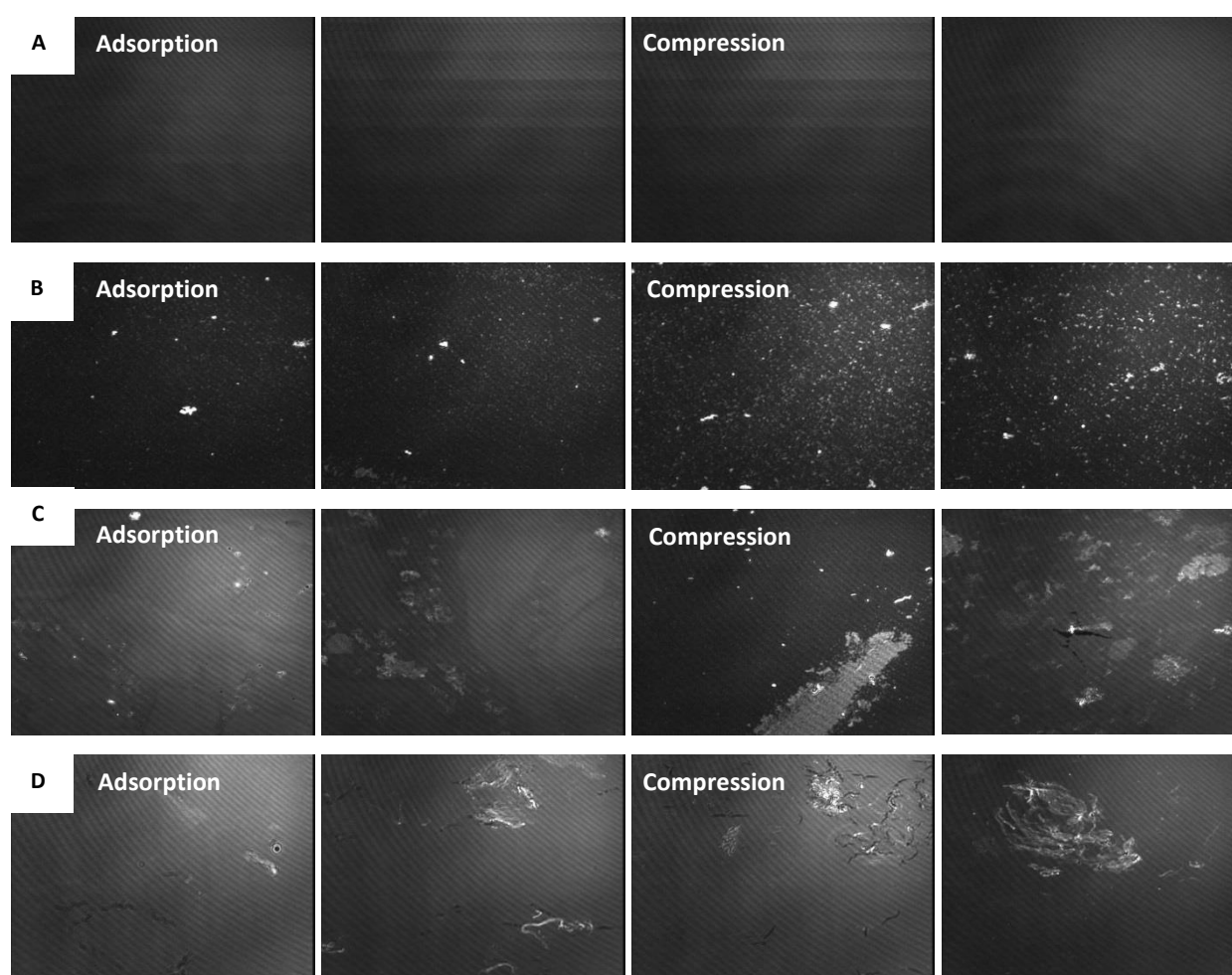


Figure 11: BAM images during adsorption and compression of A: PS 80 0.1 mg/mL, B: IgG 0.1 mg/mL + PS 80 0.01 mg/mL, C: IgG 0.1 mg/mL + PS 80 0.001 mg/mL, and D: IgG 0.1 mg/mL + PS 80 0.00005 mg/mL

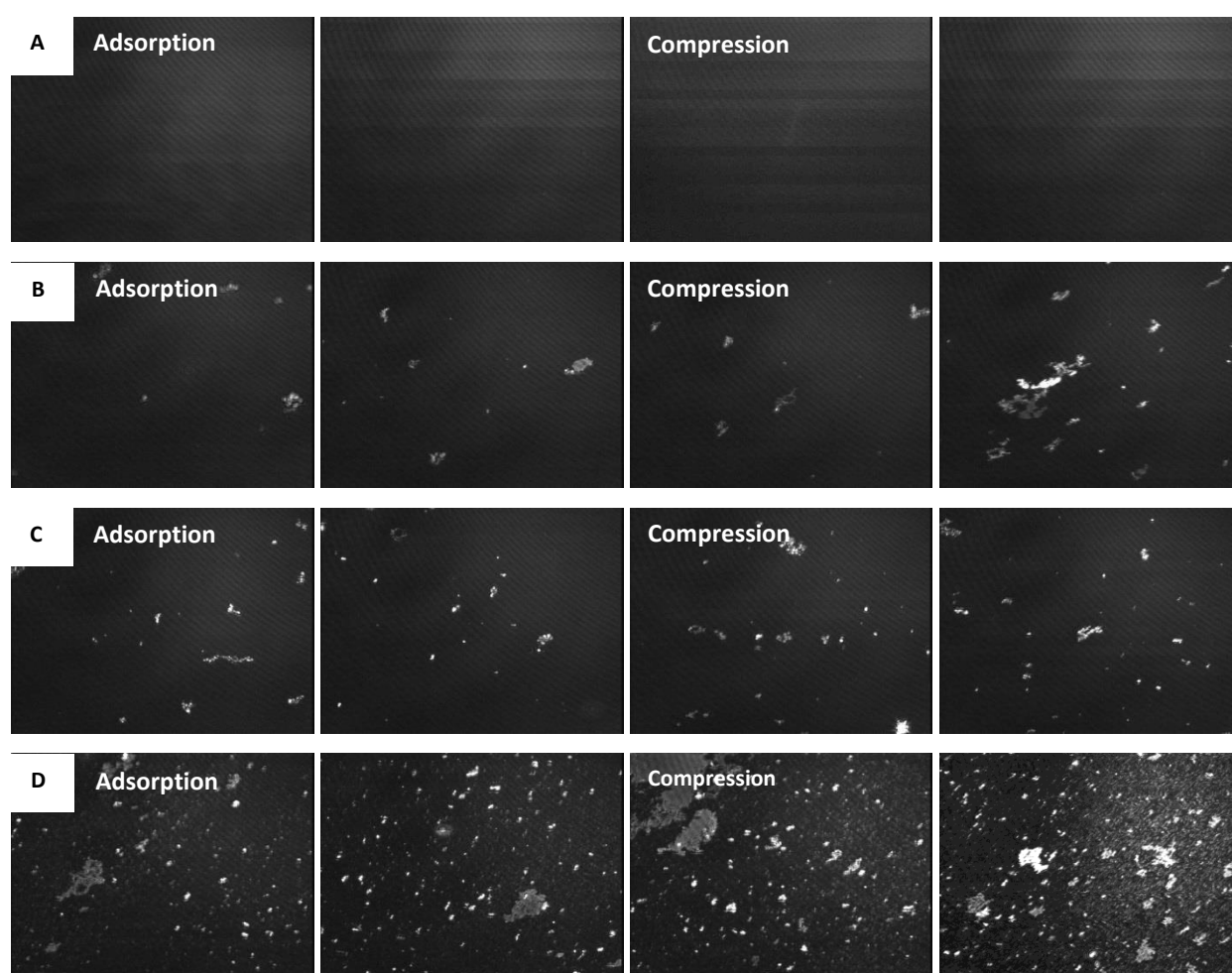


Figure 12: BAM images during adsorption and compression of A: P 188 1 mg/mL, B: IgG 0.1 mg/mL + P 188 1 mg/mL, C: IgG 0.1 mg/mL + P 188 0.1 mg/mL, and D: IgG 0.1 mg/mL + P 188 0.01 mg/mL in Glycine-NaCl buffer pH 6.8

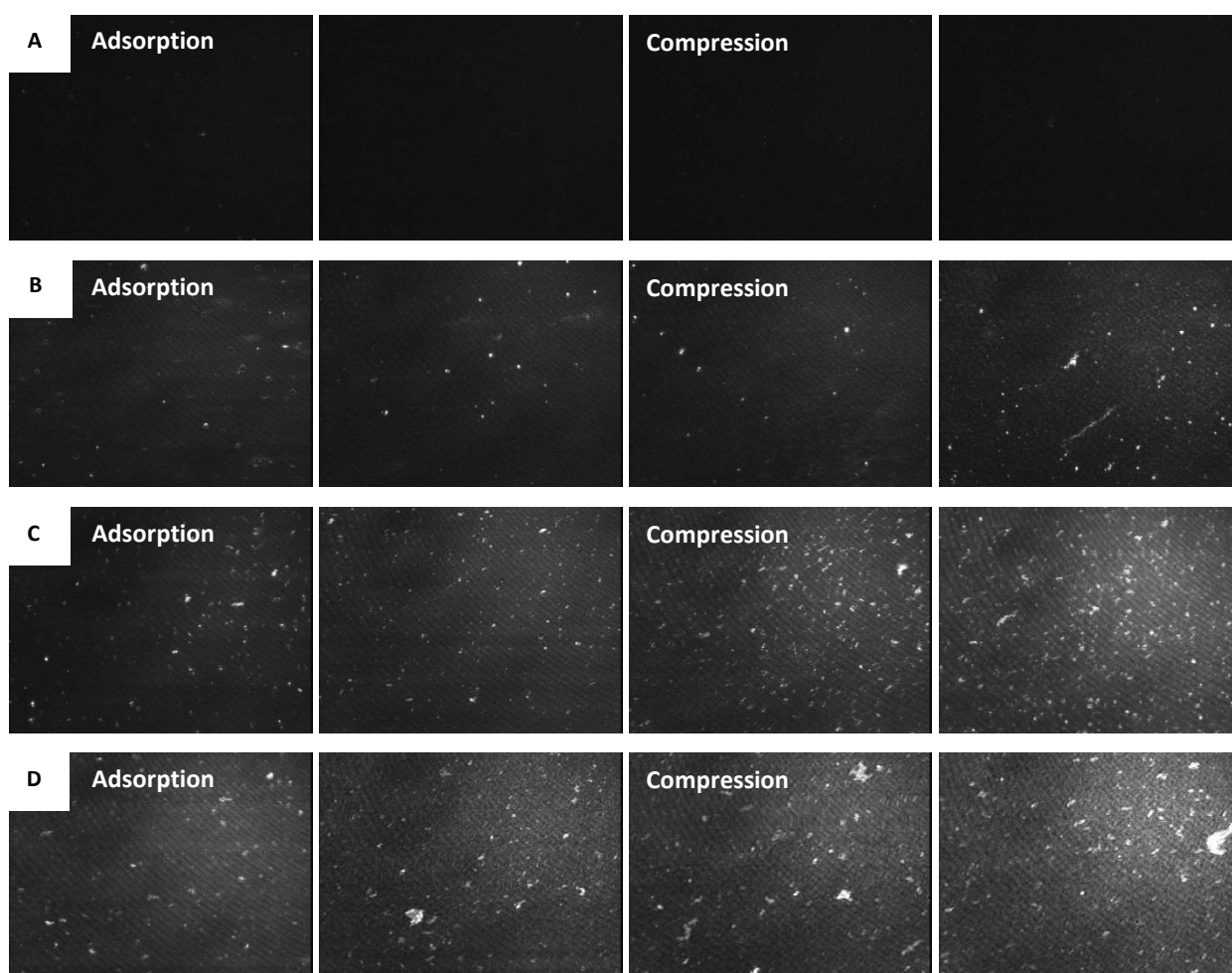


Figure 13: BAM images during adsorption and compression of A: HP- β -CD 34.9 mg/mL, B: IgG 0.1 mg/mL + HP- β -CD 34.9 mg/mL, C: IgG 0.1 mg/mL + HP- β -CD 3.49 mg/mL in Glycine-NaCl buffer pH 6.8, and D: IgG 0.1 mg/mL + HP- β -CD 0.349 mg/mL

4.5.2. Atomic Force Microscopy

For the visualization of the interfacial film submersed Atomic Force Microscopy (AFM) was used. Similar to BAM, although on a different scale, AFM demonstrated that IgG adsorption to equilibrium resulted in a coherent protein film with some agglomerates of increased height (Fig. 14A). Compression to 30 mN/m caused the formation of areas of telescoped protein material (Fig. 14B). The maximum height of the interfacial film increased from 11 nm after adsorption to 37 nm upon compression (Fig. 14A, B). With PS 80 present above CMC at 0.01 mg/mL the film appeared overall smoother and the mean roughness is markedly lower with 0.3 nm compared to the 5 nm of the IgG film (Fig. 15). Compression of the PS 80 solution did not cause a substantial increase in maximum height (1.2 nm). In a mixture with 0.00005 mg/mL PS 80, the film formed upon compression exhibited similar properties as the film of a surfactant - free IgG solution with a maximum thickness of 8 nm and a mean

roughness of 5 nm (Fig. 16A, B). Separated bright domains representing agglomerated protein material appeared and the maximum height increased to values of 23 nm after compression (Fig. 16B), comparable to the pure protein film. This is in accordance with a study by Mackie *et al.* [37] where the competitive displacement of β -lactoglobulin by SDS was investigated. They stated that the surfactant displaced the protein from the interface during adsorption as the protein film showed many holes. Wilde *et al.* [14] stated that the presence of sodium-dodecylsulfate (SDS) in mixed films with β -lactoglobulin caused crumpling of the protein network as indicated by an increase in film thickness. It has also been stated that short-range repulsive interactions between protein and additive can enhance local phase separation [38]. Hence, AFM images provide direct information on the film properties and composition based on height and roughness after equilibrium adsorption and compression.

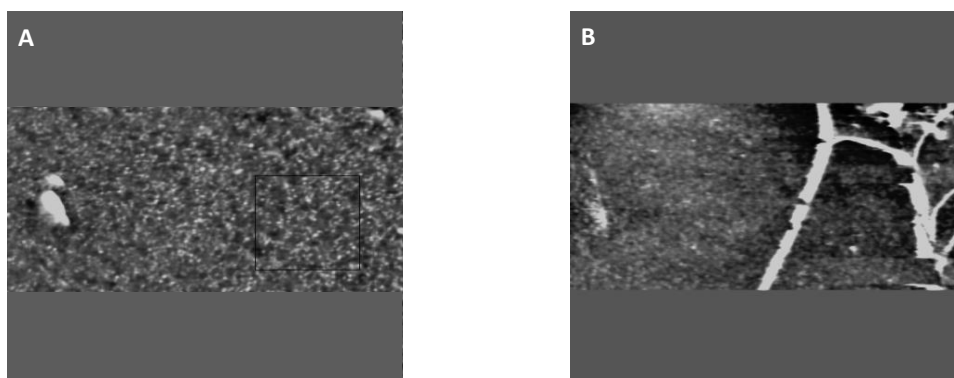


Figure 14: IgG 0.1 mg/mL after A: Adsorption to Π_{eq} (mean roughness: 1nm) and B: Compression to 30 mN/m (mean roughness: 5 nm)

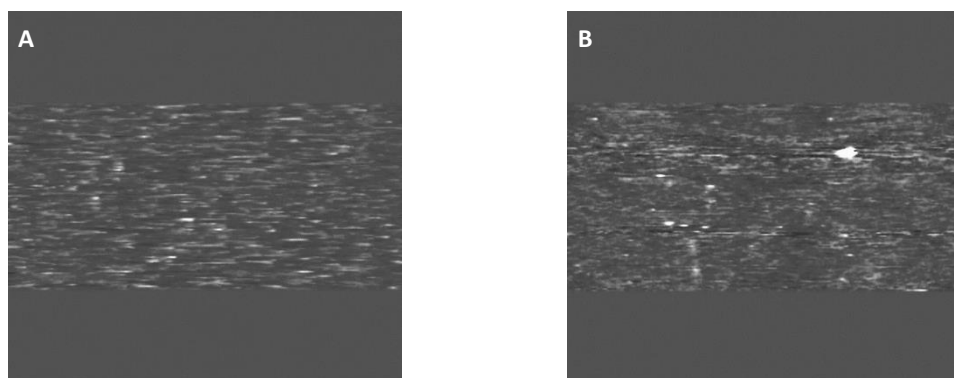


Figure 15: IgG 0.1 mg/mL + PS 80 0.01 mg/mL after A: Adsorption to $\Pi_{eq} = 24.8$ mN/m (mean roughness 0.2 nm) and B: Compression to 30 mN/m (mean roughness: 0.3 nm)

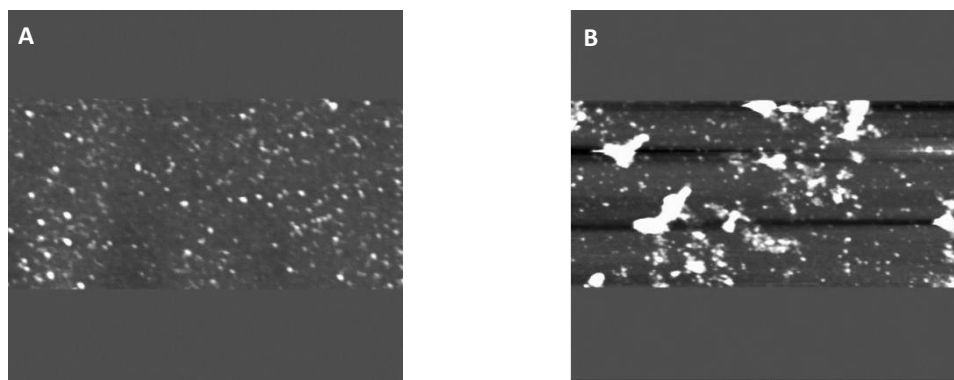


Figure 16: IgG 0.1 mg/mL + PS 80 0.00005 mg/mL after A: Adsorption to $\Pi_{eq} = 21.3$ mN/m (mean roughness 0.7 nm) and B: Compression to 30 mN/m (mean roughness: 5 nm)

4.6. Impact of the IgG-Additive Mixture Ratio on Particle Formation

4.6.1. By Agitation

Shaking studies were performed to investigate the aggregation behavior of the IgG in presence of the different additives. The number of particles per mL was determined using light obscuration (LO) and micro-flow imaging (MFI). Moreover, a visual inspection including photo documentation as well as turbidity measurements were performed. After 48 h of shaking, the pure IgG solution resulted in the formation of around 200 000 particles $>1 \mu\text{m}$ / mL, whereas the buffer control showed negligible amounts of particles (around 800 particles $>1 \mu\text{m}$ / mL) (Fig. 17A). Similarly, the number of particles of a stressed solution of PS 80 solution remained below 800 particles $>1 \mu\text{m}$ / mL. The mixtures of IgG and PS 80 showed less particle formation upon agitation compared to the surfactant free IgG solution. Addition of 0.1 mg/mL PS 80 caused a complete inhibition of protein aggregation. With decreasing PS 80 concentration the number of particles increased resulting in the formation of around 9000 particles $> 1 \mu\text{m}$ / mL at the lowest PS 80 concentration of 0.0001 mg/mL (below CMC). Figure 17B shows that the addition of P 188 also prevented agitation induced aggregation effectively, although in a less concentration-dependent manner compared to PS 80. A reduction of the P 188 concentration by factor 10 from 1 mg/mL to 0.1 mg/mL did not have a considerable effect on the absolute number of particles formed.

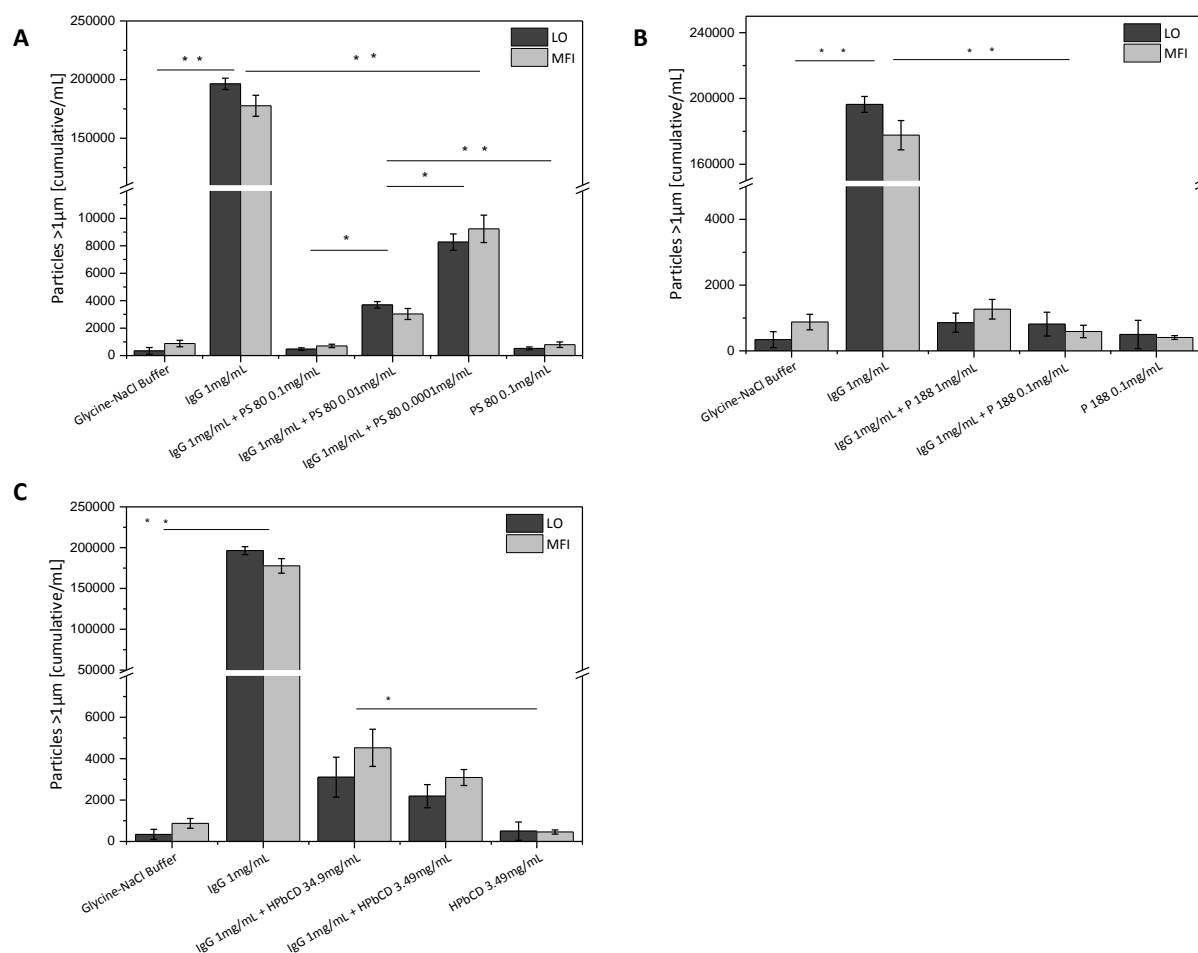


Figure 17: Number of particles >1 μm / mL of 1 mg/mL IgG in Glycine-NaCl buffer with addition of A: PS 80, B: P 188, C: HP- β -CD after 48 h of horizontal shaking in vials determined by LO and MFI (including controls)

HP- β -CD also prevented protein particle formation upon shaking considerably at the two concentrations tested (Fig. 17C). At the highest HP- β -CD concentrations tested higher numbers of particles formed compared to the formulations containing PS 80 or P 188. This supports the assumption that the occupation of the interface by the additive molecules is an important factor to stabilize proteins against interfacial stress. Because the surface activity of HP- β -CD is less pronounced compared to PS 80 and P 188, also its stabilizing effect might be lower accordingly.

4.6.2. By Liquid-Air Interfacial Stress (Mini-Trough)

To investigate the impact of only liquid-air interfacial stress on the particle formation, continuous compression-decompression cycles were performed in the Mini-Trough and analyzed for particle formation. PS 80 had a similar concentration dependent effect as described for the agitation study (Fig. 18). The presence of very low PS 80 concentrations below CMC resulted in even higher numbers of particles compared to the IgG solution without surfactant. In case PS 80 was present in a concentration of 0.00005 mg/mL around 11 000 particles $>1\ \mu\text{m}$ / mL built up. In case the pure IgG solution was stressed around 6 500 particles $>1\ \mu\text{m}$ / mL were formed only. This destabilizing effect of PS 80 at concentrations well below CMC has been previously reported [35], [37], [39]. Accordingly, P 188 successfully inhibited particle formation at all tested concentrations. Moreover, also HP- β -CD prevented the IgG from interface-induced aggregation although not as effectively as the non-ionic surfactants. Hence, these results point out that the investigated additives all evolve protein stabilizing properties at the liquid-air interface directly.

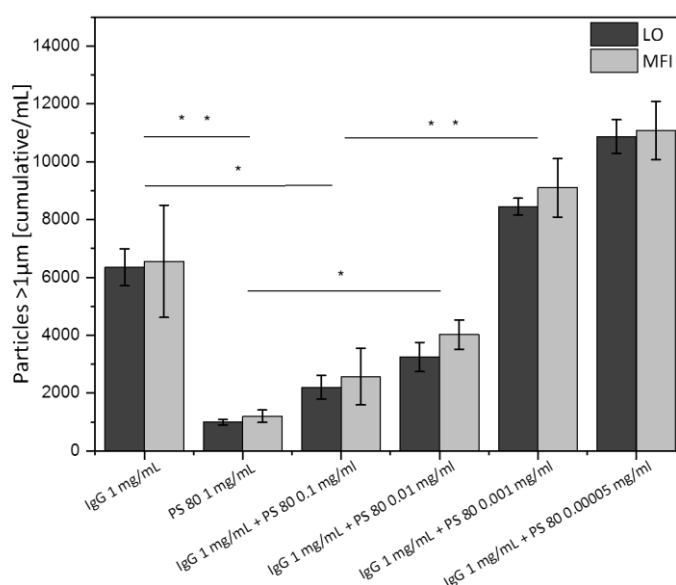


Figure 18: Number of particles $>1\ \mu\text{m}$ / mL after 100 continuous compression-decompression cycles of 1 mg/mL IgG in Glycine-NaCl buffer with and without addition of PS 80 in different concentrations

5. SUMMARY & CONCLUSION

Formulation additives, such as non-ionic surfactants, are known to successfully inhibit surface-induced protein aggregation. Nevertheless, little is known about the underlying mechanisms of stabilization [7]. In this study surface-sensitive physicochemical analytical tools were used to evaluate the effect of PS 80, P 188 and HP- β -CD on the interfacial film when co-adsorbed with an IgG. Additionally, the effect of the additives on protein particle formation upon stressing the interface by agitation and in a Mini-trough by compression and decompression was investigated. These approaches aim to improve targeted formulation development by better understanding of the liquid-air interface behavior of protein-additive mixtures.

The IgG investigated in this study shows a pronounced amphiphilic behavior. It adsorbs to the liquid–air interface in a time-dependent manner, reaching a maximum equilibrium adsorption pressure after about 4 hours. In equilibrium, a surface pressure of $\pi_{eq} = 18.5$ mN/m was reached. Adsorption of the additives occurred much faster (0.1–0.2 h), due to their lower molecular weight and the more distinct amphiphilic character [18]. A maximum surface pressure of 31 mN/m was reached for a 0.1 mg/mL PS 80 solution. The mixture of IgG with 0.00005 mg/mL PS 80 reached an equilibrium surface pressure of 15.2 mN/m after 1.3 h indicating a considerable contribution of the IgG. The mixtures with P 188 at concentrations of 0.1 mg/mL and above and HP- β -CD at 3.49 mg/mL and above reached equilibrium surface pressure already within 0.4 h. Additive and protein molecules compete for the adsorption to the interface, and the composition of the interfacial film depends on the mixing ratio [10], [35], [40]. The investigation of the interfacial film compressibility revealed that the IgG forms a highly compressible film different to the additives tested. During compression, the distribution and ordering of the molecules changes resulting in a densely-packed layer [9]. The IgG molecules rather stay at the interface and do not desorb easily upon compression as proven by the increase in surface pressure up to 44.9 mN/m [41], [42]. This effect is promoted by the formation of a strong protein network due to marked short-range protein-protein interactions [43], [44]. Decompressions initially lead to a pronounced decrease in surface pressure, followed by a re-adsorption phase. Therefore, compression must cause an increase in interfacial film thickness and / or packing density. Equilibrium surface pressure slightly decreased with each cycle which can be related to a loss of material from the interface into the bulk phase [41],

[45]. Mixtures of IgG and PS 80 at 0.01 mg/mL and above ended up at identical π_{\max} as pure PS 80 solutions. Adsorption of the small, strongly amphiphilic PS 80 molecules is kinetically favored and therefore is much faster compared to the large IgG molecules. In the IgG - PS 80 mixture at a surfactant concentration below CMC of 0.00005 mg/mL, the reduction of π_{\max} by 7.4 mN/m compared to the pure IgG indicates the additional presence of PS 80 molecules in the IgG film. Below the CMC, IgG molecules must be present at the interface in mixtures as π_{\max} was 8.9 mN/m higher compared to the pure PS 80 film. Lu and Rhodes described similar findings, with compression of PS 80 films yielding a maximum surface pressure change of 20 mN/m [46]. Overall, the change in surface pressure also depends on the compression speed and compression factor which can explain the deviation of the absolute values obtained in this study from literature [45]. The compressibility can be assigned to the hydrophobic side chains of surfactants, such as sorbitan esters, which can be condensed and therefore compressed to higher surface pressure values [46]. With this increase in surface pressure polysorbate molecules are also forced into the subphase due to their substantial water solubility [35].

Compared to pure IgG, the compressibility of mixed IgG-P 188 films was very low indicating that the film predominantly consists of poloxamer molecules for all concentrations tested. At a mixture ratio of 1:100, the difference in π_{\max} of the mixtures compared to pure surfactant was more pronounced for PS 80 (9.2 mN/m) compared to P 188 (1.3 mN/m). We determined a CMC of P 188 of 0.21 mg/mL although there is controversy about whether or not a clear CMC can be ascribed to poloxamers [17], [18], [32]. Poloxamers have been reported to occupy larger surface areas compared to polysorbates at comparable concentrations [7], [38], [47]. Hence, P 188 may be superior to PS 80 in inhibiting protein adsorption also due to a potential direct interaction with protein molecules in solution [48]. Also HP- β -CD rather effectively prohibited the protein from interface adsorption. At all concentrations investigated films of HP- β -CD-IgG mixtures did not show any protein-like behavior and the compression-decompression did not result in the formation of a considerable hysteresis. Serno *et al.* showed that 0.28 mg/mL to 1.4 mg/mL HP- β -CD can protect an IgG from liquid-air interface related aggregation [23]. Therefore, the investigated concentration range of 0.349 mg/mL to 34.9 mg/mL might have been chosen too high to identify possible protein effects. Different hypothesis for the effect of HP- β -CD have been presented and it was suggested that mixtures of IgG and HP- β -CD can coexist at the interface [49], [50]. The

surface activity of both HP- β -CD and the two surfactants PS 80 and P 188 was proven here and appears to be an important prerequisite for their mechanism of action.

IRRAS was used to prove the interfacial film composition. Except for the spectra of pure IgG and the IgG-PS 80 mixture with 0.00005 mg/mL PS 80, no amide bands referring to the IgG were detected. Rather CH₂-groups that can be assigned to the lipid chains gave evidence about the presence of PS 80 at the interface. The presence of P 188 was proven next to the weak CH₂-bands also by distinctive bands which can be assigned to ether elements (C-O-C) of the polyoxyethylen and polyoxypropylen units. HP- β -CD at the interface caused the appearance of pronounced bands that can be attributed to C-O stretching.

Although AFM and BAM have been extensively used to look at lipid films [51]–[54], little is known about the complex interplay of antibodies and pharmaceutically relevant formulation additives. The increased brightness in BAM images can be attributed to the presence of a protein film at the interface, as it was the case for IgG. For all IgG-additive mixtures with low additive concentration, BAM images revealed the typical protein island-like structures which did not change considerably during compression. As the additive solutions alone do not supply any signal, bright domains are caused by the presence of IgG. Bright, demarcated areas within the film were present even in mixtures with high surfactant concentrations above CMC (PS 80 0.01mg/mL, P 188 1 mg/mL) demonstrating that IgG is still present. Also, mixed films of IgG with HP- β -CD at a concentration of 34.9 mg/mL still showed flickering areas indicating the presence of some protein clusters at the interface. Consequently, all additives cannot entirely prevent IgG adsorption at the interface, even at high concentrations.

Although at a smaller scale compared to BAM, AFM revealed the formation of a continuous film with some inhomogeneities for the pure IgG solution. Substantial changes within the film topography upon compression could be visualized as areas of telescoped protein material with an increased height appeared. AFM images of the IgG-PS 80 mixture with PS 80 present above CMC at a concentration of 0.01 mg/mL resulted in a very smooth and thin film similar to pure surfactant films. Compression did not affect the film appearance. The presence of 0.00005 mg/mL PS 80, a concentration below CMC led to a film which exhibited areas of agglomerated protein material of increased height with thin and flat regions in between. Compression caused an increase not only in size but also in height of the agglomerates. It has been stated that in mixtures with protein, surfactant molecules adsorb

at defects in the protein network [35]. Thereby, the surfactant molecules are compressing the interfacial protein network and, upon increasing surface pressure, surfactant molecules desorb. Accordingly, the addition of small quantities of surfactant has been reported to result in strong clustering of protein material. Additionally, low surfactant concentrations were shown to promote increased particle formation and to rather destabilize protein formulations against mechanical stress [18], [35]. At higher additive concentrations, this effect was not observed as already during adsorption only few protein molecules found their way to the surface [18], [55].

The formation of protein particles upon agitation is related to the mechanical stress of the interfacial film by continuous compression-decompression. Compression leads to the formation of a condensed film with potentially pronounced protein-protein interactions [56], [57]. Clusters of protein material are formed upon adsorption as identified using BAM and AFM. Upon interfacial stress, rupture of the film results in a release of protein material from the interface [12], [41], [45]. Depending on the extent of protein-protein interactions, the protein clusters can sustain and appear as particles or disintegrate [45]. Therefore, the surface-sensitive methods applied here give a strong hint on the presence of the protein at the interface, as it directly depends on the type and concentration a surface-active additive is present in a formulation. In addition, a strong coherence between the number of particles formed and the type and mixing ratio of the additive with the IgG was observed. Mixtures with PS 80 present below CMC exhibited increasing numbers of particles with decreasing PS 80 concentration. This supports the findings obtained by BAM and AFM that additive concentrations below CMC effect protein stability negatively. Although the addition of PS 80 above CMC reduced particle formation efficiently, it was shown that still some protein is present at the interface. Thus, even the addition of surfactant at a concentration above CMC was shown not to be enough to reach full stabilization of proteins formulations against mechanical stress.

Interestingly, in mixtures with IgG P 188 revealed a strong protective effect as all physicochemical investigations at the interface were dominated by the presence of the surfactant. Also, all P188 concentrations tested prevented the IgG from interface-related stress and aggregation. The results obtained in this study therefore evinced that P 188 had the most pronounced stabilizing effect on the protein when compared to PS 80 and HP- β -CD

However, also HP- β -CD was proven to have a surface-related stabilizing effect. HP- β -CD not only successfully prevented protein adsorption but also aggregation upon interfacial stress, although to a lower extent when compared to PS 80 and P 188. Therefore, HP- β -CD represents a valuable alternative to non-ionic surfactants as disadvantages of non-ionic surfactants may not be encountered.

Consequently, the different surface-sensitive techniques applied in combination with interfacial-stress studies provided valuable insights into the liquid-air interfacial film characteristics that help to better understand how formulation additives affect interface related protein instability.

6. SUPPLEMENTAL INFORMATION

6.1. Visual Inspection and Photodocumentation

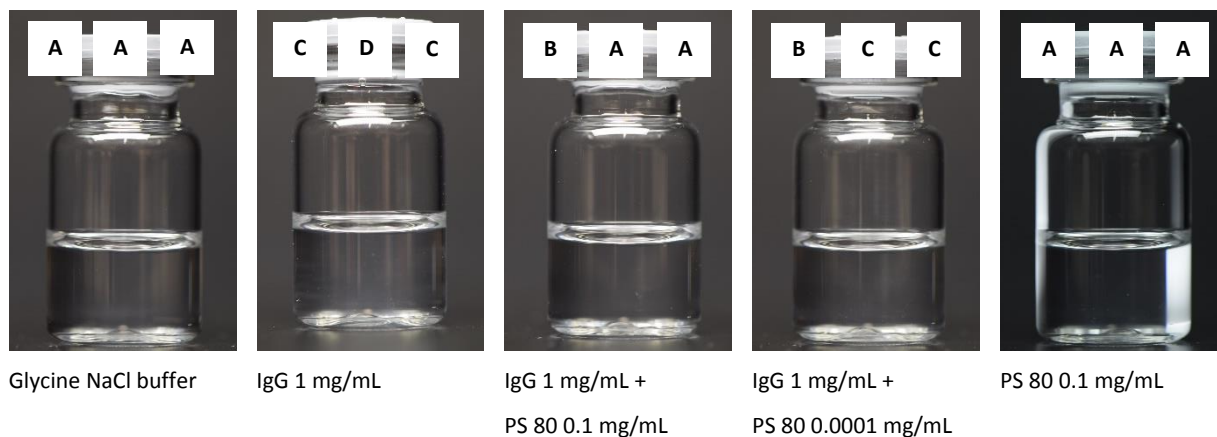


Figure 19: Visual Inspection and photodocumentation of IgG and IgG – PS 80 mixtures after 48h shaking

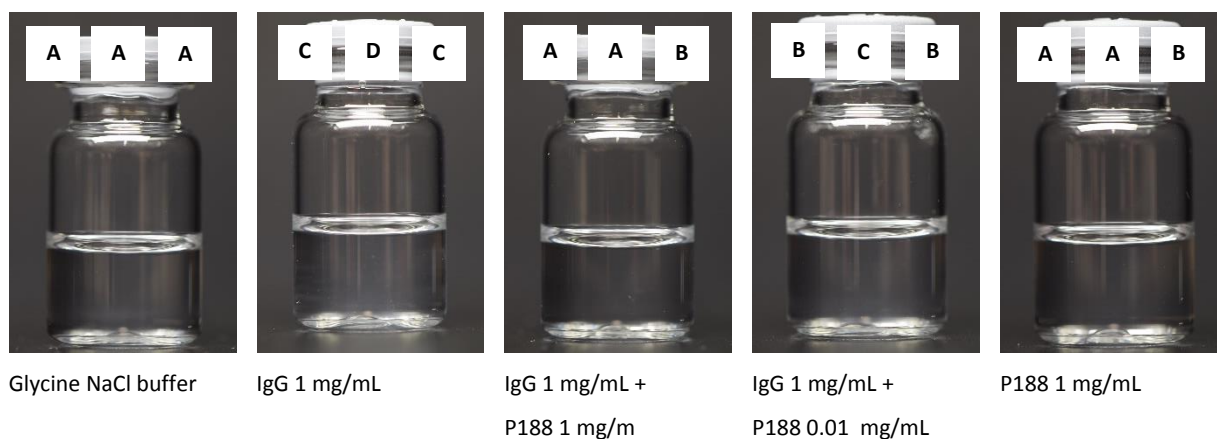


Figure 20: Visual Inspection and photodocumentation of IgG and IgG – P188 mixtures after 48h shaking

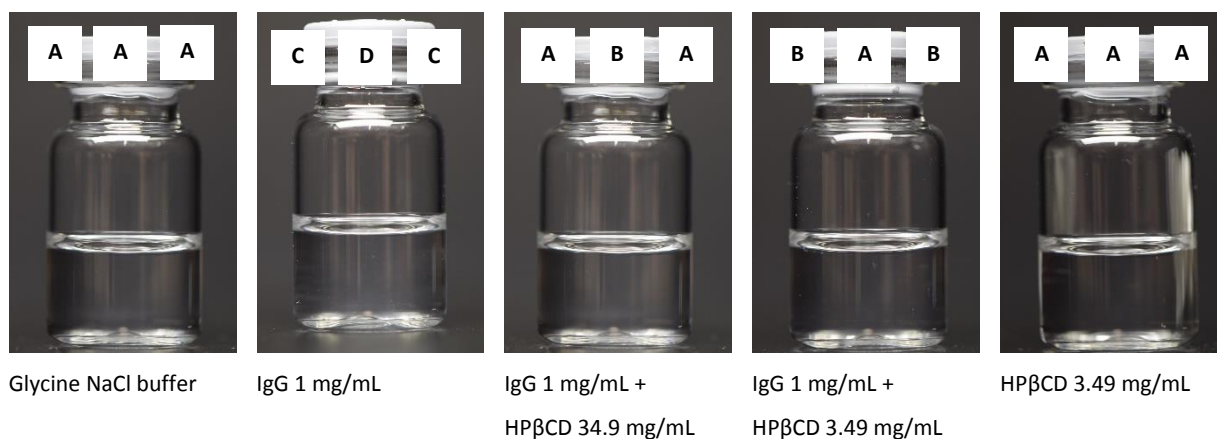


Figure 21: Visual Inspection and photodocumentation of IgG and IgG – HP- β -CD mixtures after 48h shaking

6.2. Turbidity

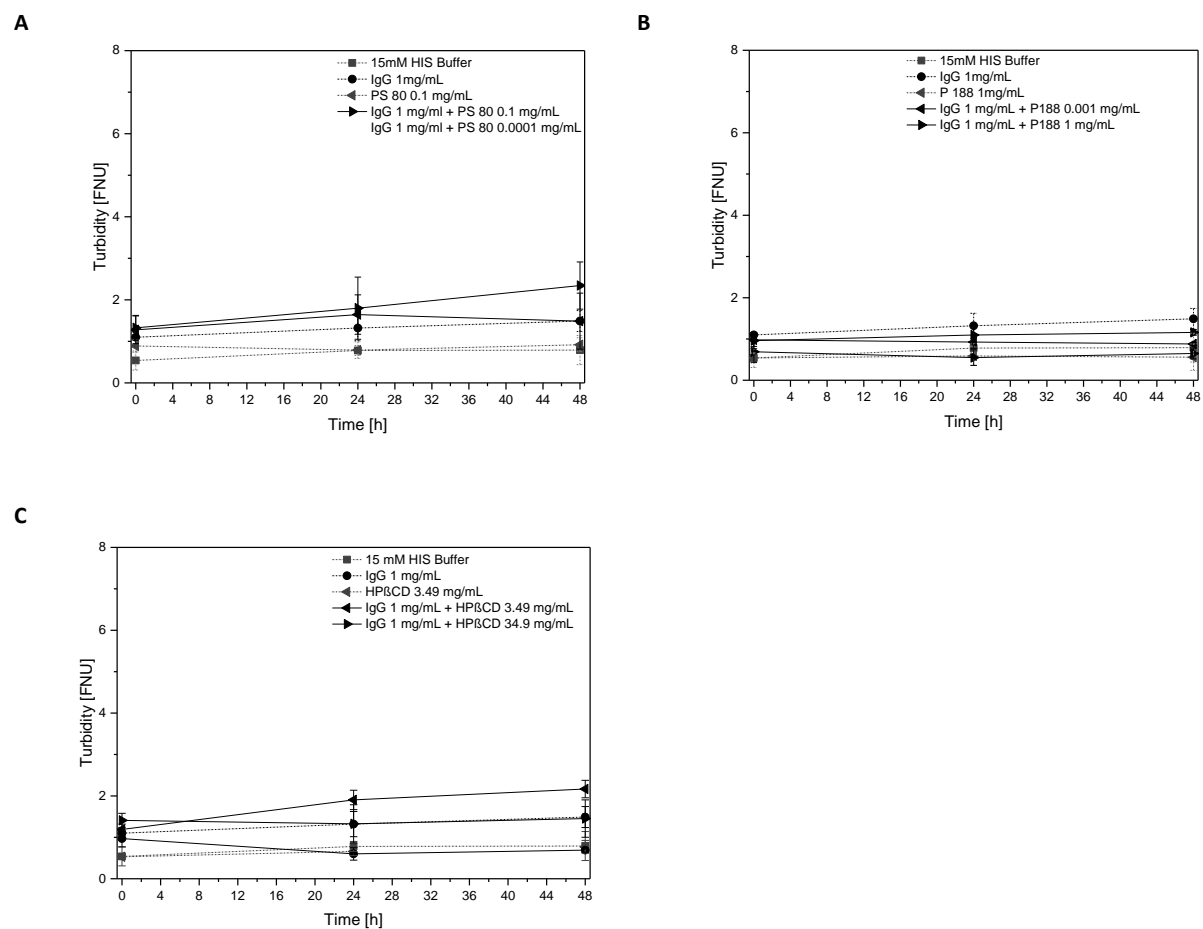


Figure 22: Turbidity during 48 h of horizontal shaking in vials determined by LO and MFI. Vials contained IgG in a concentration 1 mg/mL in Glycine-NaCl buffer in absence and presence of different additive concentrations. Glycine-NaCl buffer and additive only in the given concentration in Glycine-NaCl buffer served as controls, A: PS 80, B: P 188, C: HP- β -CD

7. REFERENCES

- [1] C. J. Roberts, "Protein aggregation and its impact on product quality," *Curr. Opin. Biotechnol.*, vol. 30, pp. 211–217, 2014.
- [2] S. J. Shire, "Formulation and manufacturability of biologics," *Curr. Opin. Biotechnol.*, vol. 20, no. 6, pp. 708–714, 2009.
- [3] J. Y. Zheng and L. J. Janis, "Influence of pH, buffer species, and storage temperature on physicochemical stability of a humanized monoclonal antibody LA298," *Int. J. Pharm.*, vol. 308, pp. 46–51, 2006.
- [4] W. Wang, S. Nema, and D. Teagarden, "Protein aggregation-Pathways and influencing factors," *Int. J. Pharm.*, vol. 390, no. 2, pp. 89–99, 2010.
- [5] A. Hawe and W. Friess, "Formulation development for hydrophobic therapeutic proteins.," *Pharm. Dev. Technol.*, vol. 12, pp. 223–237, 2007.
- [6] N. Rathore and R. S. Rajan, "Current perspectives on stability of protein drug products during formulation, fill and finish operations," *Biotechnol. Prog.*, vol. 24, no. 3, pp. 504–514, 2008.
- [7] H. L. Kim, A. McAuley, B. Livesay, W. D. Gray, and J. McGuire, "Modulation of protein adsorption by poloxamer 188 in relation to polysorbates 80 and 20 at solid surfaces," *J. Pharm. Sci.*, vol. 103, no. 4, pp. 1043–1049, 2014.
- [8] T. Serno, E. Härtl, A. Besheer, R. Miller, and G. Winter, "The Role of Polysorbate 80 and HP β CD at the Air-Water Interface of IgG Solutions," *Pharm. Res.*, pp. 1–14, 2012.
- [9] E. Koepf, R. Schroeder, G. Brezesinski, and W. Friess, "The film tells the story: Physical-chemical characteristics of IgG at the liquid-air interface," *Eur. J. Pharm. Biopharm.*, vol. 119, pp. 396–407, 2017.
- [10] V. B. Fainerman, S. A. Zholob, M. Leser, M. Michel, and R. Miller, "Competitive adsorption from mixed nonionic surfactant/protein solutions," *J. Colloid Interface Sci.*, vol. 274, pp. 496–501, 2004.

-
- [11] B. A. Kerwin, "Polysorbates 20 and 80 Used in the Formulation of Protein Biotherapeutics: Structure and Degradation Pathways," *J. Pharm. Sci.*, vol. 97, no. 8, pp. 2926–2935, 2008.
- [12] S. Kiese, A. Papppenberger, W. Friess, and H. C. Mahler, "Shaken, not stirred: Mechanical stress testing of an IgG1 antibody," *J. Pharm. Sci.*, vol. 97, no. 10, pp. 4347–4366, 2008.
- [13] A. Hawe, V. Filipe, and W. Jiskoot, "Fluorescent molecular rotors as dyes to characterize polysorbate-containing IgG formulations," *Pharm. Res.*, vol. 27, no. 2, pp. 314–326, 2010.
- [14] P. Wilde, A. Mackie, F. Husband, P. Gunning, and V. Morris, "Proteins and emulsifiers at liquid interfaces," *Adv. Colloid Interface Sci.*, vol. 108–109, pp. 63–71, 2004.
- [15] T. A. Khan, H.-C. Mahler, and R. S. Kishore, "Key interactions of surfactants in therapeutic protein formulations: A review," *Eur. J. Pharm. Biopharm.*, vol. 97, pp. 60–67, 2015.
- [16] H. J. Lee, A. McAuley, K. F. Schilke, and J. McGuire, "Molecular origins of surfactant-mediated stabilization of protein drugs," *Adv. Drug Deliv. Rev.*, vol. 63, no. 13, pp. 1160–1171, 2011.
- [17] U. Adhikari, A. Goliaei, L. Tsereteli, and M. L. Berkowitz, "Properties of poloxamer molecules and poloxamer micelles dissolved in water and next to lipid bilayers: Results from computer simulations," *J. Phys. Chem. B*, vol. 120, no. 26, pp. 5823–5830, 2016.
- [18] H. L. Kim, A. McAuley, and J. McGuire, "Protein effects on surfactant adsorption suggest the dominant mode of surfactant-mediated stabilization of protein," *J. Pharm. Sci.*, vol. 103, no. 5, pp. 1337–1345, 2014.
- [19] M. T. Yasamy, T. Dua, M. Harper, and S. Saxena, "a Growing Concern," vol. 3, no. June, pp. 4–9, 2012.
- [20] M. E. Brewster, S. H. Maninder, J. W. Simpkins, and N. Bodor, "Use of 2-hydroxypropyl- β -cyclodextrin as a solubilising and stabilising excipient for protein drugs," *Pharmaceutical research*, vol. 8, no. 6, pp. 792–795, 1991.

-
- [21] T. Serno, R. Geidobler, and G. Winter, "Protein stabilization by cyclodextrins in the liquid and dried state," *Adv. Drug Deliv. Rev.*, vol. 63, no. 13, pp. 1086–1106, 2011.
- [22] E. Härtl, N. Dixit, A. Besheer, D. Kalonia, and G. Winter, "Weak antibody-cyclodextrin interactions determined by quartz crystal microbalance and dynamic/static light scattering," *Eur. J. Pharm. Biopharm.*, vol. 85, no. 3, pp. 781–789, 2013.
- [23] T. Serno, J. F. Carpenter, T. W. Randolph, and G. Winter, "Inhibition of Agitation-Induced Aggregation of an IgG-Antibody by Hydroxypropyl- β -Cyclodextrin," *J. Pharm. Sci.*, vol. 99, no. 3, pp. 1193–1206, Mar. 2010.
- [24] F. L. Aachmann, D. E. Otzen, K. L. Larsen, and R. Wimmer, "Structural background of cyclodextrin \pm protein interactions," vol. 16, no. 12, 2004.
- [25] A. Martos, W. Koch, W. Jiskoot, K. Wuchner, G. Winter, W. Friess, A. Hawe, "Trends on Analytical Characterization of Polysorbates and Their Degradation Products in Biopharmaceutical Formulations," *J. Pharm. Sci.*, vol. 106, no. 7, pp. 1722–1735, 2017.
- [26] R. Mendelsohn, "External Infrared Reflection Absorption Spectrometry of Monolayer Films at the Air-Water Interface," *Annu. Rev. Phys. Chem.*, vol. 46, pp. 305–334, 1995.
- [27] C. R. Flach, J. W. Brauner, J. W. Taylor, R. C. Baldwin, and R. Mendelsohn, "External reflection FTIR of peptide monolayer films in situ at the air/water interface: experimental design, spectra-structure correlations, and effects of hydrogen-deuterium exchange," *Biophys. J.*, vol. 67, no. 1, pp. 402–410, 1994.
- [28] A. H. Muentner, J. Hentschel, H. G. Borner, and G. Brezesinski, "Characterization of peptide-guided polymer assembly at the air/water interface," *Langmuir*, vol. 24, no. 7, pp. 3306–3316, 2008.
- [29] S. Hénon and J. Meunier, "Microscope at the Brewster angle: Direct observation of first-order phase transitions in monolayers," *Rev. Sci. Instrum.*, vol. 62, no. 4, pp. 936–939, 1991.
- [30] D. Hoenig and D. Moebius, "Direct Visualization of Monolayers at the Air-Water Interface by Brewster Angle Microscopy," *J. Phys. Chem.*, no. 2, pp. 4590–4592, 1991.

-
- [31] D. Vollhardt, "Brewster angle microscopy: A preferential method for mesoscopic characterization of monolayers at the air/water interface," *Curr. Opin. Colloid Interface Sci.*, vol. 19, no. 3, pp. 183–197, 2014.
- [32] D. R. Devi, P. Sandhya, and B. N. V. Hari, "Poloxamer: A novel functional molecule for drug delivery and gene therapy," *J. Pharm. Sci. Res.*, vol. 5, no. 8, pp. 159–165, 2013.
- [33] S. Horiuchi and G. Winter, "CMC determination of nonionic surfactants in protein formulations using ultrasonic resonance technology," *Eur. J. Pharm. Biopharm.*, vol. 92, pp. 8–14, 2015.
- [34] J.-L. Tian, Y. Z. Zhao, Z. Hin, C. T. Lu, Q. Q. Tang, Q. Xiang, C. Z. Sun, L. Zhang, Y. Y. Xu, H. S. Gao, Z. C. Zhou, X. K. Li, Y. Zhang, "Synthesis and characterization of Poloxamer 188-grafted heparin copolymer.," *Drug Dev. Ind. Pharm.*, vol. 36, no. 7, pp. 832–8, 2010.
- [35] A. R. Mackie, A. P. Gunning, P. J. Wilde, and V. J. Morris, "Orogenic Displacement of Protein from the Air/Water Interface by Competitive Adsorption.," *J. Colloid Interface Sci.*, vol. 210, no. 1, pp. 157–166, 1999.
- [36] R. R. Niño, C. C. Sanchez, V. P. Ruiz-Henestrosa, J. M. Rodríguez-Patino, "Milk and soy protein films at the air-water interface," *Food Hydrocoll.*, vol. 19, no. 3, pp. 417–428, 2005.
- [37] A. R. Mackie, A. P. Gunning, P. J. Wilde, and V. J. Morris, "Competitive displacement of beta-lactoglobulin from the air/water interface by sodium dodecyl sulfate," *Langmuir*, vol. 16, no. 11, pp. 8176–8181, 2000.
- [38] E. Mohajeri and G. D. Noudeh, "Effect of temperature on the critical micelle concentration and micellization thermodynamic of nonionic surfactants: Polyoxyethylene sorbitan fatty acid esters," *E-Journal Chem.*, vol. 9, no. 4, pp. 2268–2274, 2012.
- [39] K. Ziegler, "Untersuchungen zur Stabilisierung und Interaktion von Cetuximab mit nicht-ionischen Tensiden," 2013.

-
- [40] Z. Liao, J. W. Lampe, P. S. Ayyaswamy, D. M. Eckmann, and I. J. Dmochowski, "Protein assembly at the air-water interface studied by fluorescence microscopy," *Langmuir*, vol. 27, pp. 12775–81, 2011.
- [41] J. S. Bee, D. K. Schwartz, S. Trabelsi, E. Freund, J. L. Stevenson, J. F. Carpenter, and T. W. Randolph, "Production of particles of therapeutic proteins at the air–water interface during compression/dilation cycles," *Soft Matter*, vol. 8, no. 40, p. 10329, 2012.
- [42] S. Ghazvini, C. Kalonia, D. B. Volkin, and P. Dhar, "Evaluating the Role of the Air-Solution Interface on the Mechanism of Subvisible Particle Formation Caused by Mechanical Agitation for an IgG1 mAb," *J. Pharm. Sci.*, vol. 105, no. 5, pp. 1643–1656, 2016.
- [43] E. A. Vogler, "Protein adsorption in three dimensions," *Biomaterials*, vol. 33, no. 5, pp. 1201–1237, 2012.
- [44] V. S. Alahverdijeva, K. Khristov, D. Exerowa, and R. Miller, "Correlation between adsorption isotherms, thin liquid films and foam properties of protein/surfactant mixtures: Lysozyme/C10DMPO and lysozyme/SDS," *Colloids Surfaces A Physicochem. Eng. Asp.*, vol. 323, no. 1–3, pp. 132–138, 2008.
- [45] E. Koepf, S. Eisele, R. Schroeder, G. Brezesinski, and W. Friess, "Notorious But Not Understood: How Liquid-Air Interfacial Stress Triggers Protein Aggregation," *J. Pharm. Sci.*, p. submitted August 14, 2017.
- [46] D. Lu and D. G. Rhodes, "Mixed composition films of Spans and Tween 80 at the air-water interface," *Langmuir*, vol. 16, no. 21, pp. 8107–8112, 2000.
- [47] M. E. Mahmood and D. A. F. Al-Koofee, "Effect of Temperature Changes on Critical Micelle Concentration for Tween Series Surfactant," *Glob. J. Sci. Front. Res. Chem.*, vol. 13, no. 4, pp. 1–7, 2013.
- [48] S. A. Maskarinec, J. Hannig, R. C. Lee, and K. Y. C. Lee, "Direct observation of poloxamer 188 insertion into lipid monolayers," *Biophys. J.*, vol. 82, no. 3, pp. 1453–9, 2002.

-
- [49] T. Serno, "Inhibition of therapeutic protein aggregation by cyclodextrins. Dissertation," Ludwig-Maximilians-Universität, Munich, Germany, 2010.
- [50] E. A. Vogler, K. B. Spencer, D. B. Montgomery, L. M. Lander, and W. J. Brittain, "Design and Operational Characteristics of a Robotic Wilhelmy Balance," *Langmuir*, vol. 9, no. 9, pp. 2470–2477, 1993.
- [51] E. Amado, A. Kerth, A. Blume, and J. Kressler, "Infrared reflection absorption spectroscopy coupled with brewster angle microscopy for studying interactions of amphiphilic triblock copolymers with phospholipid monolayers," *Langmuir*, vol. 24, no. 18, pp. 10041–10053, 2008.
- [52] C. C. Sánchez, M. R. R. Niño, A. L. Caro, and J. M. R. Patino, "Biopolymers and emulsifiers at the air-water interface. Implications in food colloid formulations," *J. Food Eng.*, vol. 67, no. 1–2, pp. 225–234, 2005.
- [53] S. Miao, H. Leeman, S. De Feyter, and R. A. Schoonheydt, "Facile preparation of Langmuir-Blodgett films of water-soluble proteins and hybrid protein-clay films," *J. Mater. Chem.*, vol. 20, no. 4, pp. 698–705, 2010.
- [54] T. S. Berzina, V. I. Troitsky, A. Petrigliano, D. Alliata, A. Y. Tronin, and C. Nicolini, "Langmuir-Blodgett films composed of monolayers of amphiphilic molecules and adsorbed soluble proteins," *Thin Solid Films*, vol. 284–285, no. Cyt c, pp. 757–761, 1996.
- [55] D. Otzen, "Protein-surfactant interactions: A tale of many states," *Biochim. Biophys. Acta - Proteins Proteomics*, vol. 1814, no. 5, pp. 562–591, 2011.
- [56] R. G. Couston, D. A. Lamprou, S. Uddin, and C. F. Van Der Walle, "Interaction and destabilization of a monoclonal antibody and albumin to surfaces of varying functionality and hydrophobicity," *Int. J. Pharm.*, vol. 438, no. 1–2, pp. 71–80, 2012.
- [57] J. Sánchez-González, M. A. Cabrerizo-Vílchez, and M. J. Gálvez-Ruiz, "Interactions, desorption and mixing thermodynamics in mixed monolayers of beta-lactoglobulin and bovine serum albumin," *Colloids Surf. B. Biointerfaces*, vol. 21, no. 1–3, pp. 19–27, 2001.

CHAPTER VI - Part 1

HOW FORMULATION PH AND IONIC STRENGTH AFFECT PHYSICOCHEMICAL PROTEIN BEHAVIOR AT THE LIQUID-AIR INTERFACE

1. ABSTRACT

Both, formulation parameters and the presence of liquid-air interfaces are known to affect the aggregation of protein drugs. In this study, the impact of pH on the liquid-air interfacial behavior of three proteins, a polyclonal and two monoclonal antibodies (IgG, mAB₁ and mAB₂) was investigated using different surface sensitive methods. Equilibrium surface pressure values revealed only a minor impact of pH and ionic strength. Infrared Reflectance Absorbance Spectroscopy (IRRAS) proved not only the presence of the proteins at the interface but also showed that the secondary structure was not considerably affected by the adsorption to the interface independent of pH between pH 3 and 9. Additionally, the physical resistance of the film as determined by the interfacial compressibility in a Langmuir trough was not affected by pH. Compression of the interfacial film caused the formation of telescoped areas which were no longer present after decompression at all pH values as investigated by underwater Atomic Force Microscopy (AFM). Brewster Angle Microscopy (BAM) showed some slight changes in the film reflectivity depending on pH, indicating changes in the interfacial film thickness. IRRAS experiments at different angles of incidence as well as section analysis of AFM images proved not only that the film thickness increased upon compression, but also that the interfacial film is thinner at pH 4 than at pH 9. Continuous compression and decompression of the protein film resulted in particle formation with increasing numbers of particles at higher pH value as detected by Light Obscuration and Micro-Flow Imaging.

The use of different surface sensitive methods provides expedient information on how liquid-air interfacial events are affected by formulation pH and ionic strength. These findings enable a better understanding of the events and processes happening at the interface and can be directly linked to the interface-related formation of particles.

2. INTRODUCTION

Protein stability is a major priority during the development of protein pharmaceuticals. Moreover, protein aggregation is one critical stability parameter for safety and efficacy of protein pharmaceuticals [1]–[4] and is described as the process by which individual protein molecules assemble into larger complexes [5]. Protein aggregates differ not only in size, ranging from dimers to oligomers to large visible particles, but also in conformation consisting of unfolded, partly unfolded, native monomers or combinations thereof. Large native-like aggregates, with essentially intact secondary and tertiary structure have been associated with immune reactions, especially when also chemically modified [5]. Typically, conformational distortion with hydrophobic amino acid residues, becoming exposed to the surface, triggers aggregation due to stronger hydrophobic protein-protein interactions [6]. In addition, solution pH and ionic strength are important factors affecting colloidal stability due to their decisive impact and charge shielding responsible for charge interaction [7], [8]. Thus, pH value and ionic strength have to be chosen carefully, as they impact colloidal as well as conformational stability [9], [10]. In presence of interfaces, aggregation processes may differ fundamentally from those described in solution. Due to their partly amphiphilic character proteins adsorb to interfaces, accumulate and form highly compressible films. Continuous rupture of the interface, e.g. by a needle [13], or continuous compression and decompression of the adsorbed protein film [14], can be correlated with protein aggregation upon shaking of protein formulations in their primary container. However, many pieces in the puzzle of protein aggregation caused by stressing the liquid-air interface of protein solutions are still missing. Several authors describe that proteins, such as lysozyme, unfold upon adsorption [13], [14]. Nevertheless, investigations of the interfacial conformation of pharmaceutically relevant proteins have not been reported yet. Furthermore, the impact of pH value and ionic strength on protein adsorption, unfolding and protein-protein interactions at the interface is complex and requires elucidation.

Besides studying surface activity itself, the impact of pH on the liquid-air interfacial film was investigated using surface-sensitive spectroscopic methods. Additionally, the number of particles formed by liquid-air interfacial stress at different pH values was analyzed. Thus, a better understanding of how the pH value affects protein interfacial behavior and the process of aggregation is reached.

3. MATERIALS AND METHODS

3.1. Materials

Human IgG (Beriglobin™, CSL Behring GmbH, Germany) was used for this study. The market product contains 159 mg/mL human IgG in 22 g/L Glycine and 3 g/L NaCl buffer at pH 6.8. Additionally, two monoclonal antibodies were investigated (mAB₁ and mAB₂) provided by AbbVie Deutschland GmbH & Co. KG, Ludwigshafen am Rhein, Germany. mAB₁ is formulated in 20mM Histidine buffer at pH 6.0 in a concentration of 126 g/L, mAB₂ in 15mM Histidine buffer at pH 5.3 in a concentration of 94 g/L. In Hydrophilic Interaction Chromatography (HIC) mAB₂ turned out to be more hydrophobic compared to mAB₁. Dilutions were performed using 15 mM histidine buffer, prepared using highly purified water (ELGA LC134, ELGA LabWater, Germany) and pH was adjusted by addition of 1mM NaOH and 1mM HCl, respectively. All samples were filtrated using 0.2µm sterile polyethersulfone (PES) syringe filters (PES, VWR, Germany). All protein solutions were diluted to a final concentration of 1 mg/mL for analysis unless otherwise stated with 15 mM histidine buffer as standard condition.

3.2. Sum Frequency Generation

Sum Frequency Generation (SFG) is a second-order nonlinear optical process and inherently specific for interfaces with inversion symmetry, such as the liquid-air interface, in the time average [15]. Two laser beams are combined at the interface, where the sum frequency of the two impinging beams is generated. One beam has tunable infrared wavelengths (IR), whereas the other one is of a fixed wavelength (vis). SFG is not only highly sensitive to changes in the interfacial composition and surface coverage, but also to the intrinsic molecular arrangement of the adsorbed layer. SFG measurements were performed with a broadband SFG spectrometer (in-house production FAU Erlangen-Nuernberg) as described elsewhere [16]. The spectrometer is equipped with a tunable femtosecond IR laser (bandwidth $>200\text{ cm}^{-1}$) and an etalon filtered pulse at 800 nm wavelength (bandwidth $<6\text{ cm}^{-1}$). Spectra were recorded with s-polarized sum frequency, s-polarized IR and vis beams. All spectra were normalized to an oxygen plasma cleaned polycrystalline aurum sample as reference spectrum. Spectra were collected from a 1 mg/mL IgG solution in 15 mM histidine buffer in a Petri dish. Each spectrum was measured by scanning the

broadband IR beam with a step width of 130 cm^{-1} . Acquisition time was set to 8 min for a frequency range between $2800\text{--}3800\text{ cm}^{-1}$.

3.3. Surface Pressure Measurements

Surface activity was expressed by surface pressure Π , with $\Pi = \sigma_0 - \sigma$, where σ_0 and σ are the aqueous subphase surface tension and the surface tension of the aqueous protein solution, respectively. Surface pressure measurements were performed in a $5.9 \times 39.7\text{ cm}^2$ PTFE Langmuir trough equipped with a metal alloy dyne probe (Microtrough XS, Kibron Inc., Finland). For the determination of equilibrium surface pressures a 3×6 Multiwell Plate ($V = 0.8\text{ mL}$) was used. Results are given as mean ($n = 3$) and standard deviation. Equilibrium adsorption pressure is defined as the maximum surface pressure that is reached by adsorption only and stable in a range of $\pm 0.2\text{ mN/m}$ within 0.5 h. 160 mL sample solution was filled into the trough for the repeated compression-decompression measurements. The surface area of the trough can be varied by two movable PTFE barriers. Temperature was kept at $20\text{ }^\circ\text{C}$ (K6-cc circulation thermostat, Peter Huber Kaeltemaschinenbau GmbH, Germany). Compression speed was set to 55 mm/min , and compression-decompression cycles were conducted from a maximum surface area of $A_{\text{max}} = 210\text{ cm}^2$ to $A_{\text{min}} = 52\text{ cm}^2$. Compression was started after the equilibrium adsorption pressure was reached.

3.4. Electrophoretic Light Scattering

The isoelectric point of the IgG was determined to 6.94 using a Zetasizer Nano ZS (Malvern Instruments, Worcestershire, UK). IgG was used at 5 mg/mL in a 15 mM histidine buffer. Using a Boltzmann fit the IEP was determined by Origin 8G (OriginLab Corporation, USA). Detailed results are described in the appendix (Fig. 16). IEP of the other mABs were already known by the provided certificate of analysis as 8.75 for mAB₁ and 6.51 for mAB₂.

3.5. FT-IR Spectroscopy

For FT-IR measurements spectra were recorded using a Tensor 27 (Bruker Optics GmbH, Germany) connected to a thermostat (DC30-K20, Thermo Haake GmbH, Germany). For each measurement, the protein was formulated at 10 mg/mL , and for each spectrum 100 absorbance scans were collected at a single beam mode with a resolution of 4 cm^{-1} . Spectra

were analyzed by Opus 7.5 (Bruker Optics GmbH, Germany) and displayed as vector-normalized second-derivative spectra (calculated with 17 smoothing points according to the Savitzky-Golay algorithms [17]). Infrared spectra of the protein in solution were recorded using an AquaSpec (transmission cell H₂O A741-1) and a BioATR or BioATR cell™ II respectively, at 20 °C.

Infrared spectra during temperature-induced unfolding of the IgG samples were recorded using the BioATR cell with buffer as reference. Temperature-dependent spectra were acquired every 4 °C from 25 – 93 °C with an equilibration time of 120 s. Infrared spectra were analyzed by Protein Dynamics for Opus 7.5.

3.6. Infrared Reflection-Absorption Spectroscopy (IRRAS)

IRRAS was used to determine the presence and the conformation of the adsorbed protein at the soft liquid/air interface. IRRAS spectra were recorded using a VERTEX FT-IR spectrometer (Bruker Optics GmbH, Germany) equipped with a liquid nitrogen-cooled MCT detector. The spectrometer was coupled to a Langmuir trough (Riegler&Kirstein GmbH, Germany), placed in a sealed container (external air/water reflection unit XA-511) to guarantee constant vapor atmosphere. The IR beam was conducted out of the spectrometer and focused onto the liquid surface of the Langmuir trough. A computer controlled KRS-5 wire-grid polarizer (thallium bromide and iodide mixed crystal) was used to generate perpendicular (s) and parallel (p) polarized light. The angle of incidence was set to 40° with respect to the surface normal. Measurements were performed using a trough with two compartments and a trough shuttle system. One compartment contained the protein solution under investigation (sample), whereas the other (reference) was filled with the pure buffer sub-phase. The single-beam reflectance spectrum (R_0) from the reference trough was taken as background for the single-beam reflectance spectrum (R) of the monolayer in the sample trough to calculate the reflection-absorption spectrum as $-\log(R/R_0)$ in order to eliminate the water vapor signal. IR spectra were collected at 8 cm⁻¹ resolution and a scatter speed of 20 kHz. For s-polarized light, spectra were co-added over 200 scans, and spectra with p-polarized light were co-added over 400 scans. To distinguish between the influence of increasing concentration and changed orientation on the signal intensity, the dichroic ratio DR of the amide I band at 1643 cm⁻¹ was calculated as $DR = A_p/A_s$, with A_p and A_s being the maximum absorption obtained with p-polarized light and s-polarized light, respectively. For the

determination of the interfacial film thickness in equilibrium and after compression to 30 mN/m, the incidence angle of the IR beam was varied with respect to the surface normal between 30° and 72° in steps of 2° or 3°. IRRA spectra were simulated using a MATLAB program [18], [19] on the basis of the optical model of Kuzmin and Michailov [20], [21]. The intensity and shape of a reflection absorption band depend on the absorption coefficient k , the full-width at half-height, the orientation of the transition dipole moment within the molecule, the molecular tilt angle, the polarization and the angle of incidence (Aoi) of the incoming light, as well as the layer thickness and its refractive index n . By using an Abbe refractometer (Nr. 322323, Carl-Zeiss AG, Germany) an average n for 100 mg/ml protein solutions was determined as 1.5 and used for the calculations of film thickness. Simulated spectra were fitted to the experimental data in a global fit, where all spectra recorded at different Aoi and different polarizations were fitted in one non-linear least square minimization using the Levenberg-Marquardt algorithm. The polarizer quality was set to $\Gamma = 0.01$. The optical constants of the water subphase were taken from Bertie et al. [22], [23]. The layer thickness was determined from a fit of the OH stretching vibrational band $\nu(\text{OH})$ in the range of 3800–3000 cm^{-1} .

3.7. Brewster Angle Microscopy (BAM)

A Langmuir Trough (KSV NIMA, Finland) was connected to a KSV NIMA Brewster Angle Microscope to enable visualization of the monolayer at the Brewster Angle (53.06°, p-polarized light). Protein solutions of 0.1 mg/mL were filled into the trough ($V = 80 \text{ mL}$). Simultaneous surface pressure measurements during adsorption and compression in the Langmuir trough enabled a direct connection of each image with the corresponding surface pressure during adsorption or compression of the protein. The lateral resolution of the BAM was approximately 3 μm . The size of the BAM images is 400 x 720 μm^2 .

3.8. Atomic Force Microscopy (AFM)

For AFM, protein films formed during adsorption to equilibrium surface pressure or after compression to a desired surface pressure were transferred by Langmuir-Schaefer deposition (horizontal transfer of the film) using 1 cm x 1 cm mica plates (Mica Sheet V5 Quality, Science Services GmbH, Germany) attached to a stamp tool. The mica was lowered onto the surface and pulled off after 2 s of contact time. The mica was removed from the

stamp tool and the transferred film was covered with 1 drop of buffer solution to prevent drying of the sample. The transferred films were analyzed by underwater AFM (Bruker / Veeco / Digital Instruments MultiMode AFM) using a cantilever (Arrow™ NCPT, resonance frequency 285 kHz, spring constant 42 N/m) in tapping mode (Nano World AG, Switzerland). Images were analyzed by NanoScope III 5.12r3 Software (Digital Instruments Inc., US).

For the determination of interfacial film thickness the film was transferred onto silica by Langmuir-Schaefer technique. A scratch was made using stainless steel tweezers. Film thickness was determined by section analysis from an average of 6 measuring points from the silica substrate to the film (area unaffected by the scratch).

3.9. Mini-Trough

The so-called “Mini”-trough was designed and built in-house. It consists of a PTFE trough with same proportions and functionality as the Kibron Langmuir Trough described before without a surface pressure measurement unit. Automated and continuous compression-decompression cycles can be performed to stress the liquid-air interface only. In relation to the Langmuir Trough the dimensions of the Mini-trough are reduced by factor 8.7 with a maximum area of 27.0 cm^2 ($=A_{\text{max}}$). This results in a trough length of 9.0 cm, a width of 3.0 cm and a depth of 0.5 cm. To maximize contact between the sample surface and the barriers, the trough was slightly overfilled and therefore, the sample volume was set constant to 14.5 mL for all experiments. Particle contamination was minimized by washing with ethanol (commercial grade, absolute) and repeated washing with highly purified water. A plastic enclosure covers the PTFE trough and the barriers (see Fig. 2). The samples were stressed by 100 cycles started after an equilibration time of 2.5 h. Compression factor (c_f), defined as the ratio of maximum surface area to minimum surface area was kept constant at 4.5 for all measurements. Compression speed was set to 55 mm/min.

3.10. Particle Analysis

3.10.1. Light Obscuration

Samples were analyzed for particles in the micrometer range by light obscuration (in analogy to USP 788 and Ph Eur 2.9.19 requirements) with a SVSS-C instrument (PAMAS, Partikelmess- und Analysesysteme GmbH, Rutesheim, Germany). After a pre-run volume of 0.5 mL, each sample was analyzed in triplicates of 0.3 mL at a filling and emptying rate of 10 mL/min. Before each run, the system was rinsed with at least 5 mL of highly purified water. Data was collected using PAMAS PMA Program V 2.1.2.0.

3.10.2. Micro-Flow Imaging

Particle size and number were additionally measured using a micro-flow imaging (MFI) system DPA4100 from Brightwell Technologies Inc. (Ottawa, Canada) equipped with a high-resolution 100 µl flowcell and the MFI™ View Application Software. Pre-run volumes of 0.3 mL and sample volumes of 0.65 mL were drawn through the flow cell by a peristaltic pump at a flow rate of 0.1 mL/min. To optimize illumination and to provide a clean baseline the system was rinsed with highly purified water before and after the measurements.

3.10.3. Statistical Significance

A t-test was performed with * for $p \leq 0.05$, ** for $p \leq 0.01$ and *** for $p \leq 0.001$.

4. RESULTS AND DISCUSSION

4.1. Determination of the interfacial pI of IgG using SFG

Potentially, the pI of the IgG molecules at the liquid-air interface may differ from that of molecules in the bulk due to differences in dissociation of preferential adsorption of charge variants. The pI in the bulk (pI_{bulk}) of the IgG was 6.94 as determined by DLS. The pI of mAB₁ amounts to 8.75 and of mAB₂ to 6.51. SFG measurements were performed to determine pI of the IgG at the interface ($pI_{\text{interface}}$). The OH-stretching vibrations of interfacial water molecules between 3100-3800 cm^{-1} show a strong dependence on pH reflecting the charged state of the interfacial molecules (Fig. 1A). Additionally, a weak band due to aromatic CH-stretching vibrations is observed at 3060 cm^{-1} . Interfacial electrical fields induce changes in SFG intensities, particularly for small and highly polarizable molecules such as water [24]. As a result, pH dependent changes of the intensity of the OH-bands can be used to determine relative changes in the strength of the interfacial electric field (Fig. 1B). The local minimum of SFG intensities of OH-bands can be assigned to $pI_{\text{interface}}$ [15], [16]. Accordingly, the $pI_{\text{interface}}$ of the IgG was determined as 5.3. Thus, it was found to be considerably lower compared to pI_{bulk} with 6.94. Engelhart *et al.* showed similar isoelectric points in bulk solution and at the liquid-air interface for bovine serum albumin and lysozyme [15]. The polyclonal IgG behaves different which may be explained by either a preferential adsorption of an IgG subtype to the interface or by changes in the dissociation of charged side chain residues. Further investigations are required for a conclusive statement. Nevertheless, these findings make clear that in discussions about electrostatic repulsions and intermolecular interactions, the bulk pI cannot be necessarily used.

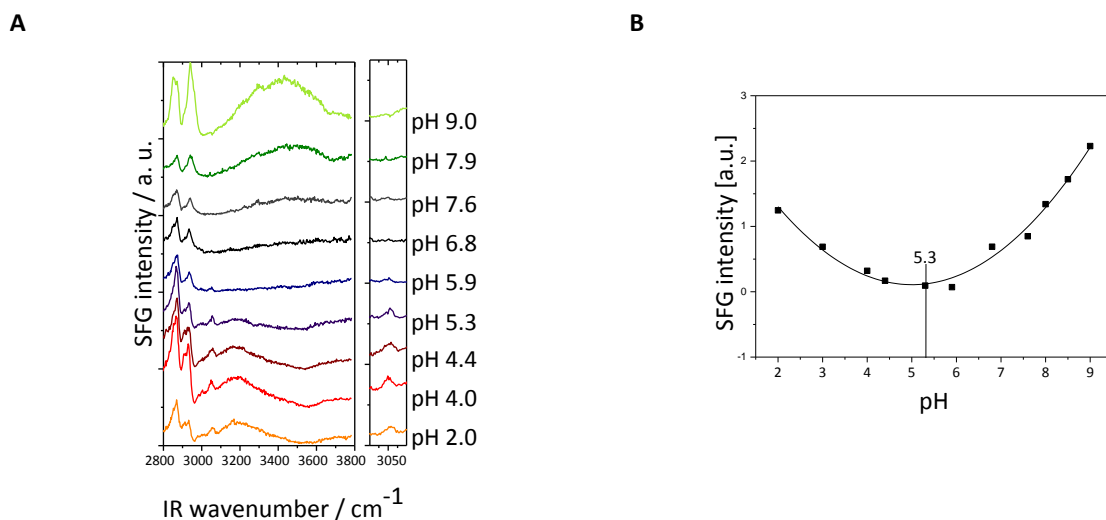


Figure 1 A: SFG spectra of IgG at different pH values and B: pH dependence of the amplitudes of the OH stretching vibration at 3443 cm⁻¹

4.2. Protein Adsorption as Function of pH

To evaluate the influence of pH on the surface activity the equilibrium surface pressure values (π_{eq}) were determined (Fig. 2). Overall, π_{eq} of the IgG remains roughly constant between pH 3 and pH 7.6 with values of 18.5 mN/m at pH 6.8 and 21.3 mN/m at pH 3. At pH 2 π_{eq} values of 24.2 mN/m indicate an increased surface activity of the IgG and thus the beginning of unfolding at this very low pH. Although the absolute values are slightly lower compared to the IgG, a similar trend was observed for mAB₁. In case of mAB₂, surface pressures range between 15.8 mN/m and 17.9 mN/m for the pH values investigated. Different authors stated that the surface activity of proteins (e.g. β -lactoglobulin) reaches a maximum around the pI, as the protein exhibits minimal repulsion at this point leading to the formation of more dense layers or multilayers at this pH value [23], [37]. This effect, however, could not be seen for β -casein [25] as was the case in our study with IgG.

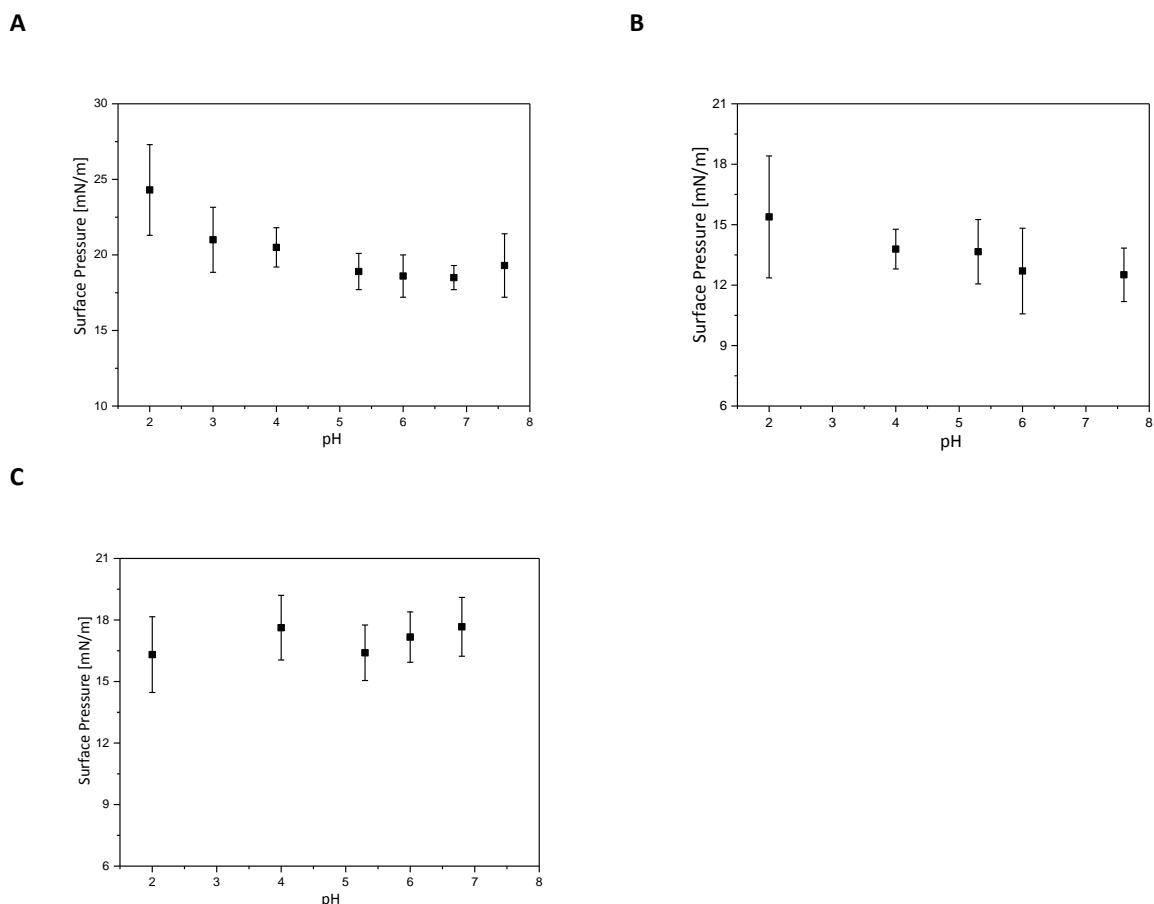


Figure 2: Equilibrium surface pressures as a function of pH of A: IgG, B: mAB₁ and C: mAB₂

4.3. Interfacial Film Compressibility

Continuous compression-decompression experiments of the interfacial film were performed at different pH values (Fig. 3). The surface pressure increase upon movement of the barriers towards each other clearly demonstrated that the protein molecules stay at the interface upon compression. Barrier movement compresses and compacts the adsorbed film and thus can be related to an increase in film thickness and / or changes in packing density [28], [29]. The high compressibility and the appearance of a considerable hysteresis substantiate the formation of a viscoelastic protein network at the interface where in addition to hydrophobic interactions, hydrogen bonds contribute substantially to the molecular association [29]–[32]. However, no considerable pH effect, neither in hysteresis profile nor in film compressibility was detected. The maximum change in surface pressure $\Delta\pi_{\max}$ upon compression amounted to 39.6 mN/m for pH 9 to 39.8 mN/m for pH 3.

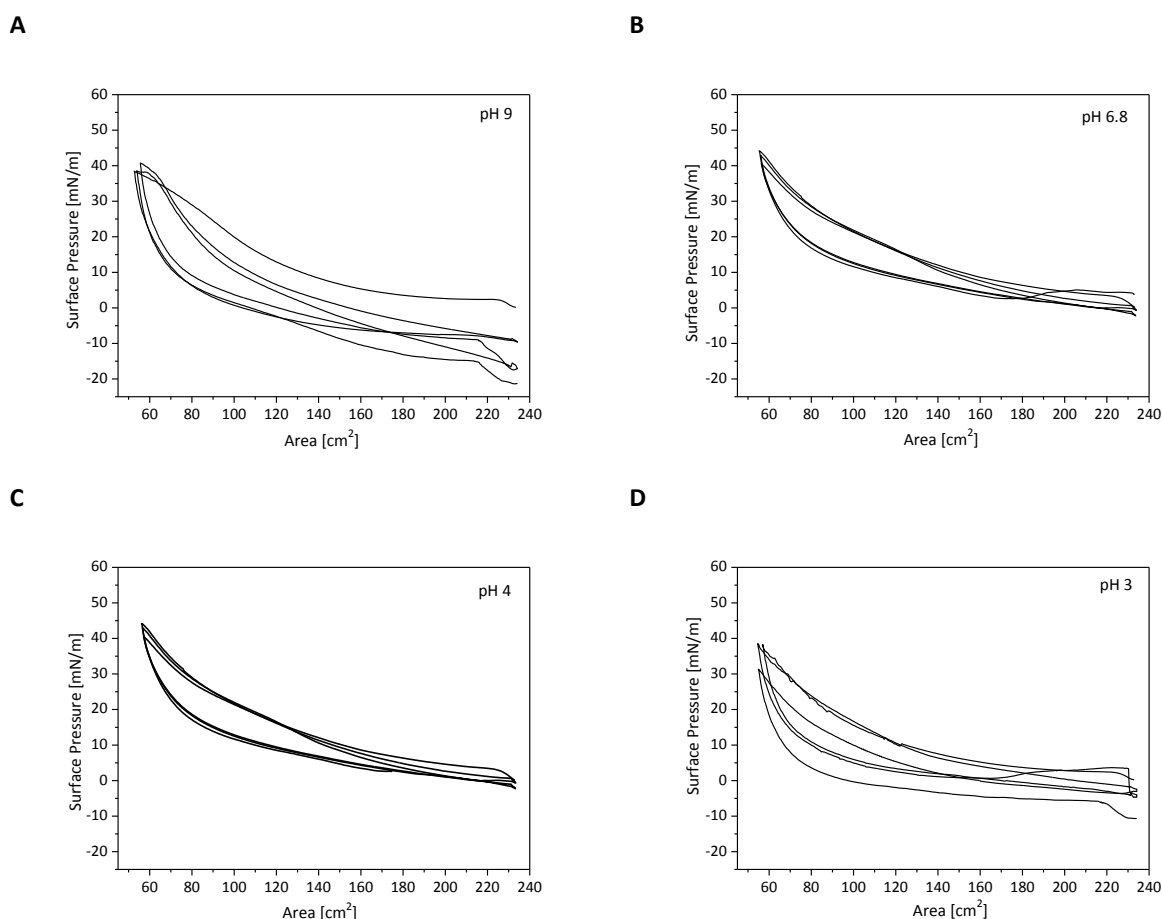


Figure 3: Compressibility of IgG 1 mg/mL at A: pH 9, B: pH 6.8, C: pH 4, and D: pH 3

4.4. Impact of pH on Secondary Structure: Bulk vs. Interface

Protein secondary structure is sensitive to the charge state and therefore to pH [33] (Fig. 4). Between pH 4 and pH 9, the absorbance maximum of the amide I region of IgG at 1639 cm^{-1} can be assigned to an intramolecular β -sheet structure of the IgG. At pH 4 as well as at pH 9 the intensity of the peak is decreased due to slight perturbations within the secondary structure [34]. A clear peak shift of the amide I band from 1639 cm^{-1} to 1631 cm^{-1} is observed at pH 2 indicating that the IgG unfolds forming intermolecular β -sheets. This is in good accordance with the increased surface pressure value at pH 2 described before. Similarly, the maximum of the amide I region of mAB₁ and mAB₂ is situated at 1637 cm^{-1} referring to an intramolecular β -sheet structure and was not affected by pH.

Additionally, the secondary structure was evaluated during heating up to 93 °C (Fig. 5). Spectral changes of all proteins were observed starting at 73 °C. The amide I absorbance maximum around 1639 cm^{-1} (or 1637 cm^{-1} respectively) decreased accompanied by an intensity increase at 1625 cm^{-1} (or 1624 cm^{-1} respectively).

Those changes were accompanied by a shift of the peak maximum at 1690 cm^{-1} to 1695 cm^{-1} . The changes represent the change from intra- to intermolecular β -sheet structure for all three proteins investigated [35], [36]. Identifying the temperature-induced structural changes should help to interpret the IRRAS results.

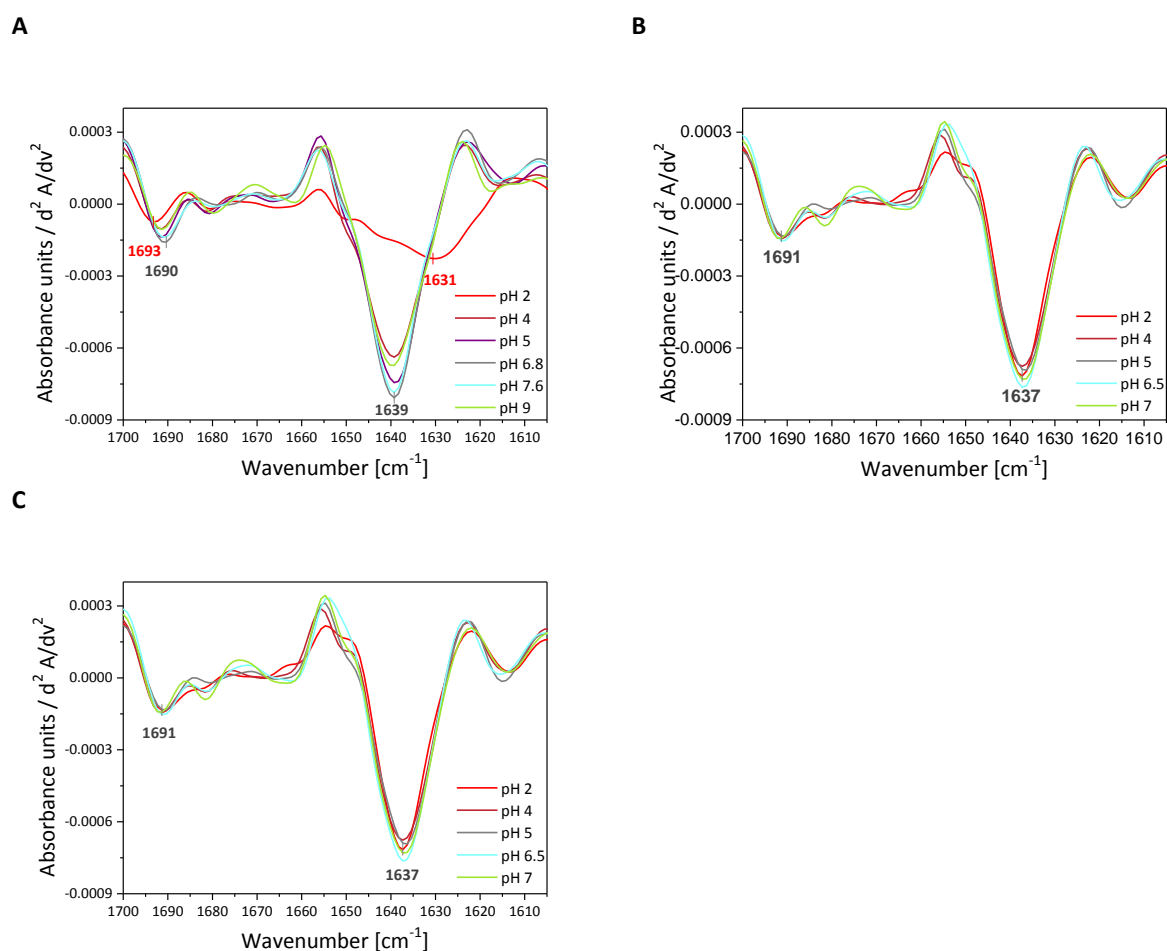


Figure 4: Impact of pH on secondary structure analyzed by FT-IR at 25 °C of A: of IgG, B: mAB₁ and C: mAB₂

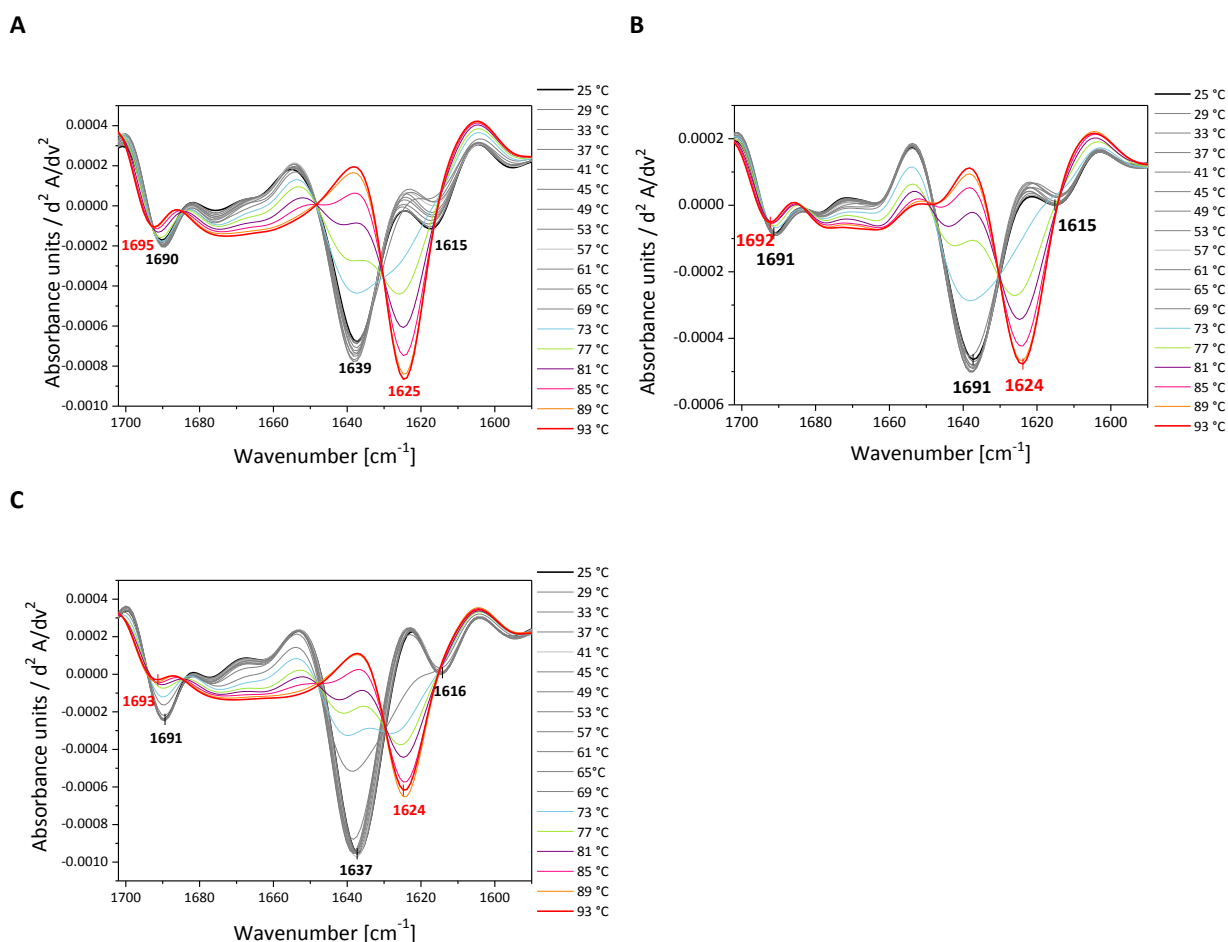


Figure 5: Temperature-induced unfolding from 25 – 93 °C analyzed by FT-IR of A: IgG, B: mAB₁ and C: mAB₂

IRRAS was used to determine the secondary structure at the interface directly (Fig. 6). Evaluation of secondary structure elements of the amide I region revealed no significant conformational changes of the IgG at the interface compared to the bulk solution, neither after adsorption nor after compression. The slight shift of the peak maxima at pH 6.8 from 1639 cm⁻¹ in bulk solution to 1643 cm⁻¹ at the interface can be explained the lower resolution or to by an overlay of slightly altered conformational modi, also indicated by broader peaks of the IRRAS spectra compared to the FT-IR spectra. Similar results were obtained for the mABs, as no pH-induced shift of the amide bands and therefore no unfolding was observed. Overall, the sensitivity to unfolding of IR spectra is limited as at least 20 % of the molecular portions must be altered to see significant changes in the peak positions [34], [37]. Nevertheless, no peak shift to lower wavenumbers as observed during heating, or at pH 2 in bulk solution were detected. Thus, the proteins essentially remain in a native-like conformation at the interface. Comparison of the IRRAS spectra at different pH values reveals no impact of pH, similar to the FT-IR results in bulk solution.

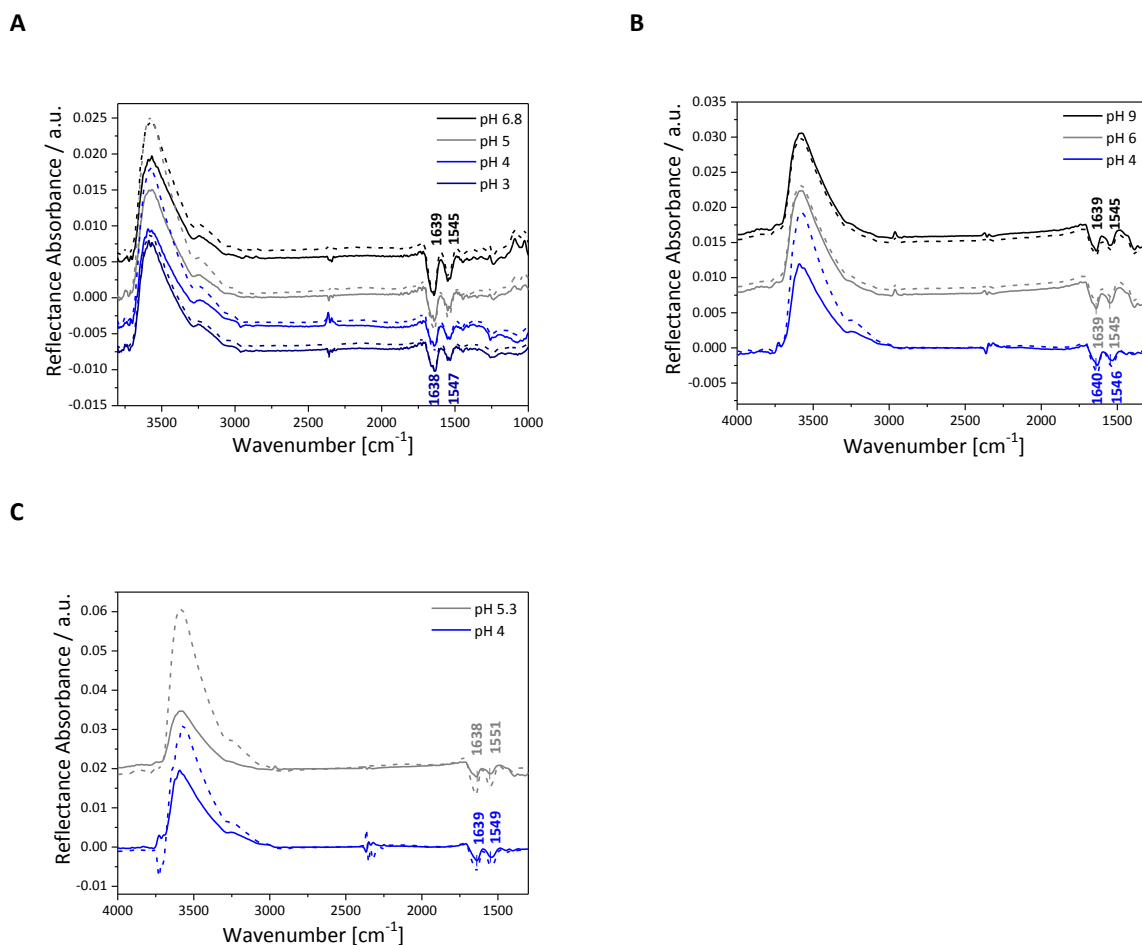


Figure 6: IRRA spectra at equilibrium surface pressure (solid lines) and after compression by 15 mN/m (broken lines) at different pH values of A: IgG, B: mAB₁, and C: mAB₂

4.5. Impact of pH on Interfacial Film Structures

4.5.1. Brewster Angle Microscopy (BAM)

BAM was performed at different pH values during adsorption as well as during compression of the film (Fig. 7). Upon adsorption a coherent interfacial film with an inhomogeneous protein distribution can be observed. Areas of increased brightness represent areas of increased packing density and / or film thickness, whereas darker regions imply a thinner protein film. Comparing the results of IgG at pH 4 and 3 to pH 6.8 it becomes obvious that the overall grey level increases with decreasing pH, particularly at pH 3. Moreover, the island-like character at higher pH changes to large elongated coherent areas of increased brightness at lower pH. The appearance of these larger coherent areas and the overall increase in brightness at lower pH suggest that the IgG molecules are more densely packed or indicate an increased interfacial film thickness. Furthermore, this effect was pronounced

in case of mAB_1 as with decreasing pH the grey level increased and the island-like structure more and more vanishes (Fig. 8). In fact, the film appears smoother at lower pH values. A similar outcome was found for mAB_2 as shown in figure 9. In this case, at pH 4 and 3 no larger areas referring to an inhomogeneous distribution of protein molecules over the interface as for pH 6 and 5.3 are detected. Further investigations focused on coherences on the topographical film appearance and the emergence of particles upon interfacial stress. Overall, slight changes in the topographical appearance of the BAM images depending on pH are observed. Also, Nino *et al.* demonstrated that the spreading of β -casein is not uniform over the liquid-air interface. Moreover, they stated that the reflected light intensity decreased with pH in case of β -casein, although other proteins such as milk or soy protein behave differently [38].

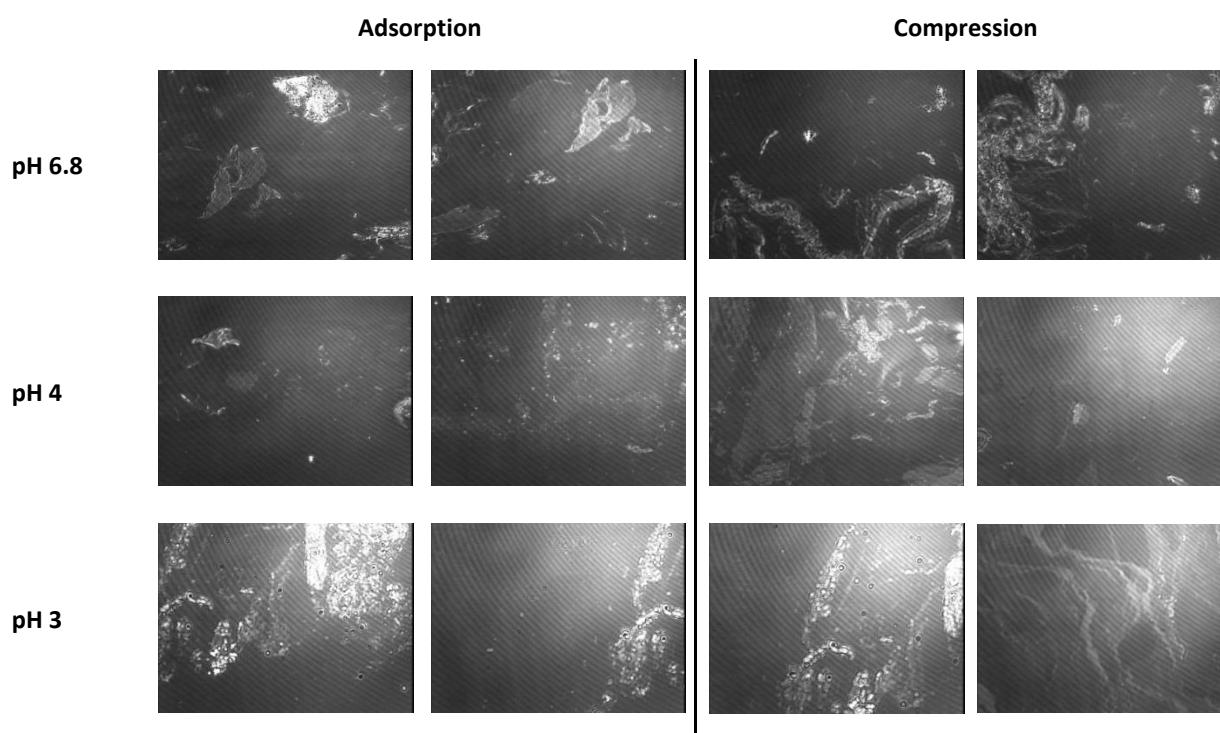


Figure 7: BAM images of IgG 0.1 mg/mL at different pH during adsorption and compression with increasing surface pressure during adsorption and compression

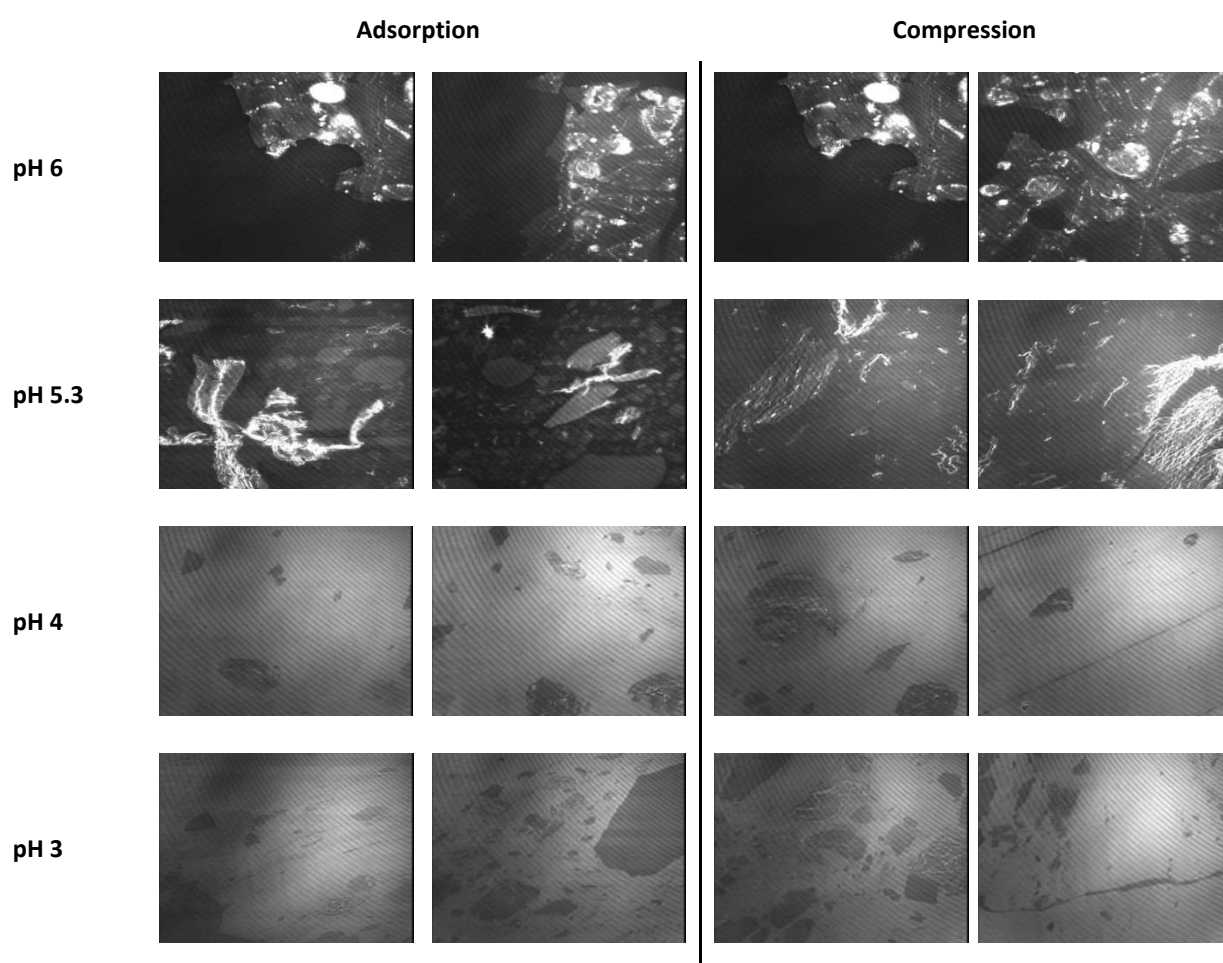


Figure 8: BAM images of mAB₁ 0.1 mg/mL at different pH during adsorption and compression with increasing surface pressure during adsorption and compression

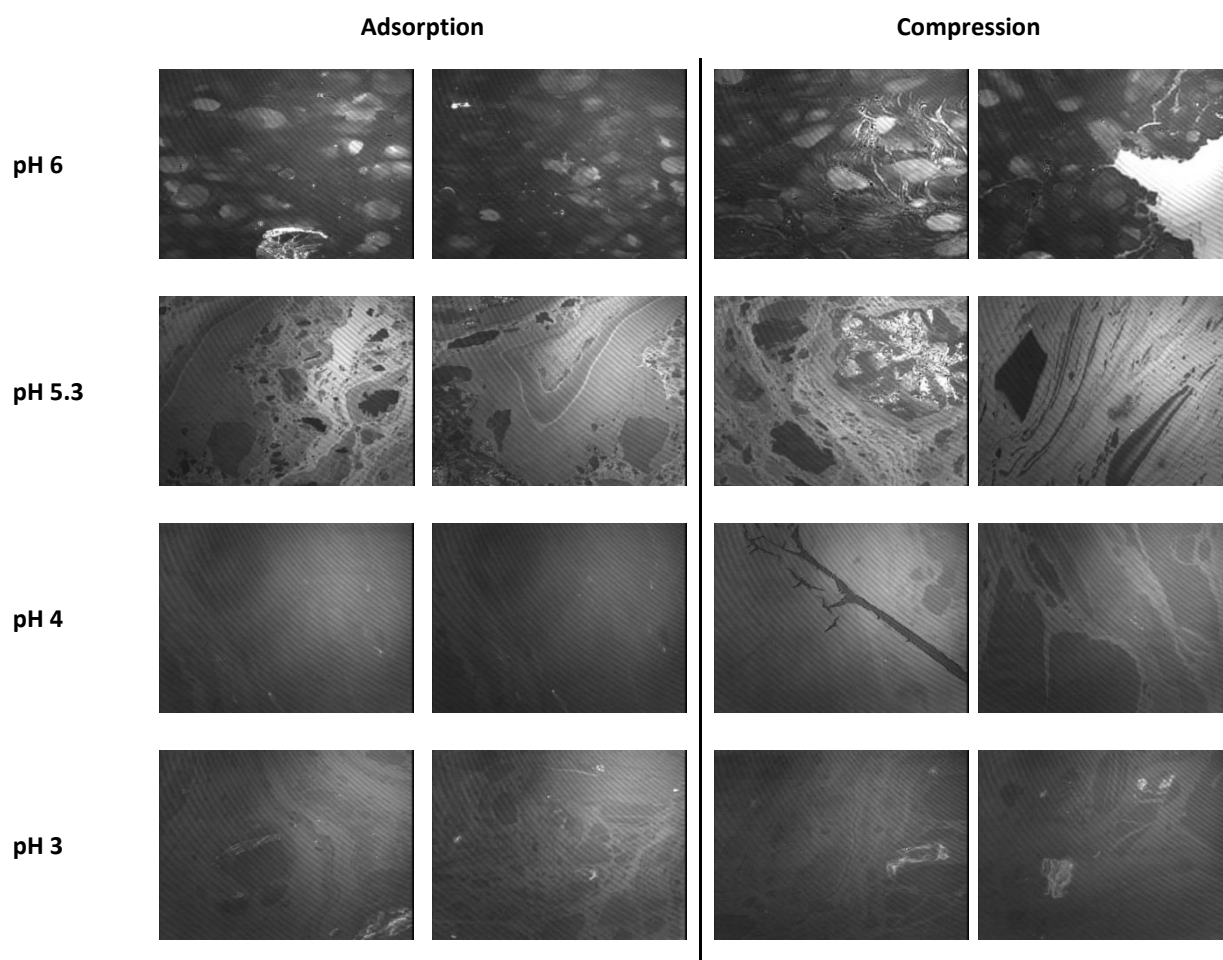


Figure 9: BAM images of mAB₂ 0.1 mg/mL at different pH during adsorption and compression with increasing surface pressure during adsorption and compression

4.5.2. Atomic Force Microscopy (AFM)

AFM is a versatile tool for the visualization of topographical features of liquid-air interfacial films after transfer on a solid substrate. After adsorption, a continuous film with small agglomerates is formed at pH 6.8 (Fig. 10). This implies clustered IgG material already after adsorption which is in good accordance with the BAM results. Compression causes the appearance of telescoped material which is no longer recognizable after decompression. A similar appearance can be observed for the films formed at pH 3 and pH 5. At pH 3 and 5, however, the distribution of IgG after adsorption to equilibrium surface pressure is slightly more inhomogeneous as circular clusters of IgG are separated by smooth and flat areas. For all samples, compression caused the formation of wrinkles and decompression resulted in smoother films compared to the adsorbed films. This is consistent with the compression-decompression experiments where the surface pressure values ended up slightly lower after each cycle. Therefore, this can be explained by a loss of material within the film upon

interfacial stress. However, only little is known about Langmuir films of protein molecules. Moreover, the effect of pH as well as compressive forces on proteins adsorbed to the liquid-air interface, have not been studied so far. Wang *et al.*, however, examined the role of charge interaction on the adsorption behavior of an IgG₁ onto a silica surface. The height profiles demonstrated a flat-on orientation of adsorbed antibody molecules at pH values between 4 and 8 [39].

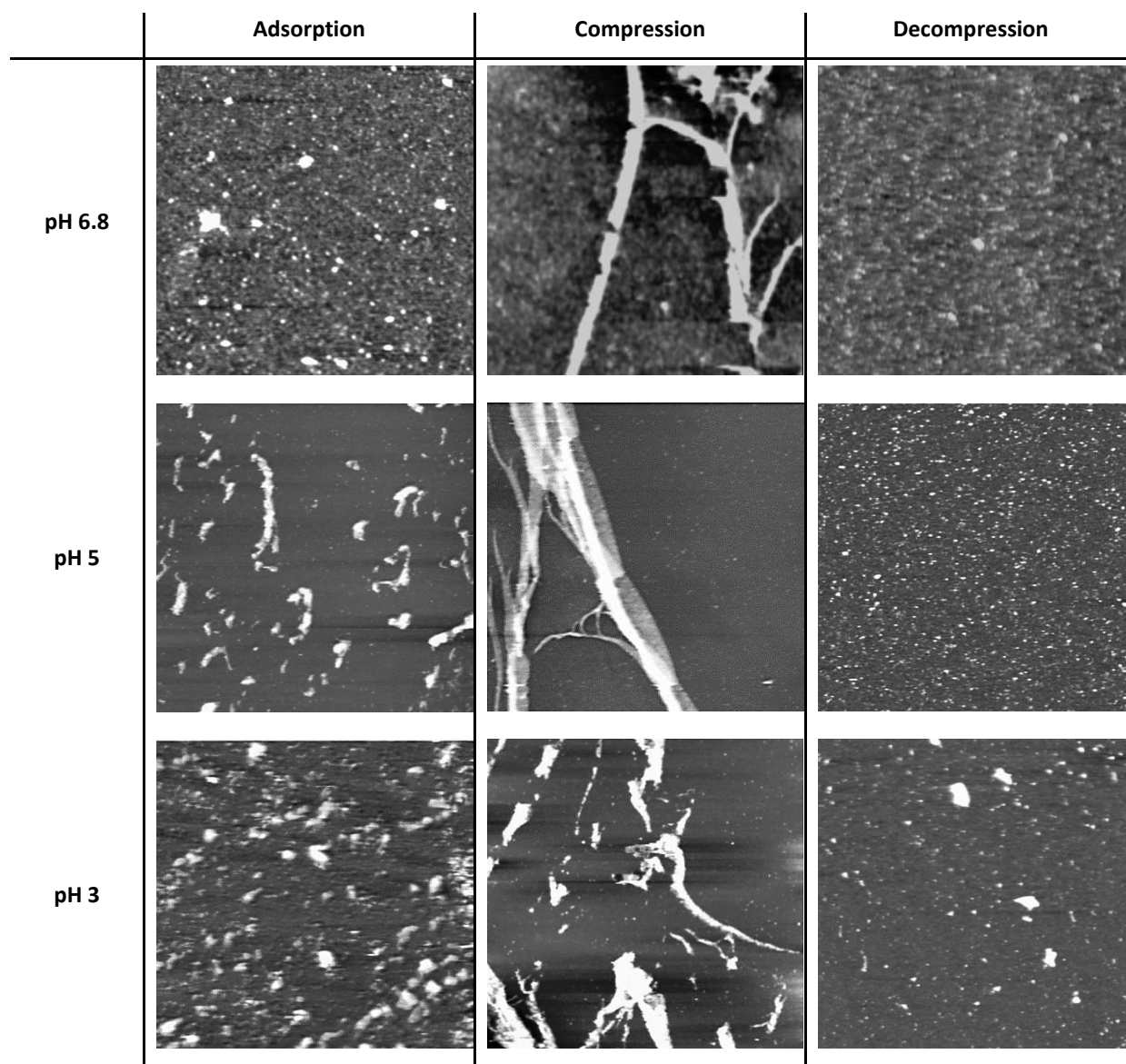


Figure 10: IgG 1 mg/mL A: in Equilibrium and B: Compression by 15mN/m and C: Decompression at A: pH 6.8, B: pH 5 and C: pH 3

4.6. Determination of the Interfacial Film Thickness

The thickness of the protein film at the interface in equilibrium and after compression at different pH values was determined by angle-dependent IRRAS measurements and compared to the values obtained by underwater AFM of the films after Langmuir-Schaefer transfer. The increase in the intensity of the OH-stretching vibration around 3600 cm^{-1} indicates an increase in film thickness upon compression. Polarized light has different reflectivity properties for p and s, respectively, around the Brewster angle ($\sim 53.1^\circ$) with a minimized intensity of the reflected p-polarized light. As exemplarily shown for IgG at pH 6.8 in figure 11, the reflectance-absorbance (RA) in the region of the OH-stretching vibration changes continuously for s-polarized light as a function of the AoI, whereas the RA of p-polarized light exhibits a discontinuity around the Brewster angle. For comparison, spectra with the OH-stretching vibration were simulated (Fig. 12). The corresponding spectra (experimental and simulated) of mAB₁ and mAB₂ can be found in the appendix.

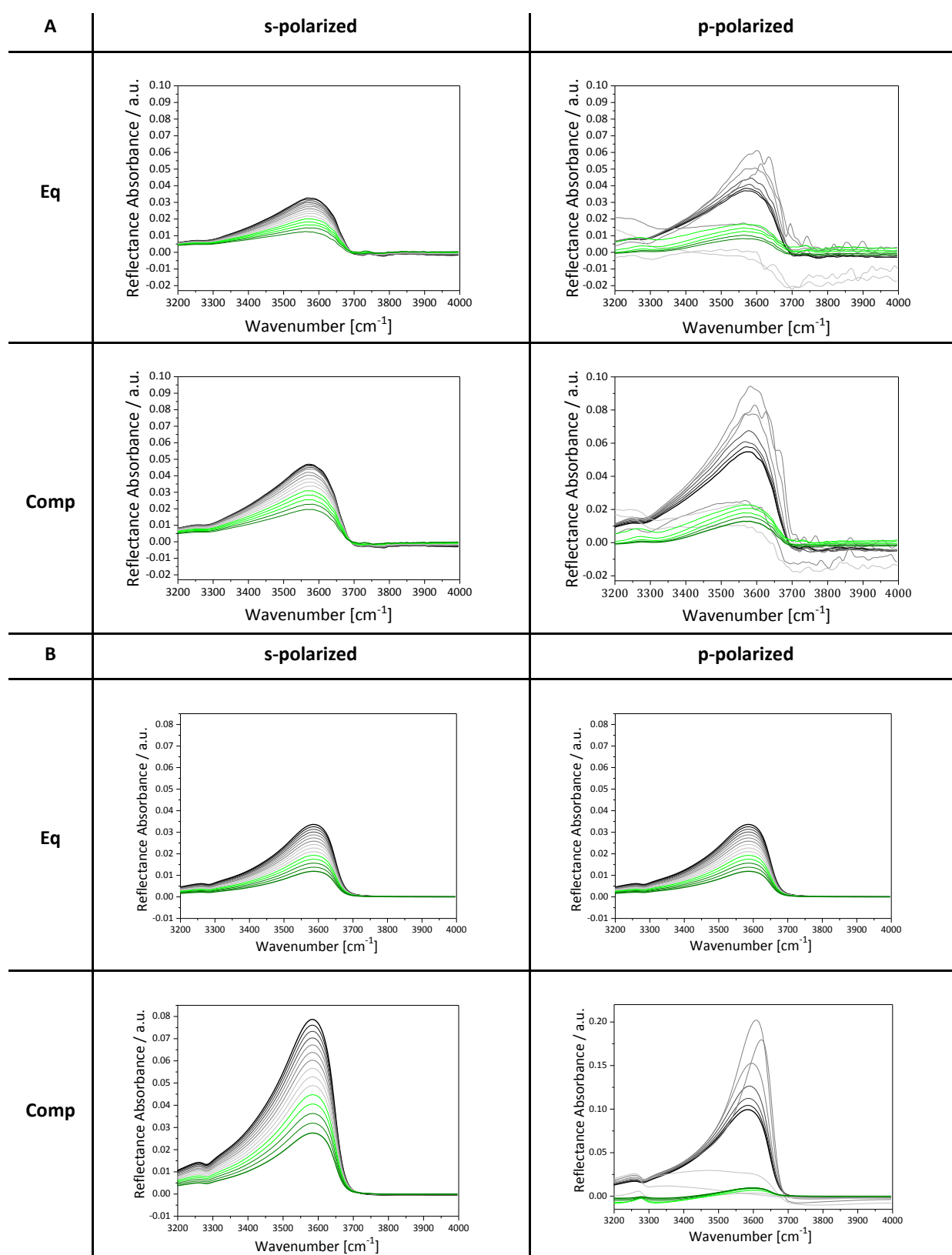


Figure 11: A: IRRA spectra of the OH-stretching vibration of IgG pH 6.8 in equilibrium Eq (top) and after compression Comp by 15 mN/m (bottom) at different Aol from 30° – 72° (from black via grey to green) in steps of 2°, s-polarized light (left), p-polarized light (right), A: experimental data and B: corresponding simulated spectra

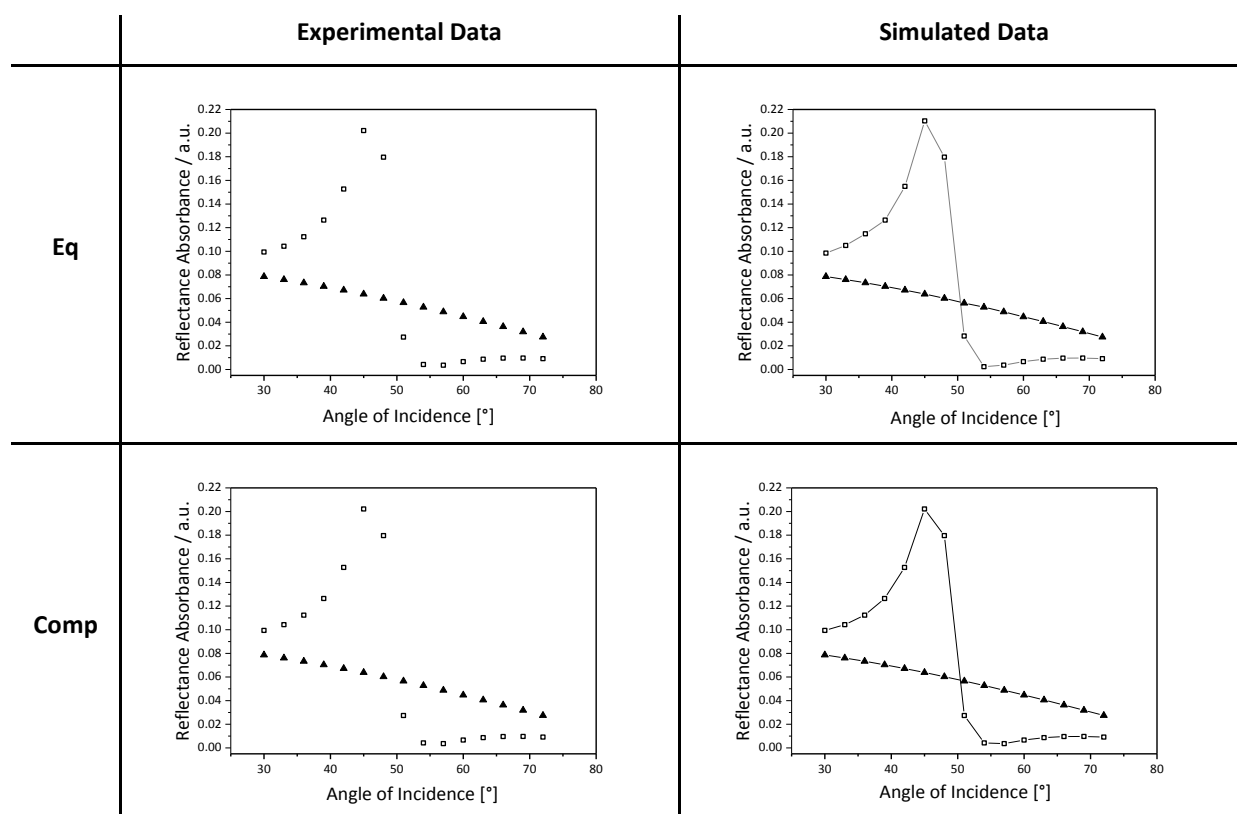


Figure 12: Experimental and simulated RA intensities using p-polarized (\square) and s-polarized (\blacktriangle) light at the maximum position of the OH-stretching vibration (2750 cm^{-1}) in equilibrium and after compression by 15 mN/m

The maxima of RA intensity of experimental and simulated spectra at different AoI were used to determine the layer thickness, assuming a refractive index of 1.5 for both the equilibrium and the compressed state which is in accordance with literature [40]. At pH 6.8, an IgG film of 3.05 nm thickness formed and upon compression by 15 mN/m it thickened to 5.59 nm (Tab. 1). At pH 9, the interfacial film thickness of the IgG amounted to 2.88 nm and 5.05 nm in equilibrium and after compression, respectively. Hence, no major difference in the interfacial film thickness can be detected between pH 6.8 and pH 9. In contrast, at pH 4 the interfacial film thickness is much lower with values of 1.67 nm in equilibrium and 3.45 nm after compression. For all three proteins investigated, the interfacial film thickness was lowest at pH 4 and compression results in an increase in film thickness. Overall comparison of the different proteins revealed highest interfacial film thickness values for the IgG and lowest for mAB₁ with 1.50 nm in equilibrium and 2.41 nm after compression at pH 4. The hydrodynamic radius of the IgG in solution was determined as 6.9 nm by DLS which corresponds to literature [41], [42]. It has been stated that IgG molecules preferentially adsorb in flat orientation, which can explain that the interfacial film thickness is thinner than

the hydrodynamic radius in solution [42], [43]. *Erickson* [44] determined the minimal radius of a sphere that could contain a protein with 100 kDa to 3.05 nm and for 200 kDa to 3.84 nm [44]. Overall, the results suggest rather the presence of a monolayer than the formation of multilayers. Moreover, Wang et al. showed that an IgG₁ adsorbed in a flat-on orientation at pH values between pH 4 and 8 [39].

Table 1: Interfacial film thickness of IgG, mAB₁ and mAB₂ in equilibrium and after compression by 15 mN/m at different pH determined by IRRAS and AFM

Equilibrium				Compression	
		IRRAS	AFM	IRRAS	AFM
pH					
IgG	4	1.67 nm	3.92 nm ± 0.61 nm	3.45 nm	4.28 nm ± 1.17 nm
	6.8	3.05 nm	5.56 nm ± 0.94 nm	5.59 nm	6.41 nm ± 1.05 nm
	9	2.88 nm	5.36 nm ± 0.86 nm	5.05 nm	6.67 nm ± 0.97 nm
mAB ₁	4	1.50 nm	4.74 nm ± 1.41 nm	2.41 nm	5.73 nm ± 1.13 nm
	6	1.57 nm	4.99 nm ± 1.79 nm	1.98 nm	5.92 nm ± 1.22 nm
	9	1.80 nm	5.47 nm ± 0.76 nm	2.57 nm	6.55 nm ± 1.73 nm
mAB ₂	4	2.19 nm	3.56 nm ± 1.33 nm	3.82 nm	4.65 nm ± 1.40 nm
	5.3	3.22 nm	3.07 nm ± 1.54 nm	5.01 nm	4.99 nm ± 1.79 nm

AFM was used as orthogonal methodology to determine the thickness of the interfacial film. Whereas artefacts may result from the film transfer on a solid substrate, AFM is not based on assumptions such as the refractive index and a mathematical simulation model. A scratch was made in a blotted film using stainless steel tweezers (Fig. 13) and the interfacial film thickness was determined as mean height from the silica substrate to the film area unaffected by the scratch. The film thickness values deduced from AFM are in the same order of magnitude as the ones determined by IRRAS but consistently higher (Tab. 1). Moreover, the percentage of increase in film thickness is slightly lower when determined by AFM compared to IRRAS. This might be explained on the one hand by a possible relaxation of the transferred film as it is not measured in situ and on the other hand by incorrect assumptions and simulation for the IRRAS data. At pH 4 the interfacial film thickness of the IgG is smallest with 3.92 nm in equilibrium. For mAB₁ the interfacial film thickness determined by AFM in equilibrium decreases from 5.47 nm at pH 9 to 4.74 nm at pH 4.

However, the interfacial film thickness of mAB₂ at pH 4 and pH 5.3 is comparable with values of 3.56 nm and 3.05 nm, respectively. As only two pH values were investigated for mAB₂ it is not possible to assess possible trends. Thus, the interfacial films of the IgG as well as for mAB₁ are thinner at pH 4 compared to pH 6.8 and 9, similar to the results obtained by the angle dependent IRRAS measurements.

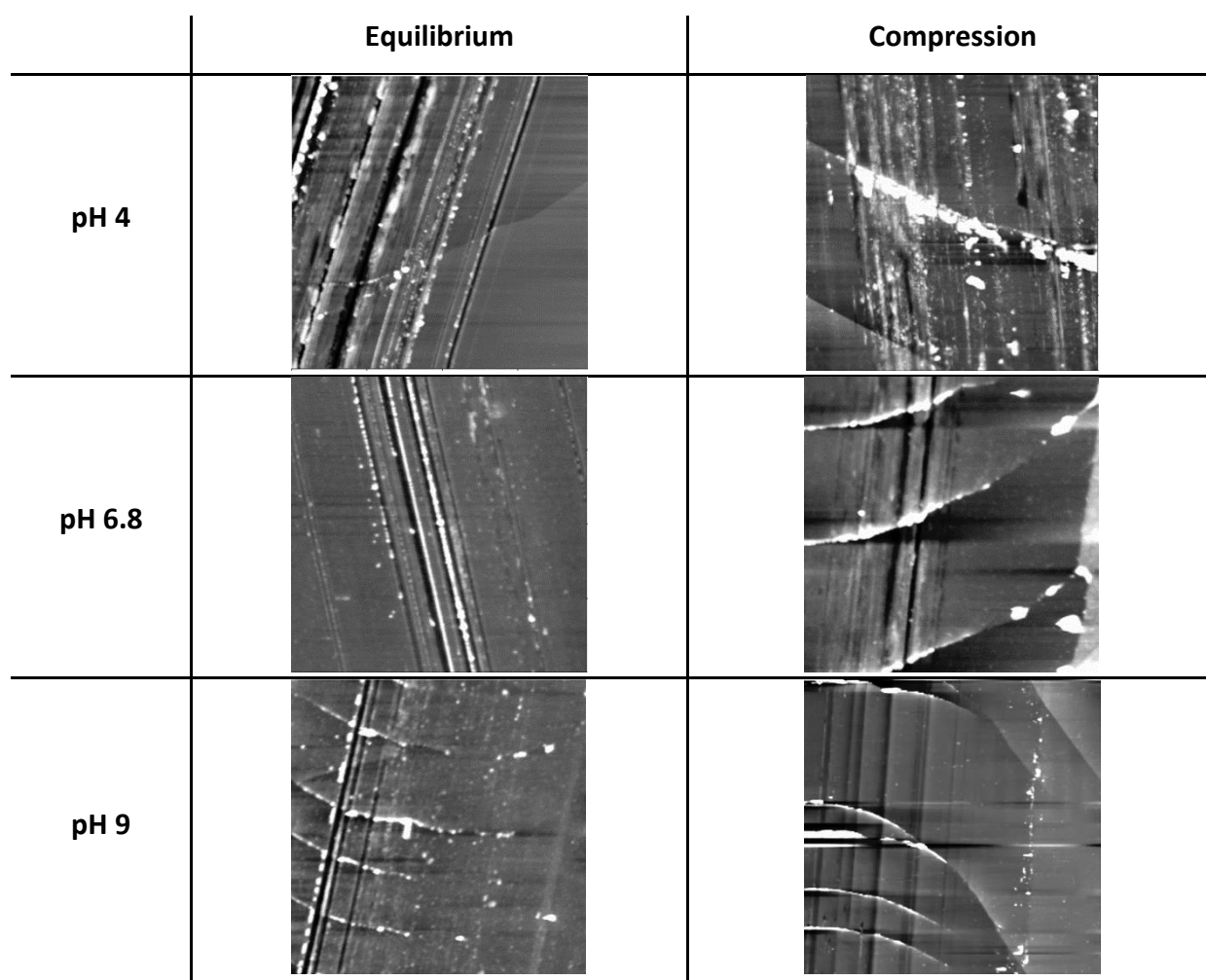


Figure 13: AFM images of IgG after adsorption to equilibrium surface pressure and after compression by 15mN/m including scratch at pH 4, pH 6.8 and pH 9. Mean height was determined as section analysis from the silica substrate to the film (area unaffected by the scratch)

At pH 4, the molecules are more heavily charged what results in more repulsive interactions between the molecules. Thus, less molecules may adsorb resulting in a thinner interfacial film [45]. Overall, the results obtained for mAB₁ and mAB₂ follow the same trend as for all proteins the interfacial film thickens upon compression. This again supports the assumption that once adsorbed, short-range interactions dominate the behavior of an interfacial protein film and that protein molecules do not easily desorb upon compressive forces.

According to literature, antibody molecules form small non-uniform clusters equivalent to 2-15 molecules as investigated by AFM [46]. Tronin *et al.* determined that the molecular orientation of IgG changes with increasing pressure as investigated by ellipsometry [47]. Transferring the liquid-air interfacial films of IgG on silicon wafers followed by drying they obtained an interfacial IgG film thickness of approximately 4 nm at low surface pressures, which coincides with the smallest dimension of IgG molecules, and about 10 nm at pressures up to 40 mN/m which is consistent with the largest molecular dimension [47]. Malmsten [48] evaluated an IgG adsorbed to a silica surface and concluded a dimension of $23.5 \times 4.5 \times 4.5 \text{ nm}^3$. Moreover, segments of the adsorbed molecules have been considered to twist and or tilt, driven by electrostatic interactions [46].

4.7. Impact of pH on Particle Formation by Liquid-Air Interfacial Stress (Mini Trough)

The impact of pH on the particle formation by liquid-air interfacial stress was investigated by 100 continuous compression-decompression cycles in the Mini-trough and subsequent particle analysis. Figure 14 demonstrates the pH-dependence of IgG aggregation. While the number of particles at pH 3 and 4 is below 3000 particles/mL, an increase in pH results in higher numbers of particles formed. Consequently, the pH directly affects the number of particles formed by liquid-air interfacial stress only, although no considerable differences in the physicochemical film characteristics were detected and only slight topographical differences were revealed using BAM and AFM. Therefore, not only the events at the interface but also the protein-protein interactions both at the interface and in the bulk solution contribute to the number of particles formed upon compression and decompression and thus mechanical stressing a protein solution.

Whereas at high pH net attraction between the protein molecules studied dominates, as indicated by the self-interaction parameter A_2 , the repulsive forces increase with decreasing pH, finally ruling at pH 4 and 3 [49]. This explains why less particles were detected at low pH values. Although partly clustered protein material, as observed by BAM or AFM, is brought into solution by interfacial stress, those loose conglomerates rather dissociate at low pH than sticking together due to the repulsive forces between the molecules. In contrast at high pH values the conglomerates formed at the interface persist in solution.

The interactions are also related to the charge state of the protein molecules at the surface and are affected by environmental conditions. Therefore, also salts providing charge shielding may both stabilize or destabilize a mAB solution against interface related stress [50], [51].

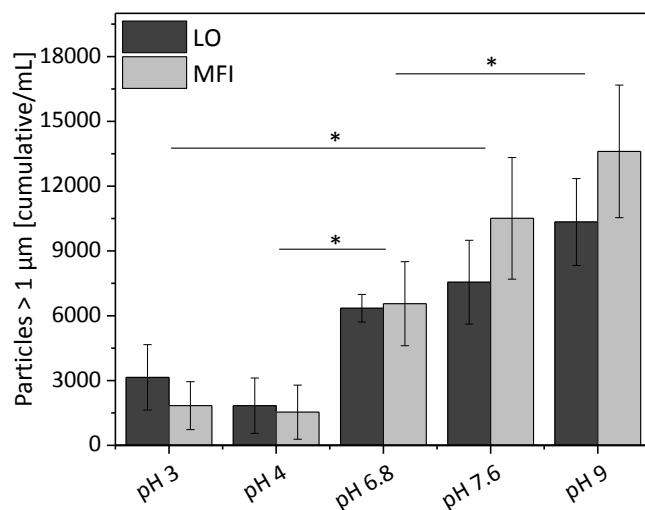


Figure 14: Number of particles $\geq 1 \mu\text{m}$ / mL after 100 continuous compression-decompression cycles of IgG at different pH in the Mini-trough determined by LO and MFI

5. SUMMARY & CONCLUSION

Proteins exhibit surface activity and therefore adsorb to interfaces, such as the liquid-air interface. Upon mechanical stress, e.g. shaking, this can cause protein aggregation [52], [53]. The mechanistic details of this effect are not fully understood yet and a rational identification of formulation conditions which can prevent this instability is highly desirable. Changes of the formulation pH are associated with a different protein charge distribution and therefore altered protein-protein interactions. Repulsive forces go along with an increased colloidal stability, whereas attraction may provoke undesired agglomeration and clustering of the molecules [54], [55]. Although both pH condition and the presence of liquid-air interfaces have been identified to decisively affect protein stability, their complex interplay has not been investigated adequately. In this study, the effect of pH protein behavior at the liquid-air interface as well as pH-dependent particle formation by interfacial stress only was examined. The charge state of the IgG molecules reflected by the pI was determined not only in bulk solution but also at the liquid-air interface by SFG. Whereas the bulk pI was identified as pH 6.94, the interfacial pI was significantly lower at 5.3. Since the investigated IgG is polyclonal, it is conceivable that a specific IgG molecule population with specific characteristics such as pI preferentially adsorb to the interface. It may also be possible that dissociation of charged moieties is affected by the interface. Further investigations are required to understand this difference between pI_{bulk} and $pI_{\text{interface}}$.

Surface pressure measurements revealed no considerable impact of pH on equilibrium surface pressure, as roughly constant values of about 20 mN/m were reached. A higher equilibrium surface pressure of 24.2 mN/m resulted at pH 2 which can be explained by an increased hydrophobicity due to unfolding [56], [57]. FT-IR measurements confirmed no effect of pH on the IgG secondary structure despite at pH 2. While mAB₁ did not reveal any pH-induced conformational changes, the secondary structure of mAB₂ is sensitive to very low pH values as indicated by the peak splitting and peak shift to lower wavenumbers at pH 2. In addition, mAB₂ precipitated above pH 6.5. The secondary structure of all proteins investigated was not affected by adsorption to the liquid-air interface. No shift or additional peaks referring to new secondary structure elements appeared. The secondary structure at the interface can be considered as essentially native-like between pH 3 and 6.8. Adsorption to the liquid-air interface results in the formation of a continuous film as visualized by BAM images for all proteins studied. The protein distribution over the interface is inhomogeneous

with areas of different reflectivity. During adsorption as well as during compression island-like structures of increased brightness were noticeable, representing areas of higher packing density or film thickness. Nino *et al.* found a significant effect of pH on topographical characteristics due to the strong impact of pH on the conformation of soy protein whereas milk protein is not affected [25]. Hence, whether or not altered charge conditions affect the interfacial film structure depend on the type of molecules used.

Compression of the film caused a considerable increase in surface pressure above equilibrium values. Repeated compression-decompression cycles revealed not only a high compressibility of the protein film but the appearance of a considerable hysteresis indicates physical changes within the film as the packing density and film thickness change with compression and decompression [12], [58], [59]. Moreover, compression did affect the BAM appearance. A slight increase in the overall grey level pointing to a higher packing density or altered molecular ordering within the film was seen at lower pH. Xu *et al.* [60] showed that protein molecules form small islands upon adsorption to biomaterial surfaces which is in good accordance with the results obtained in this study. At different scale, AFM images prove the formation of a continuous protein film with some areas of agglomerated protein at equilibrium surface pressure. Upon compression areas of telescoped material with increased height appeared which were no longer present after decompression. This is consistent with the fact that surface pressure values ended up slightly lower after each compression-decompression cycle. A formation and subsequent loss of clustered protein material from the interface upon compression and decompression can explain the topographical changes and the flattening of the film observed in AFM. This loss of clustered protein material may contribute to the emergence of protein particles in bulk solution.

The interfacial film thickness was determined from the RA intensity of the OH-stretching band. At equilibrium surface pressure, the film thickness amounts to 3.05 nm and after compression by 15 mN/m to 5.59 nm, such as in the case of IgG at pH 6.8. The thickness at pH 9 is comparable (2.88 nm in equilibrium and 5.05 nm after compression) whereas a thinner film is formed at pH 4 (1.67 nm in equilibrium and 3.45 nm after compression). For mAB₁ at pH 4 a thickness of 1.50 nm in equilibrium and 2.41 nm after compression was determined. The mAB₂ films were 2.19 nm and 3.92 nm thick at pH 4 and 3.22 nm and 5.01 nm at pH 5.3, in equilibrium and after compression, respectively. Orthogonal analysis of the film height by AFM rendered $5.56 \text{ nm} \pm 0.94 \text{ nm}$ for the IgG at pH 6.8 in equilibrium.

Compression caused an increase in film thickness to $6.32 \text{ nm} \pm 1.05 \text{ nm}$. At pH 9 film thickness values were comparable, and at pH 4 slightly lower. The two mABs formed films of similar thickness. Compression caused an increase in AFM film thickness in all cases. Hence, AFM as well as angle dependent IRRA measurements resulted in similar values for the thickness of the protein films formed at the liquid-air interface. The minimal radius of a protein sphere of 100 kDa amounts to 3.05 nm [44]. The effective hydrodynamic radius of a monoclonal antibody is with 5-7 nm slightly higher than the equilibrium interfacial film thickness [44], [61] pointing to a preferentially flat orientation of the adsorbed IgG molecules [42], [43].

Overall, the physicochemical investigations revealed no or only a minor effect of pH on the interfacial protein behavior. Mini-trough experiments connect compression and decompression of the protein film at the interface with particle formation. With increasing pH the number of particles formed upon stressing the interfacial film increased significantly. Thus, the studies demonstrate that a continuous, highly compressible interfacial film with areas of clustered, native-like protein material is formed upon protein adsorption. The considerable surface pressure hysteresis, the lowered surface pressure value after each compression-decompression cycle, and the smoother film after decompression indicate the loss of material and the transfer of protein clusters from the interface into the bulk solution. Consequently, repeated compression and decompression of the film results in the appearance of particles in the bulk. No effect of pH on the protein surface activity or folding was observed. But, pH strongly affected the number of particles formed upon stressing the film. Therefore, the bulk conditions have a vital influence on particle formation. Solution conditions which render attractive protein-protein interactions in the bulk preserve the clusters transferred from the interface into the bulk. In contrast, net repulsion of the protein molecules results in dissociation of the loosely packed protein agglomerates derived from the interface. Consequently, in the second part we complete this study with a detailed investigation of the protein-protein interactions depending on solution pH and ionic strength. A correlation with the aggregation tendency provides understanding of how the formulation conditions affect protein instability upon mechanical stress.

6. SUPPLEMENTAL INFORMATION

6.1. Determination of the isoelectric point (pI) in bulk solution

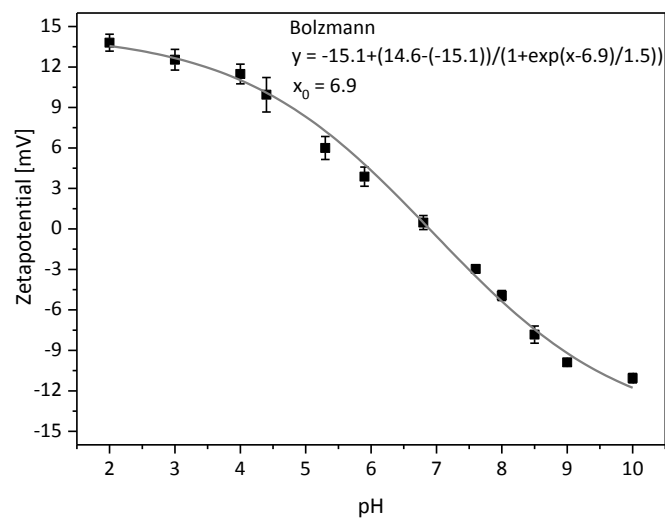


Figure 15: Zetapotential of the IgG versus pH and determination of pI using a Boltzmann fit. pI is given by the changing point of the curve and was calculated to pH 6.9 ($= x_0$)

6.2. Interfacial film thickness by IRRAS

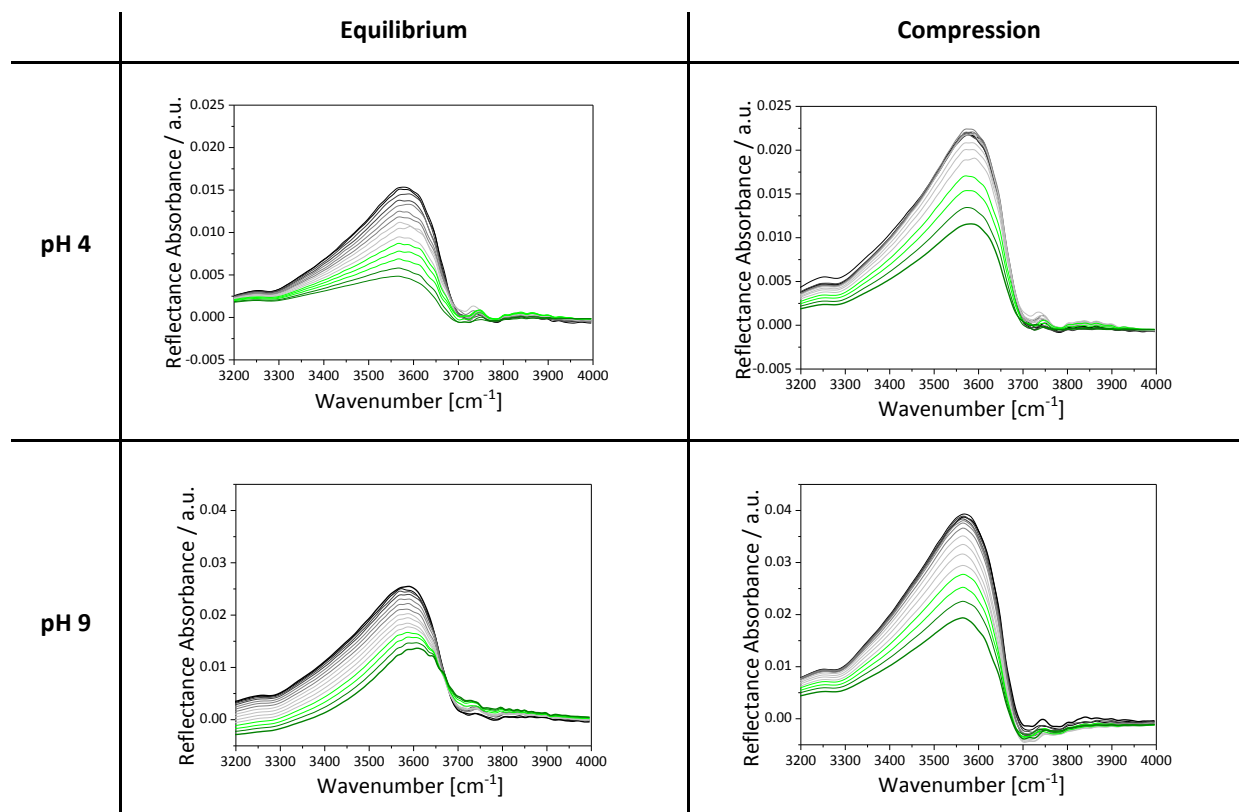


Figure 16: Experimental IRRAS spectra (40s) of IgG in equilibrium (left) and after compression by 15 mN/m (right) at different pH. Data were used for the simulation and calculation of the interfacial film thickness

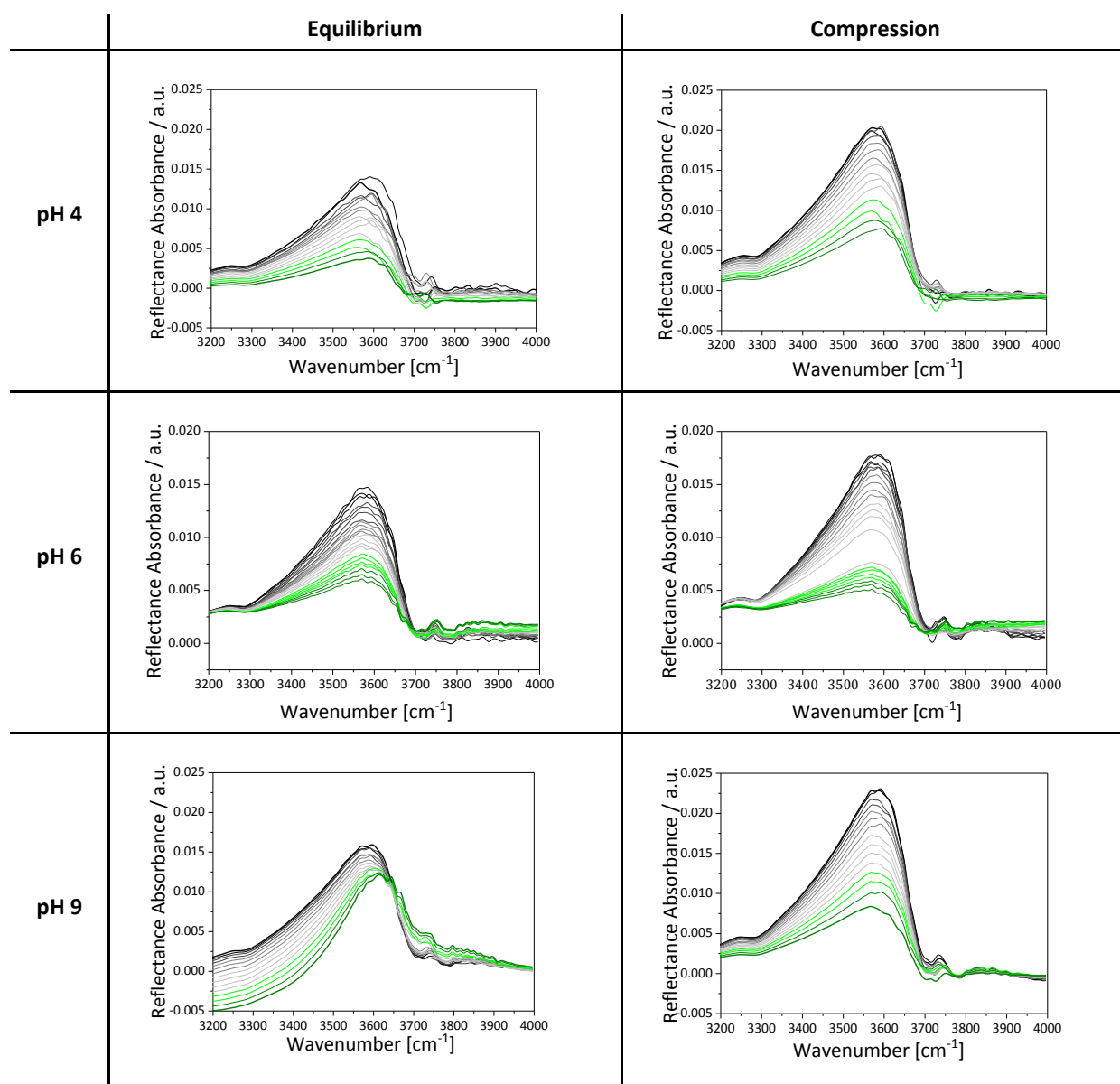


Figure 17: Experimental IRRA spectra (40s) of mAB₁ in equilibrium (left) and after compression by 15 mN/m (right) at different pH. Data were used for the simulation and calculation of the interfacial film thickness.

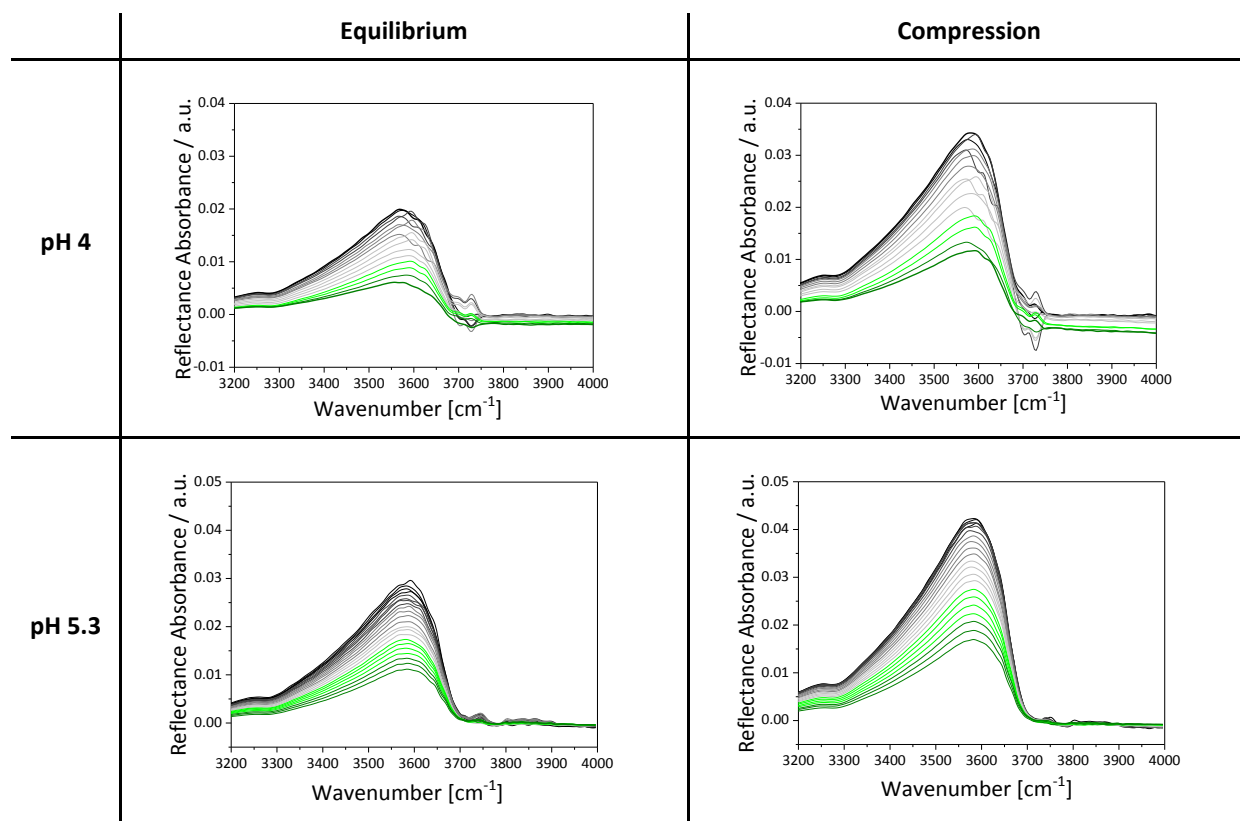


Figure 18: Experimental IRRA spectra (40s) of mAB₂ in equilibrium (left) and after compression by 15 mN/m (right) at different pH. Data were used for the simulation and calculation of the interfacial film thickness.

6.3. Interfacial film thickness by AFM

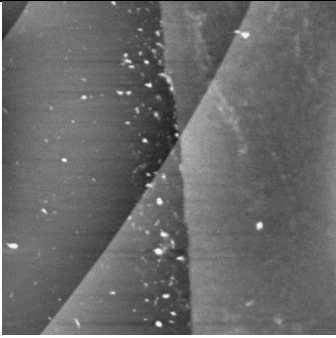
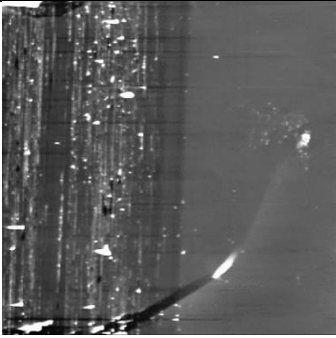

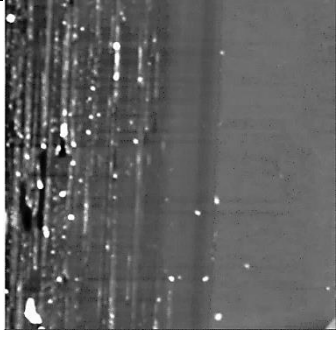
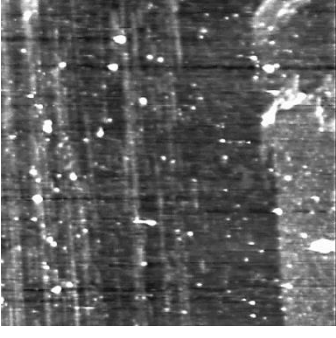
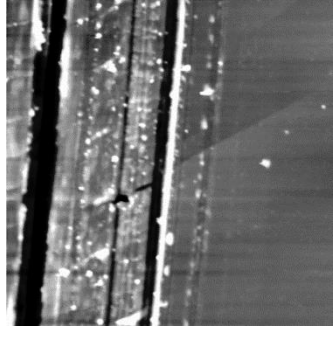
	Equilibrium	Compression
pH 4		
pH 6		
pH 9		

Figure 19: AFM images of mAB₁ after adsorption to equilibrium and after compression by 15mN/m including scratch at different pH. Mean height was determined as section analysis from the silica substrate to the film (area unaffected by the scratch)

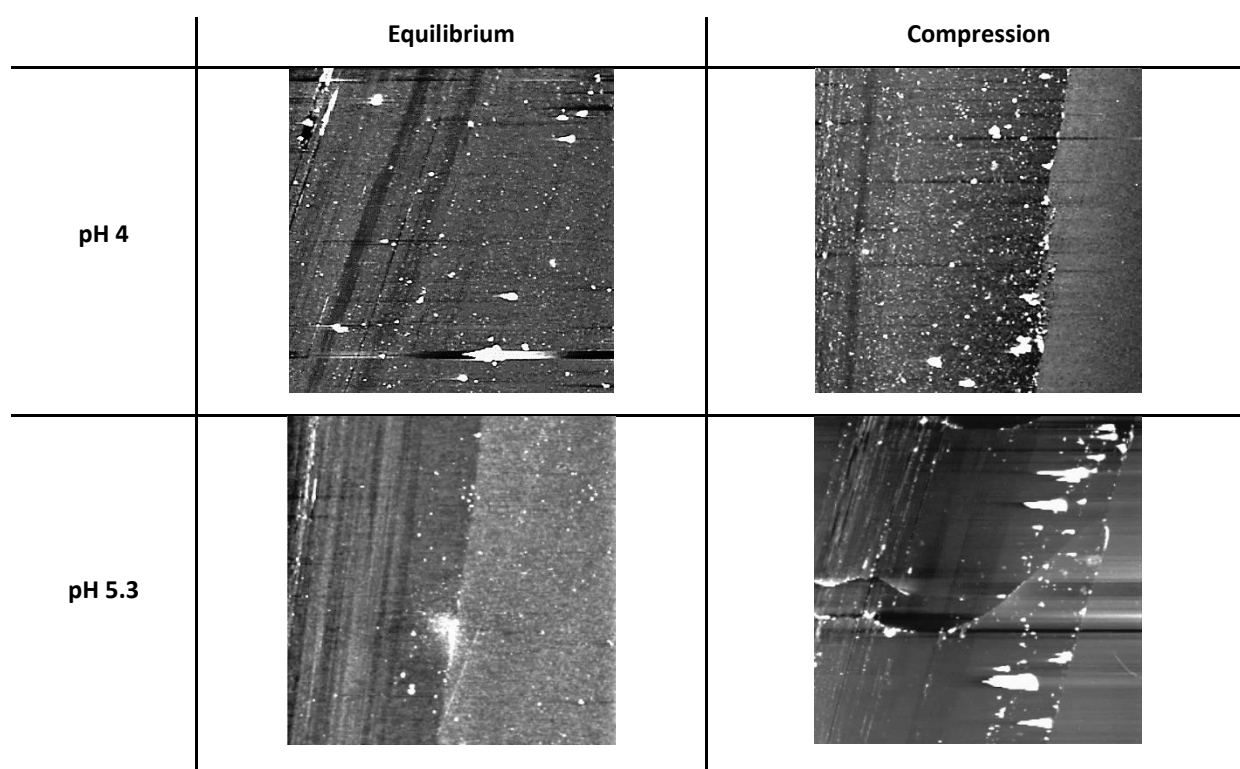


Figure 20: AFM images of mAB₂ after adsorption to equilibrium and after compression by 15mN/m including scratch at different pH. Mean height was determined as section analysis from the silica substrate to the film (area unaffected by the scratch)

7. REFERENCES

- [1] C. J. Roberts, "Protein aggregation and its impact on product quality," *Curr. Opin. Biotechnol.*, vol. 30, pp. 211–217, 2014.
- [2] M. C. Manning, D. K. Chou, B. M. Murphy, R. W. Payne, and D. S. Katayama, "Stability of protein pharmaceuticals: An update," *Pharm. Res.*, vol. 27, no. 4, pp. 544–575, 2010.
- [3] S. Uchiyama, "Liquid formulation for antibody drugs," *Biochim. Biophys. Acta*, vol. 1844, no. 11, pp. 2041–2052, 2014.
- [4] M. F. Wheeler and M. Peszyńska, "Computational engineering and science methodologies for modeling and simulation of subsurface applications," *Adv. Water Resour.*, vol. 25, no. 8–12, pp. 1147–1173, 2002.
- [5] C. J. Roberts, "Therapeutic protein aggregation : mechanisms , design , and control," vol. 32, no. 7, 2014.
- [6] C. J. Roberts, T. K. Das, and E. Sahin, "Predicting solution aggregation rates for therapeutic proteins: Approaches and challenges," *Int. J. Pharm.*, vol. 418, no. 2, pp. 318–333, 2011.
- [7] A. Hawe and W. Friess, "Formulation development for hydrophobic therapeutic proteins.," *Pharm. Dev. Technol.*, vol. 12, pp. 223–237, 2007.
- [8] T. Menzen and W. Friess, "Temperature-ramped studies on the aggregation, unfolding, and interaction of a therapeutic monoclonal antibody," *J. Pharm. Sci.*, vol. 103, no. 2, pp. 445–455, 2014.
- [9] E. Sahin, A. Grillo, M. Perkins, and C. Roberts, "Comparative Effects of pH and Ionic Strength on Protein–Protein Interactions, Unfolding, and Aggregation for IgG1 Antibodies," *J. Pharm. Sci.*, vol. 99, no. 12, pp. 4830–4848, 2010.
- [10] R. M. Fesinmeyer, S. Hogan, A. Saluia, S. R. Brych, E. Kras, L. O. Narhi, D. N. Brems, Y. R. Gokarn, "Effect of Ions on Agitation- and Temperature-induced Aggregation Reactions of Antibodies," *Pharm. Res.*, vol. 26, no. 4, pp. 903–913, 2009.

-
- [11] S. Rudiuk, L. Cohen-Tannoudji, S. Huille, and C. Tribet, "Importance of the dynamics of adsorption and of a transient interfacial stress on the formation of aggregates of IgG antibodies," *Soft Matter*, vol. 8, no. 9, p. 2651, 2012.
- [12] J. S. Bee, S. K. Schwartz, S. Trabelsi, E. Freund, J. L. Stevenson, J. F. Carpenter and T. W. Randolph, "Production of particles of therapeutic proteins at the air–water interface during compression/dilation cycles," *Soft Matter*, vol. 8, no. 40, p. 10329, 2012.
- [13] Y. F. Yano, T. Uruga, H. Tanida, H. Toyokawa, Y. Terada, M. Takagaki, and H. Yamada, "Driving Force Behind Adsorption-Induced Protein Unfolding : A Time-Resolved X-ray Reflectivity Study on Lysozyme Adsorbed at an Air / Water Interface," *Society*, no. 14, pp. 32–35, 2009.
- [14] C. Postel, O. Abillon, and B. Desbat, "Structure and denaturation of adsorbed lysozyme at the air-water interface," *J. Colloid Interface Sci.*, vol. 266, no. 1, pp. 74–81, 2003.
- [15] K. Engelhardt, W. Peukert, and B. Braunschweig, "Vibrational sum-frequency generation at protein modified air-water interfaces: Effects of molecular structure and surface charging," *Curr. Opin. Colloid Interface Sci.*, vol. 19, no. 3, pp. 207–215, 2014.
- [16] A. Rumpel, M. Novak, J. Walter, B. Braunschweig, M. Halik, and W. Peukert, "Tuning the molecular order of C60 functionalized phosphonic acid monolayers," *Langmuir*, vol. 27, no. 24, pp. 15016–15023, 2011.
- [17] A. Savitzky and M. J. E. Golay, "Smoothing and Differentiation of Data by Simplified Least Squares Procedures," *Anal. Chem.*, vol. 36, no. 8, pp. 1627–1639, 1964.
- [18] C. Schwieger, B. Chen, C. Tschierske, J. Kressler, and A. Blume, "Organization of T-shaped facial amphiphiles at the air/water interface studied by infrared reflection absorption spectroscopy," *J. Phys. Chem. B*, vol. 116, no. 40, pp. 12245–56, 2012.
- [19] S. Schrettl, C. Stefaniu, C. Schwieger, G. Pasche, E. Oveisi, Y. Fontana, A. Fontcuberta i Morral, J. Reguera, R. Petraglia, C. Corminboeuf, G. Brezesinski and H. Frauenrath, "Functional Carbon Nanosheets Prepared from Hexayne Amphiphile Monolayers at Room Temperature," *Nat. Chem.*, vol. 6, no. 6, pp. 468–76, 2014.

-
- [20] V. L. Kuzmin and A. V. Mikhailov, "Molecular Theory of Light Reflection and Applicability Limits of the Macroscopic Approach," *Opt. Spectrosc.*, vol. 51, no. 4, pp. 383–385, 1981.
- [21] V. L. Kuzmin, V. P. Romanov, and A. V. Michailov, "Reflection of Light at the Boundary of Liquid Systems and Structure of the Surface Layer: A Review," *Opt. Spectrosc.*, vol. 73, no. 1, pp. 1–26, 1992.
- [22] J. E. Bertie and Z. Lan, "Infrared Intensities of Liquids XX: The Intensity of the OH Stretching Band of Liquid Water Revisited, and the Best Current Values of the Optical Constants of H₂O(l) at 25°C between 15,000 and 1 cm⁻¹," *Appl. Spectrosc.*, vol. 50, no. 8, pp. 1047–1057, 1996.
- [23] J. E. Bertie, M. K. Ahmed, and H. H. Eysel, "Infrared Intensities of Liquids. 5. Optical and dielectric constants, integrated intensities, and dipole moment derivatives of H₂O and D₂O at 22 °C," *J. Phys. Chem.*, vol. 93, pp. 2210–2218, 1989.
- [24] K. Engelhardt, M. Lexis, G. Gochev, C. Konnerth, R. Miller, N. Willenbacher, W. Peukert and B. Braunschweig, "pH Effects on the Molecular Structure of β -Lactoglobulin Modified Air-Water Interfaces and Its Impact on Foam Rheology," *Langmuir*, vol. 29, no. 37, pp. 11646–11655, 2013.
- [25] M. Rodrigueznino. M. R. Rodriguez Nino, C. C. Sanchez, C. P. Ruiz-Henestrosa, and J. M. Rodriguez Patino, "Milk and soy protein films at the air-water interface," *Food Hydrocoll.*, vol. 19, no. 3, pp. 417–428, 2005.
- [26] J. M. Rodriguez Patino, M. R. R. Niño, C. C. Sanchez, S. E. Molina Ortiz, and C. Anon, "Dilatational properties of soy globulin adsorbed films at the air – water interface from acidic solutions," vol. 68, pp. 429–437, 2005.
- [27] R. Wüstneck, V. B. Fainerman, E.V. Aksenenko, C.S. Kotsmar, V. Pradines, J. Krägel, and R. Miller, "Surface dilatational behavior of β -casein at the solution/air interface at different pH values," *Colloids Surfaces A Physicochem. Eng. Asp.*, vol. 404, pp. 17–24, 2012.

- [28] R. R. Niño, C. C. Sánchez, and J. M. Rodríguez Patino, "Interfacial characteristics of β -casein spread films at the air-water interface," *Colloids Surfaces B Biointerfaces*, vol. 12, no. 3–6, pp. 161–173, 1999.
- [29] J. M. Rodríguez Patino, C. C. C. Sánchez, M. R. Rodríguez Niño, J. R. Patino, C. C. Sánchez, and M. R. Niño, "Structural and morphological characteristics of β -casein monolayers at the air–water interface," *Food Hydrocoll.*, vol. 13, no. 5, pp. 401–408, 1999.
- [30] I. S. Chronakis, A. N. Galatanu, T. Nylander, and B. Lindman, "The behaviour of protein preparations from blue-green algae (*Spirulina platensis* strain Pacifica) at the air/water interface," *Colloids Surfaces A Physicochem. Eng. Asp.*, vol. 173, no. 1–3, pp. 181–192, 2000.
- [31] B. A. Snopok and E. V. Kostyukevich, "Kinetic studies of protein-surface interactions: A two-stage model of surface-induced protein transitions in adsorbed biofilms," *Anal. Biochem.*, vol. 348, no. 2, pp. 222–231, 2006.
- [32] V. M. Kaganer, H. Möhwald, and P. Dutta, "Structure and phase transitions in Langmuir monolayers," *Rev. Mod. Phys.*, vol. 71, no. 3, pp. 779–819, 1999.
- [33] N. Kim, R. L. Remmele, D. Liu, V. I. Razinkov, E. J. Fernandez, and C. J. Roberts, "Aggregation of anti-streptavidin immunoglobulin gamma-1 involves Fab unfolding and competing growth pathways mediated by pH and salt concentration," *Biophys. Chem.*, vol. 172, pp. 26–36, 2013.
- [34] J. Kong and S. Yu, "Fourier Transform Infrared Spectroscopic Analysis of Protein Secondary Structures Protein FTIR Data Analysis and Band Assignment," vol. 39, no. 8, pp. 549–559, 2007.
- [35] S. Matheus, W. Friess, and H.-C. C. Mahler, "FTIR and nDSC as Analytical Tools for High-Concentration Protein Formulations," *Pharm. Res.*, vol. 23, no. 6, pp. 1350–1363, 2006.

-
- [36] J. Y. Zheng and L. J. Janis, "Influence of pH, buffer species, and storage temperature on physicochemical stability of a humanized monoclonal antibody LA298," *Int. J. Pharm.*, vol. 308, pp. 46–51, 2006.
- [37] Smith Brian C., *Fundamentals of Fourier Transform Infrared Spectroscopy*. CRC Press: Boca Raton, 2011.
- [38] R. R. Niño, C. C. Sanchez, V. P. Ruiz-Henestrosa, and J. M. Rodriguez Patino, "Milk and soy protein films at the air-water interface," *Food Hydrocoll.*, vol. 19, no. 3, pp. 417–428, 2005.
- [39] X. Wang, Y. Wang, H. Xu, H. Shan, and J. R. Lu, "Dynamic adsorption of monoclonal antibody layers on hydrophilic silica surface: A combined study by spectroscopic ellipsometry and AFM," *J. Colloid Interface Sci.*, vol. 323, no. 1, pp. 18–25, 2008.
- [40] J. Vörös, "The density and refractive index of adsorbing protein layers.," *Biophys. J.*, vol. 87, no. 1, pp. 553–561, 2004.
- [41] T. C. Werner, J. R. Bunting, and R. E. Cathou, "The Shape of Immunoglobulin G Molecules in Solution," *Proc. Natl. Acad. Sci.*, vol. 69, no. 4, pp. 795–799, 1972.
- [42] R. Saber, S. Sarkar, P. Gill, B. Nazari, and F. Faridani, "High resolution imaging of IgG and IgM molecules by scanning tunneling microscopy in air condition," *Sci. Iran.*, vol. 18, no. 6, pp. 1643–1646, 2011.
- [43] J. G. Vilhena, A. C. Dumitru, E. T. Herruzo, J. I. Mendieta-Moreno, R. Garcia, P. A. Serena and R. Perez, "Adsorption orientations and immunological recognition of antibodies on graphene," *Nanoscale*, pp. 13463–13475, 2016.
- [44] H. P. Erickson, "Size and shape of protein molecules at the nanometer level determined by sedimentation, gel filtration, and electron microscopy," *Biol. Proced. Online*, vol. 11, no. 1, pp. 32–51, 2009.
- [45] A. C. McUmbler, T. W. Randolph, and D. K. Schwartz, "Electrostatic Interactions Influence Protein Adsorption (but Not Desorption) at the Silica-Aqueous Interface," *J. Phys. Chem. Lett.*, vol. 6, no. 13, pp. 2583–2587, 2015.

- [46] H. Xu, X. Zhao, C. Grant, J. R. Lu, D. E. Williams, and J. Penfold, "Orientation of a monoclonal antibody adsorbed at the solid/solution interface: A combined study using atomic force microscopy and neutron reflectivity," *Langmuir*, vol. 22, no. 14, pp. 6313–6320, 2006.
- [47] A. Tronin, T. Dubrovsky, and C. Nicolini, "Comparative Study of Langmuir Monolayers of Immunoglobulin G Formed at the Air-Water Interface and Covalently Immobilized on Solid Supports," *Langmuir*, vol. 11, no. 2, pp. 385–389, 1995.
- [48] M. Malmsten, "Ellipsometry studies of the effect of surface hydrophobicity on protein adsorption," *Colloids Surfaces B Biointerfaces*, vol. 3, pp. 297–308, 1995.
- [49] E. Koepf, R. Schroeder, G. Brezesinski, and W. Friess, "The film tells the story: Physical-chemical characteristics of IgG at the liquid-air interface," *Eur. J. Pharm. Biopharm.*, vol. 119, pp. 396–407, 2017.
- [50] S. Saito, J. Hasegawa, N. Kobayashi, T. Tomitsuka, S. Uchiyama, and K. Fukui, "Effects of ionic strength and sugars on the aggregation propensity of monoclonal antibodies: Influence of colloidal and conformational stabilities," *Pharm. Res.*, vol. 30, no. 5, pp. 1263–1280, 2013.
- [51] M. Kastelic, Y. V. Kalyuzhnyi, B. Hribar-Lee, K. A. Dill, and V. Vlachy, "Protein aggregation in salt solutions," *Proc. Natl. Acad. Sci.*, vol. 112, no. 21, pp. 6766–6770, 2015.
- [52] S. Kiese, A. Papppenberger, W. Friess, and H. C. Mahler, "Shaken, not stirred: Mechanical stress testing of an IgG1 antibody," *J. Pharm. Sci.*, vol. 97, no. 10, pp. 4347–4366, 2008.
- [53] J. S. Bee, J. L. Stevenson, B. Metha, J. Svitel, J. Pollastrini, R. Platz, E. Freund, J. F. Carpenter, and T. W. Randolph, "Response of a concentrated monoclonal antibody formulation to high shear," *Biotechnol. Bioeng.*, vol. 103, no. 5, pp. 936–943, 2009.
- [54] O. D. Velev, E. W. Kaler, and A. M. Lenhoff, "Protein Interactions in Solution Characterized by Light and Neutron Scattering: Comparison of Lysozyme and Chymotrypsinogen," *Biophys. J.*, vol. 75, no. 6, pp. 2682–2697, 1998.

- [55] W. Wang, S. Nema, and D. Teagarden, "Protein aggregation-Pathways and influencing factors," *Int. J. Pharm.*, vol. 390, no. 2, pp. 89–99, 2010.
- [56] S. M. Kirby, X. Zhang, P. S. Russo, S. L. Anna, and L. M. Walker, "Formation of a rigid hydrophobin film and disruption by an anionic surfactant at an air/water interface," *Langmuir*, p. acs.langmuir.6b00809, 2016.
- [57] K. Nakanishi, T. Sakiyama, and K. Imamura, "On the adsorption of proteins on solid surfaces, a common but very complicated phenomenon," *J. Biosci. Bioeng.*, vol. 91, no. 3, pp. 233–244, 2001.
- [58] R. G. Couston, D. A. Lamprou, S. Uddin, and C. F. Van Der Walle, "Interaction and destabilization of a monoclonal antibody and albumin to surfaces of varying functionality and hydrophobicity," *Int. J. Pharm.*, vol. 438, no. 1–2, pp. 71–80, 2012.
- [59] S. Ghazvini, C. Kalonia, D. B. Volkin, and P. Dhar, "Evaluating the Role of the Air-Solution Interface on the Mechanism of Subvisible Particle Formation Caused by Mechanical Agitation for an IgG1 mAb," *J. Pharm. Sci.*, vol. 105, no. 5, pp. 1643–1656, 2016.
- [60] L.-C. Xu and C. A. Siedlecki, "Effects of surface wettability and contact time on protein adhesion to biomaterial surfaces," *Biomaterials*, vol. 28, no. 22, pp. 3273–3283, 2007.
- [61] Y. Baek, N. Singh, A. Arunkumar, and A. L. Zydney, "Effects of Histidine and Sucrose on the Biophysical Properties of a Monoclonal Antibody," *Pharm. Res.*, vol. 34, no. 3, pp. 629–639, 2017.

PARTS OF THIS CHAPTER ARE INTENDED FOR PUBLICATION:

Koepf E, Richert M, Braunschweig B, Schroeder R, Brezesinski G, Friess W. How Formulation pH Affects Liquid-Air Interfacial Protein Stability and Aggregation – Part 1/2, *European Journal of Pharmaceutics and Biopharmaceutics*, submitted on 2017/10/04.

CHAPTER VI – Part 2

THE MISSING PIECE IN THE PUZZLE: PREDICTION OF AGGREGATION VIA THE PROTEIN-PROTEIN INTERACTION PARAMETER A_2^*

1. ABSTRACT

The tendency of protein pharmaceuticals to form aggregates is a major challenge during formulation development, as aggregation affects quality and safety of the product. In particular, the formation of large native-like particles in the context of liquid-air interfacial stress is a well-known but not fully understood problem. So, the impact of pH and ionic strength on the interaction parameter A_2^* and its link to aggregation upon mechanical stress was investigated. A_2^* of two monoclonal antibodies (mABs) and a polyclonal IgG was correlated to the number of particles formed upon shaking in vials. A good correlation between aggregation induced by interfacial stress and formulation pH was given. A_2^* was highest for mAB₁ and lowest for IgG. Shaking of IgG resulted in overall higher particle numbers compared to the mABs. A_2^* decreased and particle numbers increased with increasing pH. Previous studies on the physicochemical behavior at the liquid-air interface pointed out that a continuous film with an inhomogeneous protein distribution over the interface is formed upon protein adsorption. Clusters of agglomerated, native-like protein material built up and are transferred into the bulk solution by compression-decompression of the interface. Whether or not those clusters lead to appearance of large protein aggregates or fall apart depends on the intermolecular forces. Thus, protein aggregation due to interfacial stress is correlated with the protein-protein interactions as determined by A_2^* . This enables to differentiate different antibodies according to their propensity to form particles upon mechanical stress and to identify optimum formulation conditions.

2. INTRODUCTION

Aggregation of monoclonal antibodies (mABs) is a known critical instability pathway. More particularly, the presence of interfaces, such as the liquid-air interface can trigger aggregate formation and especially the formation of large particles [1]–[4]. Proteins adsorb and accumulate at interfaces due to their amphiphilic nature thereby forming an interfacial protein film [5]. Rupture of this highly viscous film, e.g. by shaking, can release clusters of aggregated protein material [3], [4]. In this context the formation of large native-like protein particles has been described [2], [6]. The impact of pH on the physicochemical behavior of proteins adsorbed to the liquid-air interface was investigated in part 1 of this study using surface-sensitive analytical methods. Surface activity as well as the physical film resistance did not show a considerable pH dependency. A continuous but inhomogeneous protein film is formed during adsorption with clusters of native-like protein material. The interfacial film thickness overall slightly decreased at lower pH values. Upon compression, the protein molecules are pushed together and interact more strongly as indicated by an enormous increase in surface pressure thereby reflecting very high local concentrations [7]. Similarly, it has been stated that strong compression can cause a collapse of the protein film thereby leading to a gradual displacement of protein molecules from the interface [7]–[9]. The appearance of a considerable hysteresis upon compression and decompression, lowered surface pressure values after each cycle and a smoother film after decompression indicate a transfer of clusters of agglomerated, native-like protein material from the interface into solution upon interfacial stress. This effect has also been frequently seen in literature [3], [4], [9], [10]. However, it has also been shown that also different formulation parameters, such as pH and ionic strength, directly affect the susceptibility of a protein to aggregate [11], [12]. Thus, an investigation of the protein-protein interactions in solution may serve as the missing piece in the puzzle as it contributes to a better understanding of protein aggregation upon interfacial stress. Although the interfacial protein behavior was only slightly affected by pH, it is known that clusters of protein material are derived from the interface and brought into solution upon interfacial stress. Protein particle formation, however, is known to be strongly affected by solution pH [13]–[15]. Consequently, this study aims to link the effect of formulation pH and ionic strength on the aggregate formation by agitation to the protein-protein interactions determined via the second virial coefficient A_2^* in bulk solution.

3. MATERIALS AND METHODS

3.1. Materials

Human IgG (Beriglobin™, CSL Behring GmbH, Germany) was used for this study. The market product contains 159 mg/mL human IgG in 22 g/L Glycine and 3 g/L NaCl buffer at pH 6.8. Two monoclonal antibodies (mAB₁ and mAB₂) were provided by AbbVie Deutschland GmbH & Co. KG, Ludwigshafen am Rhein, Germany. mAB₁ is formulated in 20 mM Histidine buffer at pH 6.0 at 126 g/L, mAB₂ in 15 mM Histidine buffer at pH 5.3 at of 94 g/L. In Hydrophilic Interaction Chromatography mAB₂ turned out to be more hydrophobic compared to mAB₁ (relative perspective). Dilutions were performed using highly purified water (ELGA LC134, ELGA LabWater, Germany) and pH was adjusted by addition of 1 mM NaOH and 1 mM HCl, respectively. All samples were filtrated using 0.2 µm sterile polyethersulfone syringe filters (Sterile Syringe Filter PES, VWR, Germany). A 15 mM histidine buffer was used as standard condition. The low ionic strength solutions were prepared by 15 mM histidine buffer and pH adjustment only. The resulting ionic strength was calculated based on the amount of 1 mM NaCl or 1 mM NaOH necessary for pH adjustment (Tab. 1). High ionic strength solutions were prepared by adding NaCl in the pH-dependent required quantity to achieve 100 mM for all samples. The contribution of the polyelectrolytic proteins to the ionic strength was neglected.

Table 1: Ionic strengths of 15 mM histidine buffer at different pH values without addition of NaCl

pH	Ionic strength [mM]
2.0	28.3
4.0	16.8
6.0	12.0
6.8	9.1
7.6	8.4
9.0	12.4

3.2. Determination of A^*_2 using Dynamic Light Scattering

Dynamic light scattering (DLS) measurements were performed in 96-well plates (Greiner Bio-One Cellstar 96 well cell plate Cat.-No. 655160) using a DynaPro plate reader (Wyatt Technologies, Santa Barbara, US). A triplicate of three wells was measured for every sample with 20 acquisitions of 2 s for every well. Data were analyzed with the DYNAMICS software (version 7.1.7.16., Wyatt Technologies) at 20 °C. A viscosity of 1.019 mPa*s and a refractive index of 1.333 were used for all measurements [16]. A linear fit of D versus protein concentration data using Origin 8G gives the interaction parameter k_D [24]. The k_D values were transferred to A^*_2 values using the “TIM”-Equation [16]. For the polyclonal IgG, which consists of multiple molecular species the obtained A^*_2 value is only an apparent one.

3.3. Agitation Studies

Agitation studies of 1 mg/mL antibody solutions in 15 mM histidine buffer were performed on a horizontal orbital shaker (GfL 3017, Gesellschaft für Labortechnik mbH, Burgwedel, Germany) at 100 rpm for 48 h ($n=3$). Each vial was filled with 4 mL and sealed with 20 mm Serum NovaPure® stoppers (RS 1343 4023/50G with B2-40 FluoroTec® Coating, West Pharmaceutical Services Deutschland GmbH & Co. KG, Eschweiler, Germany).

3.4. Particle Analysis

3.4.1. Visual Inspection and Photo-documentation

Samples were analyzed for particles by visual inspection in a box with a blackboard equipped with a white light lamp for 5 s each following Ph. Eur. 2.9.19. Photodocumentation of the vials was performed using a Nikon digital camera (Nikon D5300 SLR digital camera, Nikon Corporation, Japan). Each sample was categorized according to table 2.

Table 2: Four Categories for visual inspection (following Ph. Eur. 2.9.19)

0	1	2	3
Free from particles	Practically free from particles	Several particles	Many particles

3.4.2. Turbidity

Samples were analyzed for turbidity according to Ph. Eur. 2.2.1. A sample volume of 1.8 mL was analyzed using a Nephla turbidimeter (Dr. Lange, Duesseldorf, Germany). Data are given as formazine nephelometric units (FNU).

3.4.3. Light Obscuration

Samples were analyzed for particles in the micrometer range by light obscuration (LO) with a SVSS-C instrument (PAMAS, Partikelmess- und Analysesysteme GmbH, Rutesheim, Germany). After a pre-run volume of 0.5 mL, each sample was analyzed in triplicates of 0.3 mL at a filling and emptying rate of 10 mL/min. Samples with $\geq 40\,000$ particles per mL were diluted to stay within the specification of the instrument. Before each run, the system was rinsed with at least 5 mL of highly purified water. Data was collected using PAMAS PMA Program V 2.1.2.0.

3.4.4. Micro-Flow Imaging

Particle size and number was additionally measured using a micro-flow imaging (MFI) system DPA4100 from Brightwell Technologies Inc. (Ottawa, Canada) equipped with a high-resolution 100 μ L flowcell and the MFI™ View Application Software. Pre-run volumes of 0.3 mL and sample volumes of 0.65 mL were drawn through the flow cell by a peristaltic pump at a flow rate of 0.1 mL/min. To optimize illumination and to provide a clean baseline the system was rinsed with highly purified water before and after the measurements.

3.4.5. Statistical Significance

A t-test was performed with * for $p \leq 0.05$, ** for $p \leq 0.01$ and *** for $p \leq 0.001$.

4. RESULTS AND DISCUSSION

4.1. Impact of Protein and pH on A_2^*

The protein-protein interaction parameter A_2^* was determined as function of pH for all three proteins investigated. The polyclonal IgG shows the overall lowest apparent A_2^* values (Fig. 1), whereas mAB₁ reveals the highest values. For all proteins, A_2^* decreased with increasing pH indicating an increase in attractive protein-protein interactions [18]. In case of mAB₁, A_2^* remained positive over the entire pH range between 2.0 and 9.0. The IgG showed a similar decrease with pH as mAB₁. However, mAB₂ exhibited a drastic drop in A_2^* starting at pH 5.0 and no further values could be determined above pH 6.8 due to precipitation. Consequently also no agitation studies were performed for mAB₂ above pH 6.8. Hence, mAB₁ is assumed to be the colloiddally most stable protein with the least tendency to aggregate over the entire pH range. At the same time, mAB₂ shows the most pronounced impact of pH on colloidal stability.

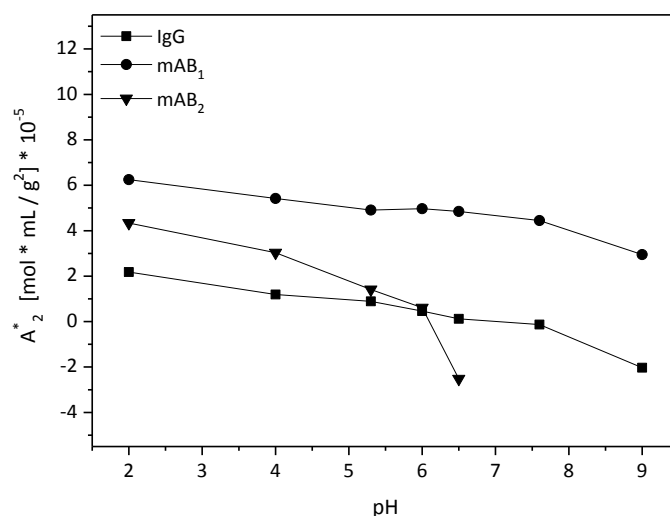


Figure 1: (Apparent) A_2^* values versus pH for IgG (■), mAB₁ (●) and mAB₂ (▼) in 15 mM histidine at low ionic strength without addition of NaCl

4.2. Impact of Protein and pH on Particle Formation by Agitation

A shaking study was carried out over 48 h for the three proteins at varying pH. The results of the visual inspection are given in figure 2. At pH 2.0, the formulations of all proteins were categorized to be free or at least practically free from particles, whereas particles were detected at all pH values above. Particularly, at pH 9.0 large protein particles were detected which is in good accordance with the hypothesis that interfacial stress can cause the formation of large protein particles.

Turbidity values increased over time and the effect was most pronounced at higher pH for all proteins. Control samples of all formulations before shaking (t_0) overall were below 1 in turbidity. In case of the IgG, no considerable increase in turbidity was observed for the formulations with a pH below 6.8, whereas the formulations at pH 7.6 and 9 exhibited elevated turbidity values of 4.1 and 5.1, respectively after 48 h. Also in case of mAB₁, the highest turbidity value of 4.6 was reached after 48 h of shaking at pH 9.0. The mAB₂ solutions reached a maximum turbidity of 5.3 at pH 6.0 and, different to the other proteins, already shaking at pH 2.0 led to a significant increase in turbidity. At pH 5.3, the IgG showed no increase in turbidity but mAB₁ and mAB₂ rendered values of 2.6 and 4.5, respectively after 48 h shaking. Similar to turbidity, the numbers of particles detected by LO and MFI were increasing with increasing pH for all proteins. In case of IgG, at pH 9.0 a maximum of 430,500 (LO) or 449,500 (MFI) particles >1 μm per mL was detected. The number of particles drastically decreased down to values well below 100,000 particles >1 μm per mL at pH values of pH 5.3 and below. Control samples of all formulations before shaking (t_0) revealed particle numbers below 800 particles by LO and below 1000 particles >1 μm per mL by MFI. A similar dependency of particle formation on pH was found for mAB₁ reaching maximum particle numbers of 61,300 (LO) and 73,800 (MFI) at pH 9.0. However, the number of particles is lower compared to the IgG. In case of mAB₂ 38,000 (LO) and 49,900 (MFI) particles >1 μm per mL were determined at pH 6. In comparison, mAB₁ exhibited only 9,000 (LO) and 7,500 (MFI) particles and thus a much lower aggregation tendency at that pH. MFI measurements overall indicated the presence of more particles compared to LO which can be explained by the presence of non-spherical protein particles as well as by the presence of particles with a similar refractive index as the surrounding solvent [19], [20].

Furthermore, also the number of large particles of $>10\ \mu\text{m}$ and $>25\ \mu\text{m}$ increases with increasing pH (Fig. 4). Following the trend of the overall number of particles formed upon shaking, mAB₁ also formed fewest large particles with e.g. only 32 (LO) or 39 (MFI) particles $>25\ \mu\text{m}$ at pH 9.0. However, it will be noted that although the IgG forms overall highest numbers of particles $>1\ \mu\text{m}$, the number of large particles $>10\ \mu\text{m}$ and $>25\ \mu\text{m}$ reaches equal values for all proteins. Particularly, in case of the IgG 73 (LO) or 82 (MFI) particles $>25\ \mu\text{m}$ build up at pH 6.8. At a similar pH of 6.0, mAB₂ forms similar numbers of large particles with 86 (LO) or 91 (MFI). At the slightly lower pH of pH 5.3, only 32 (LO) or 41 (MFI) particles $>25\ \mu\text{m}$ build up in case of mAB₂.

Overall, shaking of the IgG resulted in the highest numbers of particles $>1\ \mu\text{m}$ per mL after 48 h and both mAbs behaved rather similar. Although the absolute A_2^* values differ between the proteins, a clear trend can be observed as the number of particles directly increases with decreasing A_2^* .

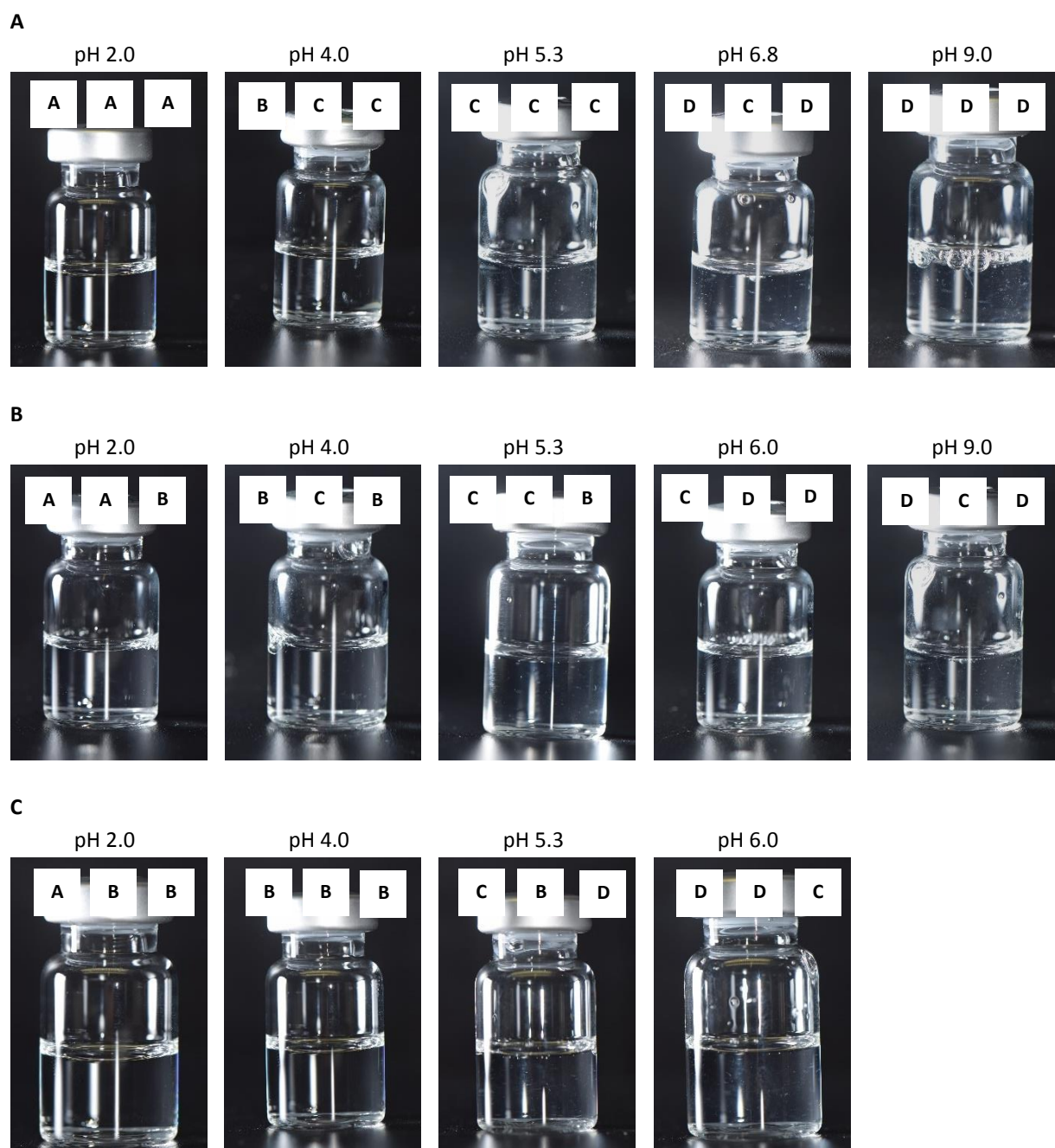


Figure 2: Visual inspection and photodocumentation of A: IgG, B: mAB₁ and C: mAB₂ after 48 h shaking at different pH values (without addition of NaCl)

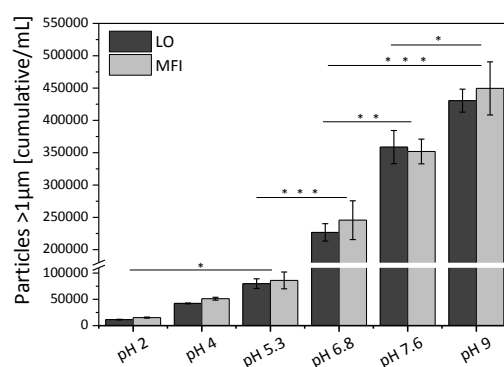
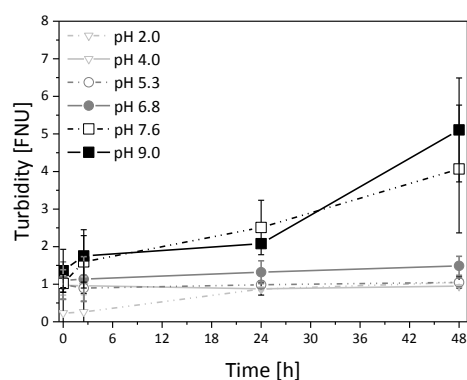
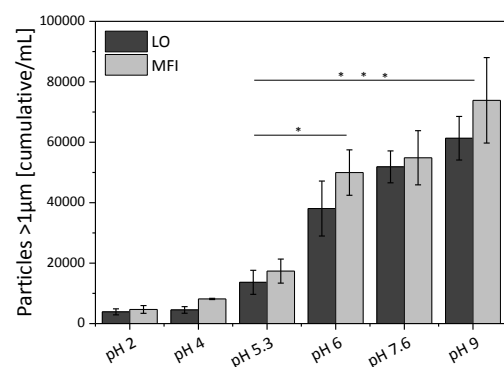
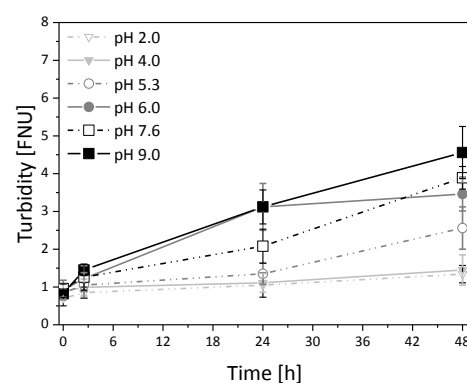
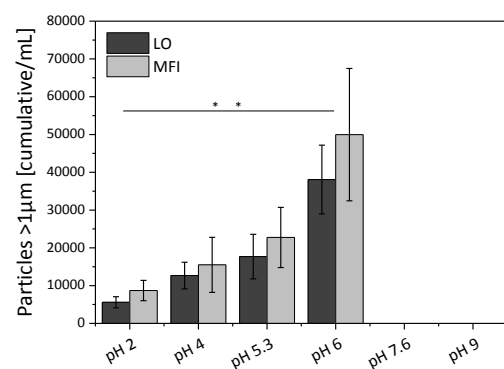
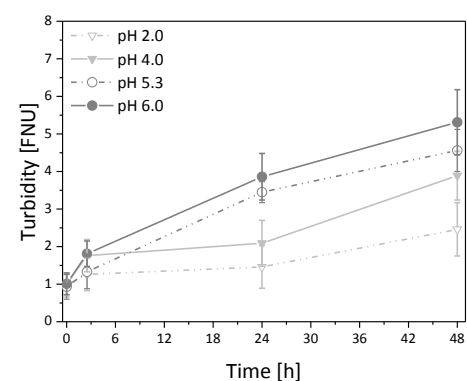
A**B****C**

Figure 3: Turbidity (left) during and number of particles > 1 μ m (right) after 48 h of shaking, A: IgG, B: mAB₁ and C: mAB₂ in 15 mM histidine without addition of NaCl

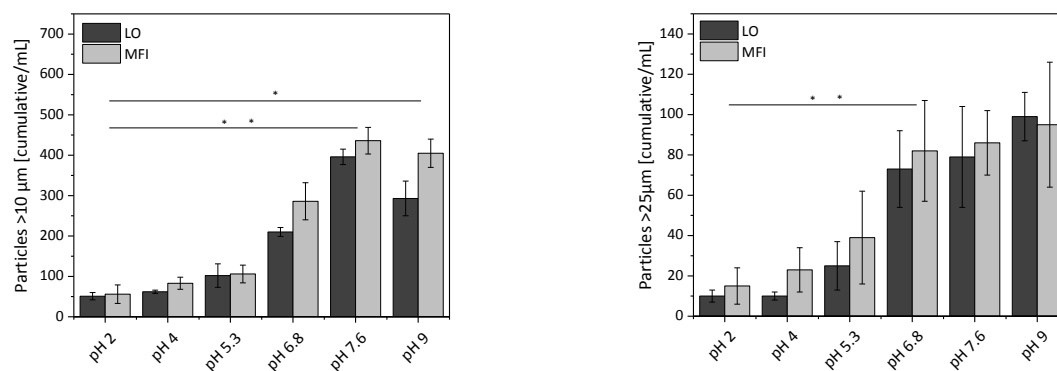
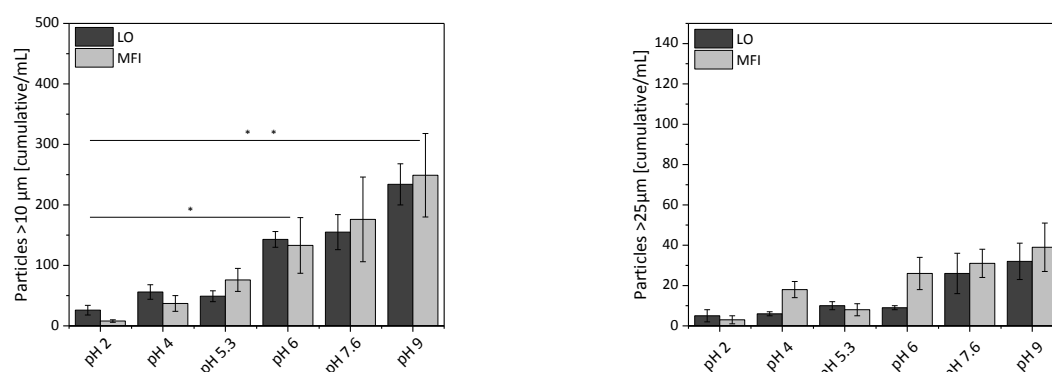
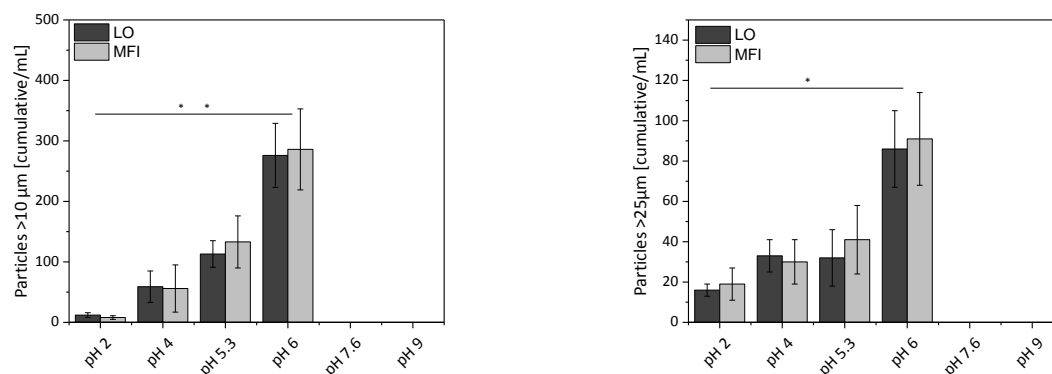
A**B****C**

Figure 4: Number of particles > 10 µm (left) and > 25 µm (right) after 48 h of shaking, A: IgG, B: mAB₁ and C: mAB₂ in 15 mM histidine without addition of NaCl

4.3. Impact of Ionic Strength on A_2^*

The impact of ionic strength on the protein-protein interaction parameter A_2^* is summarized in figure 5. In case of IgG, ionic strength does not have any considerable impact on A_2^* . Different to that, mAB₁ exhibited decreased A_2^* values at pH 7.6 and 9.0 indicating an increase in attractive interactions between the molecules at higher ionic strength. Also the A_2^* of mAB₂ became lower at higher ionic strength. Similar findings have been reported in literature thereby showing that with increasing the ionic strength protein attraction is more likely [16], [21]. Zhang *et al.* showed that protein-protein interactions between BSA molecules were dominated by an attractive potential at high ionic strengths in presence of $I = 100$ mM, whereas at low ionic strengths with less than 30 mM repulsive forces dominated [22]. Our ionic strength conditions were similar adding 100mM to achieve the high ionic strength condition for formulations which have at the most an ionic strength of 28.3 mM at pH 2.0 and 12.4 mM at pH 9.0.

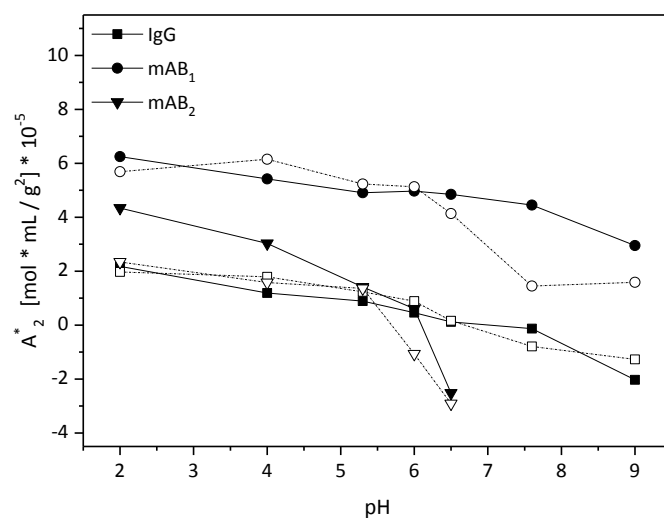


Figure 5: (Apparent) A_2^* values versus pH for IgG (■), mAB₁ (●) and mAB₂ (▼) at low (solid line, closed symbols) and high (broken line, open symbols) ionic strength

4.4. Impact of Ionic Strength on Turbidity and Particle Formation

The influence of ionic strength on the susceptibility of the three proteins to 48 h shaking stress was analyzed comparing low and high ionic strength at different pH values. At high ionic strength, the protein solutions remained clear and free from visible particles at pH 2.0, whereas with increasing pH more and more particles were formed. Particle formation was most pronounced for the IgG sample. However, mAB₁ and mAB₂ followed a similar trend as visible particles were detected at higher pH in all cases (Fig. 6). Overall, the high ionic strength samples exhibited slightly more visible particles compared to the lower ionic strength formulations described above.

Turbidity of the IgG solutions substantially increased over 48 h of shaking at pH 6.8 and 9.0. Higher turbidity resulted at high ionic strength at pH 6.8, but lower ionic strength at pH 9.0 (Fig. 7A). Similar results were obtained in sub-visible particle analysis. Only mAB₁ behaved differently, as turbidity was not much affected and remained overall low at pH 4. At pH 6.0, however, turbidity was higher in case of the high ionic strength samples. At pH 9.0, turbidity values overall were increased and revealed only slightly elevated values in case of high ionic strength. In contrast, both mABs showed higher numbers of particles measured by LO and MFI at high ionic strength, and also turbidity was higher compared to the low ionic strength samples at all pH values tested. Comparing the absolute numbers, it becomes clear that shaking of mAB₁ overall resulted in the lowest numbers of particles compared to mAB₂, and most pronounced in comparison to the IgG. Moreover, at high ionic strength more particles of >10 µm or >25 µm build up compared to low ionic strength, revealing the most pronounced effect at highest pH of 9.0 (Fig. 8).

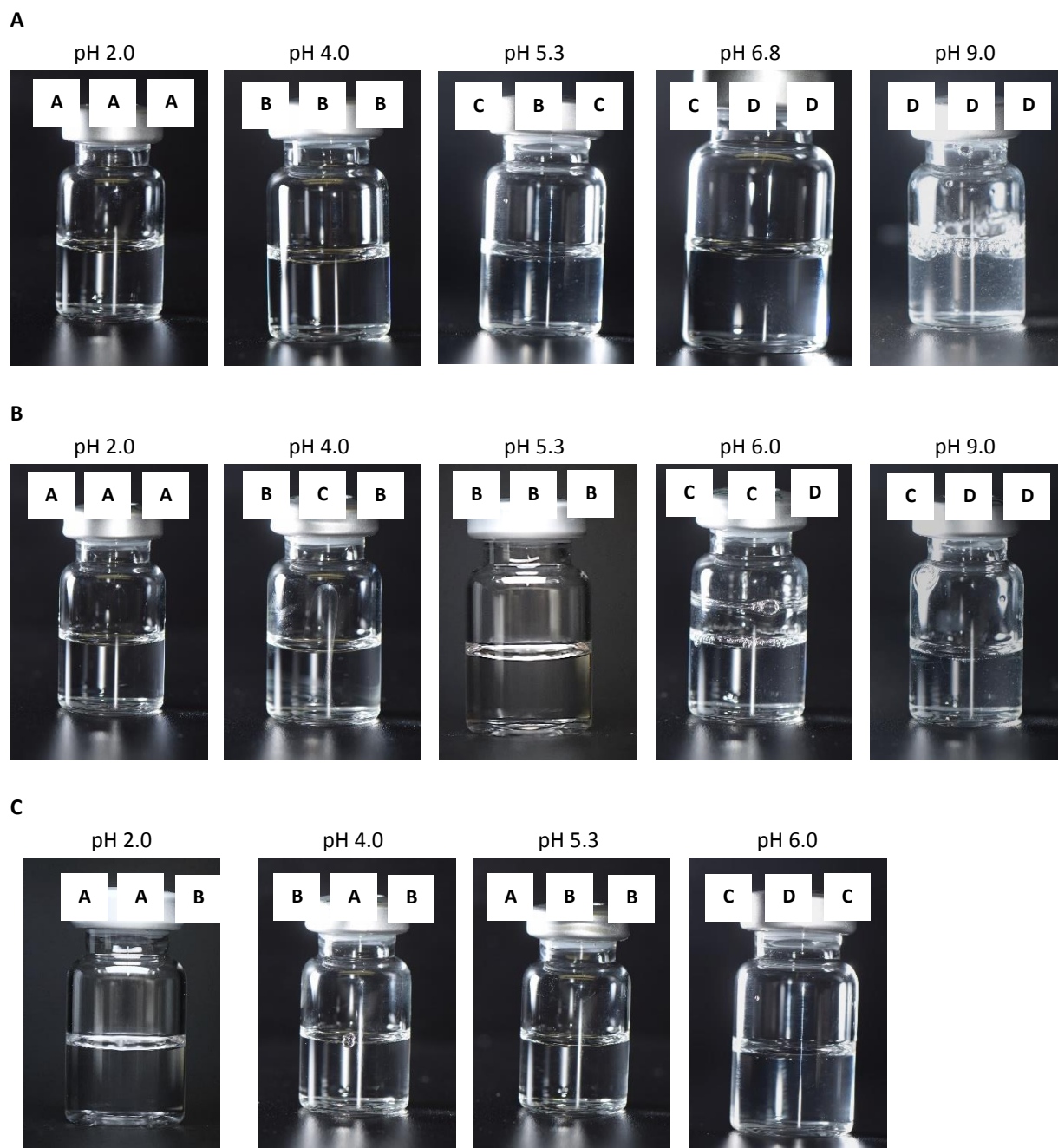
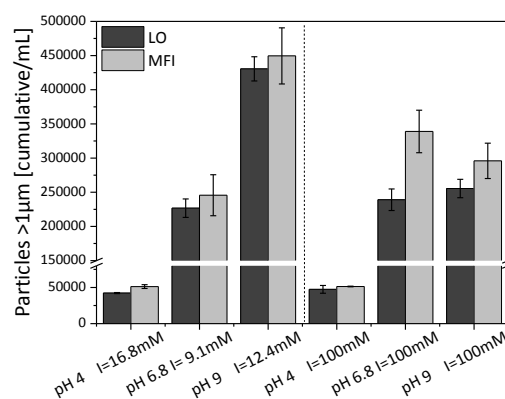
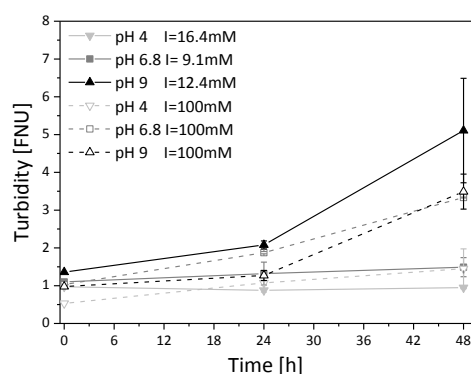
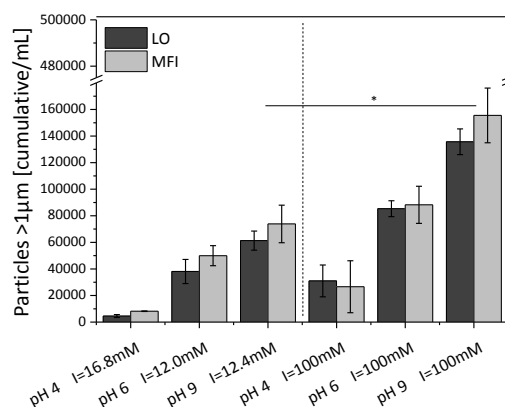
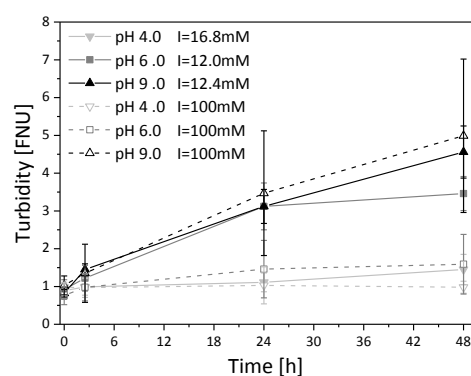


Figure 6: Visual inspection and photodocumentation of A: IgG, B: mAB₁ and C: mAB₂ after 48h shaking at different pH values at an ionic strength of 100 mM

A



B



C

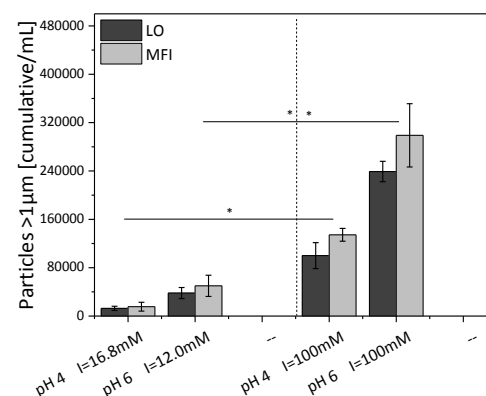
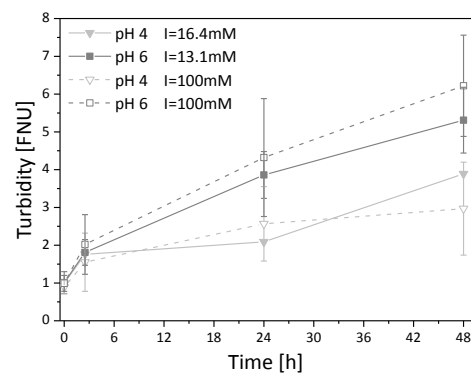


Figure 7: Turbidity (left) during and number of particles > 1 μm (right) after 48 h of shaking, A: IgG, B: mAb1 and C: mAb2 in 15 mM histidine without addition of NaCl (solid line / left part of the graph) and at an ionic strength of 100 mM (broken line / right part of the graph)

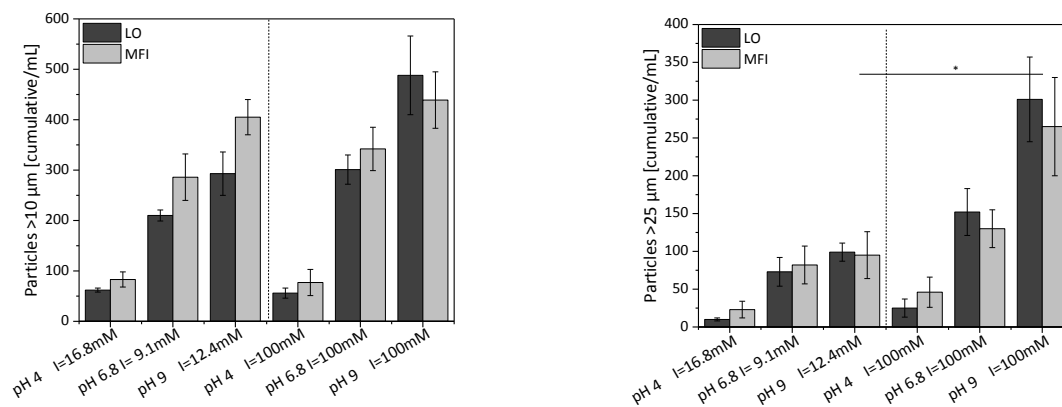
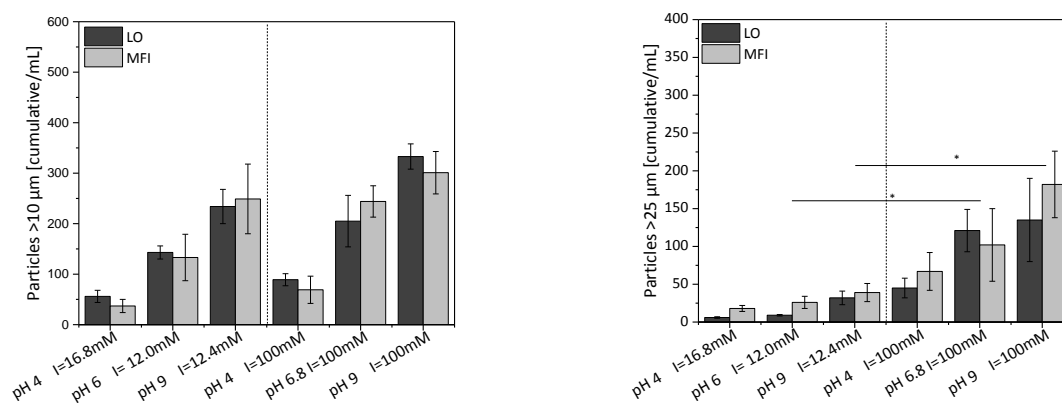
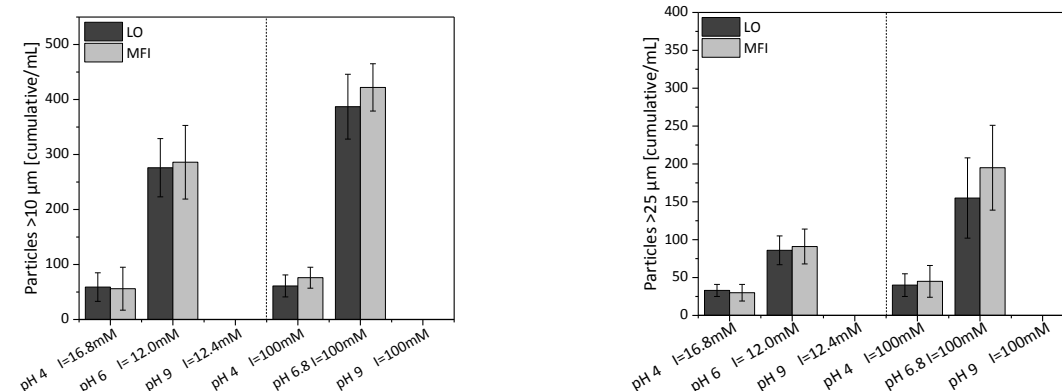
A**B****C**

Figure 8: Number of particles > 10 μm (left) and > 25 μm (right) after 48 h of shaking, A: IgG, B: mAB₁ and C: mAB₂ in 15 mM histidine without addition of NaCl (left part of the graphs) and at an ionic strength of 100 mM (right part of the graphs)

5. SUMMARY & CONCLUSION

Aggregation and particle formation is a frequently observed challenge in protein formulation development. Particularly, in the context of liquid-air interfacial stress upon shaking often large protein particles build up [28], [29]. On the one hand, various studies have been published on protein adsorption to interfaces and the effect of interfacial protein film disruption leading to particle formation [25]–[27]. On the other hand, aggregation in solution is very much dependent on protein-protein interactions which are highly affected by pH and ionic [30]–[32]. In this study, we hypothesized that protein-protein interactions in solution are also strongly affecting particle formation upon shaking.

Both the protein-protein interaction parameter A_2^* as well as the propensity to form particles upon shaking were determined for three different proteins at different pH values and two different ionic strengths. Moreover, A_2^* was found to depend on the protein itself. The repulsive interactions were most pronounced for mAB₁ which accordingly exhibited the overall lowest tendency to form aggregates. A_2^* of the polyclonal IgG was substantially lower compared to the other proteins across the entire pH range investigated. Comparison with the results of the agitation studies revealed a good correlation between A_2^* and the number of particles formed, as the number of particles overall increased with decreasing A_2^* . Additionally, also turbidity followed a similar trend. Next to the A_2^* values, also the number of particles measured for mAB₂ was found to be in between the ones of IgG and mAB₁. Thus, mAB₁ was identified as the most stable protein upon shaking and A_2^* values were overall positive. Exemplarily, even at the lowest A_2^* at pH 9.0 only 61,300 particles >1 µm per mL (LO) were formed. Furthermore, the effect of pH was most pronounced for the IgG which upon shaking formed 19,000 particles >1 µm per mL at pH 2.0 and 430,500 particles >1 µm per mL at pH 9.0 (LO). Consistent with the A_2^* values of the IgG, which became negative at pH values of 6.0 and above, at pH 5.3 less than 100,000 particles >1 µm per mL were detected whereas at pH 6.8 already 300,000 particles >1 µm per mL were formed. Therefore, it was not only shown that A_2^* is different for each protein, but also that it directly correlates with the colloidal stability of a formulation. A study by LeBrun *et al.* also pointed out small variations in the protein-protein interaction parameter of an IgG₁ by varying relevant formulation parameters, with pH and ionic strength having the most impact [21]. Differences between different antibodies can be traced back to their different structure what results in different charge distributions and net charges. Generally, antibodies carry a positive net

charge at pH values below the pI and a negative net charge at pH values above the pI. In good accordance to this, Li *et al.* demonstrated that BSA showed the lowest level in aggregation induced by liquid-gas interfacial stress directly at pI (pH 4.7) [33]. Moreover, at pH values down to 3.0, protein aggregation was found to be enhanced. In addition to charge effects, conformational instability leading to unfolding and stronger hydrophobic interaction comes into play, e.g. at highly acidic pH [34], [35]. Similarly, in a study by Majhi *et al.* the pH dependent aggregation of β -lactoglobulin was ascribed to the sensitivity to local charges in certain electrostatic domains, which have a particularly significant effect on protein-protein interactions [36]. Hence, also the net charge and the charge distribution within a molecule directly affect, next to the protein-protein interactions, its colloidal stability. Additionally, the aggregation mechanism of β -lactoglobulin was explained by an association process, where intermediate aggregates further associate and thereby form larger clusters [36]. Referring to this, the results obtained in this study agree with this assumption. Also, the pI values of the proteins investigated differ among each other, with the IgG having a pI of pH 6.9, and mAB₁ and mAB₂ values of 8.75 and 6.51, respectively. Hence, the high pI of mAB₁ also contributed to the fact that it was found to be the most stable one compared to the other antibodies. Above pI, A_2^* of all three proteins decreased due to charge shielding, and the aggregation propensity increased as indicated by the subvisible particle numbers. Different to pH, however, ionic strength only slightly affected A_2^* . Nevertheless, at high ionic strength the samples exhibit more pronounced visible particles formation. Accordingly, also the number of particles formed upon shaking was increased, i.e. large particles >25 μm were found to a greater extent, what was most pronounced at high pH. At high ionic strength, protein charges can be shielded effectively which can foster protein aggregation and the effect also depends on the mAB investigated [47, 48]. Additionally, the nature of the shielding ion can affect aggregation. For example, citrate anions were found to preferentially accumulate at the surface of an IgG₁ compared to acetate anions, resulting in different charge profiles and hence different intermolecular interactions [38]. Hence, it can be assumed, that attractive forces in bulk solution foster aggregation whereas repulsive ones promote rather a dissociation of loosely-packed protein material derived from the interface [8], [42]–[44]. Therefore, the complex interplay between interfacial film formation and transport of protein material into bulk solution upon interfacial stress can only be linked to the emergence of protein particles in bulk solution when protein-protein interactions are

taken into account. Consequently, A_2^* can serve as the missing piece in the puzzle, as it allows to rank protein formulations according to their propensity to form aggregates upon interfacial stress.

In part 1 of this study it was shown that a continuous interfacial protein film with some areas of clustered protein material is formed at the liquid-air interface, independent of pH. Upon compression, the interfacial film thicknesses increases, and the protein molecules are brought into closer contact resulting in more pronounced protein-protein interactions. Repeated compression and decompression of the concentrated interfacial layer causes release of large agglomerates of native-like protein into the bulk solution. No effect of pH or salt on surface activity or folding was observed. But, pH affected the number of particles formed upon interfacial stress. In part 2 we demonstrated that the protein agglomerates disintegrate at solutions conditions which trigger enhanced repulsive protein-protein interactions, represented by positive A_2^* values, but sustain at conditions of more attractive interactions, represented by negative A_2^* values. It can be concluded that protein molecules can remain in a native-like conformation at the interface but still form aggregates if the molecules come close enough to each other, and if attractive forces are sufficiently high within the condensed protein film. Particularly, close to the pI attractive forces between protein molecules dominate, thereby strengthening the assembly of protein clusters. Repulsive forces at pH conditions away from the pI can have an opposite effect. Additionally, the charge interactions are affected by charge shielding effects by added ions. Therefore, although similar processes happen at the interface at all pH values and ionic strengths, solution conditions and hence protein-protein interactions dictate whether or not protein particles, especially large native-like protein particles, build up. As pH strongly affected the number of particles formed upon stressing the interfacial film, the bulk conditions have a vital influence on particle formation.

Finally, a determination of A_2^* helps to identify optimum formulation conditions to increase stability of biopharmaceuticals against mechanical, specifically shaking stress. The A_2^* can also be a tool to screen different molecules for their susceptibility to undergo surface-induced protein aggregation.

6. REFERENCES

- [1] S. Kiese, A. Papppenberger, W. Friess, and H. C. Mahler, "Shaken, not stirred: Mechanical stress testing of an IgG1 antibody," *J. Pharm. Sci.*, vol. 97, no. 10, pp. 4347–4366, 2008.
- [2] J. Wiesbauer, R. Prassl, and B. Nidetzky, "Renewal of the air-water interface as a critical system parameter of protein stability: Aggregation of the human growth hormone and its prevention by surface-active compounds," *Langmuir*, vol. 29, no. 49, pp. 15240–15250, 2013.
- [3] S. Rudiuk, L. Cohen-Tannoudji, S. Huille, and C. Tribet, "Importance of the dynamics of adsorption and of a transient interfacial stress on the formation of aggregates of IgG antibodies," *Soft Matter*, vol. 8, no. 9, p. 2651, 2012.
- [4] J. S. Bee, D. K. Schwartz, J. F. Carpenter, and T. W. Randolph, "Production of particles of therapeutic proteins at the air–water interface during compression/dilation cycles," *Soft Matter*, vol. 8, no. 40, p. 10329, 2012.
- [5] S. Damodaran and L. Razumovsky, "Role of surface area-to-volume ratio in protein adsorption at the air-water interface," *Surf. Sci.*, vol. 602, no. 1, pp. 307–315, 2008.
- [6] C. J. Roberts, T. K. Das, and E. Sahin, "Predicting solution aggregation rates for therapeutic proteins: Approaches and challenges," *Int. J. Pharm.*, vol. 418, no. 2, pp. 318–333, 2011.
- [7] E. Koepf, R. Schroeder, G. Brezesinski, and W. Friess, "The film tells the story: Physical-chemical characteristics of IgG at the liquid-air interface," *Eur. J. Pharm. Biopharm.*, vol. 119, pp. 396–407, 2017.
- [8] A. H. Martin, M. A. C. Stuart, M. A. Bos, and T. van Vliet, "Correlation between Mechanical Behavior of Protein Films at the Air / Water Interface and Intrinsic Stability of Protein Molecules," *Langmuir*, vol. 21, no. 9, pp. 4083–4089, 2005.
- [9] E. Koepf, S. Eisele, R. Schroeder, G. Brezesinski, and W. Friess, "Notorious But Not Understood: How Liquid-Air Interfacial Stress Triggers Protein Aggregation," *J. Pharm. Sci.*, p. submitted August 14, 2017.

-
- [10] I. C. Shieh and A. R. Patel, "Predicting the agitation-induced aggregation of monoclonal antibodies using surface tensiometry," *Mol. Pharm.*, p. 3184–3193, 2015.
- [11] J. S. Bee, J. L. Stevenson, B. Metha, J. Svitel, J. Pollastrini, R. Platz, E. Freund, J. F. Carpenter, and T. W. Randolph., "Response of a concentrated monoclonal antibody formulation to high shear," *Biotechnol. Bioeng.*, vol. 103, no. 5, pp. 936–943, 2009.
- [12] S. J. Shire, "Formulation and manufacturability of biologics," *Curr. Opin. Biotechnol.*, vol. 20, no. 6, pp. 708–714, 2009.
- [13] E. Y. Chi, S. Krishnan, T. W. Randolph, and J. F. Carpenter, "Physical stability of proteins in aqueous solution: Mechanism and driving forces in nonnative protein aggregation," *Pharm. Res.*, vol. 20, no. 9, pp. 1325–1336, 2003.
- [14] M. C. Manning, D. K. Chou, B. M. Murphy, R. W. Payne, and D. S. Katayama, "Stability of protein pharmaceuticals: An update," *Pharm. Res.*, vol. 27, no. 4, pp. 544–575, 2010.
- [15] R. M. Fesinmeyer, S. Hogan, A. Saluja, S. R. Brych, E. Kras, L. O. Narhi, D. N. Brems, and Y. R. Gokran, "Effect of Ions on Agitation- and Temperature-induced Aggregation Reactions of Antibodies," *Pharm. Res.*, vol. 26, no. 4, pp. 903–913, 2009.
- [16] T. Menzen and W. Friess, "Temperature-ramped studies on the aggregation, unfolding, and interaction of a therapeutic monoclonal antibody," *J. Pharm. Sci.*, vol. 103, no. 2, pp. 445–455, 2014.
- [17] V. Selection, "Supplemental Information," *Exposure*, vol. 2, no. 1967, pp. 2–8, 2004.
- [18] D. W. Siderius, W. P. Krekelberg, C. J. Roberts, and V. K. Shen, "Osmotic virial coefficients for model protein and colloidal solutions: Importance of ensemble constraints in the analysis of light scattering data," *J. Chem. Phys.*, vol. 136, no. 17, 2012.
- [19] C.-T. Huang, D. Sharma, P. Oma, and R. Krishnamurthy, "Quantitation of Protein Particles in Parenteral Solutions Using Micro-Flow Imaging," *J. Pharm. Sci.*, vol. 98, no. 9, pp. 3058–3071, 2009.

-
- [20] D. K. Sharma, D. King, P. Oma, and C. Merchant, "Micro-Flow Imaging: Flow Microscopy Applied to Sub-visible Particulate Analysis in Protein Formulations," *AAPS J.*, vol. 12, no. 3, pp. 455–464, 2010.
- [21] V. Le Brun, W. Friess, S. Bassarab, S. Mühlau, and P. Garidel, "A critical evaluation of self-interaction chromatography as a predictive tool for the assessment of protein-protein interactions in protein formulation development: A case study of a therapeutic monoclonal antibody," *Eur. J. Pharm. Biopharm.*, vol. 75, no. 1, pp. 16–25, 2010.
- [22] F. Zhang, M. W. A. Skoda, R. M. J. Jacobs, R. A. Martin, C. M. Martin, and F. Schreiber, "Protein Interactions Studied by SAXS: Effect of Ionic Strength and Protein Concentration for BSA in Aqueous Solutions," *J. Phys. Chem. B Chem*, vol. 111, pp. 251–259, 2007.
- [23] S. Amin, G. V Barnett, J. A. Pathak, C. J. Roberts, and P. S. Sarangapani, "Current Opinion in Colloid & Interface Science Protein aggregation , particle formation , characterization & rheology," vol. 19, pp. 438–449, 2014.
- [24] A. Eppler, M. Weigandt, A. Hanefeld, and H. Bunjes, "Relevant shaking stress conditions for antibody preformulation development," *Eur. J. Pharm. Biopharm.*, vol. 74, no. 2, pp. 139–147, 2010.
- [25] C. J. Roberts, "Protein aggregation and its impact on product quality," *Curr. Opin. Biotechnol.*, vol. 30, pp. 211–217, 2014.
- [26] B. Patrick Werner and G. Winter, "Particle contamination of parenterals and in-line filtration of proteinaceous drugs," *Int. J. Pharm.*, 2015.
- [27] F. Jameel and S. Hershenson, *Formulation and Process Development Strategies for Manufacturing Biopharmaceuticals*. New Jersey: John Wiley & Sons, Inc., 2010.
- [28] T. Serno, E. Härtl, A. Besheer, R. Miller, and G. Winter, "The Role of Polysorbate 80 and HP β CD at the Air-Water Interface of IgG Solutions," *Pharm. Res.*, pp. 1–14, 2012.
- [29] B. A. Kerwin, "Polysorbates 20 and 80 Used in the Formulation of Protein Biotherapeutics: Structure and Degradation Pathways," *J. Pharm. Sci.*, vol. 97, no. 8, pp. 2926–2935, 2008.

-
- [30] C. J. Roberts, "Kinetics of irreversible protein aggregation: Analysis of extended Lumr1. Roberts, C. J. Kinetics of irreversible protein aggregation: Analysis of extended Lumry-Eyring models and implications for predicting protein shelf life. *J. Phys. Chem. B* 107, 1194–," *J. Phys. Chem. B*, vol. 107, no. 5, pp. 1194–1207, 2003.
- [31] E. Sahin, A. Grillo, M. Perkins, and C. Roberts, "Comparative Effects of pH and Ionic Strength on Protein–Protein Interactions, Unfolding, and Aggregation for IgG1 Antibodies," *J. Pharm. Sci.*, vol. 99, no. 12, pp. 4830–4848, 2010.
- [32] U. Nobbmann, "Protein sizing by light scattering, molecular weight and polydispersity," *Int. J. Biol. Macromol.*, vol. 19, no. 3, pp. 213–21, 1996.
- [33] R. Li, Z. Wu, Y. Wangb, L. Ding, and Y. Wang, "Role of pH-induced structural change in protein aggregation in foam fractionation of bovine serum albumin," *Biotechnol. Reports*, vol. 9, pp. 46–52, 2016.
- [34] A. Tronin, T. Dubrovsky, S. Dubrovskaya, G. Radicchi, and C. Nicolini, "Role of Protein Unfolding in Monolayer Formation on Air/Water Interface," *Langmuir*, vol. 12, no. 13, pp. 3272–3275, 1996.
- [35] Y. F. Yano, "Kinetics of protein unfolding at interfaces," *J. physics. Condens. matter*, vol. 24, p. 503101, 2012.
- [36] P. R. Majhi, R. R. Ganta, R. P. Vanam, E. Seyrek, K. Giger, and P. L. Dubin, "Electrostatically Driven Protein Aggregation: β -Lactoglobulin at Low Ionic Strength," *Langmuir*, vol. 22, no. 22, pp. 9150–9159, 2006.
- [37] Z. Liao, J. W. Lampe, P. S. Ayyaswamy, D. M. Eckmann, and I. J. Dmochowski, "Protein assembly at the air-water interface studied by fluorescence microscopy.," *Langmuir*, vol. 27, pp. 12775–81, 2011.
- [38] G. V. Barnett, V. I. Razinkov, B. A. Kerwin, T. M. Laue, A. H. Woodka, P. D. Butler, T. Perevozchikova, and C. J. Roberts, "Specific-ion effects on the aggregation mechanisms and protein-protein interactions for anti-streptavidin immunoglobulin gamma-1," *J. Phys. Chem. B*, vol. 119, no. 18, pp. 5793–5804, 2015.

- [39] A. Quigley and D. R. Williams, "The second virial coefficient as a predictor of protein aggregation propensity: A self-interaction chromatography study," *Eur. J. Pharm. Biopharm.*, vol. 96, pp. 282–290, 2015.
- [40] R. Chaudhuri, Y. Cheng, C. R. Middaugh, and D. B. Volkin, "High-Throughput Biophysical Analysis of Protein Therapeutics to Examine Interrelationships Between Aggregate Formation and Conformational Stability," *AAPS J.*, vol. 16, no. 1, pp. 48–64, 2014.
- [41] D. Roberts, R. Keeling, M. Tracka, C. F. van der Walle, S. Uddin, J. Warwicker, and R. Curtis, , "The role of electrostatics in protein-protein interactions of a monoclonal antibody," *Mol. Pharm.*, vol. 11, no. 7, pp. 2475–2489, 2014.
-

PARTS OF THIS CHAPTER ARE INTENDED FOR PUBLICATION:

Koepf E, Schroeder R, Brezesinski G, Friess W. How Formulation pH Affects Liquid-Air Interfacial Protein Stability and Aggregation – Part 2/2, *European Journal of Pharmaceutics and Biopharmaceutics*, submitted on 2017/10/04.

CHAPTER VII

SUMMARY

Protein aggregation is a major challenge in the development of biopharmaceutics as it negatively impacts product quality. The mechanisms and pathways of protein aggregation are manifold and can occur in parallel in a product. At many points during manufacturing and transportation of protein pharmaceuticals aggregation may be encountered. A better understanding of the features that influence, control and prevent protein aggregation is essential to enable a systematic and rational formulation development. Although it has already been extensively investigated that the presence of liquid-air interfaces is directly related to the emergence of protein aggregates, little is known about the aggregation mechanism at the interface itself. In particular, the formation of large native-like particles in the context of liquid-air interfacial stress is a well-known but not well understood problem. It was the aim of this thesis to provide an understanding of the behavior of immunoglobulins (IgGs) at the liquid-air interface and of the formation of aggregates, as well as to elucidate how formulation affects interface-related protein instability.

In **chapter III** surface-sensitive analytical methods such as Langmuir trough experiments, Infrared Reflection-Absorption Spectroscopy (IRRAS), Brewster Angle Microscopy (BAM), and Atomic Force Microscopy (AFM) were combined to uncover IgG adsorption and structure at the liquid-air interface. Concentration-dependent adsorption of IgG and surface-pressure / area isotherms substantiated the amphiphilic nature of the protein molecules as well as the formation of a compressible protein film at the liquid-air interface. The increase in surface pressure upon compression of the protein layer demonstrated that the protein molecules rather stay at the interface and do not readily desorb upon compression. IRRAS spectra proved not only the presence of the protein molecules at the interface, but also showed that the secondary structure does not change considerably during adsorption or compression. IRRAS experiments at different angles of incidence enabled to determine the effective film thickness (packing density) and proved that the film thickness increased upon compression. Furthermore, BAM images pointed out a coherent but inhomogeneous distribution of the protein at the interface. Topographical differences within the protein film after adsorption, compression and decompression were revealed using underwater AFM.

Different methodologies to thoroughly characterize the liquid-air interfacial behavior of two monoclonal antibodies were used in **chapter IV**. Therefore, not only physical-chemical aspects were taken into account, but also controlled stress of the liquid-air interfacial film. Therefore, a model was developed to investigate the impact of liquid-air interfacial stress only on protein aggregation. Repeated compression and decompression of the film in this newly designed test model resulted in significant formation of protein particles compared to controls, as detected by visual inspection, turbidity, Light Obscuration (LO) and Micro-Flow Imaging (MFI) analysis. The steep decrease in surface pressure upon decompression as well as the slightly decreased equilibrium surface pressure after each subsequent cycle of compression and decompression pointed towards a loss of protein material from the interface. Furthermore, the compressibility of the interfacial film was directly affected by the speed and extent of compression. Compression above a c_f of 3 caused irreversible compaction of the protein molecules within the film as observed by the emergence of a pronounced hysteresis. The number of particles formed also increased with increasing compression factor. Accordingly, compression speeds of 25 mm/min and above triggered the formation of protein particles. The island-like distribution of protein observed in the BAM images goes in line with this hypothesis. However, as no major effect on secondary structure was observed by IRRAS, the IgGs are assumed to remain in a native-like conformation. Hence, the Mini-trough method is a highly expedient method for the localization of protein particle formation by liquid-air interfacial stress only. In addition, the Mini-trough represents a valuable tool to screen different formulation candidates for their propensity to undergo interface-related protein aggregation processes.

The addition of surface active compounds is a popular option to improve the stability of a protein formulation and to prevent interface-related aggregation. Understanding of the behavior of both the protein and the additive at the interface is mandatory for the decision whether and which one to add. Therefore, physicochemical investigations and interfacial stress studies were performed with combinations of IgG and polysorbate 80 (PS 80), poloxamer 188 (P 188) or hydroxypropyl- β -cyclodextrin (HP- β -CD) in **chapter V**. Whilst IgG films were highly compressible, compression of an additive solution did not result in a considerable increase in surface pressure. The mixtures of both, revealed either IgG - or additive - like characteristics depending on the mixing ratio. The appearance of amide bands in IRRAS spectra proved the presence of IgG at the interface in case of mixtures with the

surfactant present at concentrations below the critical micellar concentration (CMC). In formulations with additive present above CMC, no amide bands but characteristic additive bands were detected. Moreover, additive solutions did not supply any signal in BAM. Therefore, bright domains could be traced back to the presence of the IgG at the interface. No aggregate formation was observed upon mechanically stressing by shaking or repeated compression and decompression of samples with PS 80 and P 188 present above CMC in the Mini-trough. Also, HP- β -CD successfully inhibited aggregation, although to a lesser extent. Residual clusters of IgG were uncovered in BAM even at PS 80 concentrations above CMC. Similarly, residual IgG clusters were detected in mixtures with P 188 above CMC and all HP- β -CD concentrations tested. In contrast, in mixtures with PS 80 far below CMC bright regions of large IgG domains emerged upon compression. Accordingly, areas of agglomerated protein material with increased height appeared in AFM images. Very low PS 80 concentrations caused a destabilization compared to a surfactant free system with a more pronounced increase in particle numbers both in shaking and compression-decompression experiments. The different surface-sensitive techniques applied in combination with interfacial-stress studies provide valuable insights into the liquid-air interfacial film characteristics that help to better understand how formulation additives affect interface related protein instability.

In **chapter VI – part 1** the impact of pH and ionic strength on the liquid-air interfacial protein behavior was investigated. Equilibrium surface pressure value was only marginally impacted by pH and ionic strength. Only at a low pH values surface pressure increased which can be traced back to an increased hydrophobicity due to IgG unfolding as investigated by FT-IR. Secondary structure and mechanical properties of the IgG film were not considerably affected by adsorption between pH 3 and pH 9. Compression of the film caused the formation of telescoped areas which are no longer present after decompression. BAM showed slight changes in the film reflectivity depending on the pH value indicating changes within the interfacial film thickness. IRRAS experiments at different angles of incidence as well as section analysis of AFM images proved not only that the film thickness increased upon compression but also that the interfacial film was thinner at pH 4 compared to higher pH values. This was in accordance with the formulation dependent formation of particles as detected by Light Obscuration (LO) and Micro-Flow Imaging (MFI) upon repeated compression-decompression of the interfacial protein film.

Subsequently, the protein-protein interaction parameter A_2^* was analyzed by DLS and its importance for interface-related protein particle formation was studied (**chapter VI - part 2**). Whereas no considerable effects of pH and ionic strength on the physicochemical characteristics of the interfacial protein film were detected, particle formation upon shaking or continued compression and decompression was strongly related to pH and ionic strength. A_2^* decreased with increasing pH value for all three proteins investigated. This correlates well with the more pronounced particle formation with higher pH upon shaking. At low pH, repulsive forces between protein molecules dominate, impeding aggregation. Moreover, A_2^* was found to be highest for mAB₁ which showed lowest numbers of particles upon mechanical stress. Overall, high ionic strength caused a destabilization, as A_2^* decreased and the number of particles formed increased compared to lower ionic strength samples. Altogether, upon compression a highly concentrated protein phase is formed. Upon decompression, clusters of agglomerated protein material may remain or fall apart depending on the extent of attractive and repulsive protein-protein interactions.

In conclusion, this work introduced valuable new surface sensitive methods that allow a better understanding of liquid-air interfacial protein behavior. The combinatorial use of physicochemical, spectroscopic and microscopic methods provided useful insights into the liquid-air interfacial protein characteristics and revealed the formation of a continuous but inhomogeneous film of native-like protein molecules whose topographical appearance is affected by compressive forces. The relevance of compression and decompression of the protein film at the liquid-air interface for the formation of protein particles was proven. Based on these achievements, the effect of formulation additives can be evaluated what helps not only to understand their mechanisms of action but also to identify the optimum additive type and concentration. Ultimately, whether aggregates and particles result after such stress depends on the protein-protein interactions and hence also on the formulation conditions. This understanding provides a good basis for the development of stable protein formulations.

